Fall 12-14-2018

Dietary Polyunsaturated Fatty Acids Regulate Mammary Tumor Growth and Metastasis by Modulating Tissue Microenvironments

Saraswoti Khadge
University of Nebraska Medical Center

Dietary Polyunsaturated Fatty Acids Regulate Mammary Tumor Growth and Metastasis by Modulating Tissue Microenvironments

By

Saraswoti Khadge

A DISSERTATION

Presented to the Faculty of

the University of Nebraska Graduate College

in Partial Fulfillment of the Requirements

for the Degree of Doctor of Philosophy

Pathology & Microbiology Graduate Program

Under the Supervision of Profs. James E. Talmadge & Geoffrey M. Thiele

University of Nebraska Medical Center

Omaha, Nebraska

September, 2018

Supervisory Committee:

James E. Talmadge, Ph.D.

Geoffrey M. Thiele, Ph.D.

Lynell W. Klassen, M.D.

Joyce Solheim, Ph.D.

In memory of beloved

Father Dwarika Lal Khadge and Mother Kamala Devi Khadge

Dedicated to the brother

Mr. Rasun Lal Khadge

ACKNOWLEDGEMENTS

It is my immense pleasure to express my sincere gratitude to my mentors Dr. James E. Talmadge and Dr. Geoffrey M. Thiele for their excellent directions and supervision to get productive outcomes from my dissertation project, and for their guidance, which helped me to grow professionally and personally. I am thankful to my mentors for providing me an opportunity to work in this collaborative project that involved multiple professors with diverse expertise. The discussions during the project meetings helped me to analyze the differential perspectives of the same research question, which is critical for multidimensional studies. I am especially thankful to Dr. Talmadge for his efforts and time in conducting discussions of papers during my initial years in the lab, which helped me to understand the roots of seminal works in cancer biology and metastasis. Similarly, I am thankful to Dr. Thiele for discussion of the original articles on isocaloric diets, pair-fed models and their importance in nutritional studies.

Besides my advisers, I would like to express my sincere thanks to Dr. John Graham Sharp and Dr. Timothy M. McGuire (collaborators of the project) who attended the weekly meetings and provided their valuable suggestions throughout the study period. I am especially thankful to Dr. Sharp for teaching me histo-pathology and the basics of human anatomy/physiology, and providing me an opportunity to observe a cadaver analysis. I am grateful to Dr. Sharp for his guidance and motivation for the study as well as for the career/personal challenges.

I am sincerely thankful to Dr. Lynell W. Klassen for his generous financial support for my studies, without which this project may not have been completed. Besides, I am thankful to Dr. Klassen for being in my supervisory committee and provided valuable suggestions for the study. I would like thank Dr. Joyce Solheim for being on my supervisory committee and providing her expert guidance for the project directions as well as a student's

curriculum development. Similarly, I am thankful to Dr. Paul W. Black, Dr. Concetta DiRusso and Jorden Beck from the University of Nebraska at Lincoln for their help in the fatty acids composition analysis.

Working as a student in a collaborative project, I am thankful to the lab members from four different labs for their cooperation throughout my studies. Firstly, I would like to thank Alicia Dafferner and Holly Britton for being wonderful colleagues. I am thankful to Alicia for her help/instructions in lab protocols in my initial days and for answering my queries, although she is not currently present in the lab. I am thankful to Holly for her help throughout the study, and for a cozy blanket, she made for me, which I have been using a lot. Additionally, I would like to thank Michel Duryee, Carlos Hunter, Erin McIntyre and Karen Easterling for all of their help, whenever needed, especially during many of the hectic experimental days. My special thanks go to Karen for being a wonderful friend and helping me personally. I will miss our meetings.

I am thankful to Dr. Sung-Ho Huh for allowing me to use equipment in his lab, and to the staffs of the tissue science facility, flow cytometry facility and animal facility for their service and co-operation. Additionally, I would like to express my sincere thanks to Dr. Rakesh K. Singh, Tuire Cechin, and Dan Teet for their excellent co-ordination of the program and providing suggestions as per need. Specifically, I am thankful to Dr. Singh for his guidance and help with experiments.

I am thankful to all of my friends at UNMC at Omaha who made my stay here enjoyable. Specifically, I am thankful to Dr. Nirakar Rajbhandari for being a wonderful friend and helping me adapt to the new place. Similarly, I would like to express my thanks to my evergreen friends Laxmi, Niroj, and Roshan for unconditionally being part of my happiness/sorrows.

In a personal note, I am thankful to my brothers and sisters for their constant support throughout my life and their solidarity with me in adversities. I am also thankful to all members of my family, including my in-laws, for providing their direct and indirect help to me and for being a wonderful family. Finally, yet importantly, I am thankful to my husband, who came into my life during this journey and brought more happiness to my life. I am thankful to him for understanding me and my dreams, and for supporting me in every possible context.

Saraswoti Khadge

Omaha, Nebraska

September 2018

Dietary Polyunsaturated Fatty Acids Regulate Mammary Tumor Growth and Metastasis by Modulating Tissue Microenvironments

Saraswoti Khadge, Ph.D.

University of Nebraska, 2018

Supervisor: James E. Talmadge, Ph.D. and Geoffrey M. Thiele Ph.D.

Omega (ω)-6 and ω-3 polyunsaturated fatty acids (PUFAs) are essential fatty acids (FAs) and the precursors of pro- and anti-inflammatory mediators respectively. Epidemiological studies have shown a lower incidence of breast cancer (BC) in the countries where long-chain (LC)-ω-3FAs consumption is higher; however, the role of ω-3FAs in BC growth and metastasis is poorly understood. We used isocaloric, isolipidic ω-6 and ω-3 (contains LC-ω-3FAs) diets and a pair-fed model to evaluate the effects of dietary PUFAs in mammary tumor metastasis. Our studies have resulted in several novel observations including that dietary LC-ω-3FAs modulate mammary gland (MG) microenvironments in non-tumor bearing (NTB) mice by lowering MG ductal density, epithelial cell proliferation, adipocyte hypertrophy and adipose tissue inflammation compared to the MGs in the ω-6 group. Similarly, we reported that dietary LC-ω-3FAs modulate the hepatic microenvironment (a common site of metastasis) by lowering hepatic steatosis, hepatocyte apoptosis, extramedullary myelopoiesis and NFκB expression relative to the respective observations in the ω-6 group. Finally, 4T1 mammary tumor studies in mice pre-exposed to these diets showed that, dietary LC-ω-3FAs delays mammary tumor induction and growth, and enhances survival of mice by lowering incidences/frequencies of spontaneous metastases to multiple organs including, lungs, liver, bone, heart, kidneys, ovaries and contralateral

mammary glands compared to the respective analyses in the mice fed a ω-6 diet. In tumor microenvironments of mice fed a ω-3 diet, there were significantly lower numbers of proliferating tumor cells, neo-vascularization and a higher incidence of apoptotic tumor cells. Similarly, there was a significantly lower infiltration of myeloid cells including F-4/80^{+} macrophages and neutrophil elastase positive cell (granulocytes), and a higher infiltration of CD3^{+} T-Cells in tumors from mice fed an ω-3 diet relative to the ω-6 diet-fed group. There was a direct correlation between the neutrophil to T-cell ratio with tumor size and macrophage infiltration with neovascularization. There was also a direct correlation between T-cell infiltration and frequency of apoptotic tumor cells, indicating their roles in tumor growth. IL10 mRNA expression in tumors of mice fed an ω-3 diet was six fold higher, relative to the expression in the tumors from the ω-6 group, indicating a potential role of IL10 in the tumor growth suppression by dietary LC-ω-3FAs. In summary, our studies using isocaloric/isolipidic diets and a pair-fed model showed for the first time that dietary LC-ω-3FAs delay tumor growth and lower metastasis, and enhance survival by modulating the tissue microenvironments including MGs and liver.

TABLE OF CONTENTS

LIST OF FIGURES

LIST OF TABLES

LIST OF ABBREVIATIONS

AA	Arachidonic acid
ALA	α-linolenic acid
CBC	Contralateral breast cancer
CFU-GM	Colony forming unit-granulocyte-macrophage
CLS	Crown like structures
CMG	Contralateral mammary gland
COX	Cyclooxygenase
DGLA	Dihomo-γ-linolenic acid
DHA	Docosahexaenoic acid
EMH	Extramedullary hematopoiesis
EMM	Extramedullary myelopoiesis
EPA	Eicosapentaenoic acid
FA	Fatty acid
G6P	Glucose 6 phosphate
HIF-1	Hypoxia induced factor-1
HO-met	Histologically observed metastases
LA	Linoleic acid

LAU	Lobuloalveolar units
LC	Long-chain
LOX	Lipoxygenase
LTs	Leukotrienes
MCV	Mean corpuscular volume
MD	Mammographic density
MFP	Mammary fat pad
MG	Mammary gland
MUFA	Monounsaturated fatty acid
NAFLD	Non-alcoholic fatty liver disease
NASH	Non-alcoholic steatohepatitis
NLR	Neutrophil to lymphocyte ratio
NTB	Non-tumor bearing
ORO	Oil Red O
PAS	Periodic Acid-Schiff
PAS-Digest	Periodic Acid-Schiff-Diastase
PDs	Protectins
PGs	Prostaglandins

PGE2	Prostaglandin E2
PHR1	Parathyroid hormone receptor 1
PHRP1	Parathyroid hormone related peptide 1
PUFA	Polyunsaturated fatty acid
qRT-PCR	Quantitative real-time polymerase chain reaction
RANK	Receptor activator of nuclear factor-κB
RANKL	Receptor activator of nuclear factor-κB ligand
RBC	Red blood cell
Rvs	Resolvins
SFA	Saturated Fatty Acid
SPF	Specific pathogen free
TAG	Triacetylglycerol
TAM	Tumor associated macrophages
TAN	Tumor associated neutrophils
TB	Tumor bearing
TDLU	Terminal ductal lobular unit
TEB	Terminal end bud
TIL	Tumor infiltrating lymphocyte

TLR	Toll like receptor
TX	Thromboxane
VLDL	Very low density lipoprotein

Chapter 1:
Introduction[1]

1.1. Commentary: Background of the project design

A team of researchers, led by Dr. James E. Talmadge (expertise in cancer biology), Dr. Geoffrey M. Thiele (expertise in immunological disorders and alcoholism-associated pathologies) and Dr. John Graham Sharp (expertise in pathology and stem cell biology), initially conceived of the project and the aims to analyze the effects of alcohol on pathological alterations and mammary carcinoma development. Dr. Thiele's lab has been using Lieber-Decarli liquid diets and the pair-feeding model for alcohol-related studies. Dr. Talmadge's lab has been studying 4T1 mammary tumor for decades. Thus, the initial project was designed to analyze the effects of chronic alcohol consumption on 4T1 tumor cell growth and metastasis. To investigate this, preliminary studies using the Lieber-DeCarli diet with altered alcohol concentrations (5.5% to 16.6%) were administered for 4-8 weeks before an orthotopic inoculation of 50,000 4T1 cells. The results showed a significant increase in tumor growth in mice fed the Lieber-Decarli alcohol diet relative to the Lieber-Decarli control diet but no difference in survival days was observed between the groups. In these experiments, we observed a few 4T1 tumor-bearing (TB) mice from both of the dietary groups had posterior paralysis, which led us to analyze bone morphology and metastasis by micro-CT and histology. As we expected, the mice with posterior paralysis had tumor metastasis in their femurs/tibia. To our surprise, we also observed mild osteopenia in non-tumor bearing (NTB) mice fed the Lieber-Decarli control

[1] A part of this chapter is derived from previously published book chapter: **Saraswoti Khadge**, John Graham Sharp, Timothy R. McGuire, Geoffrey M. Thiele, and James E. Talmadge. "**Lipid Inflammatory Mediators in Cancer Progression and Therapy."** In *Tumor Immune Microenvironment in Cancer Progression and Cancer Therapy*, pp. 145-156. Springer, Cham, 2017.

diet compared to the mice on standard chow diet. Thus, we revisited the diets' composition and their roles in the outcomes we observed.

The Lieber-Decarli control diets contain 35.5% of calories from fat, which is a higher fat level compared to the 16% calories from fat in standard chow diets. Based on this, we first analyzed the effect of fat calories in altering the histopathology and immunological markers in spleen, liver and bone marrow (BM) from NTB mice fed isocaloric diets containing moderate fat (35.5%) versus low fat (12.5%) calories. However, there were no significant differences in immunological phenotypes in liver, spleen and BM between the various dietary groups. We did observe was hepatic macro-steatosis, and micro-steatosis in moderate-fat versus low-fat pair-fed mice. Surprisingly, the fat droplets in hepatocytes of low-fat diet-fed mice were more extensive than the droplets observed in the livers from chow fed mice, which has higher calories from fat compared to the low-fat diet. These results suggested a unique role of dietary fat composition in hepatic pathology and metabolism. Thus, our results from these preliminary experiments suggested that the observations in the original alcohol studies were confounded by many factors; including, alcohol, calories from fat, and the composition of the fats. Clarification of relevant factors was necessary to evaluate the effects of a single component without overlapping effects from others. We noted that the Lieber-Decarli control diet incorporates insignificant levels of long chain (LC) omega-3 (ω-3) polyunsaturated fatty acids (PUFAs), but contained significant amounts of safflower oil, which is rich in omega-6 (ω-6) PUFA and olive oil (mono unsaturated fatty acid; MUFA). Thus, the present study has the aim of analyzing the effects of these PUFAs on the tissue microenvironments, which might play a role in regulating in mammary tumor pathogenesis.

Therefore, the role of PUFAs, in regulating tissue microenvironments and tumor progression, was the major aim of these studies. The first research section of the thesis

is oriented toward the analysis of mammary gland macro and microenvironments by dietary PUFA (Chapter 3). Since the liver is a frequent site of breast cancer metastasis; although less frequent in mice, we also analyzed alterations in the hepatic microenvironment by PUFA diets. In the second research section, we investigated PUFA modulation of hepatic tissue in NTB mice (Chapter 4). After analyzing the changes in tissue microenvironments by diets in NTB mice, we evaluated the effects of chronic exposure to PUFA diets in mammary tumor progression and metastasis to multiple organs (Chapter 5).

The introduction in this thesis is presented in the order the studies are discussed in the subsequent sections. The introduction starts with breast cancer epidemiology and the potential effects of diets; followed by a general background of PUFA, metabolism, and their role in inflammation. I then discuss mammary gland biology, the hepatic microenvironment and PUFA regulation of the metabolism and pathobiology of these organs. Finally, the pathogenesis of breast BC and the role of microenvironments and chronic inflammation in BC progression are discussed.

1.2. BC epidemiology

BBC is the most common cancer in women, regardless of race or ethnicity, and is the second most common cause of death from cancer in American women [1]. According to statistics from the National Cancer Institute, there were an estimated 3,418,124 women living with female breast cancer in the United States in 2015. About 266,120 women are expected to be diagnosed with invasive BC and 40,920 women are expected to die from BC in 2018 in the United States [2] The global pattern of BC incidence reflects the availability of BC screening as well as BC risk factors in the population. The highest BC

incidence rates are in most of Western countries including North America, Australia/New Zealand, and Europe, while the lowest rates are in Africa and Asia (Fig. 1 and Fig. 2) [3]. Besides the major risk factors relating to age, hormonal exposure, genetics and obesity [4], there are modifiable lifestyle factors such as alcohol, smoking, sedentary life, obesity and dietary factors that have been associated with an increased BC risk. The epidemiological studies investigating possible effects of dietary behavior on BC incidence are confounded by the close relationship among, dietary composition, caloric consumption and body weight, making it difficult to define the effects of one variable, independent of the others [5]. However, epidemiological and animal-based studies have shown a direct association between BC and total fat intake [6, 7], high saturated fat intake [8, 9] and a higher intake of omega (ω)-6 polyunsaturated fatty acid (PUFA), relative to the dietary level of ω-3 PUFA [10-13]. In contrast, the consumption of marine-derived long-chain (LC)-ω-3FAs have been associated with a lower risk of BC [14-17]. Despite extensive evidence of an association of dietary PUFA composition with neoplasia, the regulatory mechanisms driving such effects are little understood.

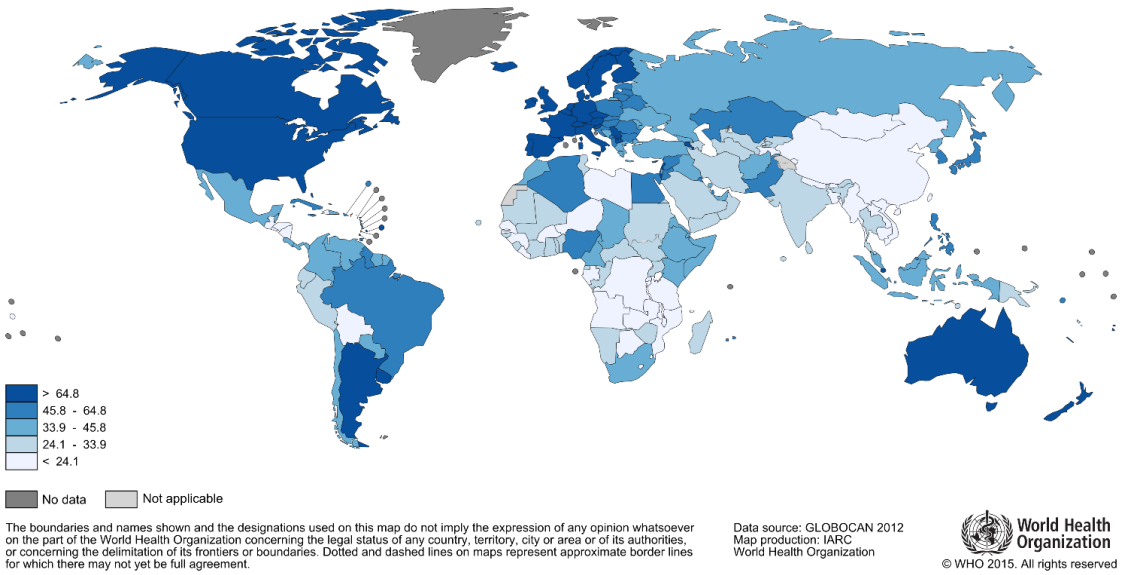

Figure 1. World BC map showing differences in incidence between countries.

The data are presented as cases per 100,000 population. Color code: the darker the color the greater the incidence [3].

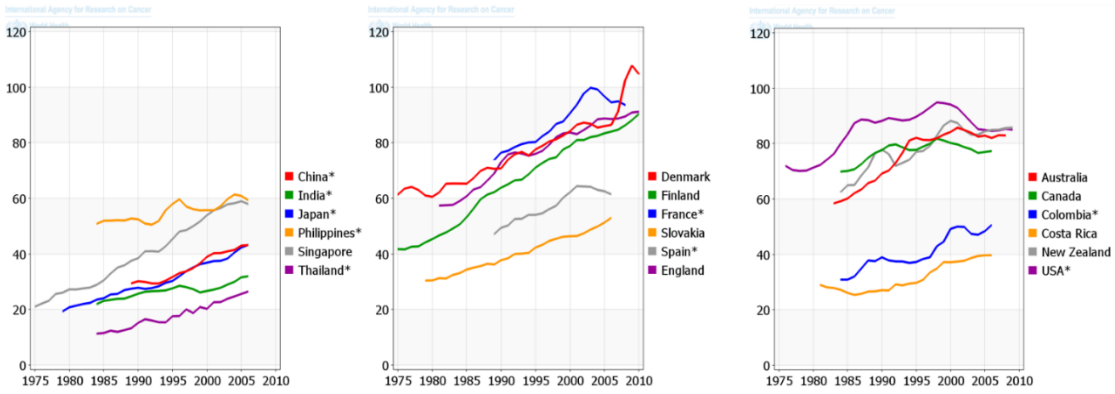

Figure 2. Breast cancer incidence between the years 1975 to 2010.

(A) Asian countries (B) and (C) many Western countries [3].

1.3. PUFAs

PUFAs are a class of lipids having two or more double bonds in their carbon chain. Among the PUFAs, ω-3 and ω-6 PUFAs are essential FAs important for human health. The name ω-3 and ω-6 are given based on the location of the last double bond relative to the terminal methyl end of the molecule (Fig. 3) [18]. The biological reactivity of fatty acids is defined by the length of the carbon chain and by both the number and position of any double bonds present. Thus, differences in the position of the last double bond between ω-3 and ω-6 PUFAs result in various biological functions. Linoleic acid (LA) (C18:2; ω-6) and α-linolenic acid (ALA) (C18:3; ω-3) are the simplest members of the ω-6 and ω-3 PUFA families, respectively, and are precursors to the long-chain (LC) series of the respective series of PUFA families. Saturated FAs (SFAs) and most monounsaturated FAs (MUFAs) can be synthesized in mammalian tissue from non-fat precursors such as glucose and amino acids. However, mammals cannot convert oleic acid (MUFA, 18:1; n-9) to LA and LA to ALA due to lack of 12-desaturase and 15-desaturase respectively [19], which are enzymes found only in plants and lower animals like *C. elegans*. Thus, LA and ALA are termed essential FAs as the human body must obtain these FAs from external sources [20]. LA is plentiful in nature and found in the seeds of most plants, except for coconut, cocoa, and palm. On the other hand, ALA is found in the chloroplasts of green leafy vegetables, and in flax, rape, chia and perilla seeds, and in walnuts [20, 21]. In the human body, most of the biological functions of PUFAs are mediated by the LC series of ω-6 and ω-3 FAs. Arachidonic acid (AA) is a LC-ω-6FA and is obtained efficiently from eggs, poultry and red meat, while LC-ω-3FAs such as eicosapentanoic acid (EPA) and docosahexaenoic acid (DHA) are obtained from cold water fish such as salmon [22]. Besides external sources, LC-ω-6FAs and LC-ω-3FAs can be derived from LA and ALA respectively in the human body by competitively using the same series of enzymes:

desaturases and elongases (Fig. 4). In general, these enzymes have greater affinity for ALA than LA, but due to increased availability of LA in diets and intake of at least 10 times more LA than ALA, more AA is formed than EPA and DHA [22-24]. As noted above, LA cannot be converted to ALA in mammals due to lack of converting enzyme ω-3 desaturase [25]. Further, studies using increased dietary ALA have shown the conversion of LA to LC-ω-3FAs, specifically to DHA, is generally poor in humans [26, 27]. Thus, the consumption levels of ω-6 and/or ω-3 FAs directly affect their bioavailability and their respective downstream biological functions. Therefore, dietary consumption of LC-ω-3FAs (EPA and DHA) might be more effective than ALA for ω-3FAs-related functions.

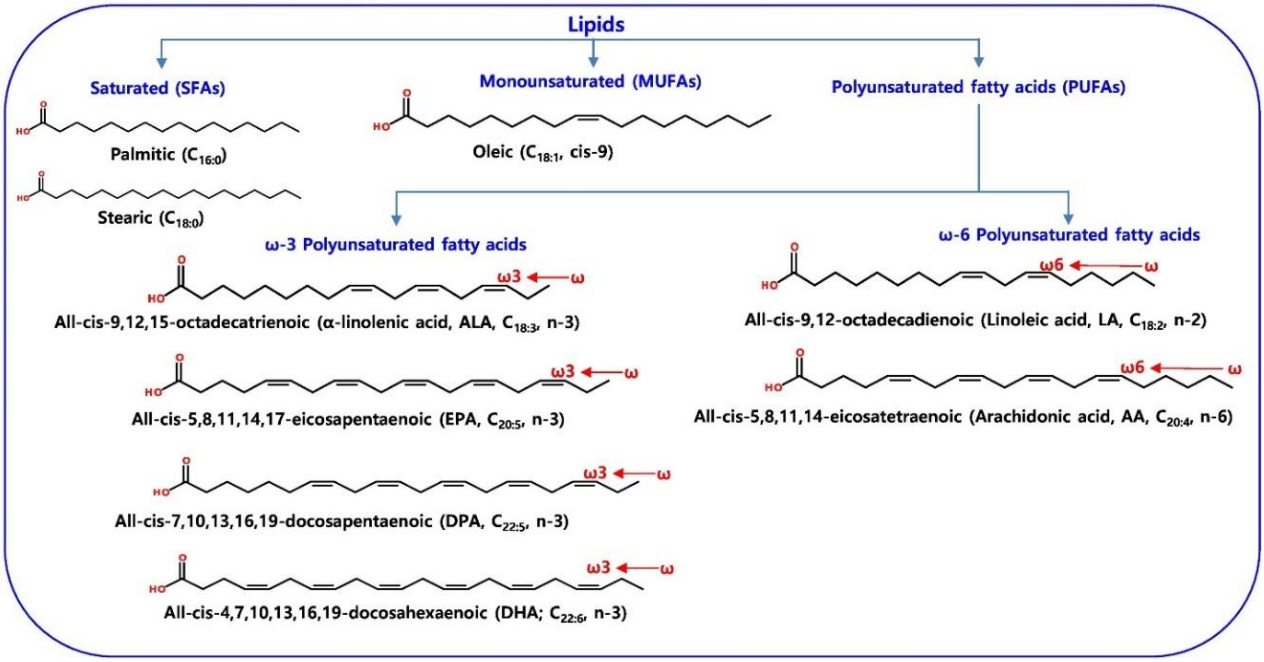

Figure 3. Molecular structure of different classes of fatty acids.

Red arrows indicating position of the first double bond in ω-3 and ω-6 PUFA. Figure source [28]

1.4. PUFAs metabolism

PUFA uptake to cells is a facilitated membrane translocation process that involves FA translocases (i.e., CD36), FA transport proteins and membrane-bound FA binding proteins [29-32]. The transported PUFAs are converted to FA acyl-CoA thioesters prior to entering one of three major metabolic pathways. The first pathway is a beta-oxidization pathway to generate energy (ATPs). The second pathway is one in which FA acyl-CoA thioesters of PUFAs are metabolized for the synthesis of neutral lipids (triglycerides, cholesterol, esters) or polar lipids such as phospholipids and sphingolipids. The third pathway occurs if PUFAs are consumed in the form of LA or ALA, where they may undergo a series of desaturation and elongation reactions and form LC-PUFAs such as AA, EPA and DHA respectively [33-35]. LA and ALA are not efficiently synthesized nor incorporated into phospholipid membranes. However, LC-ω-6FA (AA) and LCω-3FAs (EPA and DHA) can be efficiently incorporated into phospholipid membranes [24, 36]. The incorporation of LC-PUFAs affects the biological functions and/or signaling of immune cells in a variety of ways, including the fluidity of cell membranes, alterations of lipid raft composition, acting as ligands for G-receptors, or by being substrates for cyclooxygenase (COX) and lipoxygenase (LOX) enzymes for the production of bioactive lipid mediators or eicosanoids [19, 35, 37].

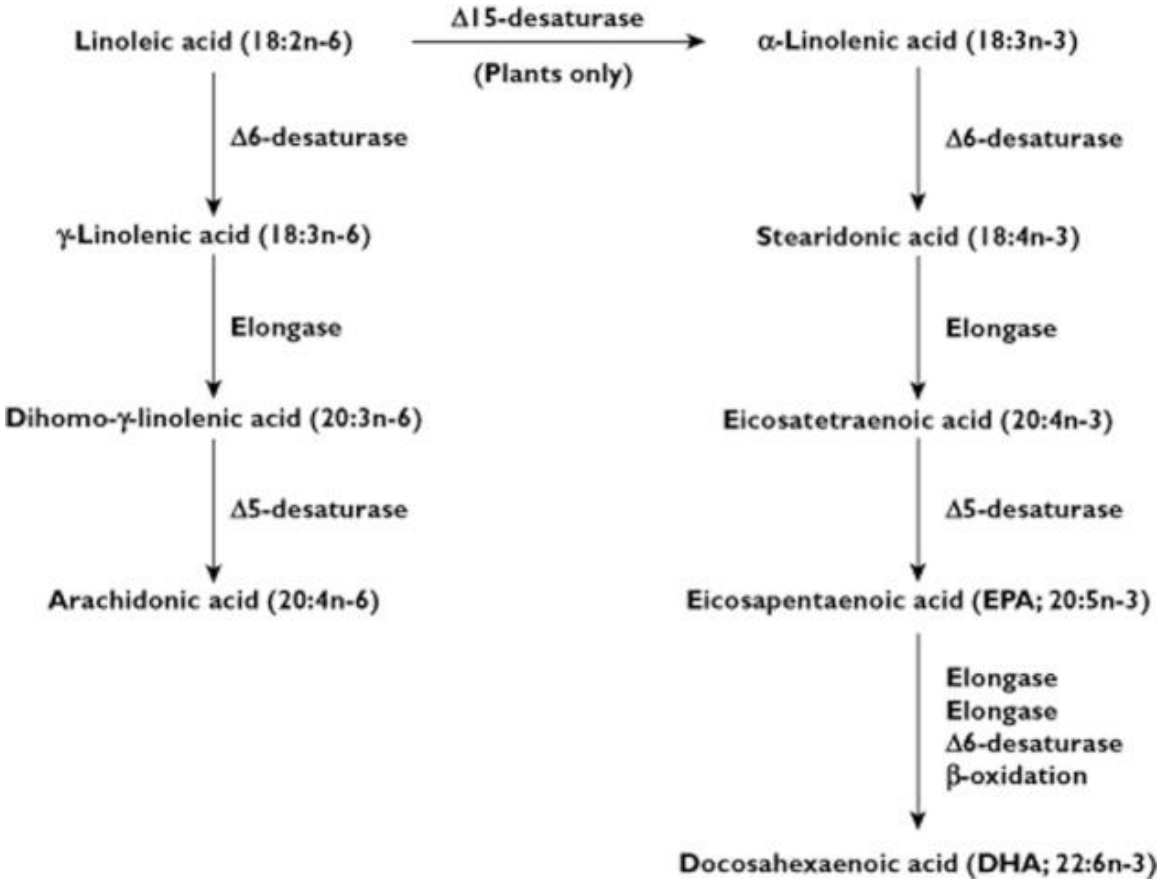

Figure 4. The metabolism of plant-derived essential ω-3 and ω-6 PUFAs.

Both ω-3 (n-3 in Fig) and ω-6 (n-6 in Fig) PUFA precursors competitively use the same set of enzymes to prepare derivatives. DHA, docosahexaenoic acid; EPA, eicosapentaenoic acid. Figure source [36]

1.5. PUFA and inflammation

Eicosanoids are a group of key, biologically active mediators that regulate inflammation signaling [38, 39]. They are typically synthesized from 20-carbon PUFAs, such as AA, dihomo-γ-linolenic acid (20:3; n=6) (DGLA) and EPA that are released from membranes by the action of phospholipase A2, after activation of the membrane receptors by growth factors or hormones [19]. These free AA, DGLA and EPA are metabolized to eicosanoids such as prostaglandins (PGs), leukotrienes (LTs) and thromboxanes (TXs) depending on the action of COX (COX-1, a constitutive enzyme, or COX-2, an inducible enzyme) and LOX (5-, 12-, or 15-LOX) enzymes. The activity of COX on AA leads to the formation of 2-series prostanoids such as PGE2 and TXA2; whereas the activity of LOX on AA generates 4-series LTs. Similarly, the activity of COX and LOX on EPA produces 3-series prostanoids (PGE3 and TXA3), and 5-series LTs and resolvins respectively. On the other hand, DGLA is metabolized by COX resulting in 1-series PGs. Since AA is the most abundant PUFA in most cells [18], relative to EPA and DGLA, eicosanoids that are synthesized are mostly derived from AA. However, the concentrations of EPA and DGLA modulate synthesis of AA derived eicosanoids as they are competitively used by the same enzyme system to generate eicosanoids [19, 22, 24]. Further, eicosanoids derived from EPA are less potent in inflammatory signaling. Thus, the competitive presence of EPA as a substrate for COX and LOX enzymes reduces inflammation by either inhibiting the production of inflammatory eicosanoids from AA or by producing fewer inflammatory eicosanoids or anti-inflammatory resolvins [40].

1.6. ω-6 PUFA- and PGE2-mediated inflammation

Among eicosanoids, PGE2 is the most abundant AA (ω-6) metabolite and has a crucial role in inflammation. Depending on the duration and extent of PGE2 production, it has pro-inflammatory functions such as induction of fever and pain [41-43], vasodilation [42], and local attraction and activation of neutrophils, macrophages, and mast cells at early stages of inflammation [44-46]. Thus, the inhibition of PGE2 synthesis is an important anti-inflammatory strategy that has been used for more than 100 years [47]. PGE2 can be produced by any cell in the body, but the major source is immune cells. Although PGE2 is unambiguously an inflammatory mediator, the finding of its role in the induction of suppressive IL10, and suppression of lymphocyte proliferation, natural killer cells activity, limitation of phagocytosis by alveolar macrophages and TNFα and IFNγ secretion, emphasizes the importance of PGE2's role as a mediator of immune suppression associated with chronic inflammatory conditions including cancer [48-53]. Further, PGE2 can enhance Th2 responses, promote Th17 differentiation, and facilitate the development of immunosuppressive macrophages and myeloid-derived suppressive cells (MDSC), all of which emphasize the critical role of PGE2 signaling in tumor progression [54-57].

1.7. Regulation of inflammation by ω-3FAs

Clinical and experimental studies have shown beneficial effects of ω-3FAs in controlling chronic inflammatory diseases. Thus, increased consumption of ω-3FA-enriched diets or endogenous synthesis of ω-3FAs are directly associated with increased incorporation of EPA and DHA in cell membranes [58-60]. The presence of higher levels of EPA in membranes competitively inhibits production of PGE2 and LTA4 from AA and elevates the production of the non-inflammatory eicosanoids PGE3 and LTB5 (Fig. 5) [61]. These effects have been shown in macrophages from fish oil-fed mice [62] and neutrophils from humans consuming fish oil supplements [63]. Further, fish oil consumption is able to decrease LTB4-mediated chemotaxis of neutrophils and monocytes [63, 64], reduce expression of adhesion molecules in endothelial and immune cells [65-67], and decrease production of inflammatory cytokines such as IL6, TNFα, MCP1, IL1B and the inflammation pathway-associated gene NFkB [68-71].

Besides modulation of classical inflammatory pathways, EPA and DHA anti-inflammatory activities can be developed by further metabolizing them to the pro-resolving/anti-inflammatory lipid mediators, including resolvins (Rvs), protectins (PDs) and maresins [72-77]. These novel, pro-resolution lipid mediators provide insight into the mechanisms of actions by ω-3FAs and their beneficial actions in the moderation of the unresolved inflammation, associated with chronic disorders. Resolvins (Rvs) are synthesized from EPA (E-series) and DHA (D-series) via differential COX-2 pathways, in the presence or absence of aspirin, while protectin D1 (PD1) is synthesized by the 15-LOX pathway using DHA as a substrate [72, 78]. Rvs are found to inhibit TNFα-induced NFkB activation, decrease polymorphonuclear leukocyte (PMN) activation by antagonistic effects of LTB4 mediated chemotaxis, and to decrease dendritic cell (DC) migration and cytokine

production [79, 80]. Similarly, PDs have tissue specific bioactivities in the resolution of inflammation. Pre-administration of PD1 dampens allergic airway inflammation and acute kidney injury-associated inflammation [81, 82]. Both Rvs and PDs protect mice from colitis [83], and improve insulin sensitivity by reducing the chronic inflammation associated with obesity [84]. Further, a recent study demonstrated that Rvs inhibit cancer progression by enhancing clearance of tumor cell debris by macrophage phagocytosis, [85] which emphasizes ω-3FA associated lipid mediators as novel therapeutic targets, that may complement cytotoxic cancer therapies. Maresins are primarily produced by macrophages, shift macrophage phenotypes by inhibiting pro-inflammatory mediators [86, 87], and have been found to suppress breast tumor growth by stimulating phagocytosis of apoptotic tumor cells and enhancing anti-inflammatory cytokines [88]. Despite recent advances in identifying the role(s) of these novel ω-3FA-derived lipid mediators in multiple inflammatory disorders and understanding their mechanisms of actions, their role(s) in the modulation of tumorigenesis and associated mechanisms of action is not fully defined.

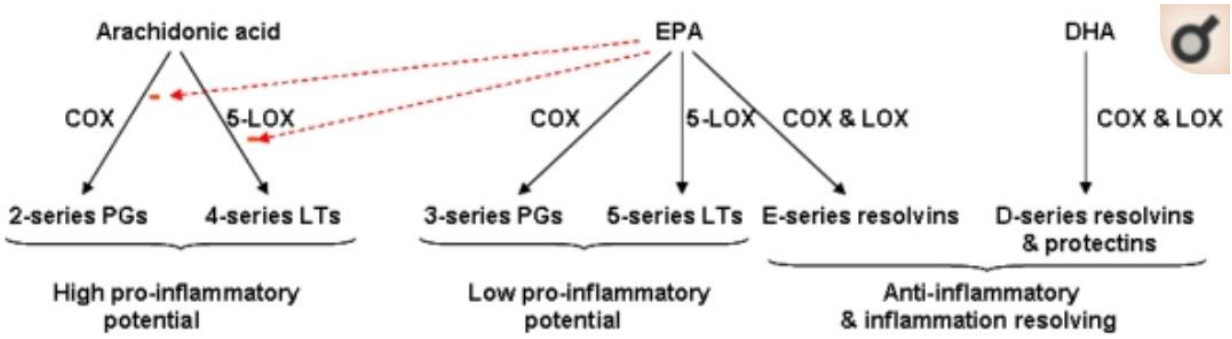

Figure 5. PUFA and inflammation.

Arachidonic acid (active metabolite of ω-6FA) metabolizes into prostaglandins (PGs) leukotrienes (LTs) with high pro-inflammatory potential. In contrast, LC-ω-3FAs such as eicosapentanoic acid (EPA) and docosahexaenoic acid (DHA) metabolize into low- pro-inflammatory PGs and LTs and anti-inflammatory resolvins and protectins respectively.

Figure source: [89]

1.8. MG: Primary site of tumorigenesis

To understand the role of macro and microenvironment in mammary tumorigenesis, the understanding of MG development and morphology is crucial. In the following section, the normal development of MG and the various factors, including PUFA-modulated alteration in morphology, that may impact mammary tumorigenesis will be discussed.

1.8.1. Breast/MG development and morphology

MG morphogenesis is similar between women (breasts) and rodents (multiple MGs). The structural and functional parts of MG develop after birth and morphogenesis occurs in different stages of life. During fetal development, MGs develop from ectodermal thickening called the milk line, that extends on each side of the body from the neck to the inguinal region [90]. One MG on each side of the milk line develops into a breast in humans while mice have 5 pairs of MGs. MG epithelium originates from the milk bud (which later develops into a nipple) and extends into the mammary fat pad as a series of branching ducts. In humans, the nipple contains outlets for 5-10 lactiferous ducts, which extend and branch out in a radial pattern to form a triangular structural lobe supported by collagenous stromal tissues [90]. In contrast, MGs in rodents contain a single lactiferous duct arising from each nipple but the duct subsequently divides into 5-10 secondary ducts. In both humans and mice, the end structures at the tip of the terminal ducts/ductules resembles bud-like structures during early puberty and are called terminal end buds (TEBs) that in humans are also known as lobular buds. These TEBs contain progenitor cells, which are highly proliferative during puberty, in the process of ductal branching and formation of MG functional units known as terminal duct lobular units (TDLU) in humans. In rodents, these units are known as lobuloalveolar units (LAU) (also called as terminal buds, side buds, alveolar buds or terminal ducts) [90, 91]. Besides cell proliferation, active cell death occurs

in TEBs during puberty, which leads to lumen formation. Both TDLU and LAU contain hormone-responsive cells and undergo continuous morphogenesis both per hormonal cycle or based on functional needs. Since these units contain proliferative cells, there is a higher chance of mutagenesis in the cells of these units and thus, they are tumor initiation sites for most mammary carcinomas [90-92]. As shown in Fig. 6, TDLU (LOB in the figure) of an adult nulliparous woman contains multiple alveolar buds of different sizes that can exist in various stages of differentiation depending on the menstrual cycle. In contrast, the LAU of an adult mouse resembles a single bud or blunt terminal duct without any subunits. During pregnancy and in a lactating woman, both the number of TDLU and the number and size of alveolar buds per TDLU will increase, forming a morphological unit (lobule or LOB 3 in Fig. 6), which resembles a cluster of grapes. In pregnant and lactating mice, LAUs undergo extensive morphogenesis, forming a lobule-like structure, but at the completion of involution, murine mammary ducts and lobule-like structures return to morphology similar to that of nulliparous mice, which contains only ductal ends but not lobules [92, 93].

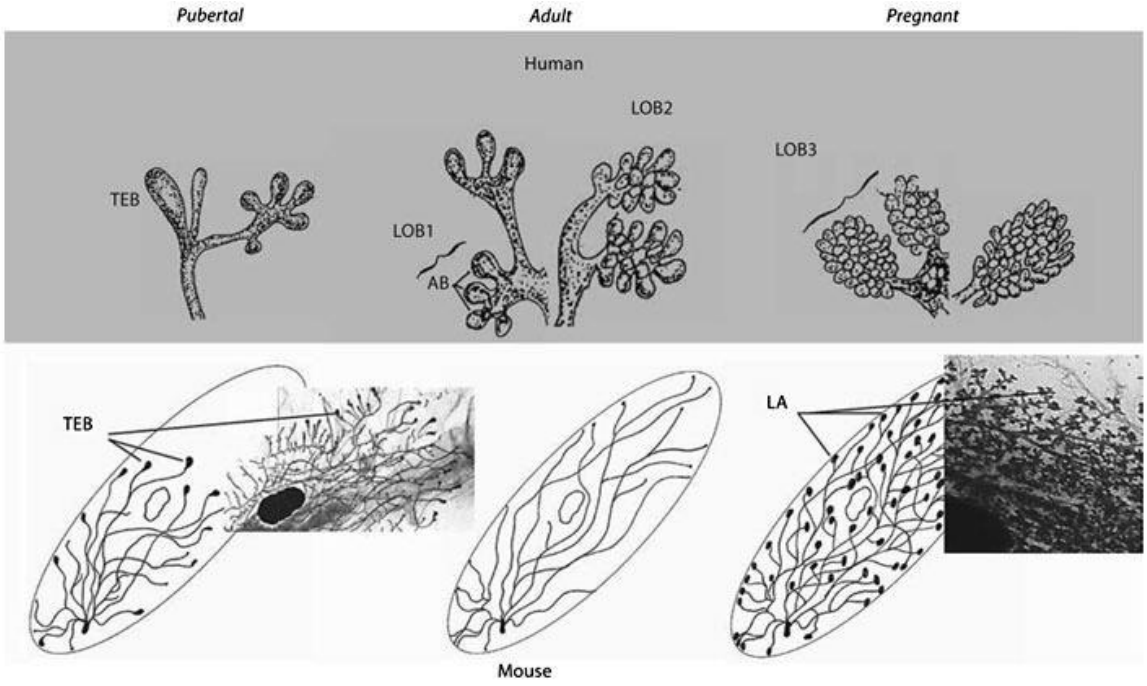

Figure 6. Different developmental phases of the mammary gland.

Human (upper part) and mouse (lower part) mammary gland. LOB = Terminal ductal lobular unit; LA = lobuloalveolar unit; TEB = terminal end bud; AB = alveolar bud [92]

1.8.2. MG morphology and BC risk

Besides the morphogenesis of MGs in response to hormonal effects in different stages of life, other external factors, including nutrition, can influence the morphology of MGs. The glandular mass of a breast/MG is represented by the total number and size of lobules and ducts in a MG of an adult nulliparous human, and total number and or size of terminal ducts and buds in a nulliparous mouse. Breast density is a measure of glandular mass, along with associated stromal tissues relative to adipose mass in the breast, and can be measured by mammographic analysis [94]. Epidemiological studies show that increased mammographic density (MD) is directly associated with the risk of BC and appears to be a major risk factor for interval BC (BC diagnosed within a year from the negative mammographic result) [95, 96]. The risk of BC development was found to be 4-6 fold higher in women with breasts that have 75% greater MD compared to the women with breasts that have 10% or lower MD [97, 98]. In murine models, MG density can be measured by the evaluation of total glandular area, ductal length, thickness and branching complexity and total number of TEB (younger mouse) and/or terminal and side ducts (older mouse) [99, 100]. Consistent with human epidemiological studies, murine studies have shown that mice with more TEBs, epithelial proliferation, and MG density develop spontaneous and carcinogen-induced mammary tumors more frequently [101-104]. Molecular mechanisms supporting an association of BC risk with dense breasts remain to be defined. However, possibilities include an increased number of epithelial cells [105] that may provide a greater chance for somatic mutations, increased epithelial cell proliferation [106, 107], alteration in stromal tissues [98, 108] and increased local inflammation in breast tissues [98, 109] of women having dense breasts. In experimental studies, higher MG density in mice was associated with a thicker ductal stroma, a higher number of proliferating ductal epithelial cells and increased infiltration of inflammatory cells

[110], and the interaction of stroma epithelium and inflammatory microenvironments [111, 112]. Further mechanistic studies are needed to evaluate the role of the microenvironment in the development of BC. The difference in MD has been found to be influenced by multiple factors, including genetic components, race, parity status, hormonal therapy and dietary factors [113].

1.8.3. Dietary PUFA composition and MG tumorigenesis

Experimental studies have shown that exposure to different levels and compositions of dietary PUFAs modulate mammary tumor carcinogenesis. Since MG morphogenesis is extensive before and during puberty, most murine studies are conducted at an early stage of life. Pregnant mice fed diets high in ω-6 have high levels of serum estrogen, which is associated with an increased incidence of mammary tumors in female offspring [114-116]. In contrast, the risk of mammary tumor development is reduced when fish oil is included in a maternal ω-6-containing diet [117]. Similarly, a delayed appearance of tumors and slower tumor growth is observed in offspring of mice fed a diet high in canola oil (ω-3FA) compared to the mice fed a corn oil diet (ω-6FA) [116]. In murine experiments using pre-pubertal mice, the results are similar, with ω-3 diet-fed mice having a lower incidence of carcinogen induced or transgenic mammary tumors [118-120] and delayed growth of transplanted xenograft tumors [121] compared to mice fed diets high in ω-6FA. However, when the results from mice fed a high-fat ω-3 diet were compared with mice fed a low fat ω-6 diet, the mice fed the high-fat ω-3 diet had a greater incidence of mammary tumors [118]. These results emphasize the importance of both dietary ω-6 and ω-3, as well as, the total dietary lipid calories in the diet with respect to mammary tumorigenesis. Further, these observations document the importance of using isocaloric diets for the analysis of FA composition on tumorigenesis.

The mechanism of action by ω-3FA in mammary tumorigenesis might be influenced by the stage of MG development and morphogenesis during LC-ω3FA exposure. Exposure to LC-ω-3FA, in-utero or early in life, modulates metabolic programming of PUFA pathways in the offspring [122, 123]. Similarly, ω-3FA exposure early in life suppresses tumorigenesis by regulating MG development as ω-3FAs enhance the differentiation of TEBs, reducing the possibility of mutations in highly proliferative TEBs [124-126]. Besides these age-dependent effects, other potential mechanisms for ω-3FA-mediated regulation of tumorigenesis may be due to the modulation of the stromal and inflammatory microenvironments. Dietary incorporation or endogenously metabolized ω-3FA, in rodents, significantly increases EPA and DHA levels, as well as decreases AA levels, and mRNA expression of fatty acid synthase, COX-2, and 5-LOX in mammary tumor tissues [125, 127]. Further, the incorporation of ω-3FA results in inhibition of NFkB activation, decreased expression of anti-apoptotic proteins Bcl-2 and Bcl-XL, increased caspase 3 activity, and reduced activation of EGFR in mammary tumor cells [128, 129].

Metabolites of ω-6 and ω-3FAs are pro- and anti-inflammatory respectively, and differential PUFA composition regulates the activity of inflammatory cells. Therefore, the regulation of the numbers and functions of inflammatory cells and their signaling pathways might be one of the mechanisms by which ω-3FAs suppresses tumor growth and metastasis as discussed in Section 1.4. Prior studies have shown that feeding LC-ω-3FA can increase natural killer cell cytotoxicity, decrease expression of related transcripts to macrophage proteins, inflammatory cytokines TNFα, IL6, CCL2, IL10, and NFkB pathway-related targets [130, 131]. However, few mechanistic studies have analyzed ω-3FA regulation of inflammatory cells in the tumor microenvironment and no published reports, to our knowledge, have used the essential controls of isocaloric, isolipidic diets in a pair-feeding model to evaluate these effects.

1.9. Liver: One site of breast/mammary tumor metastasis

Since the aim of the study is to analyze the role of diet-modulated tissue microenvironment in the regulation of metastasis to an organ, we analyzed PUFA-mediated modulation of hepatic macro and microenvironments, which may regulate hepatic metastasis. In this section, we will discuss normal histology and the metabolism by the hepatic tissue microenvironments, in response to dietary PUFA regulation. We posit that the modulated/altered microenvironments may have an impact on the arrest and survival of metastatic tumor cells in the liver.

1.9.1. Overview of anatomy and histology of liver

The liver is the largest visceral organ in the body. It is structurally and functionally heterogeneous and has been considered second only to the brain in complexity [132]. The liver has a crucial role in the efficient uptake of amino acids, carbohydrates, bile acids, cholesterol, proteins, vitamins and lipids for storage and metabolism, subsequently to release into the bile and/or blood [132, 133]. The fundamental structure of livers from humans and rodents are similar. A liver in a human has 4 lobes(right, left, quadrate and caudate) [134]. Livers of rodents (mice and rats) also have 4 major lobes named as right, left, median and caudate. The median and caudate lobes are further subdivided into 2 or more parts. Mice and humans have a gallbladder, but not the rat [134-136]. The functional unit of liver, i.e. a lobule, has the same histologic appearance, regardless of the angle a liver is sectioned [137]. Histologically, a hepatic lobule is a hexagonal region of the liver parenchyma (hepatocytes) around the central vein. At the vertices of the lobule, portal triads can be observed, which include a bile duct and branches of the hepatic artery and hepatic portal vein [138] (Fig. 7). Hepatocytes are arranged radially around the central vein, and blood sinusoids form between them. The hepatic parenchyma is divided into three zones. The hepatic parenchymal area near the portal triads is termed the peri-portal

(or zone 1), the area near the central vein is centrilobular (or zone 3) and the area in between the zone 1 and zone 3 is midzonal (or zone 2) [132, 138]. Hepatocytes (liver parenchymal cells) are the most numerous cells in the liver and comprise 60% of total cells. They perform the major functions of the liver and their cytoplasm contains varying levels of glycogen and lipids, depending on the metabolic stage. Among the non-parenchymal cells in liver, sinusoidal epithelial cells (SECs) are the primary barrier between the blood and hepatocytes and act to filter fluids and particles that are exchanged between the sinusoidal lumen and the space of the Disse [139]. Kupffer cells are resident hepatic macrophages and are derived from circulating monocytes. They represent 15% of the liver cells (30% of sinusoidal cells) and are the major producers of cytokines providing cross-talk with other cells [140]. Other resident cells in the liver include hepatic stellate cells (HSCs), which comprise 5% of the liver cells and have a major role in the regeneration and fibrogenesis of hepatic tissue [141, 142].

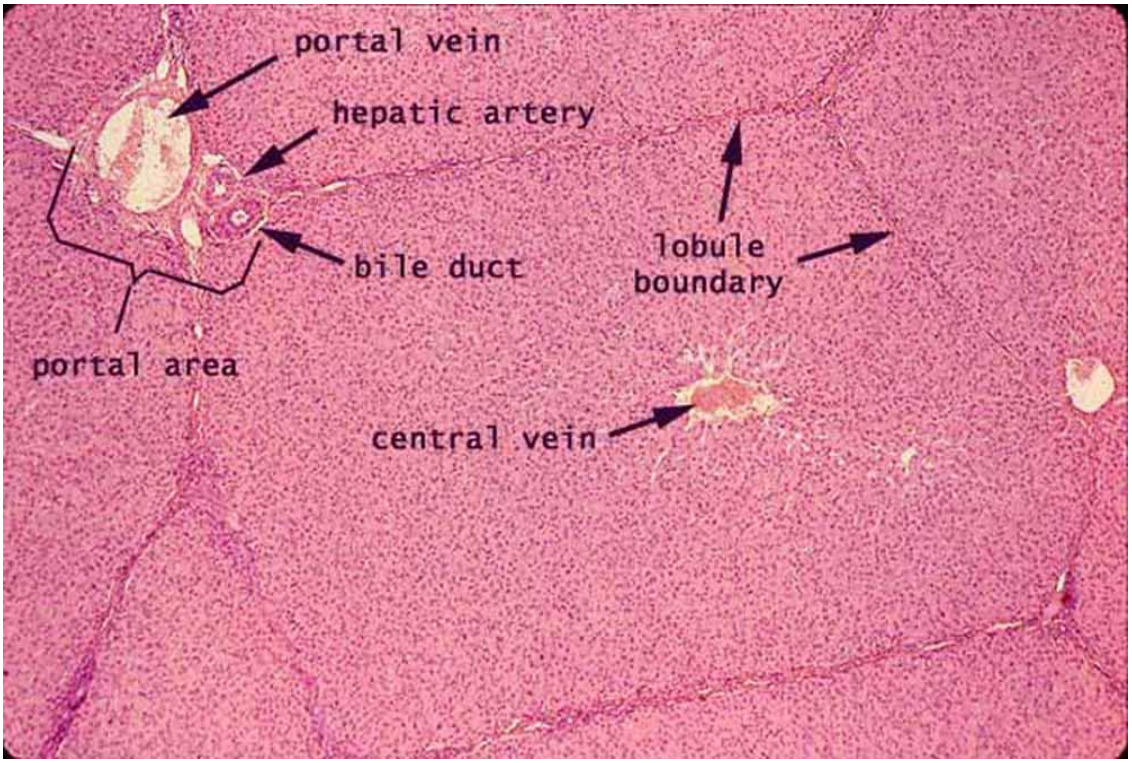

Figure 7. Hepatic lobule from a section of pig liver

Hematoxylin and eosin-stained section of a liver from pig showing hepatic lobule distinctly lined by sinusoids [143]

1.9.2. Hepatic extra-medullary hematopoiesis

Beside, the resident cells of the liver, foci of immature-inflammatory cells or hematopoietic progenitor cells are frequently observed in human fetal liver. The process of proliferation by hematopoietic progenitor cells (erythroid and myeloid progenitors), outside of the medullary space is called extra medullary hematopoiesis (EMH) [144]. Under normal circumstances, after birth, there is little proliferation of hematopoietic elements outside of the medullary space except in pathological conditions [144, 145]. In fetal life, the liver provides a niche for colonization, proliferation and differentiation of circulating hematopoietic progenitor cells, making the liver the primary site of EMH, which generally ceases after birth when the bone marrow develops. However, EMH is observed normally in neonatal life, especially following a premature birth or in pediatric patients with hepatic disorders such as hepatitis [133, 145, 146]. In contrast, hepatic EMH in adult life is associated with pathological conditions, including sepsis, solid organ and stem cell transplantation and malignancy [147-149]. While myeloid precursors are the predominant proliferating cells in EMH, the process is called extra medullary myelopoiesis (EMM) [150]. The occurrence of EMH or EMM in an adult might be the result of the arrest of immature cells that become trapped in extra-medullary tissues. Such an increase in the number of circulating hematopoietic stem cells might also be due to inadequate or inhospitable marrow space for EMH or over production of marrow elements, as a consequence of pathological conditions. Modulation of local tissue microenvironment, including an increase in hypoxia and/or inflammatory cytokines and growth factors, stimulates the proliferation of immature hematopoietic cells in extra-medullary tissue [144, 150, 151]. Hepatic EMH/EMM is mostly found in the vicinity of sinusoidal areas, which might be due to the supporting role of sinusoidal endothelial cells in the proliferation of progenitor cells [152]. Besides pathological conditions, changes of the hepatic micro-environment or

inflammatory signaling, due to life style factors such as chronic inflammation or due to alcohol consumption or diets, may influence hepatic EMH/EMM [153-155]. However, further studies are needed to examine this since the role, or effects and consequences of EMH or EMM foci and their signaling in hepatic microenvironments, is still not understood.

1.9.3. Lipid versus glycogen metabolism in liver

The liver is the primary metabolic organ for the storage or metabolism of both glucose and lipids, depending on the host energy requirement. The liver synthesizes glycogen and triglycerides as two major forms of energy storage, and metabolizes them to provide energy during different phases of food deprivation. However, how the dietary composition affects the liver's metabolic preferences, for synthesis of glycogen versus triglycerides, is not clearly understood.

1.9.3.1. Glycogen metabolism in liver

Glycogen is synthesized in the liver after consumption of food (energy sufficient or fed-state). Glucose enters hepatocytes via GLUT2 transporters and is phosphorylated by glucokinase to synthesize glucose 6-phosphate (G6P) and glycogen synthase, which uses G6P as a precursor to synthesize glycogen [156, 157]. In the fasted or energy deprivation state, due to exercise, glycogen is hydrolyzed to generate glucose by glycogen phosphorylase in the process called glycogenolysis [158]. The mechanism of glycogen synthesis versus glycogenolysis is regulated directly by the availability of glucose in the circulation and indirectly by insulin. In the fed-state, when the glucose levels are increased in the circulation, more glucose is converted to G6P, which is an allosteric activator of

glycogen synthase, whereas an inhibitor of glycogen phosphorylase thus increases G6P and enhances glycogen synthesis. Similarly, insulin is secreted by pancreatic β cells in response to an increase in blood glucose, amino acids, and fatty acids. Insulin stimulates glycogen synthase by inactivating inhibitors of glycogen synthase (glycogen synthase kinase 3) via activation of Akt (protein kinase B) [157, 158]. Insulin also stimulates acetylation of glycogen phosphorylase, which promotes dephosphorylation and inhibition of glycogen phosphorylase by protein phosphatase 1; thus, suppressing glycogenolysis [159]. Under fasting conditions, insulin secretion is downregulated, which leads to inhibition of glycogen synthase and activation of glycogen phosphorylase. Further, counter-regulatory hormones (epinephrine and norepinephrine) secreted by pancreatic α cells activate protein kinase A, which directly or indirectly activates glycogen phosphorylase, resulting in increased glycogenolysis [157-159].

1.9.3.2. Fatty acid metabolism in the liver

Hepatocytes obtain FAs from the plasma or by de novo synthesis. After a meal, dietary fat is digested, mainly in the small intestine and absorbed into enterocytes, where FAs are esterified with glycerol 3-phosphate into triacetylglycerol (TAG) and incorporated into chylomicrons before they are secreted into the gut lymphatic system [157, 160]. Those triglyceride-rich chylomicrons enter into plasma, from which 70% of FAs are delivered into adipose tissues. The remaining FAs circulate to the liver and are incorporated into hepatocytes as non-esterified FAs (NEFAs) or free FAs formed by lipoprotein lipase mediated lipolysis [160, 161]. If dietary carbohydrates are excessive to energy requirements, de novo FAs synthesis occurs from glucose in the liver. FAs convert into TAGs as described above or are esterified with cholesterol to produce cholesterol esters. TAG and cholesterol esters are either packed into very low-density lipoprotein (VLDL)

particles and delivered into adipose and extrahepatic tissues via the circulation, or stored within hepatocytes as lipid droplets, depending on metabolic circumstances. In normal metabolism, hepatic de novo lipogenesis can be driven by excess dietary carbohydrates, by multiple transcription factors related to glycolysis and lipogenesis, insulin production or the metabolic state (fed versus fasted) [157, 161, 162]. Besides the liver's metabolic role in synthesis and storage of FAs, hepatocytes also metabolize (oxidize) FAs to generate energy by the process of β oxidation. In a fasted state or when energy requirements cannot be fulfilled by the available glucose, β oxidation of FAs occurs in the mitochondria of the liver and provides energy locally, or generates ketone bodies that are exported into the circulation for delivery to energy deficient extrahepatic tissues [162]. Similarly, hepatic β oxidation is regulated by the fasting state or multiple factors related to PPARα signaling [157, 162, 163].

Although hepatic lipid metabolism is a tightly regulated process, different lifestyle modifying factors can modulate metabolic parameters, resulting in benign to pathologic hepatic conditions. The most notable factors are ethanol consumption and high calorie and high fat diets resulting in accumulation of excess fats in the liver, a condition known as fatty liver disease. Nonalcoholic fatty liver disease (NAFLD) is becoming the most common cause of liver disease in Western countries and 30% of the people of the United States have various levels of NAFLD [164, 165]. If uncontrolled, NAFLD can progress to non-alcoholic steohepatitis (NASH) and cirrhosis, and is associated with hepatic carcinoma [165]. NAFLD is directly associated with obesity, which is further associated with consumption of a high fat, high calorie diet, although the liver is not a primary site of lipid deposition. However, energy excess states, either diet or obesity can stimulate hepatic TAG synthesis and/or free FA accumulation in hepatocytes [166, 167]. Besides being hyper-caloric and high-fat, Western diets also have high amounts of ω-6 PUFA and

mostly lack ω-3 PUFAs. However, little is known about the effects of dietary PUFA composition, independent of calorie consumption and obesity, in hepatic lipid metabolism and/or storage. Recent clinical studies have shown that obese patients with diabetes and metabolic syndrome have low levels of LC-PUFAs in blood and tissue [168, 169]. Experimental studies, using obesity-resistant A/J mice and susceptible C57BL/6J, have shown an inverse regulatory role of enzymes involved in LC-PUFA synthesis in obesity associated fatty liver, so that elevated expression of these enzymes protects A/J mice from obesity and fatty liver [170-172]. Among PUFAs, ω-3FAs have been associated with decreased hepatic fat [173]. Additionally, dietary fat was found to modulate membrane lipid composition of hepatocytes, which may alter their metabolic functions and associated pathologies including NAFLD [174, 175].

Recent studies have demonstrated a correlation between lipid and glycogen metabolism in high fat diet-feddiet-fed animals [176] and shown that liver glycogen levels reduce food intake and prevent diet-induced obesity [177]. However, the mechanisms that switch lipid to glycogen metabolism in non-obese conditions is not understood, nor is the role of PUFA composition in the regulation of these metabolic processes. Altogether, an alteration in hepatic lipid or glycogen metabolism results in the modulation of liver microenvironments including steatosis, inflammation and fibrosis. The regulatory roles of diet-induced alternation in the metabolism of the hepatic microenvironment, which can modulate hepatic metastasis, are not known. Few epidemiological studies aimed to address a correlation between fatty liver diseases including NAFLD with hepatic metastasis from BC however the results from such studies are conflicting [178, 179]. Thus, further clinical, experimental and mechanistic studies are warranted to address the role of PUFAs in hepatic metastasis.

1.10. Inflammation and cancer induction progression and metastasis

In 1863, Rudolf Virchow first proposed the hypothesis that cancer cells originate at the site of chronic inflammation (irritation at that time) and that inflammation also enhances cell proliferation [180]. It is now widely accepted that chronic inflammation is a risk factor for cancer initiation and the type of inflammatory cells present in the tumor microenvironment, and their cross talk with stromal cells and tumor cells has been shown to regulate tumor progression and therapy resistance in multiple cancers, including BC. The role of inflammation in BC development can be evaluated in two stages of cancer pathogenesis: 1) chronic local or systemic inflammation modulating BC development, and 2) double edged roles of inflammatory cells in the tumor microenvironment

1.10.1. Chronic local or systemic inflammation modulating BC development

Clinical and epidemiological studies have shown an association between breast cancer and obesity [181]. Adipose tissue is an endocrine organ and able to secrete bioactive adipokines, cytokines, chemokines and hormone-like growth factors, depending on the metabolic and/or inflammatory state [182]. Adipose tissue expansion, either due to adipocyte hyperplasia (increase in cell number) or hypertrophy (increase in cell size), induce local hypoxia, which is associated with dysregulated production of adipokines and inflammatory cytokines [183, 184]. A chronic hypoxic condition results in apoptosis of adipocytes, and the release of free fatty acids, which stimulate Toll-like receptors (TLRs) on adipocytes and macrophages, and initiate the NFκB pathway, activating the expression of inflammatory cytokines including TNF-α, IL1β, IL6, IL8 and CCL2 [182, 185]. Several cytokines, specifically CCL2, attract circulating monocytes to the site of adipocyte death where they differentiate to macrophages, resulting in the formation of crown-like structures (CLS). The inflammatory signaling pathways needed to form CLS, or by the CLS, induce chronic adipose tissue inflammation. Adipocyte death and/or CLS formation is mostly

found in visceral/subcutaneous fat of humans and mice, and correlates with adipocyte size [186, 187]. However, recent findings of CLS in adipose tissue from breast cancer patients and normal weight women undergoing mastectomy for breast cancer risk reduction or therapy not only emphasize the role of local adipose inflammation in tumor progression, but also raise a potential new direction for the investigation of CLS pathways in BC development, independent of obesity [188, 189].

Adipose tissue hypoxia also induces hypoxia-inducible factor-1 (HIF-1) that acts as a molecular oxygen sensor and upregulates leptin and vascular endothelial growth factors (VEGF) and downregulates adiponectin; thus, enhancing both systemic chronic inflammation and angiogenesis [190]. Leptin levels in serum are directly correlated with obesity, and higher leptin levels are associated with increased risk of BC [191]. Further, leptin and leptin receptor expression are higher in breast adipose tissues of BC patients, and in vitro studies have shown the efficiency of leptin in enhancing the proliferation of normal mammary epithelial cells and mammary tumor cells, which further emphasizes a potential role of leptin in mammary carcinogenesis [192-194].

1.11. Inflammatory cells in the tumor microenvironment

There are complex interactions between inflammatory microenvironments and tumor cells, including the type of inflammatory cells that infiltrate tumors, and the activities regulating hallmarks of cancer, such as cell proliferation, apoptosis, angiogenesis, invasion and metastasis [195]. Immune cells can be of a cytotoxic (or tumor suppressing) phenotype, and tumor-secreted growth factors and cytokines can modulate the immune cell phenotype. Thus, tumor-infiltrating immune cells can have multiple roles in tumor pathogenesis and control. Some of the important immune cell types in the mammary tumor microenvironment are discussed below.

1.11.1. Tumor associate macrophages (TAMs)

Macrophages are one of the most abundant immune cells in the tumor microenvironment of solid tumors, including BC. Intratumoral infiltration by TAMs has been associated with a higher proliferation index and poorer disease-free survival in BC patients [196, 197]. TAMs are comprised of functionally heterogeneous populations of macrophages, and can acquire different phenotypes, depending on activation signals. M1 and M2 macrophages represent two functionally distinct phenotypes that are identified in tumor microenvironments. M1 macrophages are activated by IFNγ and bacterial lipopolysaccharides, and are associated with higher expression of proinflammatory cytokines such as TNF-α, IL1, IL6, IL12 or IL23, antigen presentation and generation of reactive oxygen species and are capable of killing pathogens and enhancing anti-tumor immune responses. M2 macrophages (alternatively activated) are differentiated by IL4 and IL13 and are associated with the production of anti-inflammatory cytokines, upregulation of scavenging receptors and participate in tissue remodeling, angiogenesis, immunoregulation, and tumor promotion [198-200].

1.11.2. Tumor-associated neutrophils

High neutrophil numbers in the circulation (neutrophilia), or increased neutrophil to lymphocyte ratios (NLR) have been associated with a poor prognosis of BC patients [201] However, there is limited information on the regulatory role of neutrophils in tumor microenvironments in BC patients. Neutrophils recruited to the tumor microenvironments are known as tumor associated neutrophils (TANs) and chemokines skewed by tumor cells recruit TANs into tumors [202, 203]. Thus, as with macrophages, tumor

microenvironments can modulate TAN frequency and phenotypes [204]. A recent study showed that TGFβ, within the tumor microenvironment, induce a pro-tumor TAN phenotype N2, and the blockade of TGFβ increased the anti-tumor cytotoxic (N1) phenotype of TANs [204]. The N2 TANs promote tumor growth by expressing matrix degrading enzymes such as metalloproteases (MMP)-9, oncostatin M and chemokines enhancing invasiveness of tumor cells and angiogenesis [202, 205]. However, additional studies are needed to improve the understanding of TAN cross talk in tumor microenvironments.

1.11.3. Myeloid derived suppressor cells (MDSCs)

MDSCs are heterogeneous population of myeloid precursor cells that were initially identified as myeloid hyperplasia associated with tumor progression [206], but later were found to be associated with other pathological conditions including bacterial infections, autoimmune diseases and obesity [207-209]. As there is cellular heterogeneity in MDSCs, the phenotypic characterization was initially contentious [206] and the markers to define MDSCs have been evolving [210]. Classically, MDSC subsets were categorized as granulocytic (G)-MDSCs versus monocytic (M)-MDSCs but G-MDSCs have also been known as polymorphonuclear (PMN)-MDSCs based on their morphological and phenotypical characteristics [210]. PMN-MDSCs are morphologically and phenotypically similar to TANs and a recent study has shown a subgroup of tumor promoting TANs (N2). Thus, it is likely that N2 TANs identified in tumor microenvironment are PMN-MDSCs [204, 211]. Tumors secrete growth factors including G-CSF, GM-CSF and M-CSF that induce myelopoiesis [144, 145], and have been correlated with MDSC numbers. Similarly, tumor-secreted chemokines, and inflammatory mediators including TNFα, IL6, IL1β and PGE2

have roles not only in mobilization but also may limit the maturation and differentiation of MDSCs, resulting in accumulation [206, 211, 212] [127, 136-138]. Further, the accumulation of their MDSCs in tumor microenvironments promote tumor growth by regulating tumor invasion, angiogenesis [212, 213], reducing T-cell frequency and/or suppressing T-cell function [206, 214]. MDSCs mediate T-cell suppression, support tumor growth and can impede tumor therapies. Thus, recent studies have been focusing on the mechanisms involved, including mechanisms of MDSC mediated suppression of T-cells: 1) down-regulation of T-cell receptor-zeta, which is required to transmit signal for activation; 2) down-regulation of L-selectin, a plasma membrane molecule necessary for homing of naïve T-cell to lymph nodes; and, 3) depletion of cysteine (an amino acid that is essential for T-cell activation) from the microenvironment [215-217].

1.11.4. T-cells (Tumor infiltrating lymphocytes)

The impact of T-cells or tumor infiltrating lymphocytes (TIL) in tumor microenvironments in the tumor progression has been studied for decades. Based on IHC evaluation of solid tumors including BC, an increase in the frequency of TILs has been positively correlated with a good prognosis and a response to cancer therapy [218, 219]. Among the subsets of T-cells, the number of $CD8^+$ cells has the greatest correlation and is most promising in predicting responses. However, Th1 $CD4^+$ infiltration has also been found to be a positive prognostic marker [220, 221]. It is unclear if the presence of $CD8^+$ in tumor microenvironments has a strong effect on the killing of tumor cells or if having $CD4^+$ in the periphery will have additional effects.

Among T-cells, regulatory T-cells (T-regs) or $Foxp3^+CD25^+CD4^+$ T-regs, play an important role during immunological self-tolerance in healthy individuals. In BC patients, increased tumor infiltration by T-regs has been correlated with poor prognosis; however, there is

limited information on the immunosuppressive mechanism and cross talk of T-regs in the tumor microenvironment [222, 223]. Tumor-derived chemokines recruit T-regs into tumor microenvironment and induce them to express high levels of $CD25^+$ by tumor-derived TGFβ and drive them to a suppressive phenotype [224]. One, well-studied T-reg-mediated immune suppression mechanism, includes the activation of immune checkpoint molecules, including T-lymphocyte associated protein 4 (CTLA-4) and program death 1 (PD1). CTLA-4 is a highly potent, co-inhibitory molecule expressed constitutively by T-regs and by conventional T-cells after activation. Since CTLA-4 has much higher affinity than CD28 for their common ligands CD80 and CD86, constitutive CTLA-4 expressed by T-regs may outcompete CD28 on conventional T-cells for binding to CD80/CD86 on antigen-presenting cells resulting in inhibition of co-stimulation of conventional T-cells [225]. The success of anti-tumor immunotherapy, using anti-CTLA-4 antibody, has been previously attributed to augment the activity of tumor infiltrating $CD8^+$ cells; however, recent studies have suggested the possibility of the role of anti-CTLA-4 antibody in depletion of T-regs, resulting in enhancing of anti-tumor immune response [226].

1.12. Breast cancer metastasis: Role of the tissue microenvironment

The metastasis of tumor cells from primary sites to distant organs is a non-random process, and the successful development of metastasis in specific organs is a result of tumor cell properties (seed) and the supportive environment of the host organ (soil). Stephen Paget first proposed the seed and soil hypothesis in 1889 [227]. Fidler and coworkers verified different aspects of the seed and soil hypothesis repeatedly in their seminal findings; including the clonal origin of metastasis [228], organ selectivity [229] and the role of cross talk between the tumor cells and the host microenvironment in the formation of the metastases [227, 229-234]. By now the hypothesis has been widely

accepted, although the definitions of seed and soil have been updated with the new insights in the molecular properties of both seed and soil [230]. However, most efforts to define therapeutic targets to control metastases have focused on the properties of the tumor cells, while modifiable properties of the host organs have been less emphasized.

Studies have shown that the tumor supportive microenvironments, known as pre-metastatic niches, occur prior to colonization by the seed (metastatic tumor cell). Tumor-derived factors or tumor-induced bone marrow-derived factors, and immune cells, have been shown to have a role in the formation of pre-metastatic niches. Additionally, modulation of the host organ microenvironments by chronic inflammation, immune suppressive cell infiltration or local PGE2 production (influenced by the tumor or other mechanisms) have a role in the preferential homing by tumor cells [235, 236]. The emerging concepts of infiltration by myeloid cells, including MDSCs in pre-metastatic sites prior to arrival of tumor cells, further indicate the role of inflammatory microenvironments in tumor metastasis [237]. However, the mechanism of dietary factor mediated regulation of the pre-metastatic niche remains to be understood. BC preferentially metastasizes to bone, liver, brain, lungs and distant lymph nodes [235], while BC metastasis to heart, kidney and ovaries are rarely reported.

1.13. Bone metastasis in BC

Around 70% of metastatic BC patients develop bone metastasis, indicating bone as one preferable metastatic site for BC cells [238]. Therapeutic targeting of bone metastasis is difficult, and the consequences of bone metastasis, including pathological bone fractures, pain, hypercalcemia, and spinal cord and nerve-compression syndromes, significantly reduce the quality of life amongst BC patients [239]. Although of great clinical importance, molecular mechanism(s) underlying bone metastasis have not been elucidated, and more

research is needed to understand the role of pre-metastatic bone microenvironments that attract tumor cells. Based on the type of bone lesions, bone metastases are classified into: osteoblastic, or osteoclastic. The major differences are that the osteoblastic lesions are the consequence of tumor growth and tumor-derived factors. In contrast, osteoclastic lesions are due to osteoclasts under the influence of tumor cells. Bone metastases in prostate cancer are predominantly osteoblastic, while BC metastases are predominantly osteoclastic [240]. In osteoblastic metastases, C-X-C chemokine receptor type 4 (CXCR-4) is a major mediator that induces migration of tumor cells towards bone microenvironments by interacting with C-X-C motif ligand 12 (CXCL12) on osteoblasts. The invaded tumor cells produce multiple growth factors that alter the remodeling process in the affected bone. Since osteoclastic metastases are important in BC, they are discussed in more detail below.

1.13.1. Mechanisms of osteoclastic or osteolytic bone metastases

As described above, osteolytic lesions are due to the activities of osteoclasts under the influence of tumor cells. BC cells produce factors such as parathyroid hormone related peptide 1 (PHRP1) that binds to parathyroid hormone receptor 1 (PHR1) on marrow stromal cells and induces the expression of receptor activator of nuclear factor-κB (RANK) ligand (RANKL). The newly formed RANKL binds the RANK receptor on osteoclast precursors and induces them to differentiate into mature osteoclasts, which resorb bone by secreting proteases and acid to dissolve the matrix and release bone mineral into the extracellular space [240, 241]. The bone resorption enhances TGFβ expression, which induces PHRP1 production by BC cells [242]. Further, bone resorption enhances local calcium levels, which promote tumor growth in bone, resulting in more PHRP1 production [243]. Thus, this reciprocal cross talk between BC cells and bone microenvironments via

PHRP1 and PHR1 results in a vicious cycle, increasing both bone destruction and promoting tumor growth in the bone. Besides PHRP1, other factors such as TNFα, IL6, macrophage colony-stimulating factor and IL1 produced by BC cells or microenvironments may play a role in osteoclast formation. PGE2 can enhance osteoclast formation by increasing expression of RANKL [244]. However, it is unclear if these factors/mediators, in pre-metastatic bone microenvironments, modulate bone metastatic BC cells to produce PHRP1 for colonization in bone, or if preselected bonetropic BC cells produce those factors/mediators to initiate the vicious cycle of the osteolytic bone metastases in BC patients. Osteopenia is also observed in post-menopausal women secondary to hormonal factors [245]. Other life style factors such as alcohol consumption can enhance osteopenia, and high fat diets lead to marrow adiposity modulating the marrow microenvironments [246, 247]. However, how such pre-existing BM microenvironments regulate BC bone metastasis is not clear and needs further evaluation.

Chapter 2:
Materials and Methods

2.1. Animals and housing:

Female BALB/c mice (6 weeks old) purchased from Charles River Laboratories were housed in micro-isolators in groups of five mice per cage, under standard conditions of temperature and humidity, with a 12 h light-dark cycle. The micro-isolators were attached to high efficiency particulate air (HEPA)-filtered ventilation blowers to provide sterile air. The animal housing facility was maintained as a specific pathogen free (SPF) area. The Institutional Animal Care and Use Committee at the University of Nebraska Medical Center approved the animal protocol for the study. After two to three weeks of acclimation to the laboratory conditions, mice were divided at random into two dietary groups based on the experimental liquid diets (ω-6 or ω-3 diet). At least n=20 mice per group were used for each pair-feeding dietary experiment. All the animal experiments were repeated at least 3 times for analysis of the outcomes. At least n=5 mice/group were used for each histological experiment in non-tumor bearing mice and at least n=10 mice/group used for histological and metastasis analysis of tumor-bearing experiments. The exact number mice/ group for each experiment is mentioned in the respective result section of each chapter (chapters 3-5).

2.2. Diets and pair-feeding:

The diets were isocaloric and isolipidic and had identical protein, fiber, and micronutrient contents. The ω-6 diet was the Lieber-DeCarli control diet (Dyets # 710027) containing 28.4 gm/L olive oil, while the ω-3 diet was customized by using the base diet (Dyets # 710166) and adding 8.4 gm/L olive oil and 20 gm/L of fish oil (NutriGold Triglyceride

Omega-3 Gold capsules; Lot # 0081-3180-2) (Table 1). Both liquid diets provided 1.0 Kcal energy per ml of diet and equal calories from macronutrients (35% derived from fat, 47% from carbohydrate, and 18% derived from protein). The ω-6 and ω-3 diets differed primarily by the absence or presence of LC-ω-3FAs from fish oil and ω-6 PUFA from olive oil respectively. Omega-3 capsules and Lieber-DeCarli powder diets were stored at 4^{o}C. Diets were prepared and delivered daily (within 24-26 hours) and daily intake was monitored. Ad libitum access to the liquid diets was provided for the first 5 days to acclimatize the mice to the liquid diets. From day 6, the ω-6 diet group mice were pair-fed based on mean consumption of the ω-3 diet group from the previous day, and this was continued throughout the study for 10 or 20 weeks. Body weights were recorded twice a week. In addition, a limited number of control studies were undertaken with age matched, chow fed (#7912, Teklad) mice, as a baseline control.

Table 1. Composition of the diets used in the study

Ingredient in Diet	**ω-6 Diet** Grams/L	**ω-3-Diet** Grams/L
Casein	41.4	41.4
L-Cystine	0.5	0.5
DL-Methionine	0.3	0.3
Corn Oil	8.5	8.5
Olive Oil	28.4	8.4
Safflower Oil	2.7	2.7
Maltose Dextrin	115.2	115.2
Cellulose	10	10
Mineral Mix	8.75	8.75
Vitamin Mix	2.5	2.5
Choline Bitartrate	0.53	0.53
Xanthum gum	3	3
Fishoil	**0**	**20**
Total	221.8	221.8

2.3. Blood Collection:

At the end of each experiment, blood was collected, without fasting, prior to the mice being euthanized and hematological parameters, such as total white blood cell count (WBC) count, red blood cell (RBC) count, hemoglobin level, hematocrit and mean corpuscular volume (MCV) were determined using a vet ABC animal blood counter (Scil animal care company, Grayslake, IL).

2.4. Fatty acid analysis:

Portions of liver, MG tissues and plasma samples were collected after 10 weeks of diet, snap frozen and stored at -80^{o}C for FA analysis. Portions of ready-to-use ω-3 and ω-6 diets were also frozen until needed for lipid extraction. Omega-3 capsules were stored at 4^{o}C and used directly for FA analysis. Total lipid extraction from tissues and diets were undertaken using antioxidant β-hydroxy-toluene (0.05%, wt/vol) as previously described [248, 249]. Heptadecanoic and nonadecanoic acid (100 µg each) were added to all samples to estimate the recovery of FA. Complex lipids were hydrolyzed by adding 0.5 ml of methanol containing 1% (wt/vol) sulfuric acid and 0.25 ml of toluene, and then were incubated at 60°C overnight. Following incubation, 1.25 ml of water containing sodium chloride (5%, wt/vol) was added, and esters were extracted using hexane (2 X 1.25 ml per sample). The hexane layer was washed using 1 ml of water containing potassium bicarbonate (2%, wt/vol), and dried over anhydrous sodium sulfate. The solvent was removed under a stream of nitrogen and the FA methyl esters were analyzed by gas chromatography-mass spectrometry (GC-MS) using an Agilent 6890 series gas chromatograph, equipped with a 5873 mass-selective detector. For assessment of sterols, 100 µg of 5α-cholestane was added to samples as an internal standard. Sterols were separated and detected by GC-MS using a DB-17ms column. FA concentration was

analyzed as µg/µl or µg/mg of the samples, analyzed, and compared between the diets and tissues from ω-3 and ω-6 diet-fed mice

2.5. Histological analysis of mammary ducts and adipocytes:

The MFP and abdominal fat tissues from non-tumor-bearing mice (Chapter 3) were fixed in zinc fixative for 24-48 hours, and transferred to 70% ethanol, prior to paraffin embedding, and sectioned at 4 µm. Sections were stained with hematoxylin and eosin (H & E) or trichrome stain for histological analysis. The sections were analyzed under light microscopy using a Zeiss Axioplan-2 microscope, and images were obtained using a HRc camera using Zeiss AxioVision Rel 4.8 software from 10 randomly selected fields at 100x or 200x magnifcation. The size of mammary ducts and stromal and epithelial layers in the ducts were analyzed in trichrome stained MFP sections using Image-J software. The average number and size of adipocytes per high power image was evaluated in H & E stained sections of MFP and abdominal fat using MRI_Adipocyte_Tools, a plug-in tool from Image-J as per the software protocol. The mean adipocyte size/number from the 10 high power field/sample were evaluated for the quantitative data. Two persons examined the sections as “blinded” group assignments and an experienced pathologist validated the results.

2.6. Hepatic steatosis analysis:

Steatosis was initially examined in H & E stained sections, then further confirmed and quantified by counting Oil Red O (ORO) stained lipid droplets in hepatocytes. For ORO staining, fresh liver tissues were embedded in optimal cutting temperature (O.C.T) compound medium (Tissue-Tek #4583, Sakura Finetek, CA U.S.A) and stored at -80^{o}C until sectioned and stained. Lipid droplets, the size of a hepatic nucleus or larger, were

enumerated to analyze macro-vesicular steatosis, whereas smaller lipid droplets were enumerated for micro-vesicular steatosis analysis. To quantify hepatic steatosis, the number of lipid droplets per 1000x magnification field were counted for 10 random fields per liver sample.

2.7. Hepatic EMM analysis:

EMM was assessed based on foci of immature myeloid inflammatory cells and their nuclear morphology in H & E stained sections. The number of foci per field and the number of inflammatory cells per focus were counted in 10 fields at 200x magnification. Biliary duct size and the area of biliary epithelium were measured in the biliary ducts present in 10 random fields at 200x magnification using Image-J software.

2.8. Hepatic glycogen storage analysis

Hepatic glycogen deposition was measured using Periodic Acid-Schiff (PAS) staining on paraffin embedded liver tissue sections. Magenta color PAS positive hepatocytes were confirmed as glycogen-deposited hepatocytes by comparing glycogen degradation in a serial section treated with PAS-diastase (PAS-digest). The average number of PAS-positive hepatocytes were counted in 10 fields of hepatic lobular regions (200x).

2.9. Immunohistochemistry (IHC) analysis:

For IHC staining, slides of paraffin-embedded tissue sections were warmed on a slide warmer for 30 minutes to 1 hour. The slides were deparaffinized and rehydrated by serial incubations in xylene (3x), 100% ethanol, 95% ethanol, 70% ethanol, 50% ethanol, and

water. For IHC analysis of liver tissue (data presented in Chapter 4), rehydrated sections were steamed in preheated sodium citrate antigen retrieval buffer (pH 6.0) for 20 minutes using a steamer (HS1000, Black and Decker, Miramar, Florida). Slides were cooled, washed 3 times in TRIS-buffered saline, pH 7.6 (TBS) containing Tween-20 (TBST). Endogenous peroxidase was blocked by hydrogen peroxide, slides were washed in TBST and blocked with 5% goat serum in TBST (ab7481; Abcam Inc.) for 1 hour at room temperature (RT). Primary antibodies were diluted in antibody diluent (BD559148; BD), and incubated at 4^{o}C overnight. For negative controls, serial sections were incubated in the diluent without the primary antibody and all other staining procedures were undertaken. Sections were washed 3 times with TBST and incubated in Signal Stain Boost IHC detection reagent (HRP, Rabbit 8114S Cell Signaling Technology; Danvers, MA.) for 30 minutes at RT in a humid chamber. The washed sections were incubated with DAB chromogen (BD550880; Becton Dickinson, New Jersey) until a mild brown color was detected. Sections were briefly dipped in a hematoxylin solution (MHS32; Sigma-Aldrich, St. Louis, MO) followed by 0.1% sodium bicarbonate for counter staining. Images were captured on a Zeiss Axioplan-2 microscope as described above. The number of CD45^{+} cells in each cluster, and the number of clusters of CD45^{+} cells per 100x field were counted in 10 random fields per sample.

For IHC analysis of mammary fat pads and tumor tissues, the same procedures and incubation times were used as discussed above, however, different reagents were used for some steps as mentioned below. For antigen retrieval, EDTA-based retrieval buffer, pH 8.0 (ab93680, Abcam) was used instead of citrate buffer. Endogenous peroxidase/phosphatase was blocked with BLOXALL (SP6000, Vector labs, Burlingame, CA). Non-specific antibodies were blocked using 2.5% normal horse serum (S-2012, Vector labs). For detection, ImmPRESS-AP, anti-rabbit Ig (MP-5401, Vector labs) was

used for 30 minutes at RT in a humid chamber and staining was detected using ImmPACT Vector Red alkaline phosphatase reagent (SK-5105). Counter staining was performed as described above. The stained sections were dehydrated with serial incubations in water, increasing concentrations of ethanol and then xylene and mounted with Permount, before evaluation of the stain-positive cells by microscopy. (Fisher, SP15-100). For analysis of staining, 10 random high power fields (HPF) were evaluated for the number of positive cells or clusters of cells (for $CD45^+$ cell clusters in liver) or $CD31^+$ vessels per HPF. All the IHC analyses of tumor tissues were performed by evaluating positive cells in sub-capsular oxic areas of the tumors.

Table 2. List of antibodies used in IHC experiments

Antibody	Reactivity	Host species	Supplier	Catalogue	Dilution
Anti-F4/80	Mouse	Rabbit	Cambridge, MA	ab111101	1:100
Anti-Ki67	Mouse,Rat, Human	Rabbit	Cambridge, MA	ab16667	1:100
Anti-Neutrophil elastase	Mouse, Human	Rabbit	Cambridge, MA	ab68672	1:2000
Anti-CD3	Mouse, Human	Rabbit	Cambridge, MA	ab16669	1:100
Anti-CD31	Mouse,Rat, Human	Rabbit	Cambridge, MA	ab182981	1:2000
Anti-CD45	Mouse,Rat, Human	Rabbit	Cambridge, MA	ab10558	1:2000

2.10. TUNEL labeling of liver tissues (Fluorescent based)

The terminal deoxynucleotidyl transferase (TdT)-mediated deoxyuridine triphosphate nick end labeling (TUNEL) assay was performed on deparaffinized liver sections according to the manufacturer's instructions (Roche, Indianapolis, IN). The label solution without TdT was used as a negative control and liver sections with known tumor metastases were used as positive controls. Slides were cured overnight, in the dark, with ProLong® Diamond Antifade Mountant with DAPI (P36971; Thermo-Fisher, Grand Island, NY). Fluorescent images were captured on a Zeiss LSM-710 confocal microscope at 630x magnification, and the images were processed using the Zeiss Zen 2012 stitching software and merged into a single image. The number of TUNEL positive nuclei and DAPI positive hepatic nuclei per field at 630x magnification were counted in 10 random fields to calculate the number of apoptotic nuclei and relative percentages of apoptotic hepatocytes.

2.11. Protein extraction of hepatic lysates and western blotting:

Freshly isolated liver sections were collected in ice-cold Tissue Protein Extraction Reagent (T-PER™; #77510; Thermo-Scientific, Grand Island, NY) containing complete™ ULTRA Tablets, EDTA-free, Protease Inhibitor Cocktail (#5892953001, Roche, Indianapolis, IN) and PhosSTOP™ phosphatase inhibitor cocktail (#04906837001, Roche, Indianapolis, IN), and then homogenized using a tissue homogenizer with disposable tips (Omni TH; Omni International, Kennesaw, GA). The homogenized tissues were centrifuged at 10,000g for 10 minutes at 4^{o}C. Protein concentrations of the whole tissue extracts were determined according to the manufactur’s protocol (Pierce™ BCA Protein Assay Kit; #23227, Thermo-Fisher, Grand Island, NY). For Western blotting, whole cell protein samples were separated by SDS PAGE using a 4-15% Mini-PROTEAN TGX Precast Gel

(456-1084, Bio-Rad), and blotted using Trans-Blot® Turbo™ Mini PVDF Transfer Packs (1704156, Bio-Rad) Trans-Blot® Turbo™ Transfer System (Bio-Rad, Hercules, California). The blotted membranes were blocked using 5% BSA in TBST for 1 hour at RT, followed by incubation in diluted primary antibodies anti-NF-kB p65 [E379] (ab32536), anti-beta Actin (ab8227) overnight at 4ºC. After washing 3 times, blots were incubated with the secondary antibody [goat anti-rabbit IgG H&L chain, HRP] (ab6721, Abcam Inc.) for 1 hr at RT. All the antibodies were purchased from Abcam Inc. The protein bands were examined by using SuperSignal™ West Pico Chemiluminescent Substrate (34078, Thermo-Fisher, Grand Island, NY). Blots were exposed and digital images were acquired using a myECL™ Imager, and relative protein quantities were determined by using myImageAnalysis™ Software (62237, Thermo-Fisher, Grand Island, NY).

Table 3. List of antibodies used in Western blot analyses

Antibody	Reactivity	Host species	Supplier	Catalogue	Dilution
Anti-NF-kB p65 [E379]	Mouse, Human	Rabbit	Cambridge, MA	ab32536	1:50,000
Anti-Beta Actin	Mouse, Rat, Human	Rabbit	Cambridge, MA	ab8227	1:25,000
Goat Anti-Rabbit IgG H&L (HRP)	Rabbit	Goat	Cambridge, MA	ab6721	1:10,000

2.12. Flow cytometry and colony forming units-granulocyte/macrophage (CFU-GM)

Freshly isolated livers were minced into small pieces, treated with collagenase-IV (17104-019, Gibco) and DNAse I (D5025, Sigma), and filtered through cell dissociation sieves to prepare single cell suspensions. Hepatic leukocytes (WBCs) were isolated using mouse cell separation media, Lympholyte M (CL5035, Cedarlane). Then the total hepatic WBC count was analyzed using a vet ABC animal blood counter and data assessed as WBC count/gram of liver. For flow cytometry, isolated leukocytes were stained with the indicated antibodies for 30 minutes at 4^{o}C. The antibodies used were anti-CD45-V450 (clone 30-F11, BD Pharmingen) anti-CD201-APC (clone ebio1560, ebioscience) and anti-CD27-BV650 (clone LG3A10, BD Pharmingen). Flow cytometry was performed using a BD LSRFortessa X50 platform, and results were analyzed using FlowJo software version 9.9.5 (TreeStar). For CFU-GM assays, 10^5 hepatic leukocytes were cultured in 1.1 ml of methylcellulose-based medium for myeloid progenitor cells (MethoCult™ GF M3534, STEMCELL technologies) as per company protocol. Colonies of at least 50 cells were scored for analysis of CFU-GM.

2.13. RNA extraction / quantitative real time PCR

Tissues were collected in RNA stabilizing solution, RNAlater (#76106, Qiagen) and stored at -20^{o}C until used. RNA was extracted by using TRIzol reagent (15596026, Invitrogen). RNA concentrations were measured using NanoDrop (ND1000, Thermofisher). In order to confirm the integrity of the RNA, the RNA (2 µg) was separated in a denaturing agarose

gel (1%) in formaldehyde, and samples with two distinct bands of RNA (16S and 23S) in the gel were used for further analyses. Complimentary DNA (cDNA) was prepared from 2 µg of RNA using a high-capacity cDNA synthesis kit (4374966, Applied Biosystems; AB) as per the kit protocol.

The qRT-PCR master mix was prepared using TaqMan gene expression master mix (4370074, AB), anti-mouse probes and 10 ng of cDNA in Micro Amp fast optical 96 well plates (4346906, AB). Pre-synthesized mouse probes from Applied Biosystems were used for the study as listed in Table 4. Negative controls were run for every probe in the plate. The samples were run using a StepOnePlus qPCR machine (Applied Biosystems) with the program: pre-heating at 95^{o}C for 10 minutes, 40 cycles of 15 seconds at 95^{o}C and 60 seconds at 60^{o}C. Each qRT-PCR experiment was carried out in triplicate (technical replicates) so that the average cycle thresholds (Cts) from technical replicates was used as a Ct value of the sample. Then the average Ct values (for each target or reference) from all samples (each tissue) in the dietary group, from the same experiment (biological replicates) were obtained for each dietary group. The relative quantities of target mRNAs was determined using the Levak method [250]. Briefly, the Ct of GAPDH was subtracted from the Ct value of the target to obtain a delta (d) Ct. Then the dCt of each of samples from the ω-6 group was compared with the average dCt from the ω-3 group to obtain ddCt values. The fold changes between the samples was calculated as 2^{-ddCt} as described previously [250].

Table 4. List of probes used in qRT PCR analyses

Gene symbol	Taqman gene expression assay ID	Target species	Supplier	Translated protein
GAPDH	**Mm99999915_g1**	Mouse	Applied Biosystem, Foster city, CA	glyceraldehyde-3-phosphate dehydrogenase
IGF1	**Mm00439560_m1**	Mouse	Applied Biosystem	Insulin like growth factor 1
IGF1R	**Mm00802831_m1**	Mouse	Applied Biosystem	Insulin like growth factor 1
ESR1	**Mm00433149_m1**	Mouse	Applied Biosystem	Estrogen receptor 1
Lep	**Mm00434759_m1**	Mouse	Applied Biosystem	Leptin
Adipoq	**Mm00456425_m1**	Mouse	Applied Biosystem	Adiponectin
IL6	**Mm00446190_m1**	Mouse	Applied Biosystem	Interleukin 6
PTGS2	**Mm00478374_m1**	Mouse	Applied Biosystem	prostaglandin-endoperoxide synthase 2 (COX-2)
IFNγ	**Mm01168134_m1**	Mouse	Applied Biosystem	Interferon gamma
PGR	**Mm00435628_m1**	Mouse	Applied Biosystem	Progesterone receptor
AREG	**Mm01354339_m1**	Mouse	Applied Biosystem	Amphiregulin
TNFα	**Mm00443258_m1**	Mouse	Applied Biosystem	Tumor necrosis factor
CCL2	**Mm00441242_m1**	Mouse	Applied Biosystem	chemokine (C-C motif) ligand 2
NFκB	**Mm00476361_m1**	Mouse	Applied Biosystem	nuclear factor NF-kappa-B
IL10	**Mm01288386_m1**	Mouse	Applied Biosystem	Interleukin 10
CSF3	**Mm00438334_m1**	Mouse	Applied Biosystem	Granulocyte colony-stimulating factor
CSF2	**Mm01290062_m1**	Mouse	Applied Biosystem	granulocyte-macrophage colony-stimulating factor

2.14. MG morphological analyses: Whole mount assays

The intact inguinal MGs (#4) were excised from the mice at necropsy. The MGs were spread onto a glass slide immediately after collection and fixed in Carnoy's solution (100% EtOH, chloroform, glacial acetic acid; 6:3:1) for 4 hours in a fume hood at room temperature (RT). The fixed MGs were then gradually rehydrated in graded ethanols (70%, 35%, 15%) ending in water. The MGs were stained using carmine alum staining solution [0.2% Carmine (C6152, Sigma, MO) and 0.5% aluminum potassium sulfate dodecahydrate (#237086, Sigma, MO) with a few flakes of thymol (#16254, Sigma, MO) overnight. The stained MGs were washed in water and dehydrated in ascending graded ethanol solutions (50%, 70%, 95%, 100%), cleared by incubating in xylene overnight and mounted with Permount (SP 15-100, Fisher scientific). Whole slide images were acquired using the Invitrogen™ EVOS™ FL Auto Imaging System. For quantitative analysis, higher magnification images were acquired using the Zeiss Discovery V8 Stereo Microscope with a Axiocam 105 color camera. We used the term "ductal terminus/termini" for all the end structures of ducts and ductules present in the high power field (HPF). The number of ductal termini were counted in 10 images (40x magnification) per sample and used to calculate the average value for each sample. The extent of ductal branching was analyzed by counting the total number of lateral branches in 3-4 primary ducts and five secondary ducts (between lymph node and distal ends of ducts) at 12.5x magnification. The results were expressed as a number of lateral branches per mm of a duct (primary/secondary). The quantitative results of ductal termini and lateral branching were discussed as ductal end-point densities and branching densities respectively, as described previously [100]. The total area of the MG ductal tree, the length of the primary duct (from nipple to end of the duct) and lymph node area, were quantified using Image-J software.

2.15. Culture of 4T1 cells and orthotopic inoculation:

Mammary adenocarcinoma 4T1 cells derived from BALB/c mice [228] were used in an orthotopic mammary tumor model. These tumor cells were a generous gift from Dr. Fred R. Miller [228]. The cells were grown in 4T1 culture media at 37^{o}C with 5% CO_2. The composition of the media is shown in Table 5.

Cells growing in log phase (40-60% confluent) were treated briefly with 0.05% trypsin-EDTA (Gibco# 25300-054), washed twice at 4^{o}C and re-suspended in Ca^{++}-Mg^{++} free (CMF) Hank's balanced salt solution (HBSS) (Gibco# 14170-112). Live cells were counted using trypan blue (Corning, 25-900CI) and re-suspended in concentrations of 5000 cells/100ul CMF-HBSS [ ]. For tumor inoculation, 100ul of 4T1 cells were injected in the left inguinal (fifth) mammary fat pad (MFP).

2.16. Tumor growth and survival analyses

The MFPs were palpated daily, from day 3 of injection until all animals had palpable tumors. Body weights and tumor volumes were measured every 3 days. Tumor volume was calculated using the formula (0.5 (short diameter) ^{2} x long diameter). For survival analysis, mice were monitored for the signs of morbidity and autopsied at morbidity or necropsied at death. The days between tumor injection and autopsy or death was recorded as survival days.

Table 5. Composition of 4T1 culture media

Reagent name	Supplier	Catalogue	Volume (ml)
Dulbecco's modified eagle medium (DMEM)	Gibco, Grand Island NY	11995-065	500
Fetal bovine serum	Atlanta biologics	S11150	50
100 X MEM Vitamins	Gibco, Grand Island NY	11120-052	10
200 mM L-Glutamate	Gibco, Grand Island NY	25030-081	5
100 mM Sodium pyruvate	Gibco, Grand Island NY	11360-070	5
50 X MEM Amino acids	Gibco, Grand Island NY	11130-051	5
100 X Non essential amino acids	GE Healthcare	SH30238.01	5
50 mg/ml Gentamycine	Gibco, Grand Island NY	15750-060	2.5

2.17. Metastases analyses:

Groups of mice were autopsied on day 35 post tumor injection for single time point metastases analyses in two independent experiments. For overt metastases (overt-met) analyses, whole organs (lungs, livers, hearts and kidneys) were fixed in Bouin's fixative for 24 hours prior to counting of the total number of nodules of overt-mets per organ (n=10/group/experiment, two independent experiments) using a Stereoscope (Zeiss # Stemi DV4). After overt-met analysis, heart and kidneys were sectioned longitudinally (including cephalo-caudal regions of each organ). One-half of the organ was embedded, and cross-sectioned from the deeper tissue side. A piece of liver and spleen were also embedded and sectioned. Both ovaries and a half of the CMGs were collected and fixed in 10% normal buffered formalin (NBF) (Fisher # SF100) for 24 hours at RT prior to embedding and cross-sectioning. Histological analyses for the presence of metastatic foci in cross/longitudinal sections of organs was performed in all animals from a single experiment (n=10/group). The histologically analyzed metastatic foci were abbreviated as histologically-observed metastases (HO-met). All the tissues were sectioned at 4 µm thickness and stained with H & E for HO-met analyses. The number and size of HO-met foci per cross-section of heart, kidney and ovaries were evaluated quantitatively using Image-J software. The presence of metastases in liver and spleen was confirmed by scanning sections of the tissue at 200x and 400x. Individual tumor cells (ITC) were identified based on 4T1 tumor cell morphology.

2.18. Bone metastasis analyses:

For bone metastasis analyses, both hind limbs were collected and fixed in 10% NBF for 24 hours, washed in 1x PBS, and muscles removed to isolate the femurs and tibias. The

bones were decalcified by immersing them in decalcification solution (15% EDTA in 1X PBS, pH 7.6) at 4ºC until the bones became soft enough to section (10-15 days). Lateral-longitudinally sectioned femurs-tibias (4 µm) were stained with H & E. Bone metastases were analyzed in medullary spaces of epiphysis/metaphysis and diaphysis of the femurs and the epiphysis/metaphysis areas of the tibia and presented as the number and size of HO-met present per longitudinal section of femurs-tibias.

2.19. Apoptotic nuclei detection in tumor tissue (Colorimetric method)

Apoptotic nuclei were detected using "*In situ Apoptosis Detection Kit*" (ab206386, Abcam) as per the kit's protocol. Briefly, deparafinized and rehydrated tumor sections were permeabilized with Proteinase K for 20 minutes followed by washing in 1X TBS. Endogenous peroxidases were inactivated by treating the sections with 3% H_2O_2. Then the sections were treated with Terminal deoxynucleotidyl Transferase (TdT) and detected with a conjugate and DAB chromogen based method, and counter-stained with methyl green. Apoptotic nuclei were analyzed in the subcapsular areas (oxic) of the tumors and evaluated in 10 HPF per each tumor sample.

2.20. Statistical Analyses:

Results are expressed as a mean ± standard error of the mean (SEM) for animal weights, liver/MG/abdominal fat weights of NTB studies and IHC quantification data, and were compared between the dietary groups by Student's t-test for independent samples. The differences in the incidences of metastases was analyzed by Fisher's exact test for the differences in the proportions between the experimental groups. Metastases analyses

data including organ, weights, metastases number, and HO-met area were presented as median values and compared by Mann Whitney's test. Longitudinal plots for change in body weights and tumor growth and dietary consumption were based on the mean ± SEM value for each time point, and the curves between the dietary groups were compared by repeated measures analysis (two-way). Graphs were plotted using Sigma Plot or Graph-pad Prism. Survival analysis was presented as Kaplan-Meier plots and statistical significance was analyzed using the log-rank test. All data were analyzed using SPSS for statistical significance. For qRT-PCR data, dCt values were compared by independent sample t-test. In all instances, differences where $p<0.05$ were considered to be statistically significant.

Chapter 3:
Long-Chain Omega-3 Polyunsaturated Fatty Acids Modulate Mammary Gland Composition and Inflammation[2]

3.1. Abstract

Studies in rodents have shown that dietary modifications as MGs develop, regulates susceptibility to mammary tumor initiation. However, the effects of dietary PUFA composition on MGs in adult life, remains poorly understood. This study investigated morphological alterations and inflammatory microenvironments in the MGs of adult mice fed isocaloric and isolipidic liquid diets with varying compositions of ω-6 and LC-ω-3FA that were pair-fed. Despite similar consumption levels of the diets, mice fed the ω-3 diet had significantly lower body-weight gains, and abdominal-fat and mammary fat pad (MFP) weights. Fatty acid analysis showed significantly higher levels of LC-ω-3FAs in the MFPs of mice on the ω-3 diet, while in the MFPs from the ω-6 group, LC-ω-3FAs were undetectable. Our study revealed that MGs from ω-3 group had a significantly lower ductal end-point density, branching density, an absence of ductal sprouts, a thinner ductal stroma, fewer proliferating epithelial cells and lower transcription levels of estrogen receptor 1 and amphiregulin. An analysis of the MFP and abdominal-fat showed significantly smaller adipocytes in the ω-3 group, which was accompanied by lower transcription levels of leptin, IGF1, and IGF1R. Further, MFPs from the ω-3 group had significantly decreased numbers and sizes of crown-like-structures (CLS), F4/80+

[2] A part of this chapter is derived from previously published original article: **Saraswoti Khadge**, Geoffrey M. Thiele, John Graham Sharp, Timothy R. McGuire, Lynell W. Klassen, Paul N. Black, Concetta C. DiRusso, and James E. Talmadge, **"Long-Chain Omega-3 Polyunsaturated Fatty Acids Modulate Mammary Gland Composition and Inflammation,"** Journal of Mammary Gland Biology and Neoplasia, Volume 23, Issue 1-2, pp 43-58, June 2018.

macrophages and decreased expression of proinflammatory mediators including Ptgs2, IL6, CCL2, TNFα, NFκB, and IFNγ. Together, these results support dietary LC-ω-3FA regulation of MG structure and density and adipose tissue inflammation with the potential for dietary LC-ω-3FA to decrease the risk of MG tumor formation.

3.2. Introduction

A growing body of evidence suggests a linkage between MG development and diet [251] that can also modify breast cancer risk [252]. The majority of studies into dietary PUFA regulation of MG development have been undertaken with *in utero*, fetal, post-natal and prepubertal manipulated rodents but are rarely undertaken in adult mice. These studies have shown that feeding a LC-ω-3FA (fish oil)-containing diet reduces the number of terminal end buds (TEB), which are a marker of MG development [114, 253, 254]. Indeed, rodent studies have suggested that ω-6 and ω-3 PUFA have opposing effects on TEB formation, with ω-3 PUFA reducing the number of TEBs [124, 251, 254] and MG-density [255], while high ω-6 PUFA diets reduce the differentiation of TEBs to alveolar buds [256]. During puberty, the majority of TEBs differentiate into terminal ducts or alveolar buds, while lateral branching of MG ducts occurs post-pubertal. As tumor initiation typically occurs post pubertal, it is critical to study the effect of PUFA on MG differentiation in adult mice. Further, it is critical that studies into dietary regulation of MG development be undertaken using isolipidic diets differing only in PUFA composition [254]; specifically, the presence or absence of LC-ω-3FA. It is clear that dietary PUFA composition can regulate carcinogenesis and tumor progression [257]; however, the potential for dietary epigenetic modification of molecular targets, in early life, requires additional investigation [258] as do the effects on post-pubertal MG structure and composition

MFPs in rodents are comprised of epithelial cells in the MG (or ductal tree), and adipose tissue, stroma and extracellular matrix which provides physical support for the MG ductal network [259]. Recently, mammary adipocytes have also been shown to have an active role in the chronic inflammation [260] that is associated with adipocyte IL6 secretion, and likely plays a regulatory role in mammary cancer induction and progression [189, 261].

Adipocytes within the MFP contribute to the regulation of MG development. For example, in the absence of mammary fat in A-ZIP/F-1 transgenic mice, abnormal MG development occurs [262]. MG adipocytes also regulate changes in mammary tissue during pregnancy, lactation, and involution, via local signals between mammary epithelium and adipocytes [261].

Emerging research suggests that the timing of PUFA exposure is critical to the increased risk of mammary cancer [263]. As MG development is age-dependent, specifically during puberty, most studies to date have used pre-pubertal exposure [264, 265]. These studies have demonstrated that pre-pubertal ω-3 PUFA incorporation into the MG regulates the morphological development of the MG during puberty [265], and reduces mammary tumorigenesis [118]. However, the role of dietary LC-ω-3FA exposure in post-pubertal life, and its regulation of the MG stromal microenvironments and morphogenesis is little studied.

Based on these observations, we examined the hypothesis that dietary LC-ω-3FA regulates mammary gland morphology. We report that in the absence of dietary LC-ω-3FA the FA composition within the adipose tissue of MG varies, resulting in local-regional inflammation and increased ductal branching density and mammary epithelial cell proliferation, all of which may potentially contribute to MG carcinogenesis.

3.3. Results

3.3.1. Food consumption, body weight, and MG and abdominal fat weights:

Pair-feeding was undertaken, as described previously [266], to assure isocaloric and isolipidic consumption. To acclimate the mice to a liquid diet, the first five days of feeding was *ad libitum.* During this time, average liquid diet intake was assessed daily, with the observation of increased diet consumption of the ω-6 diet. Based on this observation, the ω-3 diet consumption was used as the baseline for pair feeding. During this five-day period of *ad libitum* feeding the ω-6 group of mice gained more weight than the ω-3 group in association with increased liquid diet consumption. Following the initiation of pair feeding, on day 6, no significant differences in food intake occurred between the dietary groups. (Fig. 8A). The initial body weights were comparable between the dietary groups. However, mice (n=20) on the ω-3 diets had a significantly lower body weight gain throughout the study (Fig. 8B), despite the use of isocaloric diets. The weights of the abdominal fat in the mice on the ω-3 diet were 45% lower (Fig. 8C) and 42% lower as abdominal fat weight relative to the body weight (Fig. 8D) compared to the ω-6 group (n=8) (both $p<0.05$). Similarly, the weight of the fourth (left inguinal) MGs were assessed after the mice were fed the diets for 20 weeks (n=10). Significant decreases in the MG weights (-43%) (Fig. 8E) and MG weight relative to the body weight (-41%) (Fig. 8F) were observed in the mice on the ω-3 diets compared to the MGs from the mice receiving the ω-6 diets ($p<0.05$) (n=10).

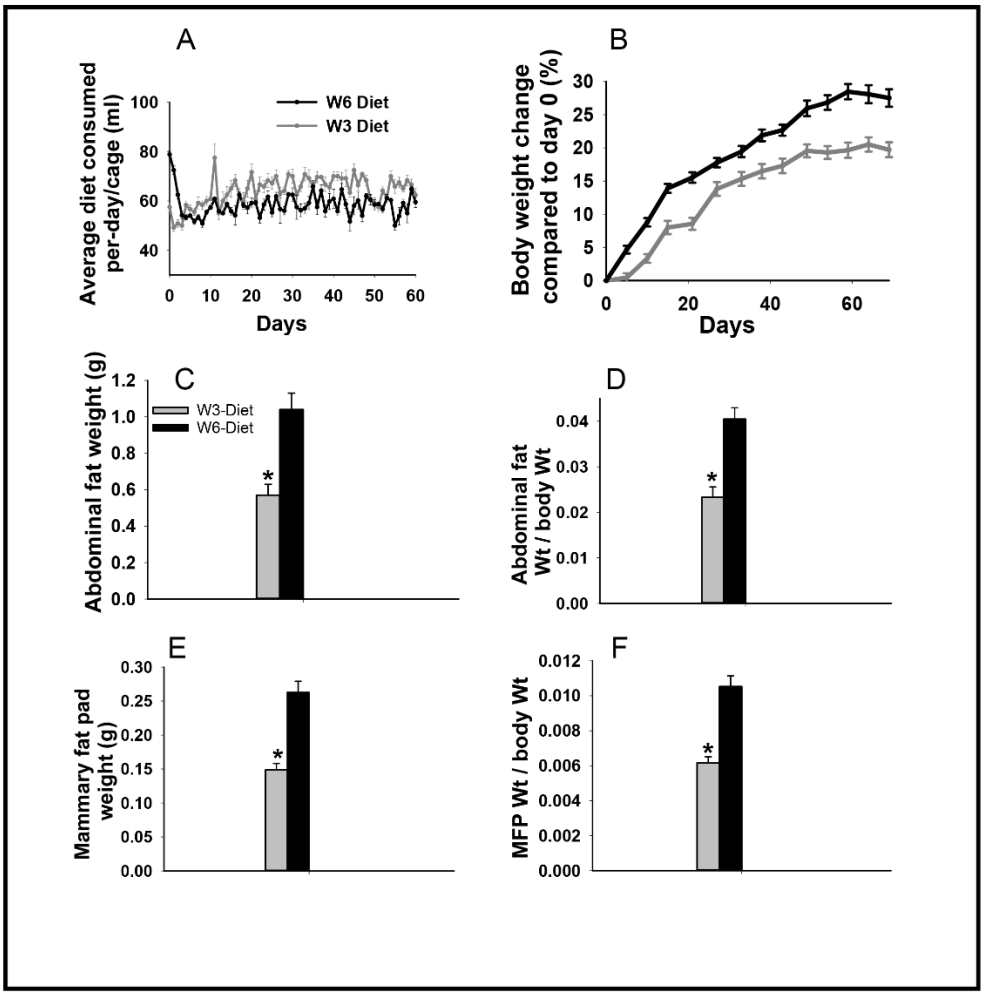
A
Average diet consumed per-day/cage (ml)
W6 Diet
W3 Diet
Days
B
Body weight change compared to day 0 (%)
Days
C
Abdominal fat weight (g)
W3-Diet
W6-Diet
D
Abdominal fat Wt / body Wt
E
Mammary fat pad weight (g)
F
MFP Wt / body Wt

Figure 8. Effects of LC-ω-3FAs on body weight, MG weight, and abdominal fat deposits

Mice were pair-fed omega-6 (ω-6) and omega-3 (ω-3) PUFA diets for 10 - 20 weeks [n=20/group]. The average amount of diet consumed/day (A). Differences in percent changes in body weights between the pair-fed groups compared by a repeated measure test (B). Differences in abdominal adipose tissues deposits (C) [n=10/group], and abdominal fat weight relative to the body weight (D). Weights of the fourth rear MG at the age of 30 weeks (E). MG weight relative to body weight (F) [n=10/group].

3.3.2. Modulation of MG, FA profile by the ω-3 versus ω-6 isolipidic PUFA diets:

The FA composition of the diets and MFPs are shown in Table 6. There was a significant effect of the dietary FA composition on the lipid profile of the MFPs from mice fed the diets for 10 weeks. The ratio of ω-6:ω-3 FA of the ω-6 and ω-3 diet were 21:1 and 0.7:1 respectively. The ω-6 diet did not have detectable levels of LC-ω-3FA such as EPA and DHA, which were major sources of ω-3FA in the ω-3 diet. Consistent with the dietary FA composition, significantly higher levels of ω-3FAs such as LNA (0.7 ± 0.2), EPA (11.1 ± 1.2) and DHA (7.5 ± 0.6) µg/mg were observed in the MFPs of mice fed the ω-3 diet. In contrast, all ω-3FAs were below the detection levels in the MFPs of the ω-6 diet-feddiet-fed mice. The levels of ω-6FAs were not significantly different between mice fed ω-6 and ω-3 diets, nor in the MFPs from mice fed the respective diets. However, a lack of Lc-ω-3FAs in the ω-6 diet significantly increased the ratio of ω-6:ω-3 FA in MFPs from the mice fed the ω-6 diet. Besides PUFA, the levels of total saturated fatty acid (SFA) were increased (1.5 fold), and oleic acid (a major monounsaturated fatty acid from olive oil) was decreased (1.5 fold) in MFPs from mice fed a ω-3 diet compared to the levels in MFP from the ω-6 diet group. The total levels of FAs were similar between the ω-6 and ω-3 diets and not significantly different between the MFPs from the mice fed the diets.

Fatty Acid (FA) Name	Carbon chain	Diet (FA µg/ml of diet)		Mammary fat pad (FA µg/mg of MFP ± SEM)	
		ω-3	ω-6	ω-3	ω-6
Saturated fatty acid (SFA)					
Tetradecanoate	C14:0	0	0.2	6.3 ± 0.7	2.8 ± 0.6
Hexadecenoic	C16:0	1.53	3.02	105.3 ± 8.8 *****	68.5 ± 8.3
Octadecenoic	C18:0	0.28	0.76	19.8 ± 2.5	13.9 ± 2.0
Monounsaturated fatty acid (MUFA)					
9-Hexadecenoic	C16:1	0	0.2	18.2 **±** 1.4	12.3 ± 2.4
9-Octadecenoic	C18:1	3.77	15.62	166.1 ± 7.0 *****	252.2 ± 31.4
cis-13-Eicosenoic	C20:1	0.7	0	9.2 ± 0.5 *****	3.0 ± 0.5
13-Docosenoic acid	C22:1	0.25	0	1.3 ± 0.1 *****	0.0 ± 0.0
Polyunsaturated fatty acid (ω-6 FA)					
cis-8,11-Octadecadienoic (Linoleic)	C18:2	6.67	5.03	71.3 ± 3.3	55.2 ± 7.4
cis-5,8,11,14-Eicosatetraenoic (Arachedonic acid; AA)	C20:4	0.51	0	0.7 ± 0.2	0.2 ± 0.2
Polyunsaturated fatty acid (ω-3 FA)					
cis-9,12,15-Octadecatrienoic acid (Linolenic)	C18:3	0.14	0.24	0.7 ± 0.2 *****	0.0 ± 0.0
7,10,13-Eicosatrienoic	C20:3	0	0	0.7 ± 0.2 *****	0.0 ± 0.0
cis-5,8,11,14,17-Eicosapentaenoic (EPA)	C20:5	7.52	0	11.1 ± 1.2 *	0.0 ± 0.0
cis-4,7,10,13,16,19-Docosahexaenoic (DHA)	C22:6	2.64	0	7.5 ± 0.6 *****	0.0 ± 0.0
cis-4,7,10,13,16-Docosapentaenoic acid	C22:5	0.26	0	1.7 ± 0.1 *****	0.0 ± 0.0
Total omega 6 FA level		**7.18**	**5.03**	**72 ± 3.5**	**55.5 ± 7.3**
Total omega 3 FA level		**10.56**	**0.24**	**21 ± 2.0 ***	**0.0 ± 0.0**
Total MUFA level		**4.72**	**15.82**	**193.5 ± 8.7**	**267.5 ± 32.6**
Total SFA level		**1.81**	**3.98**	**131.4 ± 11.9***	**85.3 ±10.0**
Total FA mass per mg/ml of MFP/diet		**24.27**	**25.07**	**420.3 ± 20.1**	**442.2 ± 47.0**
Ratio of total ω-6 FA to ω-3 FA (ω-6:ω-3)		**0.7:1**	**21:1**	**3.4:1**	**55.5:0**

Table 6. Fatty acid profiles of the diets and mammary fat pads

MFPs were collected from the mice fed respective diets for 10 weeks. (n=5/group). The ready to use diets were used for fatty acid (FA) analysis. FA profile was measured by gas chromatographic mass spectrophotometry (GC-MS) analysis. The results were expressed as microgram of fatty acid per milligram of MFP tissue.

3.3.3. Dietary PUFA regulation of mammary ductal branching

A histopathologic analysis of the inguinal MFPs of mice fed the diets for 20 weeks, was performed to evaluate structural/morphological alterations in MGs. (n=10). A significant morphological difference was observed in the ductal tree network and the total glandular area between the two dietary groups (Fig. 9A and 9B). The total area of the MG tree of MFPs from ω-3 fed mice was 20% smaller (143.3 ± 10.4 mm^2) relative to the area of the MFPs from ω-6 fed mice (177.6 ± 11.8 mm^2) ($p<0.05$) (Fig. 9C). A comparison of the quantitative differences in the ductal tree compared the number of ductal termini (end-point density) and the extent of lateral branching (branching density). Since the mice used in the study were post-pubertal adults, TEBs had differentiated into terminal ducts, alveolar buds or end buds and we use the term ductal termini for these end structures. MFPs from mice fed the ω-3 diet had 63% fewer ductal termini/HPF (25.9 ± 1.9) compared to the numbers in the MFPs from ω-6 diet-fed mice (70.9 ± 5; $p<0.05$) (Fig. 9D). Similarly, there were significantly fewer lateral branches per mm of primary ducts (0.7 ± 0.1) (a 60% decrease) and secondary ducts (1.3 ± 0.1) (a 65% decrease) compared to the numbers in each mm of primary duct (1.7 ± 0.1) and secondary ducts (3.8 ± 0.2) of MFPs from the ω-6 diet-fed group (Fig. 9E). In the microscopic analysis, there was a significant difference in the ductal morphology, including the presence of ductal sprouts, along the ductal wall in MFPs from ω-6 diet-fed mice, which were absent in the ducts of the MFPs from ω-3 diet-fed mice (Fig. 9F-9G). Despite the differences in lateral branching, there was no significant differences in the length of the primary ducts in mice fed the ω-3 diet (25.9 ± 1.2 mm) compared to the primary ductal length (28.1 ± 1.6 mm) in MFPs from ω-6 diet-fed mice. Similarly, the average lymph node (LN) area (2.7 ± 0.1 mm^2) of the ω-3

diet-fed mice were not significantly different from the LN area (2.7 ± 0.3 mm^2) of ω-6 diet-fed mice.

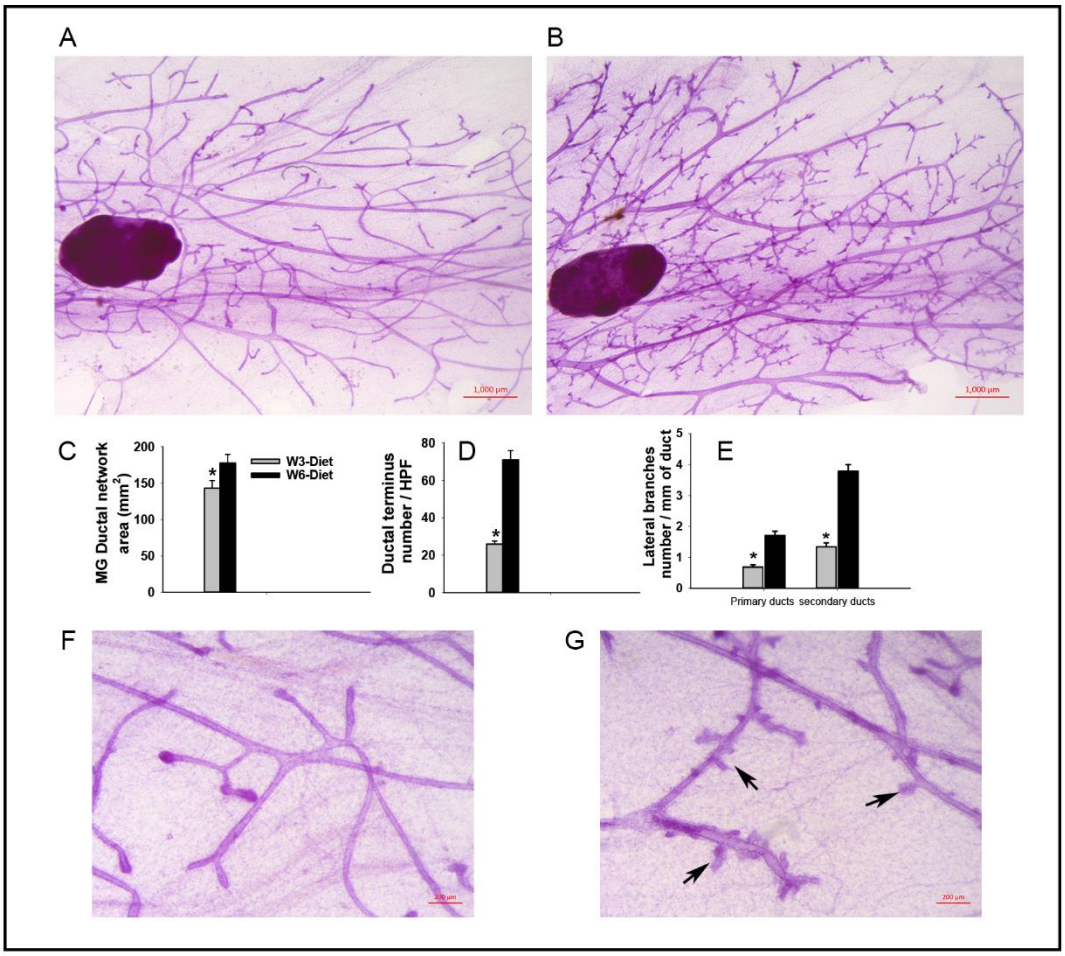
A
B
1,000 µm
1,000 µm
C
MG Ductal network area (mm²)
200
150
100
50
0
W3-Diet
W6-Diet
*
D
Ductal terminus number / HPF
80
60
40
20
0
*
E
Lateral branches number / mm of duct
5
4
3
2
1
0
*
*
Primary ducts
secondary ducts
F
G
200 µm
200 µm

Figure 9. Effects of LC-ω-3FAs on MG ductal branching and morphology

MGs were analyzed for ductal termini (end-point density), lateral branching (branching density) and sprouts in mice fed the diets for 20 weeks [n=10/group]. Whole mounts of carmine-alum stained fourth rear, MGs from 30-week old ω-3 diet-fed mouse (A) and ω-6 diet-fed mouse diets (A) [n=10]. MGs were analyzed for the number (B). The total ductal tree area (C), number of ductal terminus (D) and number of lateral branches/mm of primary or secondary ducts (E). High power analysis of ductal branches showing absence of sprouts in MFP of ω-3 diet-fed mouse (F) and presence of sprouts (shown by arrows) in MFP of ω-6 diet-fed mouse (G). Images of (A and B) are 12.5x and (F and G) are 40x magnification. [*=$p<0.05$]

3.3.4. Dietary PUFA regulation of ductal epithelial cell proliferation

The ductal histology of the MFPs from mice, fed each of the diets for 20 weeks, were analyzed using Mason's trichrome stain and proliferating epithelial cells assessed by Ki67 staining. As shown in a representative Mason's trichrome stained MG duct (Fig. 10A), we analyzed ductal lumen (DL) area, ductal epithelium (DE) area and ductal connective tissue (blue stained) or ductal stroma (DS) area. The ω-3 diet feeding for 20 weeks (Fig. 10B – 10E) resulted in a 34% decrease in the DE area (1883.3 ± 145.0 μm^2) and a 54% decrease in the DS area (3034.5 ± 377.9 μm^2), compared to the DE area (2863 ± 189.6 μm^2) and the DS area (6,593.1 ± 493.9 μm^2) respectively from mice fed the ω-6 diets for the same duration ($p<0.05$). Further, the effects on ductal size, based on a comparison of the ductal lumen (DL) area between the dietary groups, documented that mice fed a ω-3 diet had 42% smaller ducts with an average DL area of 1,497.1 ± 243.6 μm^2, compared to the MFPs from ω-6 fed mice, (2,568.7 ± 380.9 μm^2) ($p<0.05$). As there were significant differences in ductal size, we further evaluated the area of DE and DS relative to the DL. The results showed that the DS relative to DL were 33% smaller in the MFPs of ω-3 diet-fed mice (3.6 ± 0.3) compared to the same in MFPs of the ω-6 group (5.3 ± 0.5) (Fig. 10F) ($p<0.05$). However, there was no significant difference in the DE relative to DL area between the dietary groups (Fig. 10G). These results suggest that the differences in ductal connective tissue were independent of ductal size; however, the size of ducts between the dietary groups might affect the DE area. Thus, proliferating epithelial cells were evaluated to confirm the effect of dietary PUFA on DE, which showed there were 88% fewer proliferating cells in the DE of ω-3 diet-fed mice (1 ± 0.5) compared to ω-6 diet-fed mice (8.3 ± 3.1) (Fig. 10H – 10J) ($p<0.05$). The regulation of estrogen signaling is one mechanism of epithelial proliferation in MG ducts. To address this, we assessed the relative mRNA expression of amphiregulin (AREG) and estrogen receptor-1 (ESR1) as a

potential mechanism for the dietary PUFA regulation of DE cell proliferation. These studies revealed that the MFPs from mice fed the ω-6 diet had 3.1-fold and 1.4-fold higher transcription levels of AREG and ESR1, respectively, compared to MFPs from age-matched, isocaloric ω-3 diet-fed mice (Fig. 10K). However, there were no differences in the levels of progesterone receptor and prolactin mRNA levels were below the level of detection (data not shown).

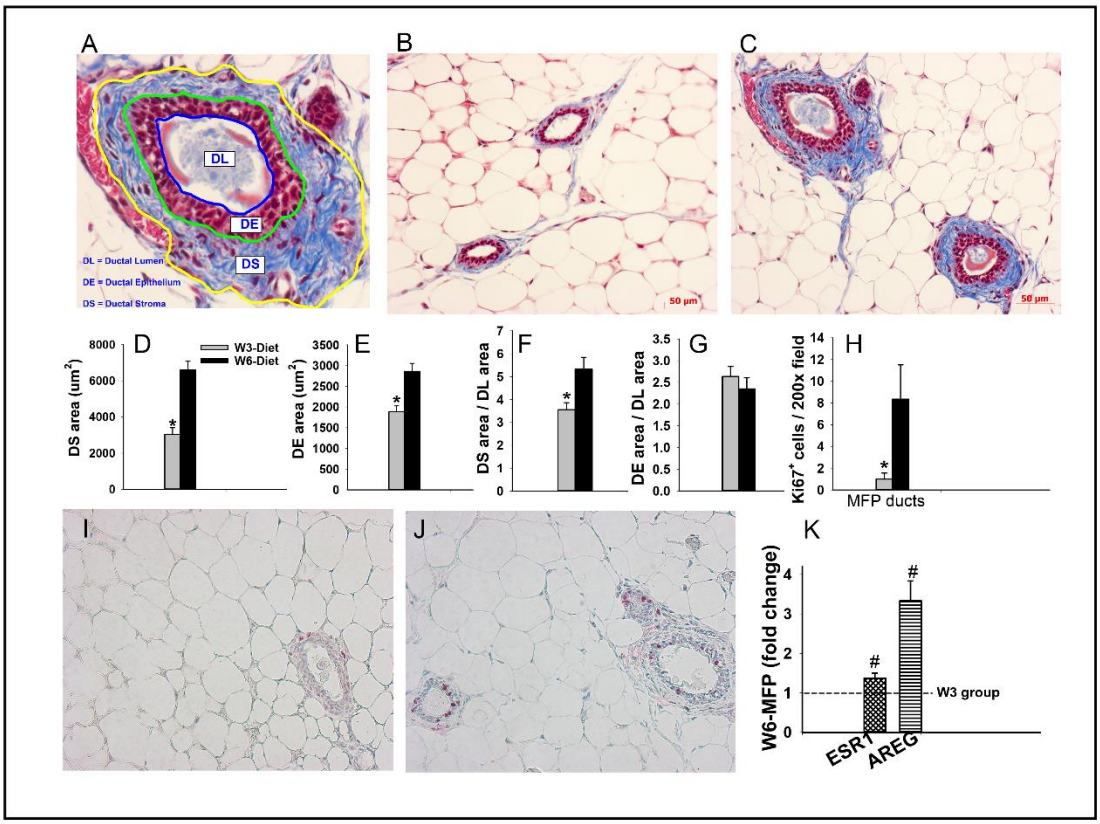
A
DL
DE
DS
DL = Ductal Lumen
DE = Ductal Epithelium
DS = Ductal Stroma
B
50 μm
C
50 μm
D
W3-Diet
W6-Diet
DS area (um2)
E
DE area (um2)
F
DS area / DL area
G
DE area / DL area
H
Ki67+ cells / 200x field
MFP ducts
I
J
K
W6-MFP (fold change)
W3 group
ESR1
AREG

Figure 10. Effects of LC-ω-3FAs on MG ductal histology

Mammary ductal histology analyzed in trichrome stained MFP sections, using 200x images (n=10fields/mouse from five mice/group). In each duct, the area of lumen marked as (DL), epithelium (DE) and stroma or connective tissue (DS) were analyzed as illustrated (A). Masson's trichrome stained MFP from ω-3 diet-fed mice (B) and ω-6 diet-fed mice (C). The difference in the area of ductal stroma (D), ductal epithelium (E), stroma relative to luminal area (F) and epithelial area relative to luminal area (G) were analyzed. MFP sections stained with the anti-Ki67 antibody were analyzed for $Ki67^{+}$ proliferating ductal epithelial cells (H). Images showing $Ki67^{+}$ cells in ducts of MFP from ω-3 diet-fed mouse (I) and ω-6 mouse (J). Relative mRNA expression (fold change compared to the ω-3 group) of ESR1 and AREG in MFP of mice fed the ω-6 diet for 20 weeks (n=15/group) [$^{\#}$ =$p<0.05$ compared to the ω-3 group]. Images were taken at a magnification of 200x (A and F) [*=$p<0.05$]

3.3.5. Dietary PUFA regulation of MFP and abdominal fat adipocytes

A comparison of adipocyte histology in the MFPs and abdominal fat deposits of mice, fed the two diets for 20 weeks, revealed (Fig. 11) that adipocytes in the MFPs of mice fed the ω-3 diet, were approximately 45% smaller compared to MFP adipocytes from ω-6 diet-fed mice ($p<0.05$) (Fig. 11A and 11B). The increase in MFP adipocyte size was validated by an analysis of the adipocyte number/100x image, which documented that the adipocyte number/field was increased 67% in the MFPs of the ω-3 diet-fed group, compared to the ω-6 diet-fed mice (Fig. 11A and 11B) ($p<0.05$). Consistent with variations in MFP adipocyte sizes, an analysis of adipocytes size and the number of adipocytes/100x field in abdominal fat showed that mice fed the ω-3 diet had 53% smaller adipocytes and 113% more adipocytes per 100X field compared to isocaloric ω-6 diet-fed mice (Fig. 11C and 11D) ($p<0.05$). We also assessed potential mechanisms for the differences in adipocyte size. This focused on alterations in fat storage/metabolism in the MFP and abdominal fat between the dietary groups by analyzing the relative mRNA expression of genes associated with fat metabolism. The results revealed that mice on the ω-6 diet had significantly increased mRNA expression for leptin (LEP) levels (3.1-fold), insulin-like growth factor-1 (IGF1) (1.8-fold) and IGF1 receptor (IGF1R) (1.7-fold) compared to the MFPs from mice fed the ω-3 diet (Fig. 11E) ($p<0.05$). Similarly, mRNA analysis of the abdominal fat showed that mice fed an ω-6 diet had significantly increased mRNA levels of Lep (5.1-fold) and IGF1 (1.9-fold) but did not differ in the expression of IGF1 (0.6-fold) compared to the mice fed diets high in ω-3 FA. (Fig. 11F).

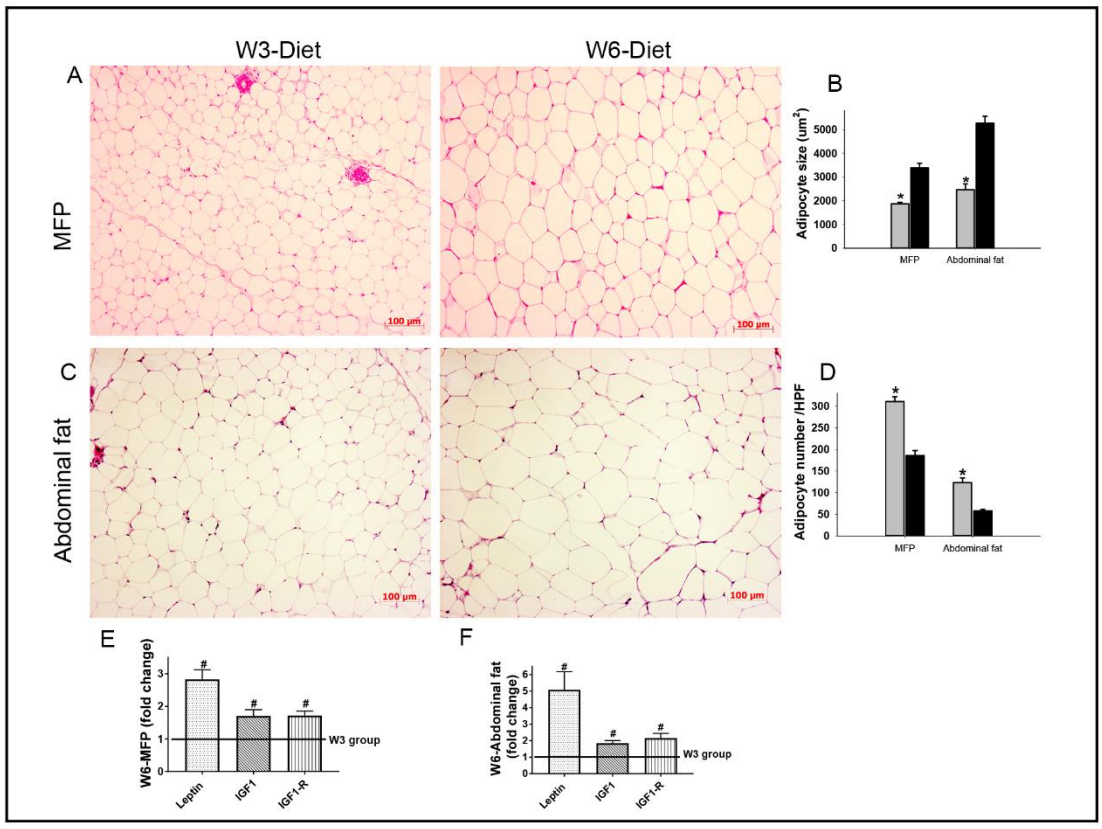
W3-Diet
W6-Diet
A
MFP
100 μm
B
Adipocyte size (um²)
5000
4000
3000
2000
1000
0
MFP
Abdominal fat
C
Abdominal fat
D
Adipocyte number /HPF
300
250
200
150
100
50
0
E
W6-MFP (fold change)
W3 group
Leptin
IGF1
IGF1-R
F
W6-Abdominal fat (fold change)

Figure 11. Effects of LC-ω-3FAs on adipocytes histology and metabolic gene expression

Analysis of adipocytes in H & E stained mammary fat pad (MFP) (A) by measuring an average adipocyte size (area) and the number of adipocytes per 100x field (B) [10 fields/mouse in five mice]. H and E stained sections of abdominal fat (C), adipocyte size and the number of adipocytes per 200x field (D) [n=10 fields/mouse in five mice]. Relative mRNA expression (fold change compared to ω-3) of leptin, IGF1, and IGF1R in MFP (E) [n=15/group] and an abdominal fat of mice fed an ω-6 diet for 20 weeks (F) [n=8/group] [$^{\#}$ =$p<0.05$ compared to ω-3 group]. Images were taken at a magnification of 100x (A and C) [*=$p<0.05$].

3.3.6. Dietary PUFA regulation of adipose tissue inflammation

The MFPs from groups of mice on the two FA diets for 10 and 20 weeks were assessed for CLS, macrophage infiltration and expression of inflammatory cytokines (Fig.12). The number of CLS per 100 adipocytes and infiltrating immune cells/CLS were analyzed in H & E stained MFP sections (Fig. 12A). Mice on the ω-3 diet had 64% fewer MFP-CLS (11.0 ± 0.8) compared to MFP-CLS (30.7 ± 3.2) in the ω-6 diet-fed mice (Fig. 12A and 12B) ($p<0.05$). Similarly, there was a 31% decrease in the number of infiltrating macrophages per CLS i.e. (2.8 ± 0.4) compared to the number of infiltrating macrophages (4.0 ± 0.6) cells/CLS in the MFPs from the ω-6 diet-fed mice (Fig. 12A and 12C). Macrophage infiltration of MFPs was confirmed by F4/80$^+$ staining (Fig. 12D). This analysis revealed that mice on the ω-3 diet had 60% fewer adipocytes with at least one adjacent F4/80$^+$ cell/s (1.5 ± 0.1) compared to adipocytes (5.2 ± 0.2) in the MFPs from ω-6 diet-fed mice (Fig. 12D and 12E) ($p<0.05$). As high levels of inflammatory mediators have been associated with the increased numbers of CLS in adipose tissue [260], we analyzed the mRNA levels of inflammatory cytokines by qRT-PCR. These studies revealed that the MFPs of mice fed an ω-6 diet, had higher levels of mRNA for Prostaglandin- Endoperoxide Synthase 2 (Ptgs2) (2.3-fold), interleukin-6 (IL6) (2.0-fold), C-C motif chemokine ligand 2 chemokine (CCL2) (2.3-fold), interferon gamma (IFNg*)* (2.8-fold), NFkB (1.5-fold) and TNFα (1.7-fold) in the MFPs from ω-6 diet-fed mice compared to ω-3 diet-fed mice (Fig. 12F).

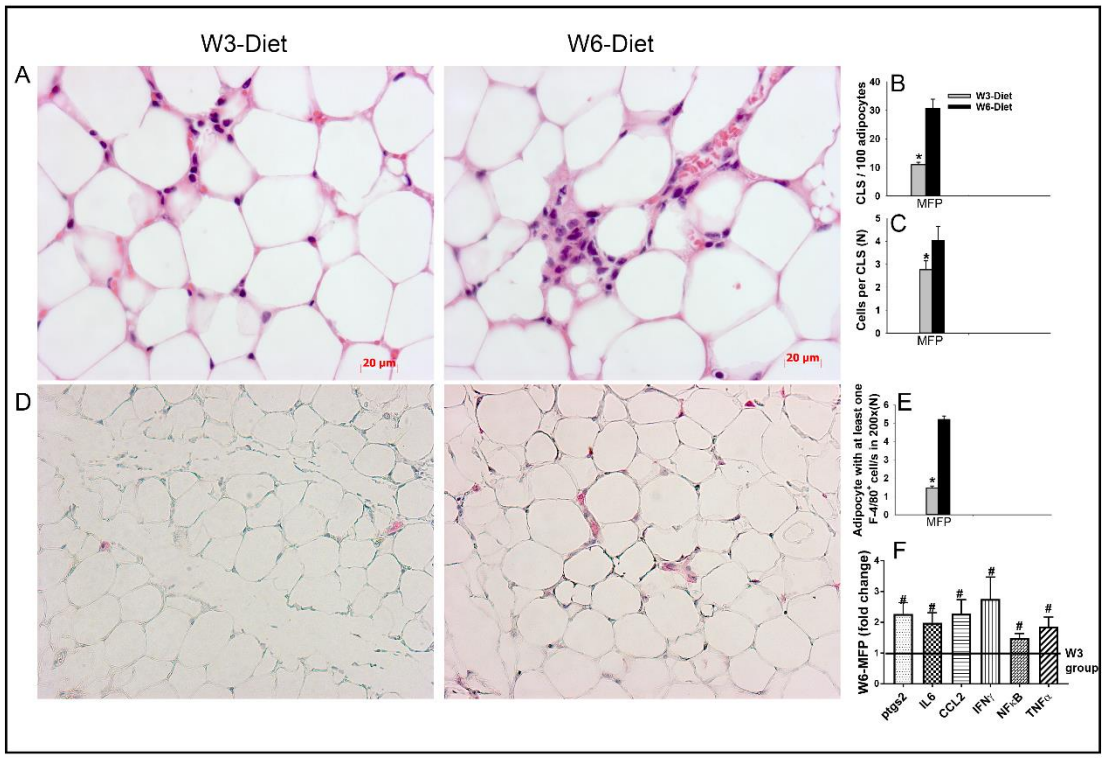
W3-Diet
W6-Diet
A
20 µm
20 µm
B
W3-Diet
W6-Diet
CLS / 100 adipocytes
MFP
C
Cells per CLS (N)
MFP
D
E
Adipocyte with at least one F-4/80+ cell/s in 200×(N)
MFP
F
W6-MFP (fold change)
W3 group
Ptgs2
IL6
CCL2
IFNγ
NFκB
TNFα

Figure 12. Effects of LC-ω-3FAs on adipose tissue inflammation

Analysis of crown-like-structures (CLS) in H & E stained mammary fat pad (MFP) (A) [n=10 fields/mouse from five mice/group]. Number of CLS per 100 adipocytes (B) and the number of inflammatory cells per CLS (C) were compared. Macrophages infiltration analyzed in F4/80-stained MFP sections (D) [n=10 fields/mouse in five mice]. The number of adipocytes surrounded by at least one $F4/80^{+}$ cell/s were counted in 200x field (E) Relative mRNA expression (fold change compared to ω-3) of inflammatory mediators, such as ptgs2, IL6, CCL2, IFNγ NFκB and TNFα in MFP of mice fed the ω-6 diet for 20 weeks (F) (n=15/group) [$^{\#}$ =$p<0.05$ compared to ω-3 group). Images were taken at a magnification of 400x (A) and 200x (D) respectively. [*=$p<0.05$]

3.4. Discussion

In this study, we provided moderate fat, isocaloric diets to pair-fed groups of mice for 10 or 20 weeks of adult life. Our goal was to assess the effects of dietary LC-ω-3FAs on the structural, inflammation and morphological alterations and differentiation of post-pubertal murine MGs. These studies demonstrated that a post-pubertal exposure to LC-ω-3FAs modulates MG FA composition, lateral branching, ductal epithelial proliferation and adipose tissue inflammation relative to the mice fed ω-6 diet, which contained high levels of ω-6FA and oleic acid but lacked LC-ω-3FAs.

A difference in dietary consumption (likely due to palatability) may be a factor when analyzing effects specific to the dietary composition, independent of total caloric intake or obesity [266]. We report that mice fed an ω-6 diet consumed significantly more liquid diet compared to the ω-3 diet during a 5-day initial *ad libitum* feeding period. This difference was subsequently controlled by pair feeding based on consumption of the ω-3 diet. Despite pair feeding and isocaloric and isolipidic diet consumption, the inclusion of LC-ω-3FA in the diet significantly decreased body weight gains and abdominal fat deposits (-45%) in mice. These results are consistent with prior studies comparing diets high in ω-3 or ω-6FA [265, 266]. In addition, studies have reported a 50% reduction in retroperitoneal fat mass [267], and a 25% reduction in epididymal fat deposits in mice fed a high ω-3FA diet [268]. This suggests that dietary LC-ω-3FA are associated with the regulation of fat mass via stimulatory or inhibitory roles of ω-6FA and ω-3FA metabolites respectively in the differentiation of adipocytes [269, 270]. Further, increasing β-oxidation and suppression of lipogenic enzymes, such as leptin in adipose tissue, may provide potential mechanisms for reducing body fat by ω-3FA exposures [271, 272].

To analyze the effects of dietary PUFA in MGs, we compared MFP weights of the fourth MG, after feeding the diets for 20 weeks, and observed 43% lighter MFPs in mice on a ω-

3 diet as compared to the ω-6 diet group. This was associated with the novel observation of a significant higher incorporation of LC-ω-3FAs in the MFPs from ω-3 diet-fed mice as compared to the MFPs from ω-6 mice. The ω-6 and ω-3 diets used in the present study contained a ω-6:ω-3 ratio of 21:1 and 0.7:1 respectively. The only ω-3FA in the ω-6 diet was ALA, whereas LC-ω-3FAs such as EPA and DHA were prominent ω-3FAs in the MGs of the ω-3 diet-fed mice (Table 2). Thus, our results document that the incorporation of LC-ω-3FAs in MFP depends directly on the dietary intake rather than *in vivo* conversion to ω-3FAs from dietary ALA. We note that dietary ALA can be endogenously converted to LC-ω-3FAs in mammals; however, the process is not efficient and <5% of ALA consumed is converted to LC-ω-3FAs in humans [273]. The observation might explain the lack of LC-ω-3FAs in the MFPs of mice fed the ω-6 diet. The LC-ω-3FA levels of mammary adipose tissue might be of clinical relevance as the breast adipose tissue from breast cancer patients has significantly higher and lower levels of ω-6FA and LC-ω-3FA respectively [274, 275]. Besides the differences in ω-3 and ω-6FA composition between the diets, the level of oleic acid was significantly higher in ω-6 diet and in MFPs of mice fed ω-6 diet compared to the levels in the ω-3 group. However, there is no significant data on oleic acid regulation of inflammation and mammary gland density published rather; oleic acid is known to prevent inflammation in adipose tissue [276]. Thus, we believe the alterations in outcomes between the dietary groups potentially be due to the differences in LC-ω-3FA levels between the diets.

Although MFP weights may be a gross indicator of MG density in animal models, significant differences in MG adiposity might influence the MG weights. Pubertal exposure to HF diets has been shown to result in heavier MGs and stunted development in C57BL/6 mice due to higher adiposity [264], while in-utero exposure to an HF-ω-6 diet increased the TEB number and enhanced susceptibility to carcinogenesis in BALB/c mice [277]. Our

data suggest that the observed difference in MFP weight might be the result of combined effects by the difference in MFP adipocyte size and alterations in MG glandular structure and composition including ductal epithelial cells proliferation and leucocytes infiltration between the dietary groups. MG development is age-dependent such that MGs undergo extensive modeling and remodeling during fetal development, puberty and pregnancy. The majority of dietary intervention studies use pre-pubertal mice that have a correlation between a higher number of TEBs and an increased risk of cancer [118, 264, 277]. However, in this study we used post-pubertal mice whose TEBs had differentiated into terminal ducts. Despite the post pubertal status, we observed that feeding an ω-3 diet in early adulthood (10-30 weeks of age) was associated with a decreased number of ductal termini, lateral branching of primary and secondary ducts, and a different total ductal area compared to isocaloric, isolipidic ω-6 diet-fed mice. Previous studies, based on ω-3 diets using a LF-ω-3 (16% energy) diet in pre-pubertal mice [118] and offspring of HF-ω-3 (39% energy) diet-fed mice, had a reduced number of TEB associating with the lower risk of tumorigenesis compared to same fat level ω-6 dietary group [278]. However, when HF-ω-3 (39% energy) were compared to LF-ω-6 (16% energy), the former developed more TEB and an increase in tumorigenesis compared to the latter, emphasizing the differential effects of fat-calories versus fat composition of the diets in MG differentiation and tumorigenesis [118]. Since we used an isocaloric diet and pair-feeding, our observation of differences are indicative of the regulation of MG structure and morphology by dietary LC-ω-3FA, independent of caloric intake and obesity. Total ductal tree area and ductal end-point and branching density represents epithelial and stromal mass of MG in animals, which can be considered equivalent to breast density as shown by mammographic scans in humans [100, 279]. Animal and clinical studies showed MG or breast density as a predictor of carcinogenic response or breast cancer risk [280, 281], while an increase in plasma DHA was associated with a decreased breast density in obese, postmenopausal

women [282]. We did not observe a significant difference in ductal lengths between the dietary groups, which might be due to the age of the mice (post-pubertal) at the start of the diet, since mice at this age have already gained full primary duct length, as a result of the extension which occurs mostly during pubertal age [265]. Rather, the effects of the diets alter the frequency of lateral branches, ductal terminus and formation of ducts (shown by a presence of sprouts in ducts in ω-6 diet-fed mice) and likely the total epithelial mass of MG. Further, future studies will need to evaluate the effects of dietary PUFA composition in mammary tumor growth and metastasis.

The observation of structural and morphological alterations in MG ductal trees was confirmed by immune-histological analysis of MG ducts. Mice fed the ω-3 diet had significantly smaller ducts, and a thinner layer of epithelium and connective tissue (stroma) in the ductal wall, as compared to the ducts from the ω-6 group. Since there was a difference in ductal size, we further evaluated those parameters relative to the ductal luminal area and found that the difference in the stroma was independent of ductal size, but the differences in epithelium thickness might be secondary to the ductal size. However, a significant decrease in proliferating ductal epithelial cells in the ω-3 group suggests a regulatory role of LC-ω-3FAs in mammary epithelial cells proliferation. Our observations of an increased ductal stroma and proliferating ductal epithelial cells in MFPs from mice receiving the ω-6 diet were in agreement with previous reports that showed higher stromal density [283] and proliferating epithelial cells [284] in mammary ducts of mice fed a high fat-diet. However, effects of isocaloric PUFA diets and/or dietary LC-ω-3FAs in ductal stromal tissue have not been reported before.

Evidence from clinical studies showed that women with cytological atypia had a higher ratio of ω-6:ω-3FA in breast tissue [285], which was associated with a reduced number of Ki-67^{+} cells with increased levels of LC-ω-3FAs in erythrocyte phospholipids [286].

Further, animal studies have shown that pre-pubertal exposure to low-fat (LF)-ω-3 was able to reduce chemical induced tumorigenesis [118] and inhibit atypical ductal hyperplasia at early stages of mammary carcinogenesis [287]. In addition, a recent finding of the regression of established pre-neoplastic lesions, by combined treatment of fish oil and tamoxifen and its correlation with tissue levels of LC-ω-3FA, demonstrated preventive and therapeutic roles of dietary LC-ω-3FAs in MG malignancies [288].

In our studies, we detected estrogen receptors in the MFPs, consistent with prior reports of their presence on adipocytes and fibroblasts, within MFPs. This supports the critical role of estrogen receptors in epithelial proliferation, mediated by both endocrine-derived and locally produced estrogen [261, 289, 290]. We also studied message levels of AREG, a ligand for epidermal growth factor receptor (EFGR), which is induced by estrogen binding to ESR1 stimulating the proliferation of mammary epithelium. Further, the overexpression of AREG has been associated with mammary tumorigenesis [291, 292]. Recent studies have shown estrogen stimulated ductal side branching by enhancing IGF-I action, while an overexpression of IGF-I was associated with ductal hyperplasia [293, 294] as observed in our studies. Further, both estrogen and IGF-I are required for progesterone-mediated formation of mature mammary gland alveoli. Thus our observation of increased lateral branching, stromal thickness and epithelial proliferation in mice fed the ω-6 diet might be due to additive effects of IGF-I to estrogen signaling, as shown by significant higher expression of AREG and ESR1 respectively in MFPs of ω-6 diet-fed mice. However, as there were no differences in progesterone receptor mRNA expression in the MFPs. These observations indicate progesterone message levels might have little effect on lateral branching of the ducts in virgin, nulliparous adult mice.

We also assessed the effects of PUFA on adipocytes, which may regulate MG ductal morphogenesis. Adipocyte hypertrophy is one mechanism for storing excess energy, and

has been observed in both omental and subcutaneous fat of obese humans [295], and in HF, high calorie-fed animals, [296] and genetically susceptible animals [297]. In our studies, we used moderate fat (MF), isocaloric diets and a pair-fed model in BALB/c mice, which are known to be less susceptible to obesity [298]. Thus, our observation of significantly smaller adipocytes in abdominal and mammary adipose tissue from ω-3 mice suggests differential regulation of lipid metabolism, storage and/or beta-oxidation in adipose tissue by dietary ω-3 and ω-6FAs [299-301]. Studies showed that ω-6FAs consumption triggered adiposity in human [302] and rodents [303] potentially by promoting pre-adipocyte differentiation or adipogenesis [304] while, DHA was able to inhibit differentiation to adipocytes and promote lipolysis [305]. In this study, the ω-3 diet-fed group had significantly higher number of adipocyte per microscopic field, which further validates our observation of smaller adipocytes in the ω-3 group. However, since we did not analyze a total adipocytes number per MFP or abdominal fat, further studies are required to analyze PUFA regulation of adipogenesis in this pair-fed model. Further, prior reports have shown that EPA can reduce hypertrophy of abdominal adipocytes [296, 306]. However, the role of LC-ω-3FAs in decreasing MFP adipocyte hypertrophy, have not been done previously, even though adipocytes have been actively researched for their crucial role in MG growth, development and carcinogenesis [261].

Adipocyte' size and fat mass are important determinants in adipokine regulation of energy homeostasis. Leptin expression increases with adipocyte size [307] and fat mass [308], while adiponectin (Adipoq) expression is inversely correlated with obesity [309]. However, the fat deposit distribution depends on the levels of leptin expression [310]. Leptin is a hormone of satiety; however, elevated plasma leptin levels do not induce a reduction of food intake nor increased energy expenditure in obese people, due to development of leptin resistance [311]. Although the mouse strain we used is less sensitive to obesity

[312], the absence of LC-ω-3FAs in the ω-6 diet led mice to gain adipose tissue resulting in a significant increase in Lep and no effects on Adipoq expression in abdominal fat tissue and MFP. Our results in Lep expression are in agreement with prior studies using HF diets with and without EPA [308, 313], while no effect in Adipoq might be due to dietary FA levels, mouse strain, or type of adipose tissue analyzed. Fish oil was able to induce epididymal adipose tissue but not subcutaneous adipose tissue [314]. Besides their role in lipid homeostasis, leptin levels have been associated with the induction of pro-inflammatory cytokines [315], and enhanced proliferation of normal and malignant breast epithelial cells [316].

In addition, we observed that a lack of dietary LC-ω-3FAs significantly enhanced expression of IGF1 and IGF1R in MFPs and abdominal fat. IGF1 was originally believed to be exclusively produced by the liver [317], but a recent study [318] showed IGF1 secretion by adipocytes and M2-macrophages. Further, ablation of IGF1R from myeloid cells results in elevated adiposity, lowered energy expenditure and increased macrophage infiltration into adipose tissue, and reduced phagocytosis [318, 319]. While IGF1 is synthesized by MG adipocytes and promotes the growth of ductal epithelium [320], overexpression of IGF1R can induce mammary epithelial hyperplasia in transgenic mice (containing human IGF-IR under a doxycycline-inducible MMTV promoter) [321] and is associated with increased risk of mammary cancer [322]. Our results are consistent with a prior study, which showed a negative correlation of dietary ω-3FA with plasma IGF1 expression and ductal density [280]. However, the effects of ω-3 in local IGF1 expression in MG and other adipose tissue have not been previously reported; thus, our results indicate a need for additional investigation. Further, the similarities in IGF1 expression, in both MFP and abdominal fat, but differential expression pattern of IGF1R, indicates

morphological similarities between adipocytes, but potentially different mechanisms of signaling.

Recent studies suggest that white blood cells, notably macrophages and eosinophils, are attracted to the end bud [323] and are essential for their development [323]. This finding raises a question regarding the regulatory role of chronic local/adipose tissue inflammation in MG pathology. Further, macrophages may also have a role in other attributes of MG morphogenesis such as lateral branching, terminal ducts, and ductal sprout formation, potential mechanisms requiring additional study. In the studies reported herein, we observed that the number/size of CLS and the number of macrophages infiltrating MGs were significantly lower in MFPs of ω-3 diet-fed mice. CLS is a hallmark of chronic adipose tissue inflammation, and increased numbers of CLS in the breast (CLS-B) have been associated with increased risk and poor prognosis of breast cancer patients in both obese individuals and those with normal BMI [324, 325]. CLS formation has been shown to enhance the expression of inflammatory cytokines/chemokines potentially further activating macrophages for clearing of apoptotic adipocytes. We observed significantly increased expression of Ptgs2, NFkB, IL6, IFNγ, and the macrophage chemoattractant CCL2 in the MFP of ω-6 diet-fed mice. These findings support an increase in pro-inflammatory signaling by ω-6 FAs and its metabolite, AA in the MFP microenvironment. In these studies, the AA levels in the MGs did not differ between the ω-6 and ω-3 diet groups; however, the MFP from ω-6 diet mice did not have detectable levels of LC-ω-3FA. Thus, our results suggested that the lack of detectable LC-ω-3FA crucial relative to the levels of AA for chronic inflammation. Local LC-ω-3FA has been shown to exert anti-inflammatory and anti-chemotactic activity regulating adipose tissue inflammation [326]. Further, constitutive expression of CCL2 by mouse mammary epithelium has been reported to increase stromal density and increase mammary tumor susceptibility [327],

emphasizing a potential role of chronic inflammation in ductal epithelial proliferation and carcinogenesis that could be modified by dietary ω-3FAs.

Findings from epidemiological, and animal studies using HF-fed or genetically obese models have provided contradictory results regarding the role of dietary LC-ω-3FA in the MG microenvironment and morphogenesis, depending on the age of mice and mixed effects of dietary calories versus composition. In summary, this research show that dietary LC-ω-3FA reduces MG density by decreasing ductal end-point density, branching density, ductal stroma and epithelial proliferation in adult mice. This occurred in an amphiregulin-estrogen and IGF-I-dependent manner, potentially by modulating adipocyte metabolism and adipose tissue inflammation. Further, an absence of detectable levels of LC-ω-3FA, such as EPA and DHA in MG might be an indicator of inflammation-associated pathologies. Future, mechanistic studies using tumor models are justified to assess a role for dietary LC-ω-3FA inhibition of mammary tumor development in adults.

After evaluation of PUFA modulations of MG microenvironments (as the primary site of mammary tumor), we extended our studies to analyze alterations in hepatic microenvironments (one of the major metastasis sites by mammary tumor) by dietary PUFA composition that are discussed in the next chapter (chapter 4).

Chapter 4:
Dietary Omega-3 and Omega-6 Polyunsaturated Fatty Acids Modulate Hepatic Pathology[3]

4.1. Abstract

Recent evidence has suggested that dietary PUFAs modulate inflammation; however, few studies have focused on the pathobiology of PUFA using isocaloric and isolipidic diets and it is unclear if the associated pathologies are due to dietary PUFA composition, lipid metabolism or obesity, as most studies compare diets fed ad libitum. Our studies used isocaloric and isolipidic liquid diets (35% of calories from fat), with differing compositions of ω-6 or LC-ω-3FAs that were pair-fed and assessed hepatic pathology, inflammation and lipid metabolism. Consistent with an isocaloric, pair-fed model we observed no significant difference in diet consumption between the groups. In contrast, the body and liver weight, total lipid level and abdominal fat deposits were significantly higher in mice fed an ω-6 diet. An analysis of the fatty acid profile in plasma and liver showed that mice on the ω-6 diet had significantly more AA in the plasma and liver, whereas, in these mice ω-3 fatty acids such as EPA were not detected and DHA was significantly lower. Histopathologic analyses documented that mice on the ω-6 diet had a significant increase in macrovesicular steatosis, extramedullary myelopoiesis (EMM), apoptotic hepatocytes and decreased glycogen storage in lobular hepatocytes, and hepatocyte proliferation relative to mice fed the diet containing LC-ω-3FAs. Together, these results support PUFA

[3] A part of this chapter is derived from previously published original article: **Saraswoti Khadge**, John Graham Sharp, Geoffrey M. Thiele, Timothy R. McGuire, Lynell W. Klassen, Michael J. Duryee, Holly C. Britton, Alicia J. Dafferner, Jordan Beck, Paul N. Black, Concetta C. DiRusso, and James E. Talmadge, **"Dietary omega-3 and omega-6 polyunsaturated fatty acids modulate hepatic pathology."** *The Journal of Nutritional Biochemistry,* Volume 52, pp 92-102, Feb. 2018.

dietary regulation of hepatic pathology and inflammation with implications for enteral feeding regulation of steatosis and other hepatic lesions.

4.2. Introduction

Omega (ω)-6 and ω-3 PUFA are essential FAs, which cannot be interconverted in humans due to a lack of ω-3 desaturase [328]. Besides their role in energy storage and production, PUFA are important constituents of biological membranes and are precursors to prostaglandin and pro-resolving lipid mediator pathways [329, 330]. Many lipid mediators derived from ω-6FA have pro-inflammatory functions [331], whereas; those synthesized from ω-3FAs have anti-inflammatory properties [332, 333]. Both ω-3 and ω-6FAs are metabolized by the same enzymes, resulting in signaling molecules with opposing bioactivities. Studies have suggested that humans evolved on a diet containing approximately a 1:1 ratio of ω-6:ω-3 PUFA [25]; however, current western diets have a high ω-6:ω-3 ratio [334]. A diet high in ω-6 PUFAs, such as LA, results in decreased tissue levels of LC-ω-3FAs, including EPA, DHA [335], and a heightened risk of chronic inflammatory disease processes [336]. In contrast, a diet containing a low ω-6:ω-3 PUFA ratio, or one that is supplemented with LC-ω-3FAs, reduces risk factors for chronic inflammatory diseases, including cardiovascular disease [337, 338], cancer [339, 340], and obesity [341, 342]. Dietary LC-ω-3FAs can also reduce hepatic inflammation, fibrosis, and steatosis in non-alcoholic fatty liver diseases (NAFLD), and non-alcoholic steatohepatitis (NASH) [343, 344].

Although hepatic lipid storage is normal, excessive intrahepatic lipid accumulation (>5.6% of liver weight) [345] is associated with steatosis, inflammation and cardiometabolic syndromes. Several mechanisms are involved in the accumulation of intrahepatic lipids, including increased accumulation of triglycerides in the liver, increased de novo lipogenesis, and/or reduced clearance and obesity [167]. Approximately 30% of Americans have a fatty liver [345], and this is increased up to 75% amongst obese

individuals [346]. Further, hepatic steatosis occurs rapidly with excess calorie consumption, independent of dietary composition [347]. In contrast, in humans a hypocaloric diet reduces steatosis [348, 349], suggesting that it is crucial to differentiate between the effects mediated by total caloric intake versus obesity to understand the role of dietary composition in the modulation of the hepatic microenvironment. The majority of studies on hepatic steatosis have used high-fat diets (60% of calories from saturated fatty acids (SFAs)) and overfeeding to provide an animal model of NAFLD [350, 351]. To date, little is known about the effects of ω-6 and ω-3FAs dietary composition, independent of caloric intake on the hepatic microenvironment.

Mature myeloid cells are terminally differentiated and continuously renewed by the proliferation of committed hematopoietic precursors, such that myelopoiesis is critical to expand and replenish the myeloid cell pool. Numerous pathologic conditions stimulate myelopoiesis, including infections, autoimmune and inflammatory conditions, neoplasia and obesity in association with neutrophilia, splenomegaly and multifocal, hepatic EMM, i.e. the formation of myeloid tissue outside of the bone marrow [352]. Hepatic EMM is normal during fetal and early development [144, 150]; however, EMM in adult tissues is associated with pathological conditions. Hepatocyte apoptosis indicates liver injury and found significantly increased in patients with NASH [353]. High fat diets have also been reported to increase the osmotic fragility of red blood cell (RBC) membranes resulting in decreased RBC counts and hemoglobin concentration [354].

In the present study, we used an isocaloric, isolipidic liquid diet combined with pair feeding that allows for controlled dietary caloric intake and limited weight changes between groups. Using this model, we examined the effects of dietary ω-6 and ω-3FAs composition on hepatic pathobiology and report that dietary PUFA composition regulates hepatic steatosis, proliferation, apoptosis and EMM using a dietary model containing

comparatively lower fat calories as a percent of total relative to previously reported studies [350, 351].

4.3. Results

4.3.1. Pair-feeding, food consumption and body weight

During the initial 5-day *ad libitum* diet acclimation period (Fig. 13A), mice on the ω-6 diet consumed more feed than those in the ω-3-diet group ($p<0.05$). Therefore, when pair-feeding was initiated on day 6, the average amount of ω-3 diet consumed was used as the baseline for the ω-6 diet (Fig. 13B). Studies of changes in body weight over time with the isocaloric and isolipidic diets using a repeated measures test revealed significant increases in weight in the mice (n=20/group) given the ω-6 diets (Fig. 13C). In part due to the increased consumption of the ω-6 diet during a brief acclimation period a significant difference in body weight was observed between the groups on day 5 (Fig. 13D). Similarly, at the pair-feeding mid points (day 20, and day 40) and at autopsy on day 69 (Fig. 13D) significant differences in body weights were also observed. Consistent with the higher body weights at autopsy (20 weeks), mice fed the ω-6 diet had significantly more abdominal fat (Fig. 13E) and abdominal fat weight relative to the body weight (Fig. 13F), as compared to ω-3 diet-fed mice. On gross examination of the livers from the ω-3 (Fig. 13G) and ω-6 diet-fed mice (Fig. 13H), livers from ω-6 diet-fed mice were lighter in color (pink) and significantly smaller than those from the ω-3 diet-fed mice, which were red-brown in color (Fig. 13H). In both groups, liver weights (Fig. 13I) and liver body weight ratios (Fig. 13J) were significantly lower in mice fed the ω-6 diet.

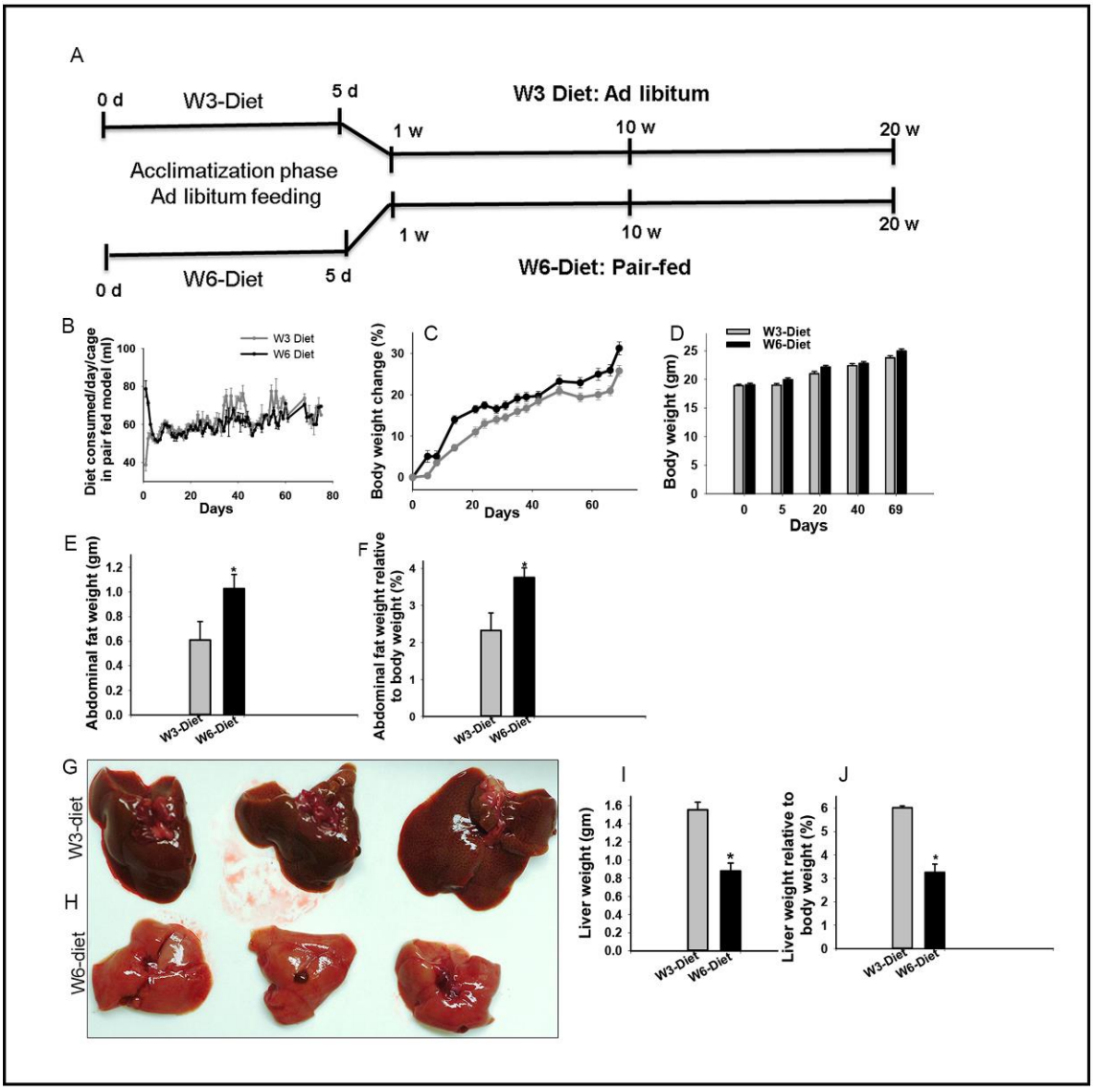
A
0 d
W3-Diet
5 d
W3 Diet: Ad libitum
1 w
10 w
20 w
Acclimatization phase
Ad libitum feeding
1 w
10 w
20 w
W6-Diet
5 d
W6-Diet: Pair-fed
0 d
B
Diet consumed/day/cage in pair fed model (ml)
W3 Diet
W6 Diet
Days
C
Body weight change (%)
Days
D
Body weight (gm)
W3-Diet
W6-Diet
Days
E
Abdominal fat weight (gm)
W3-Diet
W6-Diet
F
Abdominal fat weight relative to body weight (%)
W3-Diet
W6-Diet
G
W3-diet
H
W6-diet
I
Liver weight (gm)
W3-Diet
W6-Diet
J
Liver weight relative to body weight (%)
W3-Diet
W6-Diet

Figure 13. Isocaloric and isolipidic diets, pair-fed model and their impact on body weight

Mice were pair-fed omega- (ω-6) and omega-3 (ω-3) PUFA diets for 10 or 20 weeks. Experimental design for a pair-fed model (A). Mice were acclimatized to liquid diets by feeding *ad libitum* amounts for the first five days. Thereafter, the ω-6 diet group mice were pair-fed based on the diet consumed by the ω-3 mice on a cage basis on the preceding day. The average amount of diet consumed/day (B). Differences in percent changes in body weights between the pair-fed groups [n= 20] compared by a repeated measure test (C). Body weights before the start of the liquid diet [day 0], at the start of pair-feeding [day 5], on day 20, and day 40, of pair feeding and before autopsy on [day 69] (n=20) (D). Comparison of abdominal adipose tissues between the groups (E and F) (n=3), based on abdominal fat weight (E), as well as, fat weight relative to body weight (%) at autopsy (F). Photographs of representative livers document differences in color and size from mice fed ω-3 (G) or ω-6 (H) diets. Comparison of liver weight (I) and liver weight relative to body weight (J) (n=3). * = $p \leq 0.05$

4.3.2. Effect of PUFA diet composition on the lipid profile of plasma and liver

The lipid composition of the plasma and livers were analyzed following autopsy at 10 weeks post dietary initiation (Table-7). These studies revealed an 8-fold higher level of AA (0.64 µg/µl) in the plasma of ω-6 fed mice. However, as the ω-6 diet contained no AA (C20:4); the AA is of a metabolic origin from the ω-6FA precursor, linoleic acid (C18:2), which is contained in both diets. Both of the diets and the plasma of mice on these diets had a comparable level of C18:2, but AA product:precursor ratio (C20:4/C18:2) was 5.8 fold higher in the plasma of ω-6 diet-fed mice. Further, there was a 2.8-fold higher level of total ω-6 FAs in the plasma of ω-6 diet-fed mice compared to ω-3 diet-fed mice ($p<0.05$); even though both of the diets had comparable amounts of total ω-6 PUFAs. In contrast to ω-6 FA levels, the ω-3 PUFA, EPA was not detected in the plasma or livers of mice consuming the ω-6-diet. Similarly, levels of the ω-3FAs, DHA were 2.8-fold lower (0.05 vs. 0.14 µg/µl) in the plasma of mice fed the ω-6 diet ($p<0.05$). There were also 1.9-fold and 2.4-fold increases in the level of linoleic acid and AA respectively in the liver, resulting in a significantly higher level of total ω-6 PUFA in livers of ω-6 diet-fed mice as compared to ω-3 diet-fed mice ($p<0.05$). However, the C20:4:C18:2 FA ratio was not significantly different between the livers of ω-6 versus ω-3 diet-fed mice. Consistent with the plasma EPA levels, EPA was not detected in the livers of mice fed the ω-6 diet and the DHA content was significantly (11-fold) lower (1.5 vs. 16.5 µg/mg), compared to mice fed the ω-3 diet ($p<0.05$). We note that the mono unsaturated fatty acid (MUFA) content was significantly higher in the liver, but not in plasma of mice fed the ω-6 diet. Table 2 also has an analysis of the FA composition of the fish oil used in the diet, which contained 83.2% of total FAs in the form of ω-3FA (from C20:5 and C22:6) resulting in a ω-6:ω-3FA ratio of 0.7:1 in the ω-3 diet compared to 21:1 in the ω-6 diet. The ω-6: ω-3FA ratios of the plasma was similar to the dietary ratio.

Carbon chain length and double bonds	Fatty Acid (FA) Name	Concentration						
		Diet (µg/µl)		Plasma (µg/µl ± SEM)		Liver (µg/mg ± SEM)		Fish Oil (µg/µl)
		ω-3	ω-6	ω-3	ω-6	ω-3	ω-6	
14:0	Tetradecanoate	0.00	0.20	0.01 ± 0.01	0.00 ± 0.00	0.00 ± 0.00	0.00 ± 0.00	0.00
16:0	Hexadecanoic	1.53	3.02	0.79 ± 0.08	0.79 ± 0.10	12.32 ± 4.12	15.83 ± 1.30	9.65
16:1	9-Hexadecenoic	0.00	0.20	0.00 ± 0.00	0.01 ± 0.01	1.01 ± 0.29	1.42 ± 0.18	0.00
18:0	Octadecanoic	0.28	0.76	0.57 ± 0.14	0.38 ± 0.01	5.18 ± 1.42	5.19 ± 0.21	0.00
18:1	9-Octadecenoic	3.77	15.62	0.20 ± 0.01	0.35 ± 0.02 *	8.35 ± 0.85	42.87 ± 3.11 *	27.44
18:2	cis-8,11-Octadecadienoic (Linoleic) (ω-6)	6.67	5.03	0.31 ± 0.01	0.44 ± 0.03	5.78 ± 0.62	11.22 ± 0.83 *	4.73
18:3	cis-9,12,15-Octadecatrienoic acid (Linolenic) (ω-3)	0.14	0.24	0.00 ± 0.00	0.00 ± 0.00	0.00 ± 0.00	0.00 ± 0.00	0.00
20:1	cis-13-Eicosenoic	0.70	0.00	0.01 ± 0.01	0.00 ± 0.00	0.10 ± 0.10	0.86 ± 0.05 *	26.99
20:3	cis-7,10,13-Eicosatrienoic	0.00	0.00	0.00 ± 0.00	0.00 ± 0.00	0.69 ± 0.21	0.49 ± 0.04	0.00
20:4	cis-5,8,11,14-Eicosatetraenoic (AA) (ω-6)	0.51	0.00	0.08 ± 0.01	0.64 ± 0.03 *	2.13 ± 0.38	5.14 ± 0.20 *	37.60
20:5	cis-5,8,11,14,17-Eicosapentaenoic (EPA) (ω-3)	7.52	0.00	0.19 ± 0.01	0.00 ± 0.00 *	5.58 ± 1.07	0.00 ± 0.00 *	409.70
22:1	13-Docosenoic acid	0.25	0.00	0.02 ± 0.02	0.00 ± 0.00	0.09 ± 0.09	0.00 ± 0.00 *	12.54
22:5	cis-4,7,10,13,16-Docosapentaenoic acid (ω-3)	0.26	0.00	0.00 ± 0.00	0.00 ± 0.00	2.22 ± 0.33	0.68 ± 0.08 *	17.97
22:6	cis-4,7,10,13,16,19-Docosahexaenoic (DHA) (ω-3)	2.64	0.00	0.14 ± 0.01	0.05 ± 0.01 *	16.55 ± 2.92	1.50 ± 0.06 *	159.78
	Total omega 6 FA level	7.18	5.03	0.39 ± 0.01	1.08 ± 0.04 *	7.91 ± 0.73	16.36 ± 0.85 *	42.33
	Total omega 3 FA level	10.56	0.24	0.33 ± 0.01	0.05 ± 0.01 *	24.35 ± 3.13	2.18 ± 0.10 *	587.45
	Total MUFA level	4.72	15.82	0.23 ± 0.02	0.36 ± 0.02 *	9.55 ± 0.91	45.15 ± 3.12 *	66.97
	Total SA level	1.81	3.98	1.37 ± 0.16	1.17 ± 0.10	17.50 ± 4.35	21.02 ± 1.32	9.65
Total Fatty Acid Concentration (µg/mg or µg/uL)		24.27	25.07	2.32 ± 0.16	2.66 ± 0.11	60.00 ± 5.49	85.20 ± 3.49	706.40
Ratio of total ω-6 FA to ω-3 FA (ω-6:ω-3)		0.7:1	21:01	1.2:1	21.6:1 *	0.32:1	7.5:1 *	

Table 7. Fatty acid profiles of diets, liver, and plasma

Sections of livers and plasma were collected from the mice fed respective diets for 10 weeks. (n=5/group). The ready to use diets and fish oil were used for fatty acid (FA) analysis. FA profile was measured by gas chromatographic mass spectrophotometry (GC-MS) analysis. The results were expressed as microgram of fatty acid per mg or ml of the sample.

4.3.3. Effect of dietary ω-3:ω-6 PUFA hepatic histopathology and steatosis

Histopathologic analysis of H & E stained liver sections from mice fed the different diets for 10 weeks (Fig. 14A) revealed significant effects on hepatocyte steatosis. The livers from mice fed the ω-3 diet had occasional hepatocyte lipid microvacuoles; whereas mice on the ω-6 diet had an increase in macro- and micro-vesicular steatosis in their hepatocytes (Fig. 14A). Steatosis was quantified by counting the ORO positive fat droplets that were about the size of a hepatic nucleus. There was a 7-fold increase in macrovesicular steatosis in mice fed the ω-6 diet, compared to the ω-3 diet-fed mice ($p<0.05$) (Fig. 14B and 14C). Moreover, an increase in microvesicular steatosis was observed in the livers of ω-6 diet-fed mice (Fig. 14C). This suggested that the increase in the dietary hepatic ω-6:ω-3 ratio in mice receiving the ω-6 diet (Table 6) enhanced hepatic macro-steatosis, independent of total caloric consumption.

Hepatic glycogen storage was assessed by the histological analysis of PAS (+/- diastase digestion) stained liver sections of mice fed the diets for 20 weeks (Fig. 15). The result showed that livers from mice fed the ω-3 diet had significant glycogen storage in hepatocytes around portal triads and central veins of hepatic lobules, which was absent in mice fed the ω-6 diet (Fig. 15A- 15C). The presence of glycogen deposits in PAS positive cells was confirmed by a comparison to a serial section that underwent glycogen digestion (Fig. 15C). Thus, the results indicate that the dietary ω-6:ω-3FA ratio might modulate energy storage and metabolism pathways, such that increasing consumption of a diet with a high ω-6:ω-3FA ratio enhances hepatic fat storage whereas consumption of LC-ω-3FA reduces fat storage but enhances energy storage in the form of glycogen. Collectively, the increase in the dietary ω-6:ω-3FA ratio results in macrosteatosis, and decreased glycogen deposition in lobular hepatocytes. We also undertook a histological analysis of liver tissues from mice fed a chow control diet using H & E and ORO stained

sections (Fig. 17A-17C). The histological features of livers from chow controls were distinct from the mice receiving liquid diets and had intermediate levels of steatosis (more than the ω-3 group but less than the ω-6 group. Also, there were a few microgranulomas in the liver from chow fed mice, but the size, number and features of those immune cells were more distinct than what we reported as EMM in this study (Fig. 17B). Thus, mice in a chow control group were not used in further analysis as their dietary composition had multiple differences from our experimental liquid diets including lipid types, percentages, protein and carbohydrate levels and calorie consumption.

The total WBC count of blood and liver was determined. There was no significant difference in the peripheral blood WBC count between the dietary groups, i.e.; 11.3×10^6 +/- 1.1×10^6 and 9.3×10^6 +/- 1.0×10^6 WBC cells per ml of blood in mice from ω-3 and ω-6 diet groups respectively (n=20). In contrast, mice fed an ω-6 diet had a significant (10-fold) increase in the number of WBC cells per gram of liver (7.9×10^6 +/- 1.3×10^6) compared to ω-3 diet-fed mice (0.8×10^6 +/- 0.5×10^6). We also evaluated hepatic inflammatory cell infiltration by H & E and anti-CD45 staining from mice receiving the diets for 10 and 20 weeks (Fig 16A-16G). The differentiated inflammatory cells were observed in cellular clusters composed of immature myeloid cells with variable size and nuclear morphology (Fig. 16A), supporting hepatic EMM. Mice given the ω-6 diet for 10 weeks had a significant (9-fold) increase in EMM foci (0.9+/-0.2 per 100x magnified field), compared to ω-3 diet-fed mice (Fig. 16A and 16B). Similarly, mice given the ω-6 diet for 20 weeks had an inflammatory appearance, with a significantly higher number of EMM foci (2-fold) compared to ω-3 diet-fed mice (0.2+/-0.06 per 100x magnified field) (Fig. 16B). However, there was no significant difference in the number of EMM foci between the 10- or 20-week diet-fed groups (Fig. 16B). Further, the EMM foci in ω-6 fed mice were larger and located adjacent to the central veins, whereas the EMM foci in ω-3 diet-fed animals

were smaller and located randomly in the hepatic sinusoids (Fig. 16A). The presence of inflammatory cells (individually distributed or in clusters) was confirmed by staining the liver sections with the anti-CD45 antibody (Fig. 16C-16G). The ω-6 diet-fed mice had significantly higher numbers of individual $CD45^+$ cells compared to the ω-3 diet-fed groups, in both the 10 and 20 weeks' diet-fed studies (Fig. 16C & 16D). Morphologically, these $CD45^+$ cells included both myeloid and lymphoid cells. In addition, ω-6 diet-fed mice had a significantly higher number of $CD45^+$ inflammatory cell foci (6.8+/0.4) compared to ω-3 diet-fed mice (0.4+/-0.3 per 100x magnified field). The foci were approximately 3 times larger (23.2+/-2.4 cells/cluster) in the livers of ω-6 diet-fed mice compared to the ω-3 diet-fed mice (8+/-5.3 cells/cluster) (Fig. 16E-16G). Similar results were observed in the livers of mice maintained on the diets for 20 weeks. Additionally, the number of inflammatory cells per EMM foci were significantly increased in the 20-week diet-fed mice compared to the 10-week mice, when studied using mice from both dietary groups. (Fig. 16F and 16G). Confirmation of the increase in hepatic hematopoietic progenitor ($CD201^+CD27^+$) cells [355] was obtained by flow analysis of isolated hepatic non-parenchymal cells and found as a 24.4+/-4.9% of $CD45^+$ cells in ω-6 diet-fed mice versus 3.7+/-1 % of $CD45^+$ cells in ω-3 diet-fed mice were of progenitor phenotype respectively. The myeloid phenotypes of progenitor cells were further confirmed by CFU-GM analysis, which showed that ω-6 and ω-3 dietary groups had 14.9+/-1.1 and 9.4+/-2.1 CFU-GM colonies/100,000 cells plated respectively.

Since NFκB expression is associated with myelopoiesis, we examined the expression of NFκB protein in the livers of mice fed the diets for 10 weeks and found that livers from ω-6 diet-fed mice had a significantly higher level of NFκB expression (Fig. 16H and Fig. 16I) ($p<0.05$, $n=5$), indicating inflammatory cell activation. Collectively, the higher ω-6:ω-3FA

ratio in the diets appeared to be associated with inflammation and EMM in the hepatic microenvironment.

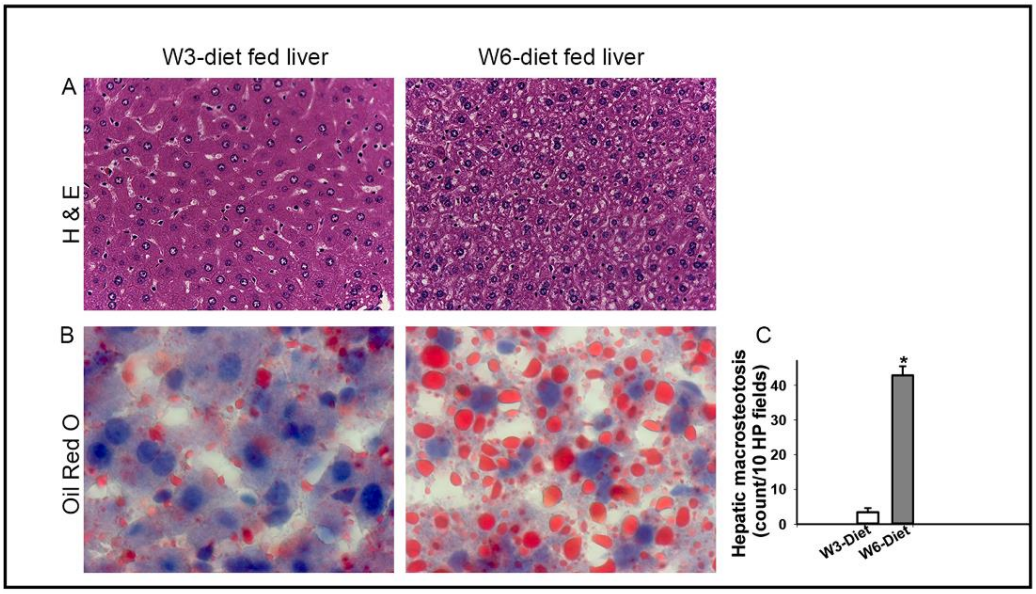
W3-diet fed liver
W6-diet fed liver
A
H & E
B
Oil Red O
C
Hepatic macrosteotosis (count/10 HP fields)
0
10
20
30
40
*
W3-Diet
W6-Diet

Figure 14. Differential effects of dietary PUFA on hepatic steatosis

Hepatic steatosis analysis of livers by hematoxylin and eosin (H & E) staining (A). Oil Red O-stained liver sections analyzed for hepatic steatosis (B and C). Images were taken with magnification of 400x (A) and 1000x (B) (n=5) [*=$p<0.05$].

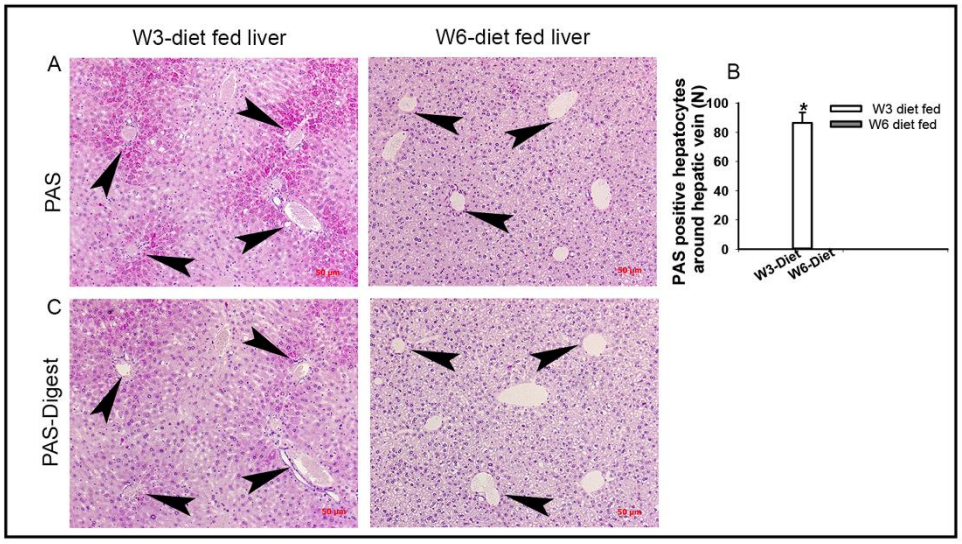
W3-diet fed liver
W6-diet fed liver
A
PAS
B
PAS positive hepatocytes around hepatic vein (N)
100
80
60
40
20
0
*
W3 diet fed
W6 diet fed
W3-Diet
W6-Diet
C
PAS-Digest

Figure 15. Differential regulation of hepatic glycogen storage by dietary PUFA

Liver sections stained with Periodic Acid-Schiff (PAS) showed glycogen-containing hepatocytes around the regions of central vein and portal area of hepatic lobules in mice fed ω-3 diet but absent in ω-6 diet group (A and B). The hepatic glycogen was digested using PAS-diastase staining (PAS-Digest) (C). Images were taken with magnification of 200x (A and C) and (n=5) [*=$p<0.05$].

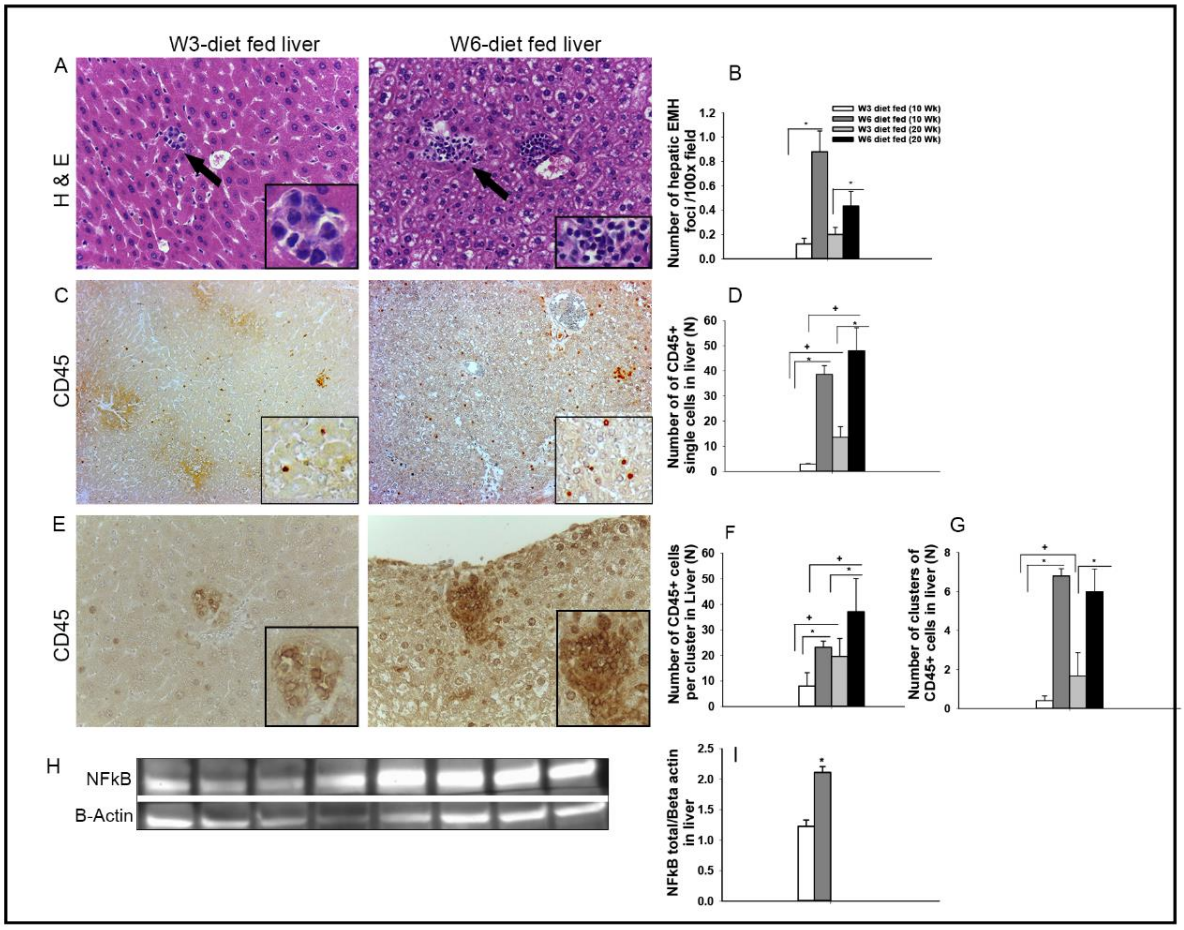
W3-diet fed liver
W6-diet fed liver
A
H & E
B
W3 diet fed (10 Wk)
W6 diet fed (10 Wk)
W3 diet fed (20 Wk)
W6 diet fed (20 Wk)
Number of hepatic EMH foci /100x field
C
CD45
D
Number of of CD45+ single cells in liver (N)
E
CD45
F
Number of CD45+ cells per cluster in Liver (N)
G
Number of clusters of CD45+ cells in liver (N)
H
NFkB
B-Actin
I
NFkB total/Beta actin in liver

Figure 16. Differential regulation of hepatic EMM by PUFA

Livers of mice were compared for hepatic EMM by counting the number and size of EMM foci in 10 microscopic fields/sample by H & E staining (A) (n= 3 to10). Arrows indicate a focus of EMM. Comparison of EMM foci between 10 weeks and 20-week diet-fed mice of the dietary groups (B). Analysis of 100x magnified fields of CD45 stained liver sections for $CD45^+$ single cells (C and D). Analysis of number and size of $CD45^+$ cell clusters in dietary groups (E, F, and G). Images were taken at a magnification of 400x (A) and 100x (C and E). Hepatic NFκB protein expression was significantly higher in the ω-6 as assessed based on Western blots (H and I) [*=$p<0.05$].

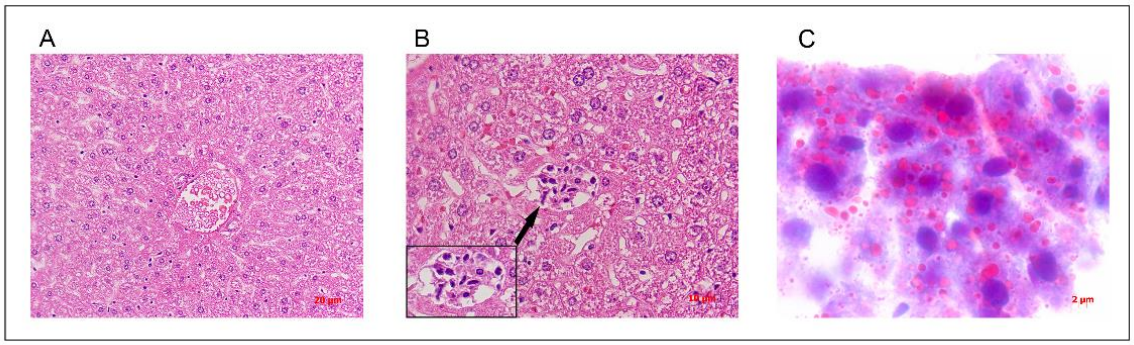
A
B
C
20 µm
10 µm
2 µm

Figure 17. Hepatic histology and fat accumulation in chow fed mice liver

Sections of liver from control mice fed chow diet. (A-B) Hematoxylin & eosin stained liver sections at the magnification of (A) 200x and (B) 400x. (B) Cluster of immune cells in hepatic tissue. (C) Oil red O stained hepatic section showing fat droplets in hepatocytes at 1000x magnification.

4.3.4. Dietary ω-3:ω-6 PUFA regulation of hepatocyte proliferation, degeneration, and apoptosis

We examined hepatocyte proliferation (Ki67) and apoptosis (TUNEL) by IHC using mice fed the experimental diets for 10 or 20 weeks. Mice fed the diet for ten weeks did not have a difference in hepatocyte proliferation (data not shown). However, mice fed the ω-6 diet for 20-weeks had a significantly lower number of proliferating hepatic nuclei (1.5-fold) as compared to ω-3 diet-fed animals (Fig. 18A and 18B). In contrast to hepatocyte proliferation, a 4-fold increase in the number of TUNEL positive hepatocyte nuclei was observed in the livers of mice fed the ω-6 diet for 20 weeks (Fig. 18C and 18D). When the number of TUNEL positive nuclei relative to total hepatocyte nuclei were compared, a significantly higher frequency of hepatocytes in the livers of ω-6 diet-fed mice were TUNEL positive (41%) as compared to 15% of the hepatocytes in the livers of ω-3 diet-fed mice (Fig. 18E). Collectively, these results suggest a potential mechanism for the decrease in liver weight in the ω-6 diet-fed animals.

Additionally, morphological differences were observed in the bile ducts of ω-3 versus ω-6 diet-fed mice although no differences were observed in RBC count and properties between the dietary groups (Fig. 19).

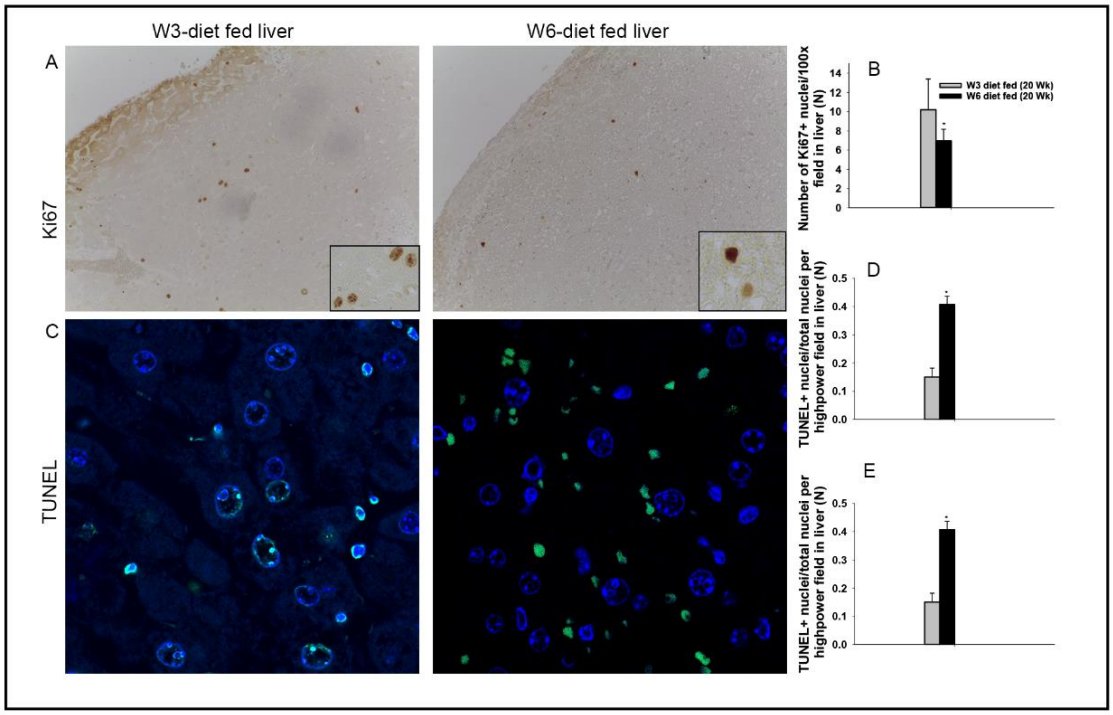
W3-diet fed liver
W6-diet fed liver
A
Ki67
B
W3 diet fed (20 Wk)
W6 diet fed (20 Wk)
Number of Ki67+ nuclei/100x field in liver (N)
C
TUNEL
D
TUNEL+ nuclei/total nuclei per highpower field in liver (N)
E
TUNEL+ nuclei/total nuclei per highpower field in liver (N)

Figure 18. Dietary PUFA regulation of hepatocyte proliferation, and apoptosis

The livers of mice fed ω-3 and ω-6 diets for 20 weeks were compared based on proliferation (Ki67) and apoptosis (TUNEL) by counting the number of positive cells per 10 microscopic fields per sample (n=3). The number of proliferating hepatocytes observed are shown in A and B. The number of $TUNEL^{+}$ (apoptotic) nuclei (C and D) and apoptotic nuclei relative to total nuclei (C and E) observed in are shown. Images were taken at a magnification of 100x (A) and 630x (C) respectively [*=$p<0.05$].

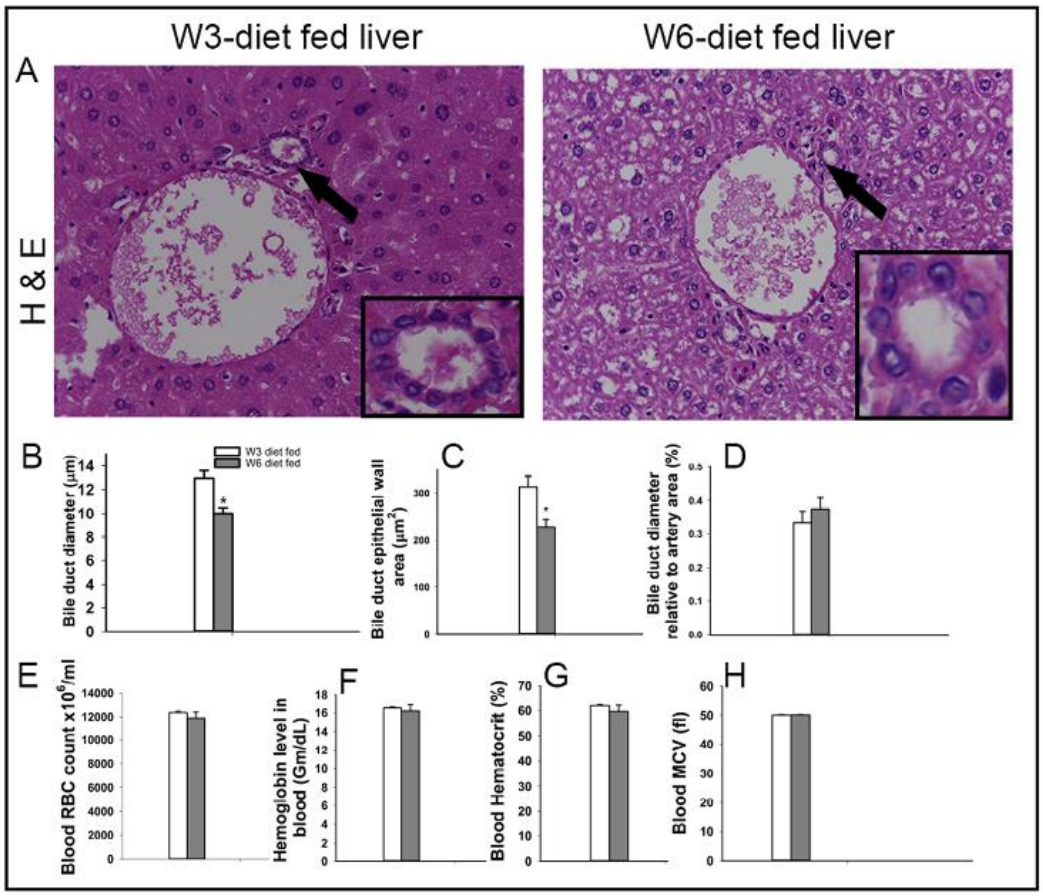
W3-diet fed liver
W6-diet fed liver
A
H & E
B
Bile duct diameter (μm)
W3 diet fed
W6 diet fed
C
Bile duct epithelial wall area (μm²)
D
Bile duct diameter relative to artery area (%)
E
Blood RBC count x10⁶/ml
F
Hemoglobin level in blood (Gm/dL)
G
Blood Hematocrit (%)
H
Blood MCV (fl)

Figure 19. Biliary histology and blood parameters

(A) H & E stained sections of liver (400x) showing bile duct histology, comparative analysis of bile duct (B) diameter, (C) thickness of epithelial cell layer in bile duct and (D) bile duct diameter relative to are of the adjacent artery. Blood samples were collected from heparinized mice at autopsy from the mice fed the diets for 10 weeks and analyzed for (E) RBC count (F) hemoglobin level, (G) hematocrit % and (H) blood mean corpuscular volume (MCV) [*=$p<0.05$].

4.4. Discussion

In the present study, we compared the biological effects of feeding ω-3 versus ω-6 PUFA using Lieber-DeCarli, isocaloric liquid diets and a pair-fed model. During acclimatization, the dietary preference was for the ω-6 diet, which was consistent with our earlier observations. Thus, the ω-3 diet consumption was used as the base-line for pair feeding. In contrast to prior reports of pair-fed mice given isocaloric diets [356, 357], in our studies significant differences in body weight were observed between mice fed an isolipidic ω-3 versus ω-6 diet. It is noted that in the referenced prior studies, diets differed in components other than PUFA and so are not directly comparable. This is relevant as in the one published study, in which mice were pair fed, isocaloric and isolipidic diets differing in PUFA composition (safflower oil (ω-6) versus fish oil (ω-3)) mice on the safflower oil diet for nine months had a 31% increase in weight versus mice on the fish oil diet.[358] These observations support a need for pair-feeding to achieve an isocaloric diet due to dietary preferences by laboratory rodents, and a need for isolipidic diets to study PUFA regulation of body weight. Further, despite providing isocaloric and isolipidic diets, we observed a significant difference in fat mass measured as abdominal fat in ω-6 diet-fed mice, suggesting differential metabolism between the two groups. This is consistent with prior reports of PUFA regulation of dietary fat content and body fat deposition and distribution [359, 360]. In one clinical study, consumption of PUFA diets was reported to decrease visceral fat and increase lean muscle mass as compared to individuals receiving high saturated fat diets [359]. Among the subtypes of PUFA, ω-3 can limit hypertrophy of abdominal fat deposits [267] and reduce weight gain in pre-obese animals and humans by a reduction in visceral fat [361-364]. Potential mechanisms for the divergent effects of ω-3 and ω-6 FAs in adipose tissue biology include the regulation of adipogenesis [365],

lipid homeostasis [366], brain-gut-adipose tissue axis [367], and systemic inflammation,[368] suggesting that lowering the dietary ω-6:ω-3 ratio might help control obesity [20]. The levels of LC-ω-3FAs used in this study was higher than the dose used in clinical study [369], because the current study was primarily designed to analyze the effects of a ω-6:ω-3 ratio of 1:1, which has been reviewed in literatures as the ω-6:ω-3 ratio upon which humans evolved [25].

The FA composition of diets can modulate the composition of stored and structural lipids [370], including the FA profile of plasma and tissues [371, 372] In the present study, we observed a significant increase in total ω-6FA, AA, and a decrease in DHA, and an absence of EPA in the plasma of mice fed a ω-6-diet. These observations are in agreement with a previous report, in which rats were fed a diet with a 1:1 ratio of ω-6:ω-3 FA resulting in a significantly higher levels of plasma EPA, DHA, and a lower level of AA, compared to the rats fed a diet with a 30:1 ratio of ω-6:ω-3 PUFA [371]. The results are also consistent with a clinical study in which the plasma FAs in humans were associated with their dietary FA composition [373].

Our results suggest that the plasma level of LC-ω-3FAs, such as EPA and DHA, reflect dietary intake. In contrast, plasma AA (C20:4) levels could only be explained by the elongation and desaturation of the ω-6 linoleic acid (C18:2) in mice given the ω-6 diet. Further, the ω-6 and ω-3FAs compete for incorporation into phospholipids and as substrates contributing to these differences [374]. In this study, the concentration of total ω-6 PUFAs and linoleic acid (precursor to AA) did not differ between the experimental diets, although the AA: precursor linoleic acid was 5.8-fold higher in the plasma of mice fed ω-6 diets. Thus, the decreased level of plasma AA in the ω-3 diet-fed mice is apparently regulated by dietary LC-ω-3FAs, as a modulator of AA biosynthesis. This observation is supported by reports that both EPA and DHA can reduce pro-inflammatory

cytokines [375] and hepatic steatosis [376]. The observation of significantly higher MUFA level in mice fed ω-6 reflected the dietary composition of the ω-6 diet. Previous studies into the bioactivity of olive oil showed that an iso-energetic MUFA diet can reduce liver fat in diabetic patients [377], higher oxidation of MUFA in the liver of rats [378] and protects against experimental inflammation [379]. Thus, we posit that our observations of inflammatory signals in ω-6 diet-fed mice is primarily due to changes in dietary ω-6:ω-3 or the absence of LC-ω-3FAs, rather than an increase in MUFA with the ω-6 diet. In our studies, we evaluated DHA and EPA in the livers of mice fed ω-3 and ω-6 diets. In a previous report, a decrease in total hepatic ω-6FA and AA levels were observed in a mouse model of NAFLD, which was associated with the metabolic utilization of AA during chronic inflammation [380]. A Majority of NAFLD studies were based on diet induced obesity models including; over-consumption/hypercaloric diet compared to a control diet [381], *ad-libitum* feeding of a high saturated fat diet (>60% calories from fat) [351, 382] or a high fat Lieber-DeCarli diet (71% of energy from fat) compared to the Lieber-DeCarli control diet (35% fat, that we used herein) [383]. Thus, the role of PUFA composition, as opposed to obesity in the pathogenesis of “fatty liver” has been poorly evaluated. In these studies, we report an increase in macro-vesicular steatosis in ω-6 diet-fed mice, an observation consistent with previous clinical and animal model studies, which emphasized that a western diet-induced hepatic steatosis [382, 384]. However, unlike previous animal studies, we observed lower relative liver weights and higher steatosis in the ω-6 diet-fed mice [382], supporting a role for dietary PUFA composition on the hepatic microenvironment, independent of total caloric intake [385]. Most studies used high fat/high caloric /high saturated fat diets to induce hepatic steatosis and compared the results with liver from control mice fed a standard laboratory chow diet, which has ω-6:ω-3 ratio of around 10:1 with variable dietary composition [386, 387]. The present study compared the results between two liquid diets differed in FA composition only. Further, an

increase in liver weights in diet induced NAFLD/NASH studies might be a consequences of severe steatosis along with induction of fibrosis in liver. Thus, it is possible that feeding the moderately fat ω-6 diet for 20 weeks may be insufficient for the development of other NASH symptoms such as fibrosis, which might be responsible for increasing liver weight in steatosis studies using NAFLD/NASH model. In this study, the lobular hepatocytes from ω-6 diet mice lacked glycogen storage (Fig.15) which is supported by the significant increase in macrosteatosis in lobular and portal regions of the ω-6 mice (Fig. 14I). Hepatic steatosis and glycogen storage levels vary depending on the strain of mice and the percent of glycogen positive cells decrease with an increase in steatosis in high fat diet-fed BALB/c mice [388]. Similarly, increased macrosteatosis in the livers of mice fed a high carbohydrate diet was associated with a decrease in glycogen storage, which recoverd by inclusion of ω-3FA in the diet [389]. The difference in hepatic glycogen storage might be due to specific regulatory roles of ω-6 and ω-3FA in metabolic pathways. [390] However, a comparison of hepatic glycogen content between moderately fat, isocaloric, isolipidic and pair-fed model has not been reported previously, suggesting a need for further studies to understand the metabolic regulation of the diets which might have modulated mechanisms of energy storage in the form of fat or glycogen. In summary, the decreased glycogen content (Fig. 15), together with increased steatosis (Fig. 14), decreased hepatocyte proliferation and increased hepatocyte apoptosis (Fig. 18) might contribute to the lower hepatic weight of the ω-6 diet-fed mice observed in the current study.

In these studies, we observed a significant increase in hepatic inflammatory cells in an absence of leukophilia in the ω-6 diet group suggesting that the outcome of higher number of inflammatory cells in the liver was independent of a systemic inflammatory response. Further, histological analysis documented a significant increase in the number and size of inflammatory cell foci, containing immature myeloid cells in the livers of mice fed a high

ω-6:ω-3 diet. The foci closely resembles hepatic EMH as defined by National Toxicological program [72] however, as majority of cells in the foci were early myeloid cells, likely myeloid progenitor cells with a lack of erythroid progenitor cells [as defined in EMH], we addressed the foci as EMM. We further confirmed the increase in hematopoietic progenitors in livers of the ω-6 diet-fed mice by flow analysis and CFU-GM counts. Unlike humans, mice have a smaller medullary space resulting in EMH during early development; however, our observation of a significant increase in number and size foci of EMM in 30 weeks old mice fed an ω-6 diet compared to age matched ω-3 diet-fed mice cannot be considered as a normal developmental phenomenon and needs further evaluation. An increase in EMM foci in association with hepatic steatosis has not been reported previously; however, prior hepatic steatosis studies were based on a NASH model, which might have an infiltration of mature inflammatory cells, such that enhanced EMM was obscured by regional inflammation. Modulation of the hepatic microenvironment and the production of growth factors such as granulocyte-monocyte colony stimulating factor (GM-CSF) by inflammatory cells may result in EMM [145]. Further, our observation of degenerating hepatocyte morphology with large lipid inclusions, higher numbers of apoptotic hepatocytes, and an increase in NFκB levels support an inflammatory cell role in the modulation of the hepatic microenvironment resulting in the mobilization of hematopoietic precursors leading to hepatic EMM in mice fed a high ω-6:ω-3 PUFA diet.

Hepatocyte proliferation [391] maintains hepatic mass and in our studies we observed decreased hepatocyte proliferation in the ω-6 diet-fed mice. However, this differs from a previous report of an increased hepatocyte proliferation in NAFLD hepatic steatosis [392]. The basis of this difference needs further evaluation, but likely contributes to the decreased liver size in the ω-6 diet-consuming mice. Further, hepatocyte apoptosis is a prominent clinical feature of NASH and positively correlates with hepatic inflammation

[353]. Thus, the observation of increased apoptotic hepatocytes in livers of mice fed ω-6 diet, steatosis and EMM supports a role of for dietary PUFA in the initiation of liver inflammation.

The significant increase in bile duct diameters at comparable levels of the biliary tree and morphological alterations on the biliary epithelium in mice fed ω-3 versus ω-6 diet may be secondary to the changes in liver mass between the dietary groups (Fig. 19). However, additional mechanistic studies are needed to analyze a potential role for dietary PUFA on the biliary system.

In summary, employing a pair fed, liquid diet with a lipid composition of 35% of dietary calories, the present study demonstrates that consuming a high ω-6:ω-3 PUFA diet regulates hepatic steatosis, EMM, glycogen deposition, and hepatocyte apoptosis. These results indicate that dietary LC-ω-3FAs suppresses steatosis and prevents the “first hit” mechanism of fatty liver development, and potentially lowers the risk of NAFLD and liver injury associated hepatic disorders. This may support a role for a ω-6:ω-3FA ratio, but not the average calories consumed from fat, (~35%) in the initiation of the formation of a “fatty liver”. However, other attributes of metabolic changes due to hypercaloric consumption and obesity might promote progression to NAFLD and NASH.

After evaluating the modulation of tissue microenvironments (MG and liver) by dietary PUFA composition, we extended our studies to understand how pre-modulated modulated tissue microenvironments by dietary PUFA regulate mammary tumor growth and metastasis. The finding from our studies on 4T1 mammary tumor bearing mice are discussed in the next chapter (Chapter 5).

Chapter 5:
Long-chain Omega-3 Polyunsaturated Fatty Acids decrease Mammary Tumor Growth, Multiorgan Metastasis and Enhance Mouse Survival[4]

5.1. Abstract

Epidemiological studies show a reduced risk of B) in women consuming high levels of LC-ω-3 FAs compared with women who consumed low levels. However, the regulatory and mechanistic roles of dietary ω-6 and LC-ω-3FAs on tumor progression, metastasis and survival are poorly understood. Female BALB/c mice (10-week old) were pair-fed with a diet containing ω-3 or an isocaloric, isolipidic ω-6 diet for 16 weeks prior to the orthotopic implantation of 4T1 mammary tumor cells. Major outcomes studied included: mammary tumor growth, survival analysis, and metastases analyses in multiple organs including pulmonary, hepatic, bone, cardiac, renal, ovarian, and contralateral MG (CMG). The dietary regulation of the tumor microenvironment was evaluated in mice autopsied on day-35 post tumor injection. In mice fed the ω-3 containing diet, there was a significant delay in tumor induction and prolonged survival relative to the ω-6 diet-fed group. The tumor size on day 35 post tumor injection in the ω-3 group was 50% smaller and the frequencies of pulmonary and bone metastases were significantly lower relative to the ω-6 group. Similarly, the incidence/frequencies and or size of cardiac, renal, ovarian metastases were significantly lower in mice fed the ω-3 diet. The analyses of the tumor microenvironment

[4] This chapter is derived from previously submitted original article: **Saraswoti Khadge**, Geoffrey M. Thiele, John Graham Sharp, Timothy R. McGuire, Lynell W. Klassen, and James E. Talmadge, **"Long Chain Omega-3 Polyunsaturated Fatty Acids decrease Mammary Tumor Growth, Multiorgan Metastasis and Enhance Mouse Survival."** Clinical and Experimental Metastasis, July 2018.

showed that tumors in the ω-3 group had significantly lower numbers of proliferating tumor cells ($Ki67^+$)/high power field (HPF), and higher numbers of apoptotic tumor cells ($TUNEL^+$)/HPF, lower neo-vascularization ($CD31^+$ vessels/HPF), infiltration by neutrophil $elastase^+$ cells, and macrophages ($F4/80^+$) relative to the tumors from the ω-6 group. Further, in tumors from the ω-3 diet-fed mice, T-cell infiltration was 102% higher resulting in a neutrophil to T-lymphocyte ratio (NLR) that was 76% lower ($p<0.05$). Direct correlations were observed between NLR with tumor size and T-cell infiltration with the number of apoptotic tumor cells. qRT-PCR analysis revealed that tumor IL10 mRNA levels were significantly higher (six-fold) in the tumors from mice fed the ω-3 diet and inversely correlated with the tumor size. Our data suggest that dietary LC-ω-3FAs modulates the mammary tumor microenvironment slowing tumor growth, and reducing metastases to both common and less preferential organs resulting in prolonged survival. The surrogate analyses undertaken support a mechanism of action by dietary LC-ω-3FAs that includes, but is not limited to decreased infiltration by myeloid cells (neutrophils and macrophages), an increase in $CD3^+$ lymphocyte infiltration and IL10 associated anti-inflammatory activity.

5.2. Introduction

Breast cancer (BC) is one of the leading causes of cancer deaths of women in the United States [393]. However, there is a significant difference in BC incidence between populations consuming Western diets, with those, who consume an Asian diet, typically due to a higher intake of fish, supporting dietary PUFA composition as a risk factor for BC [394-397]. A typical Western diet contains higher levels of ω-6FAs relative to ω-3FAs, mainly LC-ω-3FAs [25]. The LC-ω-3FAs such as EPA and DHA are metabolized to bioactive lipid mediators important in inflammation resolution [398]. In contrast, ω-6FA metabolites such as AA are pro-inflammatory mediators and chronic production of AA has been associated with inflammation-associated morbidity including BC patients [329]. Thus, the ratio of dietary ω-3 and ω-6 FA has a critical role in determining the inflammatory status of tissue microenvironments, which can modulate tumor growth, metastasis and the efficacy of therapeutic treatments [399, 400].

In murine studies, dietary LC-ω-3FAs early in life results in reduced incidences and growth of mammary tumors compared to the mice fed diets high in ω-6FA [118, 401]. Further, feeding LC-ω-3FA enriched diets in adult life results in significantly lower MG ductal density, proliferation of epithelial cells in the MG, and adipose tissue inflammation, all of which are associated with reduced risks of BC [110, 402, 403]. However, dietary LC-ω-3FAs regulation of mammary tumor microenvironments, tumor progression, metastasis and survival, has been little studied.

Despite recent advances in the development of molecularly targeted therapies, most deaths due to cancer result from the progressive growth of therapy-resistant metastases [234]. Metastasis is regarded as a highly inefficient process so that less than 0.01% of circulating tumor cells eventually succeed in forming secondary tumor growths [404]. The

growth of a metastatic lesion in a specific organ is determined by the intrinsic properties of the tumor cells (seed) and the supportive role of the microenvironment of the target organ (soil) so that some cancer cells grow preferentially in one organ while not in other organs [227, 230]. Most invasive BC cells preferentially metastasize to bone, lungs, liver and brain [230] while ovarian [405], cardiac [406] and renal [407] metastases have been less frequently observed. Similarly, 4T1 mammary tumor cells predominantly metastasize to lungs in the spontaneous metastasis model whereas metastases to liver, heart, kidneys and bone have been less frequently reported, and there are no published data on ovarian metastases by 4T1 cells [408-411]. In animal models and in-vitro studies, ω-3 and ω-6FA have been shown to modulate tissue microenvironments of MG, liver, bone, ovaries, heart and kidneys [110, 266, 412-416]. However, the role of the modulated microenvironments by pre-exposure to PUFA in the regulation of metastasis to those organs has not been studied. Further, the role of dietary PUFA composition in mammary tumor microenvironments such as inflammation, neo-vascularization and apoptosis have been little studied.

In this study, we hypothesize, that LC-ω-3FA diets can suppress mammary tumor cell proliferation and metastasis by modulating tumor and metastatic microenvironments. By pair-feeding isocaloric and isolipidic diets in an orthotopic model of mammary tumor, we uniquely analyzed the effects of dietary LC-ω-3FA on tumor microenvironments, measured as tumor cell proliferation and apoptosis, neo-vascularization and infiltrating leukocytes with pro-and anti-tumor inflammatory activities. Further, with the injection of low numbers of 4T1 cells, we established a tumor model capable of assessing the differential regulation of dietary PUFA on spontaneous metastases to different organs including bone, heart, kidneys, ovaries and CMG, which have not previously been reported.

5.3. Results

5.3.1. Dietary LC-ω-3FA regulate mammary tumor induction, growth and mouse survival

Mice (n=20/group) were fed the experimental diets for 10-16 weeks before use in two independent tumor experiments. The Fig. 20 shows the data from pair-fed groups of mice in a single experiment (n=20/group). There was no difference in the average dietary consumption between the groups during the non-tumor bearing (NTB) period; (Fig. 20A) but the dietary consumption levels significantly decreased in the ω-6 group during the tumor bearing (TB) phase of the experiments (Fig.20B).

The effects of dietary LC-ω-3FAs on the regulation of mammary tumor induction, growth and survival from pooled data of two independent studies are shown in (Fig. 21). Out of n = 40 mice/group used in the study, 100% (40/40) of the mice from the ω-6 group and 95% (38/40) of mice from the ω-3 group developed palpable tumors within the experimental period (89 days). Among the mice which developed tumors, the median time to a palpable tumor were significantly delayed for the ω-3 group (10 days, range: 6 - 32 days) compared to a median of 7 days, range: 5 - 22 days for the ω-6 diet group (Fig. 21A). Similarly, mice fed the ω-3 diet had a significantly slower mammary tumor growth compared to the ω-6 diet-fed mice (Fig. 21B). These data are supported by a 50.2% smaller tumor volume (446.3 ± 52.3 mm^3), and 48.8% lower tumor weight (0.6 ± 0.1 g) in mice fed the ω-3 diet compared to the tumor volume (888.5 ± 115.2 mm^3), and weight (1.2 ± 0.2 g) in the mice fed the ω-6 diet on the day-35 post 4T1-tumor injection autopsy (n=20/group, $p<0.05$) (Fig. 21C-21D). The body weights of the mice were evaluated at different times during the experiment to analyze the effects of dietary PUFA composition on body mass, before and during tumor growth (Fig. 21E). There was no difference in body weights when the

experimental diets were started at the age of 10 weeks. However, after feeding the diets for 16 weeks, mice given the ω-3 diet had significantly lower body weights compared to the mice on ω-6 diet, resulting in a significant difference in the body weights on the day of tumor injection. When the tumors are palpable, changes in body weights are influenced by multiple factors in addition to diet, including tumor growth and weight, and tumor-associated metabolic changes (cachexia). Thus, we analyzed the body weights at autopsy (day 35 post tumor injection Fig. 21E(c)) and after subtracting the weight of the tumor on that day (fig. 21E (d)). Both dietary groups of mice lost significant body weight by the day of autopsy compared to their weights at tumor injection. The ω-3 diet mice had significantly lower body weights (with or without tumor) on day 35 post tumor injection; although, the % change in body weights (-tumor weights) relative to their weights on tumor injection day were not different between the groups (Fig. 21E(e)).

Among the mice used in the study, 20/group that were pooled from two studies were autopsied on day 35 post injection and the extent and sites of metastases assessed and the survival of the remaining 20 mice/group was monitored. During the study period of 89 days, two mice from the ω-3 group did not develop tumors, and one mouse had a palpable tumor, which did not grow to a measurable size by 89 days post tumor injection, when the study terminated. The survival analysis showed that a mice fed the LC-ω-3FA diet for 16 weeks of adult life, prior to tumor challenge, significantly prolonged overall survival (a median survival time (MST) of 46.5 days) compared to the MST of 35.5 days for the ω-6 diet-fed mouse group ($p<0.05$) (Fig. 21F).

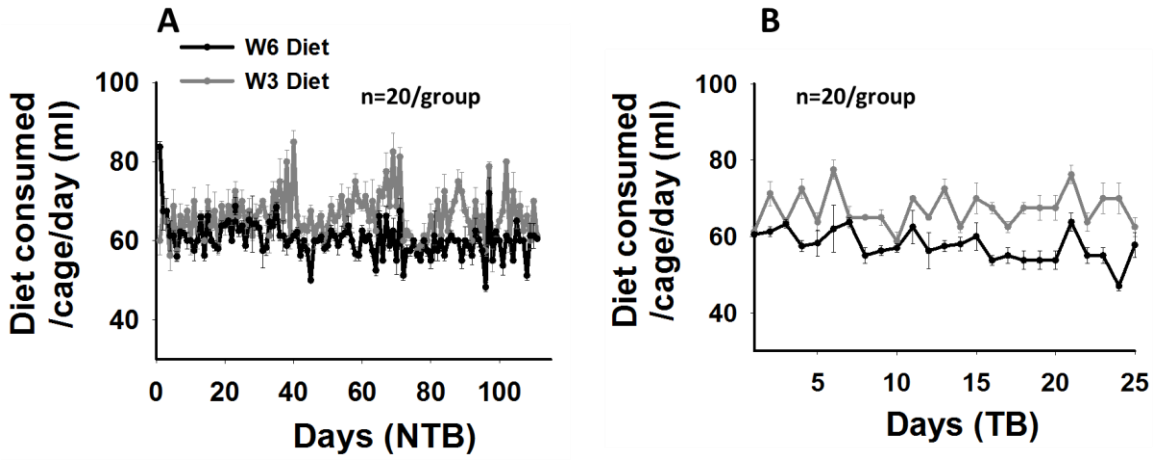
A
W6 Diet
W3 Diet
n=20/group
Diet consumed /cage/day (ml)
100
80
60
40
0
20
40
60
80
100
Days (NTB)
B
n=20/group
Diet consumed /cage/day (ml)
100
80
60
40
5
10
15
20
25
Days (TB)

Figure 20. Dietary consumption in pair-fed model

Dietary consumption levels in a single study were presented. Experimental diets were started in mice (n=20/group) at the age of 10 weeks. Ad libitum amounts of diets were provided for first 5 days of the experiment. Thereafter, mice on an ω-6 diet were pair-fed depending on the average amount consumed by the mice on an ω-3 diet. (A) Diet consumption levels during non-tumor-bearing (NTB) phase. (B) Diet consumption levels after injection of 4T1 tumor.

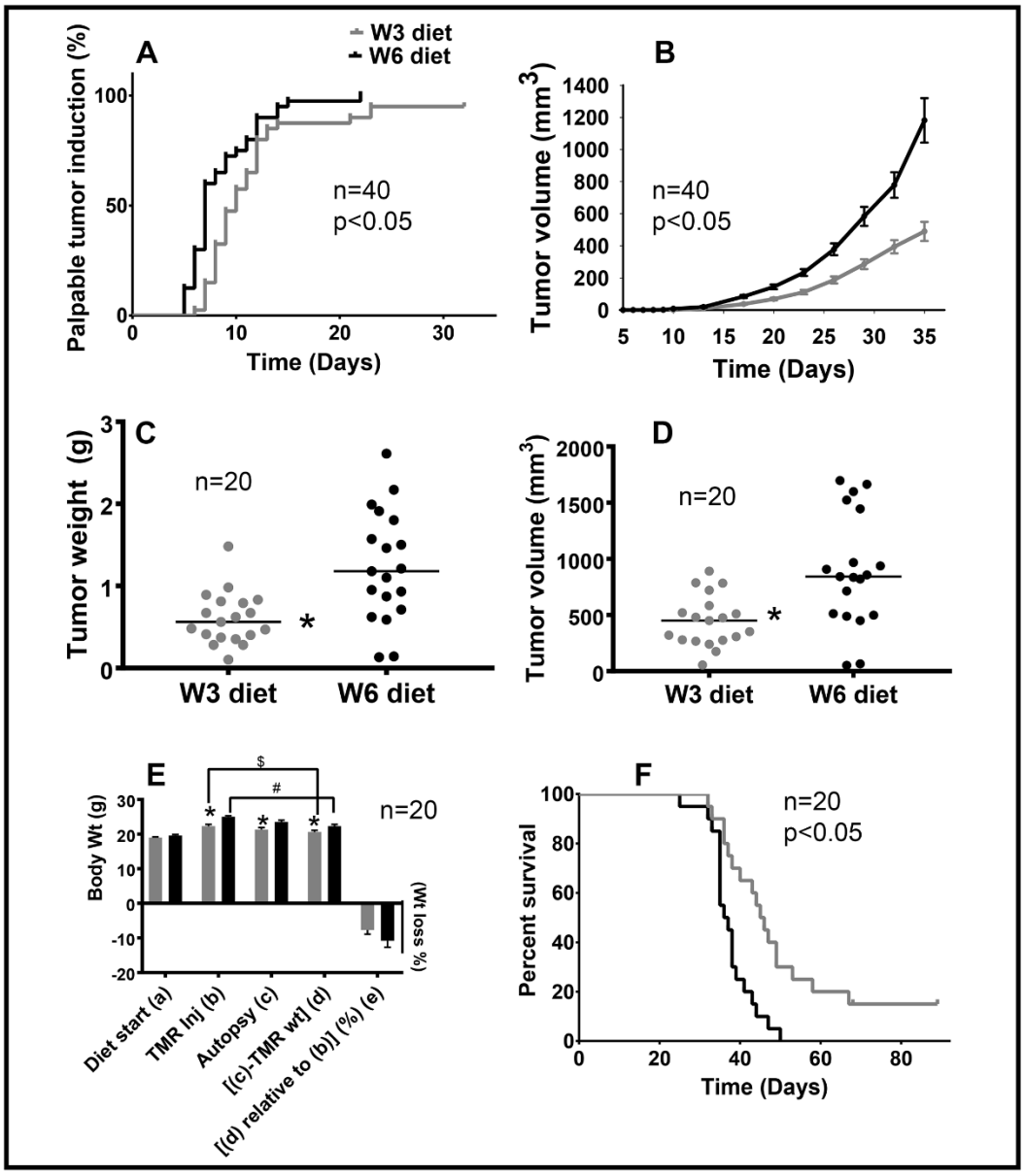
A
W3 diet
W6 diet
Palpable tumor induction (%)
n=40
p<0.05
Time (Days)
B
Tumor volume (mm3)
n=40
p<0.05
Time (Days)
C
Tumor weight (g)
n=20
*
W3 diet
W6 diet
D
Tumor volume (mm3)
n=20
*
W3 diet
W6 diet
E
$
#
n=20
Body Wt (g)
(Wt loss %)
Diet start (a)
TMR Inj (b)
Autopsy (c)
[(c)-TMR wt] (d)
[(d) relative to (b)] (%) (e)
F
n=20
p<0.05
Percent survival
Time (Days)

Figure 21. Dietary PUFA regulation of 4T1 tumor induction, growth and survival.

Mice were fed an isocaloric, isolipidic pair fed ω-3 (W3 in figure) or ω-6 (W6 in figure) diet for 10 weeks prior to orthotopic injection of 4T1 cells in left rear mammary gland (MG). Pooled data from two experiments is shown and analyzed. (A) Graph is a Kaplan-Meier plot of the time to development of a palpable tumor (log-rank test). (B) Longitudinal changes in tumor volume (repeated measures test). (C) Tumor volume and (D) tumor weights were compared from mice autopsied on day 35 post-tumor injection. Horizontal line represents median values and Mann-Whitney test was used to analyze the difference between the dietary groups. (E) Body weights of the mice were compared at key study landmarks: body weights at the start of the experimental diets, at the time of tumor injection, at autopsy on day-35 post tumor injection, host weight at autopsy (body weight minus tumor weight) and percent body weight loss at autopsy relative to the day of tumor injection. $ and # indicate $p<0.05$ for the change in host body weight at autopsy in ω-3 and ω-6 group respectively compared to the respective weights on tumor injection day (t-test). (F) Kaplan-Meier survival plot of mice on ω-3 and ω-6 diets (n=20/group) (log-rank test). *$p<0.05$ compared to mice fed the ω-6 diet.

5.3.2. Effect of dietary PUFA in 4T1 tumor MET to lung, liver and bone

Metastasis analysis was performed on day 35 on autopsied mice from two independent experiments (n=10/group/experiment). The extent of metastasis was determined by counting overt metastases on the organ surfaces [417] and by evaluating the weights of organs autopsied on the same day. Further, smaller and deep tissue metastases were evaluated by analyzing histologically-observed metastases (HO-met in figures) in H & E stained tissue sections. Among the organs investigated, the lungs had the highest number of metastases in both dietary groups and metastases were detected in all animals (Table 7). However, the ω-3 diet group mice had a 64% lower number of pulmonary overt-metastases (median=28; range: 2 - 187) compared to the ω-6 group (Median = 78; range: 8 - 312) ($p<0.05$) (Fig. 22B). This observation was supported by the lower lung weights in mice fed the ω-3 diet that were 36% lighter (median = 0.27g; range: 0.16 – 0.74g) relative to the lungs of the ω-6 fed group (median = 0.47g; range: 0.16 – 0.96g) ($p<0.05$) (Fig. 22C). Histopathological analysis of lung metastases showed that the majority of metastatic pulmonary foci were localized superficially on the lungs while metastatic foci in the lungs from mice given the ω-6 diet were localized throughout the pulmonary parenchyma (Fig. 22A). An analysis of hepatic metastases (Table 8) (Fig. 22D-22F) showed that there was a 47% lower incidence of mice with hepatic overt-metastases in the mice that received the ω-3 diet (8/20 mice) compared to the incidence in the ω-6 group (15/20 mice) ($p=0.05$). However, there were no significant differences in the median number of hepatic overt-metastases nor the weights of livers between the dietary groups (Fig. 22E-22F). Histopathological analysis showed that the livers from ω-3 diet-fed mice had fewer and smaller metastatic foci deeper in the hepatic parenchymal tissue compared to mice in the ω-6 fed group (Fig. 22D). There were individual tumor cells and clusters of few tumor cells in the livers from the ω-3 fed group, while the histologically observed metastases in the

livers from the ω-6 group were macrometastases (≥2mm in size). Quantitative analysis of the hepatic metastases size was challenging due to extensive extramedullary myelopoiesis (EMM) within the metastatic foci, preventing reliable analyses of the metastasis area. The tumor weights were directly correlated with the weights of lungs, the number of overt metastases in lungs and the weights of and liver were directly correlated with the tumor weights suggesting a direct relationship to tumor growth with metastasesMETs to these organs (Fig. 23A -23C).

The effects of dietary PUFA on the spleen was evaluated based on weights and histological analyses. There were significantly lower spleen weights in the ω-3 dietary groups compared to the ω-6 group (Fig. 22H). Further, the spleen weights directly correlated with tumor weights in both groups of mice (Fig.22I). Histological analyses of spleen sections showed splenomegaly was predominantly due to increases in EMM in the sub-capsular and red pulp areas, as previously reported [418]. Individual tumor cells and/or clusters of a few tumor cells were observed in all spleens independent of the dietary group (Fig. 22G). However, the incidence of distinct histologically observed metastasis was non-significantly (33%) lower in the spleens from ω-3 diet-fed mice (4/10) compared to the ω-6 group (6/10) (p=0.6).

Bone metastases by 4T1 tumors have been rarely reported, with the exception of sub-clone 4T1.2 tumor cells which were selected for their propensity to develop bone metastases [419]. In the current study, we report dietary PUFA regulation of bone metastases in this 4T1 orthotopic primary tumor bearing mice model. The presence of osseous metastases was suggested by the observation of hind-limb paralysis in the ω-6 group of mice. We analyzed bone metastasis in the longitudinal sections of femurs and tibias from both hind limbs of mice autopsied on day 35 post tumor injection to evaluate

the effects of dietary PUFAs on bone metastases (n=10 mice/group). Mice fed the ω-3 diet had an 80% lower incidence of bone metastasis in at least one leg (1/10 mice) relative to the incidence in the ω-6 group (5/10 mice) (p=0.1). Similarly, (3/10) mice on ω-6 diet had metastases in the femur and/or tibias from both hind limbs, which was not observed in mice fed the ω-3 diet (0/10) (p=0.08) (Table-8). Further, there were significantly fewer (median=0; range: 0-1) and smaller (median=0; range: 0-0.099mm^2) HO-met/s per femurs/tibias in ω-3 diet-fed mice, compared to the retrospective analyses of number (median=0; range: 0-6) and size (median=0; size: 0-0.346 mm^2) of metastases in the ω-6 diet-fed mice (Fig. 22J-22K). Histopathological analyses showed the larger metastases of the ω-6 group were localized to the femur metaphyses, specifically around the growth plate, while smaller metastases were present throughout the distal and proximal epiphyses and diaphyses of the femurs and epiphyses of the tibias. The only metastasis detected in an ω-3 diet-fed mouse was localized in the femur diaphysis medullary space (Fig. 22J). Despite variations in the location of metastases, all of the detected metastases in long bones were adjacent to trabecular bone, indicating potential interactions of tumor cells and sites of active hematopoiesis/osteogenesis in bone microenvironments.

Metastases Incidence						
Organ	**mice/ group (n)**	**Mice with overt-met [n (%)]**		**mice/group (n)**	**Mice with HO-met [n (%)]**	
		W3	**W6**		**W3**	**W6**
Lung	20	20(100%)	20(100%)	n/a	n/a	n/a
Liver	20	8 (40%)	15 (75%)	n/a	n/a	n/a
heart	20	2 (10%)*	12 (60%)	10	2 (20%)	6 (60%)
Kidney (at least one)	20	2 (10%)*	15 (75%)	10	1 (10%)	6 (60%)
Kidneys (Both)	20	2 (10%)	7 (35%)	10	0 (0%)	2 (20%)
Ovary (at least one)		n/a	n/a	10	1 (10%)*	9 (90%)
Ovary (both)		n/a	n/a	10	0 (0%)*	6 (60%)
Bone (one leg)		n/a	n/a	10	1 (10%)	5 (50%)
Bone (both leg)		n/a	n/a	10	0 (0%)	3 (30%)

Table 8. Dietary LC-ω-3FA regulation of incidences of metastasis

Mice autopsied on day 35 post tumor injection were analyzed for incidence of overt metastases (overt-met) (n=20 mice/group) and histologically observed metastases (HO-met) (n=10 mice/group). The results are presented as number of mice with at least one metastasis in the indicated organ (n) and percent representation per total animal analyzed in the group (%). *$p<0.05$ ω-3 versus ω-6 diet-fed mice. Fisher exact test for the difference in proportions was used to analyze statistical difference. n/a indicates either the analysis was not applicable or not done.

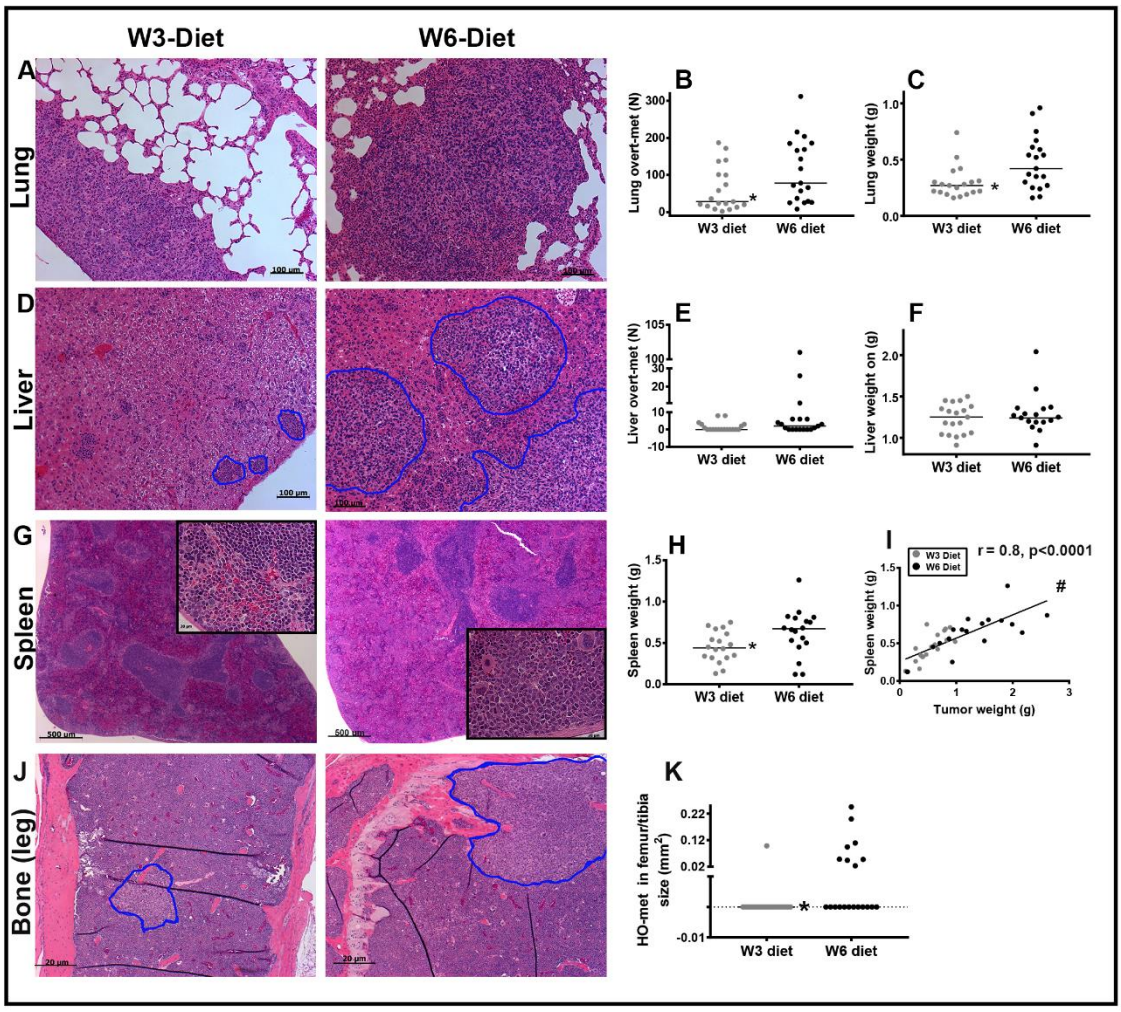
W3-Diet
W6-Diet
A
Lung
B
Lung overt-met (N)
W3 diet
W6 diet
C
Lung weight (g)
D
Liver
E
Liver overt-met (N)
F
Liver weight on (g)
G
Spleen
H
Spleen weight (g)
I
W3 Diet
W6 Diet
r = 0.8, p<0.0001
Tumor weight (g)
J
Bone (leg)
K
HO-met in femur/tibia size (mm2)

Figure 22. Dietary PUFA regulation of 4T1 metastasis to the lungs, liver and femur. Mice from two experiments were autopsied on day 35 post tumor injection and analyzed for overt metastases (overt-met) (n=20/group) and histologically observed metastases (HO-met) (n=10mice/group). (A) Hematoxylin and eosin (H & E) stained section of lungs with HO-met. (B) Median number of overt-mets and (C) median lung weights at autopsy. (D) H & E liver sections with HO-met. (E) Median number of overt-met on the liver surface and (F) median liver weights at autopsy. (G) H & E stained sections from spleens showing foci of myeloid cells. (H) Spleen weights. (I) Linear regression analysis of tumor weight. (J) H & E stained sections of decalcified femurs that had HO-met. (K) One mouse from the ω-3 group has one smaller HO-met while 5 mice in the ω-6 group had small to large sized HO-met. Images (A), (D), (J) and (K) were taken at 100x. Images of G and J were taken at 25x and 400x magnification respectively. *$p<0.05$ compared to the mice fed ω-6 diet (Mann-Whitney test).

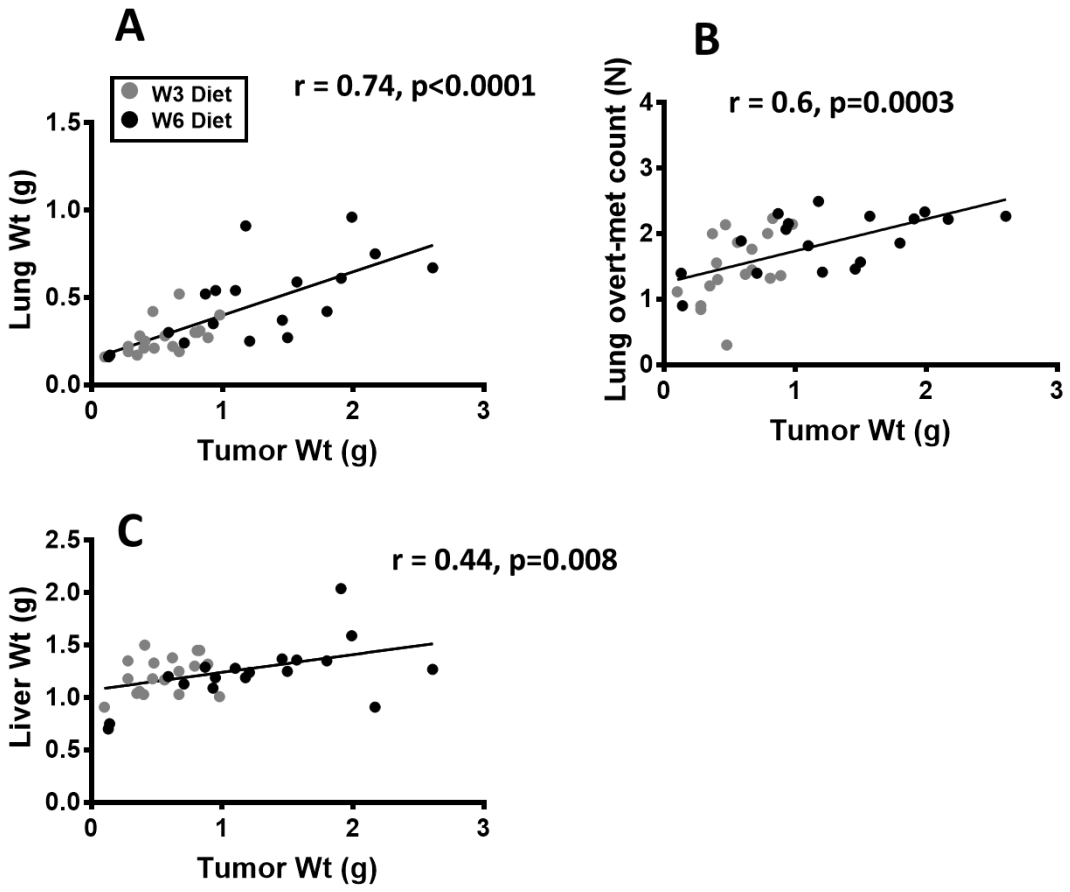
A
W3 Diet
W6 Diet
r = 0.74, p<0.0001
Lung Wt (g)
Tumor Wt (g)
B
r = 0.6, p=0.0003
Lung overt-met count (N)
Tumor Wt (g)
C
r = 0.44, p=0.008
Liver Wt (g)
Tumor Wt (g)

Figure 23. Influence of tumor weight on lung and liver weight

Mice autopsied on day 35 post tumor injection (n=20) were evaluated for lung, liver and tumor weight. Relationship of tumor weights with (A) lung weights and (B) lung overt metastases counts and (C) liver weights at autopsy. Pearson’s correlation analysis was performed.

5.3.3. Effect of dietary PUFA in 4T1 tumor metastasis to heart, kidneys and ovaries

Heart, kidneys, and ovaries are not primary targets of 4T1 mammary tumor metastases [409, 420, 421] and therefore are infrequently reported. In this study, we observed an 83% lower incidence of cardiac metastases in mice receiving dietary LC-ω-3FAs (2/20 mice) compared to the incidence in mice on the ω-6 diet (12/20 mice) ($p<0.05$) (Table-8). Mice from the ω-3 group with cardiac metastases had a single nodule of overtmetastases (median=0; range: 0-1) on the pericardium, which was a significantly lower number compared to the frequency found on the pericardium from the mice fed ω-6 diet (median=1; range:0-5). Histological analysis of myocardial metastases deeper in the cardiac tissue was performed by evaluating the frequency and size of histologically observed metastases per cross section of cardiac tissue (n=10/group) (Fig. 24A-24B). The results showed the incidence of cardiac histologically observed metastasis in cardiac tissue was 67% lower in mice fed the ω-3 diet (2/10) relative to the incidence in the ω-6 group (6/10) ($p=0.16$). Both of the mice from the ω-3 group with myocardial metastases had a single histologically observed metastasis (median=0; range: 0-1) while mice on the ω-6 diet had a median=1; range of 0-5 metastatic foci in heart tissue ($p=0.07$). The median size of cardiac histologically observed metastatic foci in the ω-3 group was significantly lower (median=0; range: 0-1.730) mm^2 compared to metastases size in ω-6 group (median= 0.491; range: 0-7.698) mm^2 ($p<0.05$). The cardiac metastases in mice fed the ω-3 mice were limited to the pericardium; while the metastatic foci were present in pericardium, as well as deeper in the cardiac tissue of the mice from the ω-6 group.

Renal metastases were analyzed by counting the number of overt metastases nodules on the renal membrane, histologically observed metastases per renal cross-section and by

determining the size of the histologically observed metastases (Fig. 24C-24D). We analyzed metastases in both kidneys of the mice and expressed our data as the incidence of metastases in one kidney or both kidneys per mouse. The incidence of having overtmetastases in at least one kidney of the mice fed ω-3 diet (2/20) was significantly (87%) lower relative to the incidence in the ω-6 group (15/20). Similarly, there was a 72% lower incidence of overtmetastases in both kidneys of mice fed ω-3 diet (2/20) relative to the ω-6 group (7/20) (p=0.4) (Table-7). Further, the median number of overt metastases per kidney for the ω-3 group (median: 0 range: 0-2) was significantly lower from that of the ω-6 group (median:1, range:0-4). Histological analysis (Fig. 24C - 24D) confirmed that the incidence of histologically observed metastasis in at least one kidney was 83% lower in the mice fed ω-3 diet (1/10 mice) relative to the ω-6 group (6/10 mice). None of mice from the ω-3 group had histologically observed metastases on both kidneys in the ω-3 group; while, (2/10) of mice on the ω-6 diet had metastasis in the histological sections from in both kidneys. The single metastatic lesion found in the kidney of a mouse from the ω-3 diet was found attached to the renal peri-capsular area, but did not invade into the renal parenchyma. In contrast, amongst the 20 metastatic lesions analyzed in the kidneys from mice fed the ω-6 diet, 35% were located in the peri-capsular fat and attached to the renal capsule, 45% were located on the adrenal gland and 20% were located in the renal parenchyma. The median size of histologically observed renal metastases in a ω-3 diet-fed mice (median=0; range:0-0.222 mm^2) was significantly lower compared to the median size from kidney of ω-6 diet-fed mice (median=0; range: 0-3.554 mm^2). Overall, the results suggest that the incidence of kidney metastases (both overt and histologically observed) were significantly lower in the mice fed the ω-3 diet compared to the mice fed the ω-6 diet.

Representative images of an ovarian cross-section with histologically observed metastases and variations in their size between the dietary groups are presented in (Fig.

24E-24F) (n=10/group). Among the ovarian cross-sections examined, the ovaries with intact capsule, cortex, medulla and follicles were included in the quantitative analysis of histologically observed metastases. The incidence of having metastasis in at least one ovary was significantly lower (89%) in mice fed ω-3 diet (1/10 mice) relative to the incidence in the ω-6 diet-fed group (8/9 mice). Similarly, in the ω-3 diet-fed group, none of mice had metastasis in both ovaries (0/9 mice), while 86% (6/7mice) had metastasis in both ovaries in mice on the ω-6 diet. There was significantly fewer number of metastatic lesions met (median=0; range: 0-3), and the lesions were significantly smaller in size (median=0; range: 0 - 0.010 mm^2) in the mice fed the ω-3 diet compared to the frequency (median=3; range: 0-8), and size (median= 0.088; range: 0 - 0.939 mm^2) of ovarian metastases in mice fed the ω-6 diet. Collectively, these results suggested that mice on the ω-3 diet had a significantly lower incidence/frequency and smaller ovarian metastases compared to the respective observations in the mice fed the ω-6 diet.

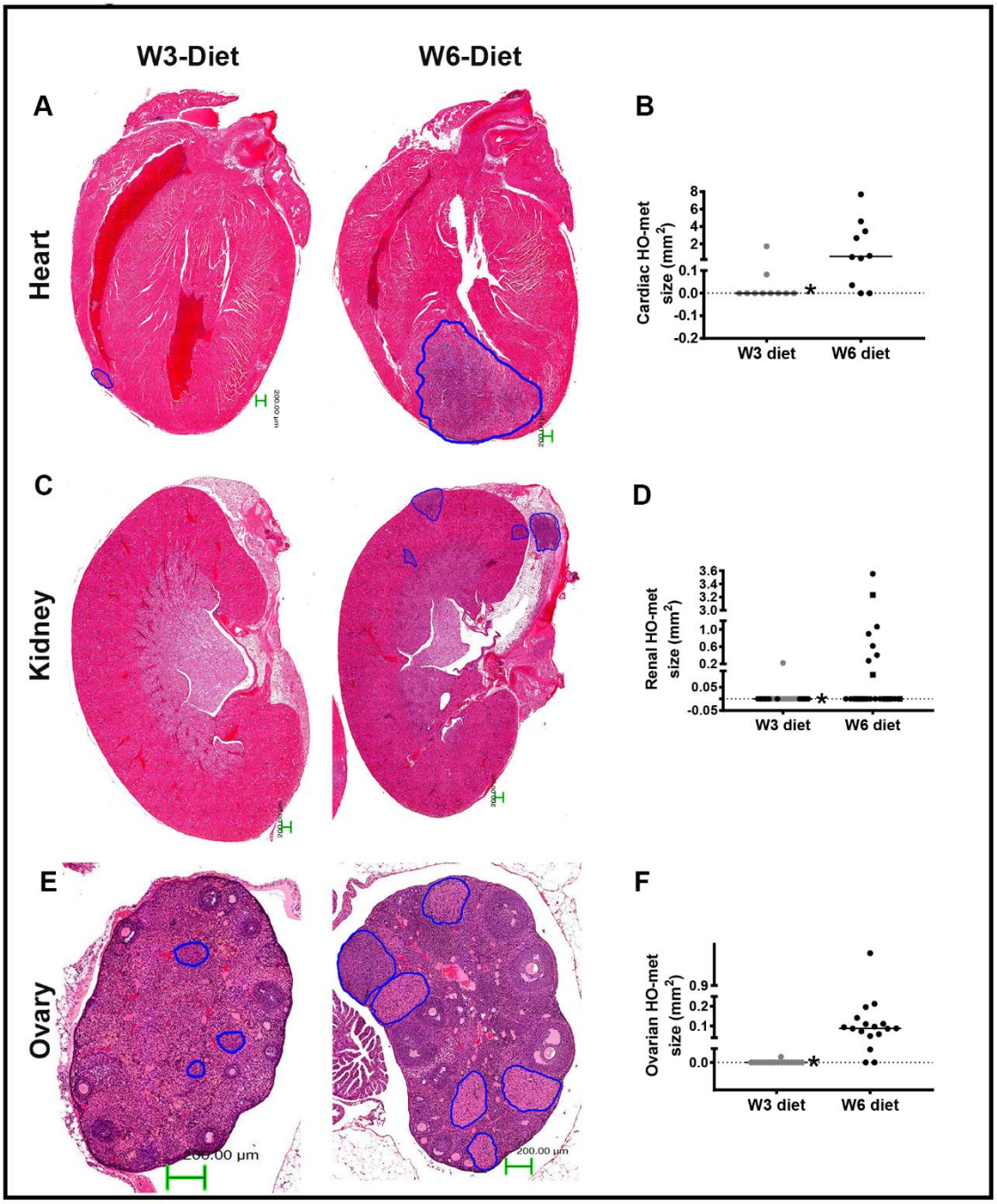
W3-Diet
W6-Diet
A
Heart
B
Cardiac HO-met size (mm²)
8
6
4
2
0.1
0.0
-0.1
-0.2
W3 diet
W6 diet
C
Kidney
D
Renal HO-met size (mm²)
3.6
3.4
3.2
3.0
1.0
0.6
0.2
0.05
-0.05
W3 diet
W6 diet
E
Ovary
200.00 µm
200.00 µm
F
Ovarian HO-met size (mm²)
0.9
0.2
0.1
0.0
W3 diet
W6 diet

Figure 24. Dietary PUFA regulation of 4T1 metastasis to the heart, kidneys and ovaries.

Mice (n=10/group) autopsied on day 35 post tumor injection were analyzed for histologically observed metastases (HO-met). (A) Hematoxylin & eosin (H & E) stained cardiac cross section showing myocardial HO-met. (B) Two of the ten mice fed the ω-3 diet had small cardiac HO-met and six of the ten mice on the ω-6 diet had larger HO-met. (C) H & E stained renal cross-sections showing HO-met in each dietary group. (D) One of the ten mice fed the ω-3 diet had one small renal HO-met in one kidney, while six of the ten mice on the ω-6 diet had larger HO-met. (E) H & E stained ovarian cross-sections showing HO-met in each dietary group. (F) One of the ten mice fed the ω-3 diet had small ovarian HO-met, while eight of the nine mice on the ω-6 diet had larger HO-met. Scale bars in images (A), (C) and (E) represent 200 μm length. Horizontal line in (B), (D) and (F) represents median. *$p<0.05$ mice fed ω-3 versus ω-6 diet.

5.3.4. Metastases in the contralateral mammary gland

The fifth left MG was injected with tumor cells and the fourth right MG was assessed for the presence of metastasis in CMG that is distant to the primary tumor. Out of n=10 mice/group in which metastases were analyzed histologically in CMGs, metastases were observed in three mice in the ω-3 group (range: 0-1 /CMG) and four mice in ω-6 group (range 0-6 /CMG) respectively (p=0.4). In addition to studies into metastases to the CMG, we also examined metastases to the associated MG lymph node (Fig. 25A - 25B). Among the analyzed lymph nodes in the CMG sections, metastases were observed in 100% of lymph nodes from both dietary groups. We did not find any lymph node in the tumor injected MGs, which might be due to the aggressive growth of the tumor throughout the MG.

In a histological analysis, tumor cell morphology of the CMG metastases from the ω-6 diet appeared more proliferative, compared to metastases in CMGs from ω-3 mice, an observation confirmed by Ki67 staining. In the Ki67 IHC studies, the frequency of proliferating tumor cells in the CMGs from ω-3 diet-fed mice were 74% lower compared to tumor cells from the CMG from the ω-6 group (n=3, $p<0.05$) (Fig. 25C-25D). In addition to the CMG metastases, the mammary ducts in the CMG from ω-6 fed mice had a significantly higher number of proliferating cells ($Ki67^{+}$), which was rarely observed in the mammary ducts from the ω-3 group. Our analysis of 10 fields/sample for n=10 mice/group showed that ω-3 diet-fedmice had 97% fewer proliferating cells in the ductal epithelial layer (Fig. 25E-25F) relative to mice on the ω-6 diets ($p<0.05$). We previously showed that NTB mice on the ω-3 diet had thinner epithelia, ductal stroma, and fewer proliferating epithelial cells and macrophages in adipose tissue of MFPs compared to mice in the ω-6 fed group [110]. The current analysis of CMGs from TB mice support these previous

observations; but the extent of effects may be influenced by the presence of the primary tumor. In the current study, the 4T1 TB mice fed the ω-3 diet had 59% fewer F4/80^{+} macrophages in the periductal area and 52% fewer in the adipose tissues of the CMG, compared to the respective analysis in CMG from TB mice fed ω-6 diet ($n=10$, $p<0.05$) (Fig. 25G-25J). The infiltrating macrophages in the CMG from 4T1 TB mice were increased (data not shown) and appeared to be larger and morphologically activated, with multiple cytoplasmic granules, compared to those observed in the MGs from NTB mice independent of the dietary group (Fig. 26A-26B). These results suggest, dietary PUFA might influence the number of infiltrating macrophages in both NTB MGs and TB CMGs but the presence of primary tumor further enhance the number and activity of infiltrating macrophages. Additionally, individual tumor cells were observed around the ducts in association with an increased number of infiltrating macrophages, notably in the CMGs from the ω-6 group. Collectively, our data document that prior exposure to dietary PUFAs modulate the CMGs microenvironments to be tumor promoting or suppressing, depending on the type of PUFA, and might further regulate the proliferation of tumor cells in the CMG metastases.

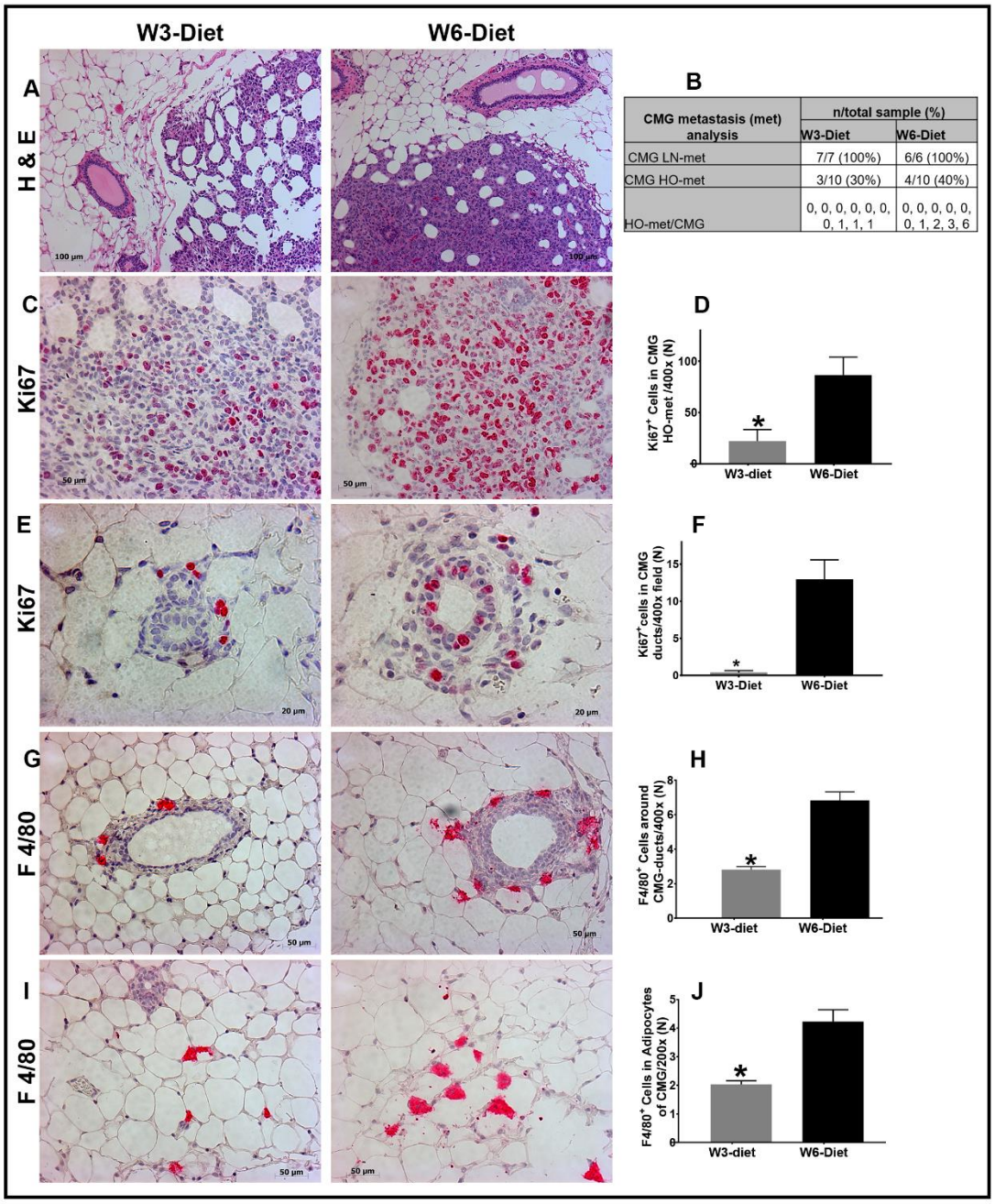

CMG metastasis (met) analysis	n/total sample (%)	
	W3-Diet	W6-Diet
CMG LN-met	7/7 (100%)	6/6 (100%)
CMG HO-met	3/10 (30%)	4/10 (40%)
HO-met/CMG	0, 0, 0, 0, 0, 0, 0, 1, 1, 1	0, 0, 0, 0, 0, 0, 1, 2, 3, 6

Figure 25. Dietary PUFA regulation of contralateral mammary gland metastasis.

Mice (n=10/group) autopsied on day-35 post tumor injection were analyzed for histologically observed metastases (HO-met) in contralateral mammary gland (CMG). (A) H & E stained CMG sections showing tumor HO-met arrested in the CMG (B). Incidences of HO-met in the CMG lymph node (LN) and the CMGs. Note, that a CMG LN was sectioned in only six of the ten CMG. (C) Proliferating tumor cells in CMG HO-met as shown by Ki67 staining. (D) Quantitative analysis of proliferating tumor cell frequency in the HO-met of the CMGs. (E) Ki67 staining for proliferating cells in the ductal wall of CMGs and (F) their frequency. (G) F4/80+ macrophages in the ductal wall of CMGs and (H) their frequency. (I and J) F4/80+ macrophages in adipose tissue of CMGs. Images of (A) were taken at 100x and those of (C), (E), (G) and (I) were taken at 200x. *$p<0.05$ mice fed ω-3 versus ω-6 diet and were analyzed using t-test.

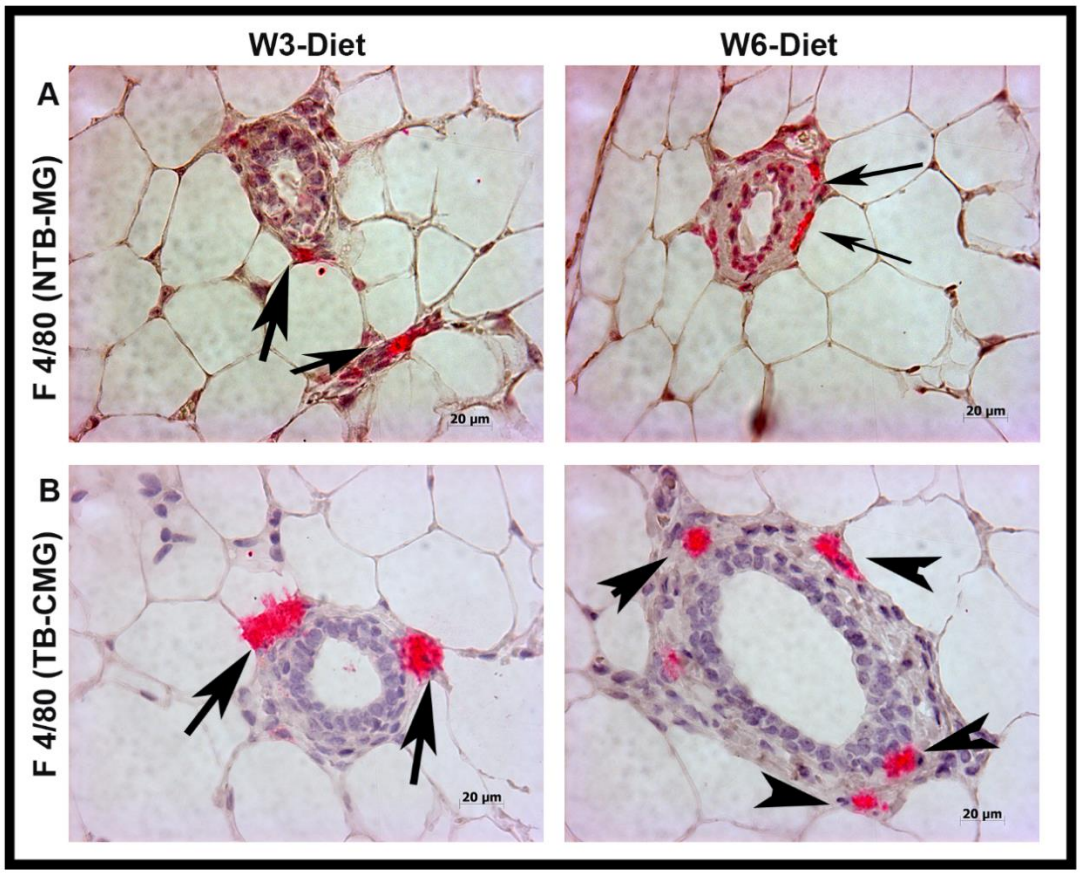
W3-Diet
W6-Diet
A
F 4/80 (NTB-MG)
B
F 4/80 (TB-CMG)
20 µm
20 µm
20 µm
20 µm

Figure 26. Differential morphology of F 4/80^{+} macrophages in MGs from NTB and TB mice

Mammary glands (MGs) from NTB mice were collected after feeding the diets for 16 weeks. Contralateral MGs were collected from mice autopsied on day 35 post tumor injection. The morphological differences of F 4/80^{+} macrophages were shown in (A) MGs from NTB mice and (B) CMGs for TB mice from the each of dietary group. Arrows showing F 4/80^{+} macrophages.

5.3.5. Dietary PUFA regulation of mammary tumor cell proliferation, apoptosis and neo-vascularization

Mammary tumors from mice (n=10 mice/group) were collected on day 35 post tumor injection for the analysis of dietary PUFA regulation of the tumor microenvironment. We obtained representative CS from these tumors containing oxic, hypoxic and necrotic tumor zones. The sub-capsular, oxic areas of tumors were used for all IHC evaluations. Our data showed that a diet high in LC-ω-3FA, fed for 16 weeks, prior to tumor challenge decreased the number of proliferating ($Ki67^+$) primary tumor cells by 44% (49 ± 7 cells/HPF) compared to the tumors from the mice fed the ω-6 diet (87 ± 7 cells/HPF) ($p<0.05$) (Fig. 27A and 27B). In contrast, the tumors in the ω-3 fed mice had a 50% higher frequency of apoptotic tumor cells (8 ± 1 cells/HPF) relative to the tumors from the mice fed ω-6 diet (4 ± 1 cells/HPF) ($p<0.05$) (Fig. 27C-27D).

PUFA regulation of intra-tumoral neo-vascularization was also evaluated as $CD31^+$ vessels in oxic areas of the tumors. These studies showed that mice fed an ω-3 diet had 34% fewer neo-vascular vessels (14 ± 1 vessels/HPF) relative to the counts in the ω-6 diet-fed mice (22 ± 2 vessels/HPF) ($p<0.05$) (Fig. 27E-27F). Morphologically, the vessels in the tumors from the ω-3 group were smaller and of uniform size; while the vessels in ω-6 fed mice were larger, connecting with an irregular structure. The number of CD31+ vessels, and the number of proliferating tumor cells were positively correlated with the size of the tumors, while an inverse correlation was observed between the number of apoptotic cells in the tumors and the tumor size (Fig. 27G-27I). We note that the tumor sizes of the mice on ω-3 diet were significantly smaller relative to tumors of mice on the ω-6 diets (Fig. 21C-21D). Further, a direct correlation was found between the $CD31^+$ vessels and the number of $F4/80^+$ cells in tumors (Fig. 27J) indicating a potential role of tumor infiltrating macrophages in enhancing neo-vascularization.

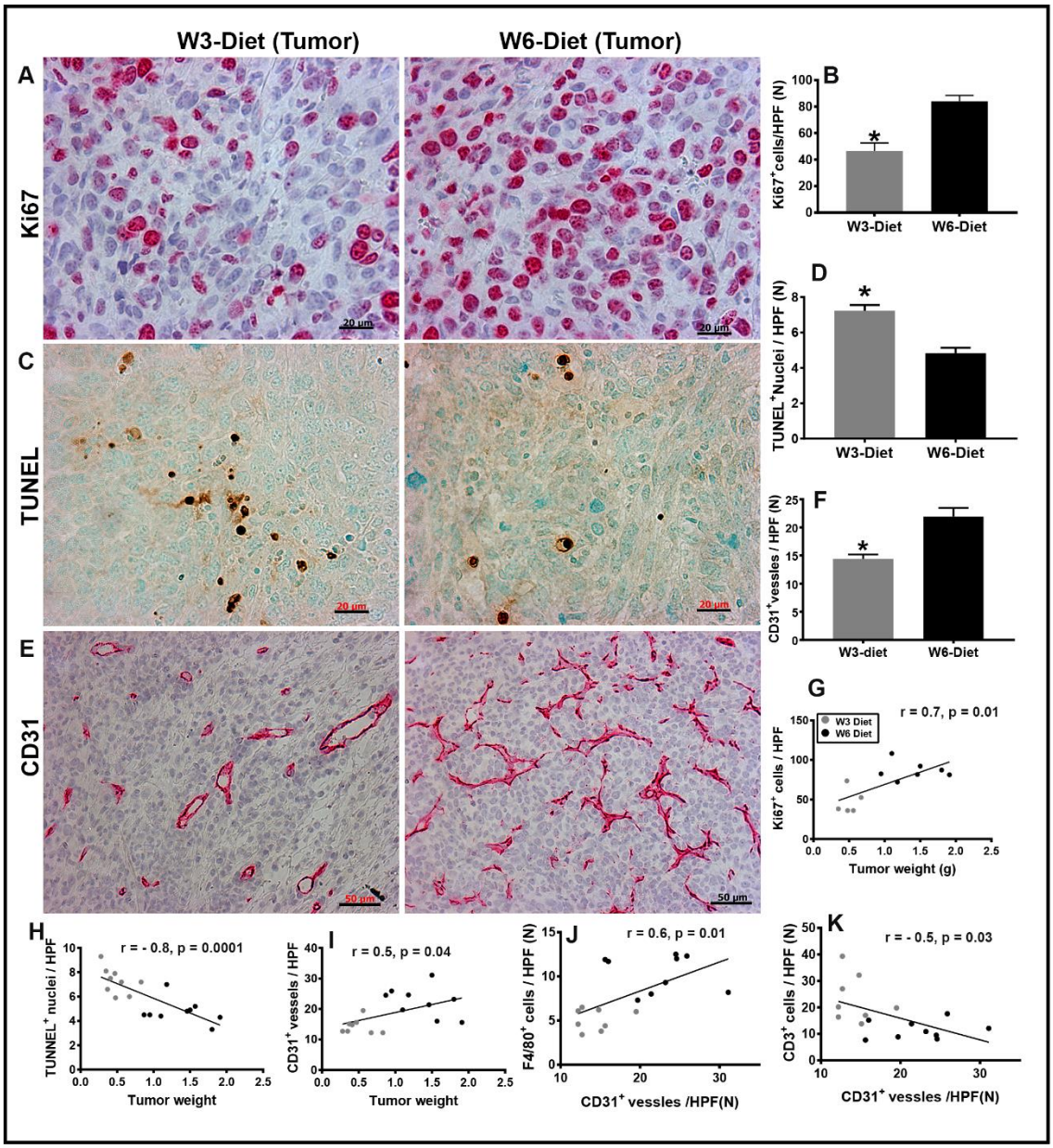
W3-Diet (Tumor)
W6-Diet (Tumor)
A
Ki67
20 μm
B
Ki67+cells/HPF (N)
W3-Diet
W6-Diet
C
TUNEL
D
TUNEL+Nuclei / HPF (N)
E
CD31
50 μm
F
CD31+vessles / HPF (N)
W3-diet
G
r = 0.7, p = 0.01
W3 Diet
W6 Diet
Ki67+ cells / HPF
Tumor weight (g)
H
r = - 0.8, p = 0.0001
TUNNEL+ nuclei / HPF
Tumor weight
I
r = 0.5, p = 0.04
CD31+ vessels / HPF
J
r = 0.6, p = 0.01
F4/80+ cells / HPF (N)
CD31+ vessles /HPF(N)
K
r = - 0.5, p = 0.03
CD3+ cells / HPF (N)

Figure 27. Dietary PUFA regulation of 4T1 tumor proliferation, apoptosis and neo-vascularization.

Mice (n=10/group) were autopsied on day 35 post tumor injection and well oxygenated, peripheral tumor sections analyzed by immunohistochemistry (IHC). (A) Representative images of tumor tissue stained with Ki67 staining. (B) Frequency of proliferating tumor cells. (C) Tumor tissue showing $TUNEL^+$ nuclei. (D) Differences in TUNEL positive apoptotic cells between the dietary groups. (E) Intra-tumoral neo-angiogenesis as shown by $CD31^+$ vessels in actively growing areas of tumor. (F) Differences in tumor associated neo-angiogenesis between the dietary groups. Correlation analysis between tumor weights and (G) $Ki67^+$ cells. (H) $TUNEL^+$ nuclei. (I) $CD31^+$ vessels per high power field (HPF). Relationship between the number of $CD31^+$ vessels in tumor with (J) the number of $F4/80^+$ cells and (K) the number of $CD3^+$ cells in tumor. Pearson's correlation analysis was used for statistical test. Images (A), (C) and (E) were taken at 400x. *$p<0.05$ compared to the mice fed ω-6 diet.

5.3.6. Dietary PUFA regulation of mammary tumor inflammatory microenvironments

Tumor infiltrating neutrophils were assessed as the frequency of elastase positive (NE^+) cells, as were the frequency of $F4/80^+$ macrophages and $CD3^+$ T-cells to characterize the tumor microenvironment between the dietary groups (n=10). There were 52% fewer neutrophils infiltrating the tumors from mice fed the ω-3 diet (10 ± 2 cells/HPF) compared to tumors from mice fed the ω-6 diet (22 ± 4 cells/HPF) ($p<0.05$) (Fig. 28A-28B). Similarly, infiltrating F4/80 positive macrophages were 49% lower in mice fed the ω-3 diet (5 ± 1 cells/HPF) compared to the mice on the ω-6 diet (10 ± 1cells/HPF) ($p<0.05$) (Fig. 28C-28D). In contrast, mice on the ω-3 diet had a 102% more infiltrating T-cells (23 ± 3 cells/HPF) compared to tumors from mice on the ω-6 diet (11 ± 1 cells/HPF) ($p<0.05$) (Fig. 28E-28F). Based on studies that have shown that the neutrophil to lymphocyte ratio (NLR) can be used as an independent prognostic factor and that a high NLR is associated with shorter survival of patients [422] we assessed these ratios as well. Feeding a LC-ω-3FA diet for 16 weeks prior to tumor challenge significantly lowered the NLR by 76% in 4T1 mammary tumors compared to the mice fed the isocaloric, isolipidic ω-6 diet. Further, the NLR directly correlated with tumor size (Fig. 28J). In addition, a direct correlation between tumor size and infiltration by neutrophil-elastase positive (NE^+) myeloid cells and macrophages, but an inverse correlation with infiltrated T-cells (Fig. 28G-28I) was noted. Further, the number of T-cells in tumors was inversely correlated with the intra-tumoral neo-vascularization (Fig. 27K) and directly correlated with the number of apoptotic tumor cells (Fig. 28K) Thus, the differences in the tumor microenvironments may be associated with both tumor size and indirectly or directly associated with diet. This suggests a critical role for dietary PUFA composition in the regulation of the inflammatory tumor microenvironment, and that an increase in a dietary LC-ω-3FA may regulate tumor growth by decreasing inflammatory cells and increasing lymphocyte infiltration.

Cytokines and chemokines are mediators of inflammation, including myeloid cell proliferation and infiltration, and can have a critical role in tumor growth and progression, depending on the type and function of the cellular mediator. The mRNA expression of inflammatory and immune regulatory mediators in tumors and spleens was analyzed from mice autopsied on day-35 post tumor injection (n=10/group). Sections of tumors from subcapsular, actively growing tumor areas were collected for the evaluation of mRNA expression to avoid the influence of hypoxic condition on the mRNA expression of the target genes. Among the analyzed target genes, there was no difference in mRNA expression levels of NFkB, G-CSF, GM-CSF, TNFα, CCL2, PTGS2, LEP, IGF1, CXCL5, CXCL1 and AREG in tumors between the dietary groups. Unexpectedly, we observed a significant (6 fold) higher expression level of IL10 mRNA in the tumors from mice fed ω-3 diets relative to the expression in tumors from ω-6 diet-fed mice (Fig. 29A). We compared the expression levels of the indicated genes in tumors of both groups with the respective gene expression levels in NTB spleens to evaluate if mRNA expressions was directed by tumor growth and/or dietary PUFA differences. Our data showed that the tumor mRNA levels of PTGS2, CCL2 and G-CSF from both dietary groups were significantly higher relative to the respective mRNA levels in NTB spleens. In contrast, IL10 mRNA level was not different in the tumors of the ω-3 group but significantly lower in the tumors from ω-6 group relative to the level in NTB spleens (Fig. 29B). Further, there was a indirect correlation between the mRNA levels of IL10 with tumor size (Fig. 29C) but no relationship was observed in the levels of G-CSF, PTGS2 and CCL2 with tumor size (Fig. 29D-29F). Collectively our data showed that the mRNA expression of PTGS2, CCL2 and G-CSF were associated with the presence of 4T1 tumors and that diets may have minimal effects on their expression; however, the IL10 expression in the tumors might have been modulated by dietary PUFA composition.

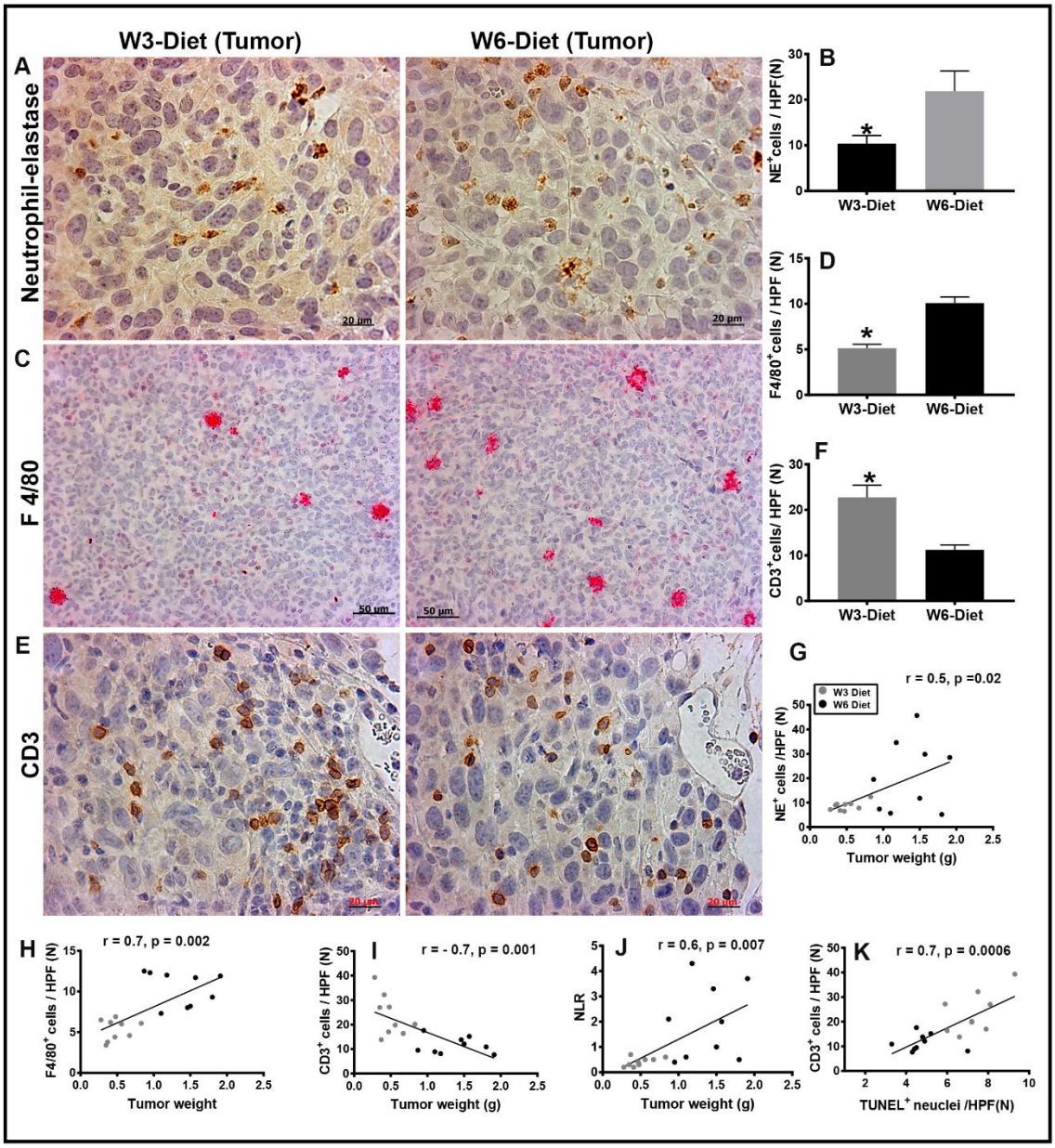
W3-Diet (Tumor)
W6-Diet (Tumor)
A
Neutrophil-elastase
20 µm
B
NE+cells / HPF(N)
W3-Diet
W6-Diet
C
F 4/80
50 µm
D
F4/80+cells / HPF (N)
E
CD3
F
CD3+cells/ HPF (N)
G
r = 0.5, p =0.02
W3 Diet
W6 Diet
NE+ cells /HPF (N)
Tumor weight (g)
H
r = 0.7, p = 0.002
F4/80+ cells / HPF (N)
Tumor weight
I
r = - 0.7, p = 0.001
CD3+ cells / HPF (N)
Tumor weight (g)
J
r = 0.6, p = 0.007
NLR
Tumor weight (g)
K
r = 0.7, p = 0.0006
CD3+ cells / HPF (N)
TUNEL+ neuclei /HPF(N)

Figure 28. Dietary PUFA regulation of 4T1 tumor inflammatory cell infiltration.

Mice (n=10/group) autopsied on day 35 post tumor injection were assessed by IHC for leukocyte infiltration of well oxygenated, peripheral tumor sections. (A) Infiltration of neutrophil-elastase positive (NE^+) myeloid cells in tumor. (B) Quantitative differences in the number of infiltrated cells per high power field (HPF) between the groups. (C) Infiltration by $F4/80^+$ macrophages in tumors. (D) Differences in the number of invading macrophages per HPF between the groups. (E) T-cell infiltration assessed as $CD3^+$ cells. (F) Plot comparing the frequency of T-cells per HPF infiltrating the tumors. Correlation analysis of tumor weights. (G) Neutrophil-elastase$^+$ cells. (H) F4/80+ nuclei and (I) $CD3^+$ cells per HPF (Pearson's correlation analysis). (J) Relationship between neutrophil to lymphocyte ratio (NLR) (evaluated by NE^+cell number/ T-Cell number) and tumor weight (Pearson correlation analysis). (K) Correlation analysis of $CD3^+$ T-cells with apoptotic cells in tumor. Images (A), (C) and (E) were taken at 400x. *$p<0.05$ fed ω-3 versus ω-6 diet (independent sample t-test for IHC data and one sample t-test for qPCR data).

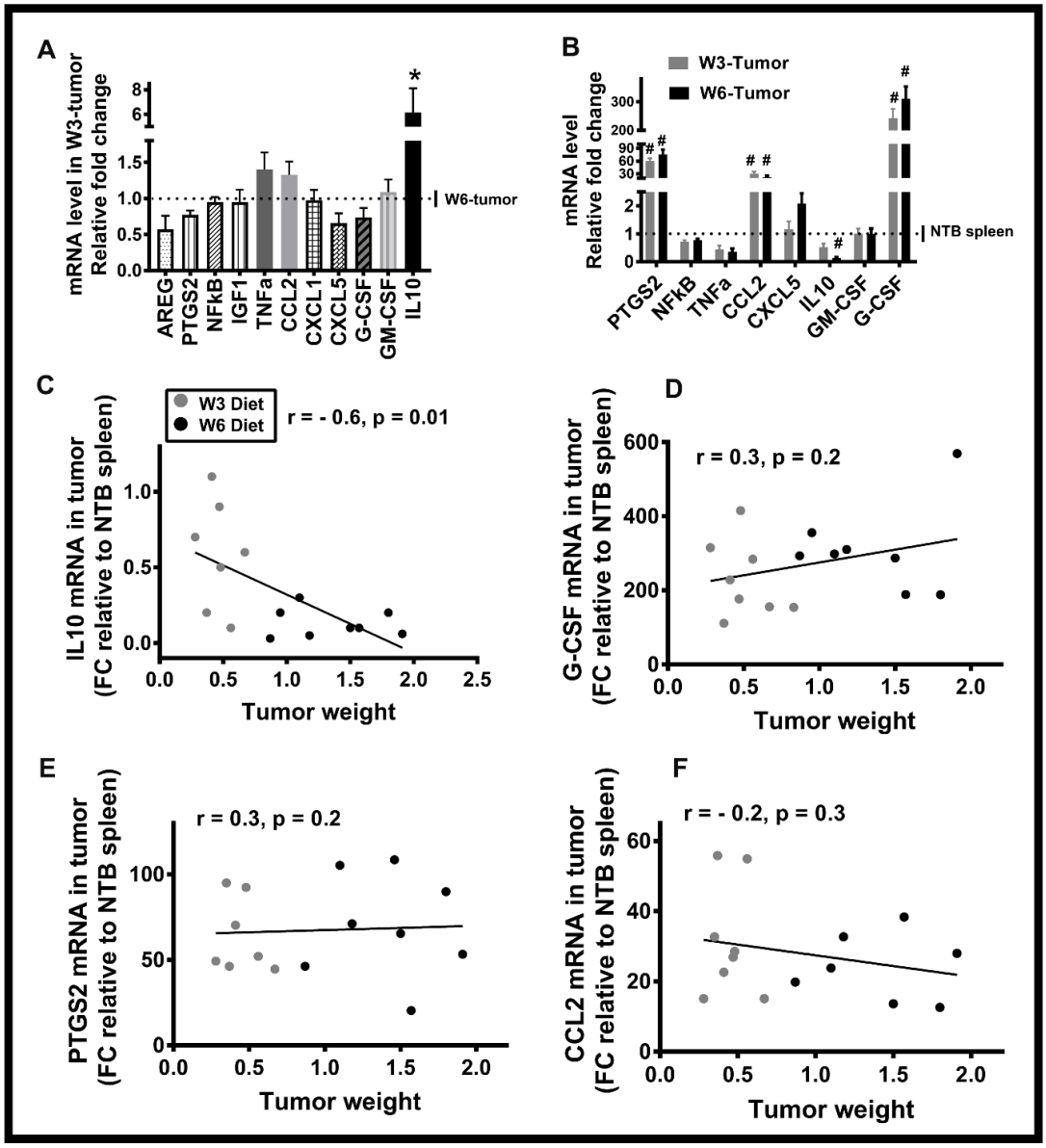
A
mRNA level in W3-tumor
Relative fold change
W6-tumor
AREG
PTGS2
NFkB
IGF1
TNFa
CCL2
CXCL1
CXCL5
G-CSF
GM-CSF
IL10
B
W3-Tumor
W6-Tumor
mRNA level
Relative fold change
NTB spleen
PTGS2
NFkB
TNFa
CCL2
CXCL5
IL10
GM-CSF
G-CSF
C
W3 Diet
W6 Diet
r = - 0.6, p = 0.01
IL10 mRNA in tumor
(FC relative to NTB spleen)
Tumor weight
D
r = 0.3, p = 0.2
G-CSF mRNA in tumor
(FC relative to NTB spleen)
Tumor weight
E
r = 0.3, p = 0.2
PTGS2 mRNA in tumor
(FC relative to NTB spleen)
Tumor weight
F
r = - 0.2, p = 0.3
CCL2 mRNA in tumor
(FC relative to NTB spleen)
Tumor weight

Figure 29. Dietary PUFA regulation of inflammatory mediators

Tumor tissue from peripheral tumor sections, and sections of spleen were collected from mice autopsied on day 35 post tumor injection for evaluation of mRNA expression by qRT-PCR (n=10/group). (A) qPCR analysis of the mRNA levels of the indicated genes in the tumors from ω-3 (W3) diet-fed mice. Data are expressed as the fold change (FC) relative to the corresponding mRNA levels in the tumors from ω-6 group. (B) mRNA levels as a FC of the indicated genes in tumors from ω-3 and ω-6 diet-fed mice relative to the expression levels in the spleen from NTB control mice. (C) Correlation analysis of comparing FC of IL10 mRNA in tumors (D), G-CSF, (E) PTGS2 and (F) CCL2 relative to the levels in NTB spleen versus tumor weight (D). For statistical analysis, dCts were compared by Student's t-test in (A) and (B). *$p<0.05$ versus ω-6 diet group and #$p<0.05$ versus NTB spleen. Pearson's correlation analysis was performed for (C-F).

5.4. Discussion

In this study, we present evidence that LC-ω-3FAs-containing diets in adult life significantly decreased 4T1 mammary tumor induction, growth, metastasis to multiple organs and enhanced survival of mice compared to mice pair-fed with an isocaloric, isolipidic ω-6FA diet. The outcomes were consistent with the observed differences in tumor microenvironments including tumor cell proliferation, apoptosis, neo-vascularization and infiltrating immune cells between the two dietary groups. We have previously shown that feeding a LC-ω-3FAs diet for 16 weeks of adult life resulted in decreased MG density, ductal epithelial cell proliferation and decreased expression of inflammatory mediators in MGs [110] and liver [266]. In our current study, we extended these observations to dietary PUFA-mediated alterations in mammary tumor microenvironments that regulate tumor growth and metastasis.

The observations of significantly lower body weight gains in mice fed an ω-3FA diet compared to the mice fed an ω-6FA diet during NTB phase is consistent with our previous studies using the same dietary model [110, 266]. BALB/c mice are refractory to obesity [7], such that their body weights did not increase significantly , following consumption of a high fat diet (60% calories from fat) for 16 weeks [7]. Thus our observation of significant differences in body weights, on diets with 36% calories from fat, after a 16 week diet feeding period, may be due to lack of body fat deposits on the mice fed LC-ω-3FAs diets, rather than a significant increase in body weights on the ω-6 diet group [110]. The potential mechanisms behind the difference in the body fat depositions are more likely by differential regulation of metabolism and adipogenesis by dietary PUFAs [361, 365]. During tumor bearing phase, mice fed the ω-6 diet lost more weight compared to their body weights prior to tumor injection. During tumor growth, body weight is more influenced

by tumor associated metabolic disorders, including cachexia and adipose tissue atrophy than the effects by a dietary calories and composition [423, 424]. Further, when the energy generated from dietary calories is not sufficient to fulfil the requirement for hyper-proliferative tumor cells, beta-oxidation of body fats occur to generate energy endogenously, resulting in the weight loss [425]. In these studies, tumors were initiated earlier, growing faster resulting in around double sized tumors on day 35 and had more metastasis in the mice fed a ω-6 diet compared the mice from ω-3 group, so it is likely that they lost more weight due to tumor growth associated factors as discussed before.

Whether tumor growth and metastasis are regulated by PUFA composition or specific PUFA metabolism is not directly addressed in our studies. However, we have separated PUFA composition from caloric composition with the use of an isocaloric diet. This provides a model to address the role of ω-3 versus ω-6FA composition on tumor growth and metastasis. Further, the timing (in utero, pre/puberty or adult) of dietary PUFA consumption may also have a critical role in these parameters as well as mammary tumorigenesis. The results from the studies based on in utero/prepubertal dietary exposure helps to understand the role of PUFAs in mammary tumorigenesis during MG development. Studies with autochthonous mammary tumors have shown that fish oil-based diets markedly suppress mammary tumor incidence, multiplicity and MG hyperplasia in murine mammary tumor virus (MMTV)-HER-2/neu transgenic mice [426, 427]. Similarly, pre-pubertal consumption of a low-fat (16% calories from fat) ω-3 diet but not a high-fat (39% calories) ω-3 diet induced mammary epithelial differentiation by reducing TEBs**,** increasing apoptosis and reducing cell proliferation**,** as well as, decreasing mammary tumor incidence, compared to a low-fat ω-6FA diet [118, 428]. These results

emphasized the critical role of calories from FAs as well as dietary composition in mammary tumorigenesis.

The current study is based on dietary consumption during adult life using isocaloric and isolipidic diets to assess the role of PUFA composition on the growth of orthotopically implanted mammary tumors. . As we started the diets earlier than tumor injections, our study emphasizes the potential prophylactic role of dietary LC-ω-3FAs in the control of tumor growth and metastasis by modulating microenvironments by prior exposure of the diets. Among the 40 mice/group in two studies, two mice from the ω-3 group did not develop tumors. Potential reasons for this might be due to technical issues related to the low number of tumor cells injected (5,000 4T1 cells), compared to most prior reports [7, 429, 430]. Alternatively, the delay in tumor development in the ω-3 group may be due to ω-3FAs mediated microenviromental changes. We report that mice fed the ω-3 diet had a significant delay in tumor induction resulting in 50% smaller tumors at autopsy on the day 35 post tumor injection, compared to the mice fed the ω-6 diet. These findings are consistent with previous studies using autochthonous mammary tumors in rodents fed ω-3FA-enriched diets [426, 427] or studies with the fat-1 transgenic mice capable of endogenously producing ω-3FA [125] and orthotopic mammary tumor models [431, 432]. However, this is the first study using rodents receiving isocaloric and isolipidic diets and pair feeding in the analysis of tumor growth and metastases to multiple organs.

4T1 mammary carcinoma tumors spontaneously metastasize to multiple organs [433] in a process involving both soil and seed properties [227, 230]. BCs usually metastasize to lymph nodes, bone, lungs and liver [230, 434] and less frequently to the ovaries [405], heart, and kidneys [406, 407]. The 4T1 mammary tumor is an aggressive tumor spontaneously metastasizing to the lungs [228] and less frequently to other organs

including the liver, brain, bone [7, 408-411, 420], heart, and kidney [408, 411] while, no report published to our knowledge, has described metastasis to ovaries and CMGs by the parental 4T1 tumor cells. In our present study, we report dietary PUFA regulation of a frequency and number of spontaneous metastasis to both common and infrequent organs. The presence of pulmonary metastases was anticipated, as lungs are preferential site of metastasis in most murine mammary tumor models. Further, the direct correlation of lung weights and pulmonary overt metastases with the tumor size indicates the potential role of slower tumor growth in ω-3 diet-fed mice in having less burden of pulmonary metastases compared to the ω-6 group is a novel observation.

Although, the incidence of hepatic metastasis was lowered by 35% in the ω-3 group, we did not observe significant differences in either hepatic overt metastases counts or liver weights between the dietary groups. We previously reported that the liver weights of NTB mice fed an ω-6 diet were significantly lower compared to the livers from mice fed the ω-3 diet. The differences in liver weights were accompanied by differences in hepatic storage of fat versus glycogen in mice given ω-6 or ω-3 diets respectively [266]. Thus, our observation of similar liver weights in TB mice between the dietary groups may be due to an increase in liver weights of TB mice on the ω-6 diet, potentially by the presence of a greater number of metastases in the hepatic parenchyma (Fig. 22D). Spontaneous bone metastases are infrequently reported by primary 4T1 tumors, compared to their occurrence following intra-cardiac or intra-tibial inoculation of 4T1 cells or the bone trophic variant that favors colonization of the femurs/tibias (4T1.2) [419, 435, 436]. In the current study, using a low number of 4T1 parent cells, we observed dietary PUFA regulation of bone metastases and an 80% lower incidence of spontaneous femur/tibia metastases in mice fed an ω-3 diet relative to mice given an ω-6 diet. Previous studies have shown that dietary fish oil prevents osteolytic lesions following intra-cardiac injection of MDA-MB-231

breast cancer cells and bone metastases [437]. These data were supported by the findings that DHA and EPA significantly attenuated the migration/invasion of MDA-MB-231 BC cells in-vitro as well as reduced cell migration to bone [437, 438]. Further, other studies have shown a beneficial role of fish oil in bone health, including inhibitory activities of DHA for osteoclastogensis [413] and calcium bioavailabity [439], and a negative correlation of the dietary ω-6:ω-3 ratio with bone formation [412, 440]. Thus, it is unclear, if a dietary PUFA modulation of osteolytic pre-metastatic niches in bone acts as a chemoattractant for metastases to bone, or PUFA modulated bone metastases regulate osteolysis suggesting that further mechanistic studies of bone metastases are needed.

Cardiac and renal metastasis are rarely reported metastatic sites for any tumor type. The lower incidence may be due to the lymphatic network in these organs, composition of the tissue microenvironments or physiological functions of the organ (for example, myocardial contractions) [406, 441]. However, it is also possible that metastases to these sites may have been overlooked when focusing on the burden of metastases in the more common metastatic sites. This is supported by the frequent findings of cardiac metastases in post-mortem examinations [442-444]. In this study, a diet enriched in ω-3FA was associated with lower incidences of cardiac and renal metastases, relative to the respective incidences in mice fed an ω-6 diet. Further, the observation of a significantly lower number and size of histologically observed metastases in the heart and kidney of mice given the ω-3 diet suggests a role of the dietary LC-ω-3FAs on the establishment and growth of metastatic cells in those tissues, potentially due to modulated tissue microenvironments. However, our study is the first reporting dietary PUFA regulation on cardiac and renal metastasis of a murine carcinoma, thus further mechanistic studies are warranted.

Although the ovary is not a preferential site for BC metastasis, ovarian metastasis have been detected in autopsies from young women with BC [405, 445]. Differential diagnosis

of ovarian metastasis by BC are challenging because ovarian cancer is frequently diagnosed as a primary tumor rather than a metastatic lesion [446]. We did not find any previous reports of spontaneous 4T1 ovarian metastasis or for any other mammary tumors. Interestingly, we observed a significant decrease in number of mice with ovarian metastasis that were fed the LC-ω-3FA diet relative to mice in the ω-6 group. Further, metastasis were found extensively in the follicular regions in mice fed an ω-6 diet, while the growth was limited to medullary region of ovaries in mice fed the ω-3FA diet, indicating the critical role of PUFAs in growth of tumor cells in the ovarian microenvironment. Potential mechanisms are the regulation of prostaglandin E2 and estrogen levels by LC-ω-3FA, as reported with ovarian cancer growth [447-449]. However, further mechanistic studies in animal models of mammary tumors are needed to evaluate the specific roles of LC-ω-3FAs in BC ovarian metastasis.

CBC metastases have been diagnosed in 11% of BC survivors [450]. CBC can be a new cancer or invasion of metastatic tumor cells in the second breast, but due to challenges in differential diagnosis of the clonal origins, most CBC are treated as a second BC [450, 451]. A recent study reported a direct relationship between breast density and incidence of CBC in women with a primary BC [452]. Recently, we showed that the MGs of NTB mice fed a LC-ω-3FA diet had significantly lower ductal densities and macrophage infiltration, relative to the MGs from NTB mice given an ω-6 diet [453]. However, there are no reports on the association of LC-ω-3FA in the induction of CBC, nor murine studies on the role of ω-3FA, on metastasis to CMG. In the current study, we did not find significant differences in the incidence of CMG metastases between the dietary groups. Nevertheless, there were significantly fewer proliferating tumor cells in the metastases of CMG of mice fed an ω-3 diet, which was accompanied by fewer proliferating epithelial cells in the ductal epithelium and infiltrated macrophages relative to the respective findings

in mice given an ω-6 diet (Fig. 25C-25H). Additionally, the macrophages infiltrated in tumor tissue were larger and granulated compared to the macrophages we observed in MGs from NTB mice (Fig. 26). These data suggest that tumors' growth might regulate the activation of macrophages in CMGs from TB mice, however further studies are warranted to evaluate the macrophage phenotypes. Collectively, our previous data from NTB mice [453] and our current analyses of CMG metastases in 4T1 TB mice, suggests that the consumption of LC-ω-3FAs may suppress pro-inflammatory mediators and growth factors, thus modulating the microenvironment, inhibiting successful 4T1 metastasis in the CMG of mice fed the ω-3 diet. These observations are supported by previous findings of the ability of ω-3FA to inhibit mammary tumor growth in-vitro [454] and in-vivo [401, 455].

Splenic BC metastases are a rare event in humans [456] and have been infrequently reported in mice bearing 4T1 murine carcinomas [408, 457]. Splenomegaly in a 4T1 tumor bearing mouse is strongly associated with extramedullary hematopoiesis, driven by myeloid growth factor secretion by 4T1 cells [206, 458, 459]. In these studies, as we expected, we observed splenomegaly in TB mice from both dietary groups compared to a normal mouse spleen; however, mice from the ω-3FA group had significantly smaller spleens, relative to those from ω-6FA diet-fed mice. Spleen weights were directly correlated with tumor size in both groups and the histology demonstrated sub-capsular myeloid hyperplasia. Thus, the observation of smaller spleens in the ω-3 groups may be associated with the decreased tumor size.

The tumor microenvironment has a crucial role in tumor progression. In these studies, we observed a significantly lower number of proliferating tumor cells, a greater number of apoptotic tumor cells and less neo-vascularization in the sub-capsular oxic areas of tumors from mice fed an ω-3 diet, relative to the same analyses in the ω-6 fed groups. DHA has been shown to induce tumor cell apoptosis and reduce proliferation in vitro and in vivo,

potentially by increasing lipid peroxidation [460], tumor cell cytotoxicity [400], inhibition of pro-inflammatory eicosanoids [461] and cell cycle arrest [462, 463]. The induction of tumor cell apoptosis has an important role in cancer therapy and represents a target for many treatment strategies. As LC-ω-3FAs appear to cause selective cytotoxicity towards cancer cells with little or no toxicity to normal cells, many studies have assessed the role of ω-3 PUFAs as a therapeutic adjuvant, to improve the efficacy and tolerability of traditional anticancer therapies [400, 464-466].

Neo-vascularization is essential for tumor metastases, thus it is an important target in the treatment of solid tumors, including BC [467, 468]. Our observation of lower numbers of $CD31^+$ vessels in tumor tissue from an ω-3 diet-fed mice suggests a decrease in tumor neo-vascularization by dietary LC-ω-3FAs. In addition to a direct effect of active metabolites of LC-ω-3FAs on mediators of neo-vascularization, such as vascular endothelial growth factor (VEGF) [469], modulation of tumor infiltrating inflammatory cells might also indirectly regulate neo-vascularization. Recent evidence indicates that tumor-associated immune cells, including macrophages, neutrophils, and mast cells can stimulate tumor angiogenesis [470-473]. We found that infiltration of macrophages and neutrophils in tumor oxic areas from mice fed ω-3 diets was significantly lower, relative to their infiltration in the tumors from ω-6 diet-fed mice. Further, the number of neutrophils and macrophages in tumor tissue directly correlated with tumor size and a direct correlation was observed between the numbers of macrophage with the extent of neo-vascularization in tumors. These results suggest that macrophages mediating downregulation of neovascularization might be one of the potential mechanisms of tumor growth suppression by dietary LC-ω-3FA. Our results are supported by previous findings on the effects of LC-ω-3FA metabolites in the suppression of tumor-associated

macrophage infiltration and the association of macrophages with tumor angiogenesis [130, 474-476].

The presence of tumor infiltrating T-cells has been associated with a better prognosis and response to cytotoxic treatments in BC patients [477]. In contrast, a neutrophilic response can inhibit immunity by suppressing the cytotoxic activity of T-cells and is associated with a poor prognosis in cancer [478]. The NLR of blood is an indicative of systemic inflammation and clinical studies have demonstrated the prognostic value of a systemic NLR in multiple cancers, including BC [201, 422]. We evaluated NLR in tumor microenvironment in this study as an index of pro-tumorigenic immune response. Our finding of a greater number of T-cells and fewer neutrophils in tumors from mice fed a diet rich in LC-ω-FAs, relative to the numbers in the ω-6 diet group, and a direct correlation of NLR with tumor size indicates the potential of dietary LC-ω-3FAs in tumor growth suppression by decreasing tumor supporting inflammation. Further, our results also support a potential role of LC-ω-3FA as an adjuvant to enhance tumor therapies [479-481].

In an analysis of potential mediators of inflammation and/or immune-regulation in the tumor microenvironment, the expression of IL10 was significantly higher in tumors and spleens of ω-3 diet-fed mice relative to the ω-6 group And IL10 expression in tumors was negatively correlated with tumor size. These data suggest a potential role for dietary LC-ω-3FAs in the regulation of tumor and systemic inflammation via IL10 mediated pathways. In tumor immunology, IL10 has multifaceted roles and has been associated with both poor and good cancer prognoses [482-484]. It has been suggested that IL10 contributes to an immune suppressive tumor microenvironment, however, recent studies have shown a role for IL10 in stimulating antitumor activity of $CD8^+$ T-cells [485] suggesting IL10 as a potential therapeutic target for cancer treatment [486, 487]. The ω-3FAs have been

associated with increased IL10 production in in-vitro and in-vivo studies, [488, 489] but the role of LC-ω-3FA mediated IL10 in tumor microenvironment has not been fully elucidated. In the present study, since increased IL10 expression in tumors was associated with tumor size, our data indicates a potential novel mechanism of dietary ω-3FA mediated tumor growth suppression; however, future mechanistic studies are warranted.

In our studies, we did not observe any significant difference in the expression of the cytokines and growth factors we analyzed in tumors between the dietary groups, although the expression of PTGS2, CCL2 and G-CSF were significantly higher in the tumors from both groups relative to the respective levels in NTB spleens. Studies have shown 4T1 tumor message level of G-CSF [490, 491], PTGS2 (COX-II) [492] and CCL2 [493] were associated with tumor growth and metastasis. It is noted that in our prior study [490], the G-CSF message was associated with tumor cells and not infiltrating leukocytes, consistent with in vitro studies showing high levels of G-CSF message and protein with 4T1 tumor cells [491, 494]. Thus, our data indicate that the increase in intra-tumoral expression of G-CSF, COX-II and CCL2 might be tumor cells dependent phenomenon and the dietary PUFA may not significantly regulate those inflammatory mediators.

In this study, we reported the effects of dietary PUFAs in mammary tumor using 4T1 murine cell line and BALB/c mice. To validate that these effects are not limited to a single tumor cell line and mouse strain, further studies are warranted using different mammary tumor cell lines and mouse strains. Our findings suggest a potential prophylactic role of dietary LC-ω-3FAs in breast cancer, and also emphasize for the need of future studies (mechanistic/translational/clinical) to evaluate the therapeutic role of LC-ω-3FAs in breast cancer growth, metastasis and in clinical management of co-morbidities in survivors. There are ongoing clinical trials on the role of ω-3FAs in breast cancer prevention (https://clinicaltrials.gov/ct2/show/NCT02295059) and a recent clinical study showed the

beneficial effects of ω-3FAs. They are able to reduce arthralgia associated with aromatase inhibitors treatment in obese breast cancer patients. Moreover, clinical studies focusing on the role of LC-ω-3FAs as an adjuvant therapy and translational studies in understanding of modulation of microenvironments of primary tumor and metastatic sites would provide an insight on targeting LC-ω-3FAs associated pathways for an advancement of anti-cancer therapies.

In summary, using isocaloric, isolipidic diets in a pair-fed model, we conclude that dietary LC-ω-3FAs suppress mammary tumor growth resulting in lower frequency of metastases to the preferential sites such as lungs and prolonged survival of the mice. Moreover, considering the difference in the metastatic burden (incidence/frequency/size) in multiple organs (specifically low preference metastatic sites: heart, kidney, ovaries, bone and CMGs) between the ω-3 and ω-6 dietary groups, out data indicate dietary PUFA composition have additive effects in metastasis, in addition to the regulation of metastasis by primary tumor growth. Further, analyses of the tumor microenvironments showed significantly lower neo-vascularization, macrophage infiltration, and NLR and higher T-cell infiltration, tumor cell apoptosis and increased IL10 expression in the ω-3 diet-fed mice. Together, these factors might contribute the suppressive effects on to the tumor growth by dietary ω-3 PUFAs.

Chapter 6:
Discussion/Summary and Future Directions

6.1. General discussion and summary

Dietary calories versus dietary composition are crucial factors in studies analyzing the role of nutritional components in pathological outcomes. For instance, both hypercaloric and hyperlipidemic diets induce obesity, which is a co-morbidity for multiple metabolic disorders and a risk factor for BC development and negative outcomes [495-497]. Animal studies have shown that high-fat diets stimulate increased food consumption and weight gain through its low satiety properties [498]. Thus, balancing of total dietary calories, calories from fat and food intake is important in the studies of fat composition as regards to downstream effects. Among dietary FA studies, both ω-6 and ω-3FAs are essential FAs that are competitive substrates for downstream pro- and anti-inflammatory pathways, respectively. Evolutionary studies have indicated that humans evolved on diets that contained an ω-6:ω-3 ratio of about 1:1; however, most current Western diets are high caloric, high fat and have an ω-6:ω-3FA ratio of 20-25:1 and mostly lack significant amounts of LC-ω-3FAs [25]. Animal studies evaluating the effects of dietary fats have focused on high versus low fat diets; which also have a differential ratio of ω-6:ω-3FAs and caloric consumption from fats [7, 118]. Thus, the present studies used isocaloric, isolipidic diets and pair-feeding to evaluate dietary ω-6 and LC-ω-3FAs effects on tissue microenvironments, in the regulation of mammary tumor growth and metastasis.

During preliminary optimization studies for the pair-fed model, we found that mice administered the ω-3 diet consumed less diet compared to the mice receiving the ω-6 diet. These observations suggested that the presence of fish oil in ω-3 diets makes them less

palatable to mice or decreased satiety, resulting in thecconsumption of lower amounts of food than isocaloric, isolipidic ω-6 diets, which have higher levels of olive oil and safflower oil. Thus, we used the ω-3 diet as the baseline diet for pair-feeding and the same amount of the diet consumed by the ω-3 group was given to mice from the ω-6 group on the next day, so that the overall food intake by each group was balanced throughout the studies.

Using the optimized pair-feeding model, we investigated the effects of dietary PUFAs on tissue microenvironments of the MG, which is the primary site of mammary tumor growth (Chapter 3), the hepatic microenvironment; one of the major sites of metastasis (Chapter 4) and the cumulative effects of those pre-modulated microenvironments on mammary tumor growth, metastases and survival (Chapter 5). We extended our analyses of metastases to common and uncommon sites of metastases indicating dietary PUFA may modulate the microenvironments of multiple organs, rendering them hospitable sites for metastatic cell seeding and growth.

Our first series of studies evaluating MG macro- and microenvironments (Chapter 3) showed that dietary ω-6 and ω-3 PUFAs have differential effects on MG morphologies including ductal density, including the thickness and morphology of ductal end structures. Mice fed ω-3 diets had significantly thinner ducts, fewer lateral branches and lack ductal sprouts, resulting in a significantly lower MG density relative to mice consuming ω-6 diets. This is an important observation as increased breast density has been associated with increased risk for BC development [95]. Increases in breast density is most often attributed to either increased stroma or epithelial mass in the breast. In histological analyses, both ductal stroma and epithelium were significantly thinner and fewer numbers of proliferating epithelial cells were observed in the mammary ducts of mice fed an ω-3 diet compared to the ω-6 group. MG morphogenesis including ductal epithelial cell proliferation during pubertal life is mainly regulated by estrogen, progesterone and growth hormones, while

IGF1 also plays a role in branching morphogenesis. During pregnancy and lactating phases, progesterone and prolactin have major roles in alveolar development and their differentiation into milk secreting lobules [499]. In our studies, the expression of ESR1 was significantly lower in MGs from the ω-3 group. However, we did not observe differences in the mRNA expression of the progesterone receptor and prolactin expression was undetectable. These results can be explained by the use of mice in the studies that were adults and virgin. It also indicates that the morphological differences we observed are potentially regulated by other factors/cells in the MG microenvironment. Thus, we analyzed local adipose tissue, whose fundamental function is to provide physical support for the MG ductal network, but also has an active role in MG development [261], and tumorigenesis [500].

The histological analyses of adipocytes in local MG microenvironments, as well as, in abdominal adipose tissues showed that PUFAs regulate the hypertrophy of adipocytes independent of total fat calories in the diets. We observed significantly smaller adipocytes in MFPs and abdominal fat from mice fed ω-3 diets, a finding paralleled by higher mRNA expression of adipokines including; leptin, IGF1 and IGF1R in the respective tissues. Excessive adipocyte hypertrophy can induce hypoxic microenvironments in local adipose tissues [501], which stimulates adipocyte apoptosis followed by the induction of pro-inflammatory mediators and recruitment of macrophages to clear the apoptotic bodies. Our results showed that the MG microenvironments had significantly lower inflammation as shown by fewer numbers of CLS/macrophages and a lower mRNA expression of inflammatory mediators in mice fed ω-3 diet compared to the ω-6 group. Thus, it is likely that dietary ω-3 and ω-6 PUFA may regulate FA metabolism in adipose tissues such that increased dietary levels of ω-3FAs prevent FA storage by adipocytes compared to the same levels of dietary ω-6FAs. Further, the prevention of local adipocyte hypertrophy

might be one of regulatory mechanisms by which ω-3FAs limit pro-inflammatory microenvironments in MGs.

Thus, our studies examining dietary PUFA regulation of MG microenvironments, showed that the increased consumption of LC-ω-3FA lowers MG density and can prevent chronic inflammation of local adipose tissue, potentially by controlling adipocyte hypertrophy and associated adipokine and cytokine expression. Local expression of leptin can regulate proliferation of both normal and malignant breast epithelial cells [316] and local adipose tissue, and chronic inflammation has been found to contribute to BC development [403]. Therefore, we postulate that alterations in MG macro/microenvironments by ω-3 and ω-6 PUFAs regulate MG tumorigenesis by providing an unfavorable or favorable microenvironment for tumor growth.

Since the liver is a common metastatic site in breast cancer, the second phase of our studies investigated dietary PUFA modulation of the hepatic macro/microenvironment. Hepatocytes metabolize dietary macromolecules, and depending on the excess energy state, they can transiently store glycogen and FAs. The chronic storage of FAs by hepatocytes leads to fatty liver disease, and if uncontrolled, progresses to hepatic inflammation and fibrosis. Chronic consumption of alcohol or high caloric/high fat diets have been associated with fatty liver diseases. Our studies showed that dietary LC-ω-3FA limits hepatic FA storage compared to mice fed an isocaloric and isolipidic ω-6 diet. In contrast, lobular hepatocytes from mice fed the ω-3 diet had significantly more glycogen deposits compared to the mice given the ω-6 diet. These results indicate that dietary ω-3 and ω-6 have differential metabolic preferences/fates such that increased levels of ω-3FAs potentially promote FA metabolism and/or distribution of FAs/energy to extrahepatic tissue as needed. In contrast, high levels of ω-6FAs (or lack of LC-ω-3FA) may promote FAs storage in hepatocytes and metabolism of glycogens to generate energy and

distribution as needed. In either situation, the difference in hepatic storage of fat versus glycogen can influence the hepatic microenvironment in many ways. The observation of increased hepatic steatosis in the ω-6 diet group was also accompanied by increased EMM, lower numbers of proliferating hepatocytes and higher numbers of apoptotic hepatocytes, all of which might contribute to significantly lower liver weights of mice from the ω-6 group relative to the ω-3 group. Collectively, dietary PUFA composition modulates hepatic macro and microenvironments such that an absence of LC-ω-3FAs and increased ω-6:ω-3 FAs promote hepatic steatosis, which may further regulate hepatocyte apoptosis, proliferation and hepatic myelopoiesis. Therefore, we hypothesize that these alterations in the hepatic microenvironment by PUFA composition might differentially regulate hepatic metastasis from mammary tumor..

After evaluating the effects of dietary PUFA composition on the primary tumor site (MG) and one of the major metastatic sites (liver) in NTB mice, we investigated the effects of chronic dietary pre-exposure of PUFAs on 4T1 mammary tumor growth and metastases. Our data showed that diets high in LC-ω-3FAs, consumed for 20 weeks, resulted in a significant delay in tumor induction, smaller tumor size, and prolonged survival. Metastasis is the main factor that regulates primary tumor survival. Thus, we analyzed mammary tumor metastases in multiple organs and analyzed the tumor microenvironments of 4T1 TB mice autopsied on day 35-post tumor injection. Mice fed diets high in LC-ω-3FAs had lower frequencies and/or incidences of spontaneous metastases in both common and uncommon sites compared to the mice fed ω-6 diets. The lungs are the most common site of metastases in the 4T1 mammary tumor model. We observed lung metastases in 100% of mice from both of the groups; however, there was a significantly lower frequency of overt-metss and pulmonary weights. Additionally, histological analyses suggested that dietary LC-ω-3FAs lowers pulmonary metastases. Hepatic metastases are also reported

in imaginable 4T1 models. In this study, quantitative analysis of the hepatic metastasis burden was difficult to evaluate. In the studies on NTB mice (Chapter 4), we showed that liver weights of mice fed ω-6 diets were significantly lower due to hepatic steatosis compared to the observations in the ω-3 diet-fed mice. In 4T1 TB mice, there was no difference in liver weights between the dietary groups. Altogether, the differential outcomes of liver weights in NTB and TB mice indicates that mice fed ω-6 diet potentially had increased hepatic metastases replacing hepatic fat content such that liver weights increased in TB mice compared to NTB mice fed the same diet. Further, histological analysis confirmed our hypothesis that hepatic metastases in mice fed the ω-3 diet were mostly limited to subcapsular areas, while METs grew extensively in deeper hepatic tissue in the mice from the ω-6 fed group.

Bone is also a common metastasis site in breast cancer patients but less commonly reported in rodent's mammary tumor models including in 4T1 (parent) mammary tumors [238, 419]. Analysis of bone metastases in the hind limbs of mice fed an ω-3 diet, there was an 80% lower incidence of bone metastases and the metastases were significantly smaller relative to the mice fed a ω-6 diet. A single bone metastasis was found in only one mouse in the ω-3 group, which was significantly smaller and located in the medullary space of the femural diaphysis. Further, all analyzed bone metastases were located in trabecular bone, which indicates a potential role of osteoclasts in the formation of bone metastases. However, further studies are required to validate the role of a diet modulated pre-metastatic niche in the establishment of bone metastases.

In addition to metastases in common sites, our data showed the incidence/frequency of metastases in uncommon sites including heart, kidneys and ovaries were significantly lower by feeding diets containing LC-ω-3FAs. The metastases in mice fed ω-3 diets were significantly smaller and were limited mostly to the subcapsular regions of the heart,

kidneys and ovaries. In the ovaries, the metastases were located outside of follicular regions unlike the metastases in the deeper tissue of heart, kidney and inside follicular regions of ovaries from mice fed an ω-6 diet. The difference in the metastatic growth in the mentioned organs might be regulated by the metastatic niche in these sites [235]. However, in our current study, we did not analyze the effects of dietary PUFAs on the modulation of microenvironments in these organs, nor did we evaluate the metastatic sites. Thus, further studies are warranted to evaluate the mechanism(s) behind the outcomes of the current study.

Our studies in NTB mice (discussed in Chapter 3) showed that dietary LC-ω-3FAs lowers MG ductal density, ductal epithelial cell proliferation and local inflammation in MGs relative to the mice fed an ω-6 based diet. As discussed above, modulation of the MG microenvironments due to ω-3 consumption suppressed primary tumor growth. We extended our studies to evaluate the role of modulated MG microenvironment in metastases to the CMG. There were metastases in the CMG associated LNs analyzed in all of mice, which is expected as we evaluated metastases in the late stage of tumor growth (day 35 post tumor injection). Further, there were insignificantly fewer mice with CMG metastases in mice from the ω-3 group. However, when the metastatic microenvironments were analyzed, we observed that there were significantly lower levels of proliferation by tumor and ductal epithelial cells and lower infiltration by macrophages to the CMGs from ω-3 diet-fed mice compared to the ω-6 group. The macrophages in the CMGs of TB mice morphologically resembled activated (large and granulated structure) macrophages as compared to macrophages in the MGs of NTB mice. Collectively, our data showed that feeding of PUFA diets for 20 weeks prior to tumor injection modulated CMG microenvironments, which potentially regulated the growth of metastases number by suppressing or promoting proliferation of tumor cells in CMGs.

Major factors that regulate local tumor growth and metastases are related to the modulation of tumor microenvironments including neovascularization and recruitment of pro- or anti-tumor inflammatory cells. The analysis of the tumor microenvironment showed that tumors in the ω-3 group had significantly lower numbers of proliferating tumor cells (Ki67+)/high power field (HPF), lower neo-vascularization measured as CD31+ vessels and infiltration by neutrophil elastase+ cells, and macrophages (F4/80+) relative to the tumors from mice in the ω-6 group. Tumor cell proliferation, intra-tumoral neovascularization and infiltration of macrophages and neutrophils directly correlated with tumor size indicating their direct roles in the promotion of tumor growth. In contrast, tumors from the ω-3 fed mice had significantly higher numbers of apoptotic tumor cells ($TUNEL^+$)/HPF and infiltrating $CD3^+$ T-cells, both of which indirectly correlated with tumor size indicating their role in the suppression of tumor growth. Further, the macrophage infiltration is directly correlated with neovascularization, while infiltration of T-cells is directly correlated with the number of apoptotic tumor cells. Collectively, our data on the inflammatory microenvironment of tumors on day 35 showed that the increased infiltration of T-cells and decreased infiltration by tumor promoting myeloid cells including neutrophils and macrophages might regulate tumor microenvironments in mice fed ω-3 diets resulting in the suppression of tumor growth compared to the mice on an ω-6 diet.

Finally, we analyzed the mRNA expressions of cytokines/adipokines and growth factors to understand their potential role in dietary PUFA mediated regulation of tumor microenvironments. When the mRNA expression in tumors were compared to the respective mRNA expression in spleens from NTB control mice, G-CSF, PTGS2 and CCL2 were highly expressed in 4T1 mammary tumors in both dietary groups and the expression was not different between the tumors from the dietary groups. These results indicates that the expression of G-CSF, PTGS2 and CCL2 is largely regulated by 4T1

tumors such that, the effects of dietary PUFA interventions in their expression was minimal during tumor growth. Further, we did not observe any difference in the expression of NFkB, GM-CSF, LEP, IGF1, CXCL5, CXCL1 and AREG either as compared to the expression in NTB spleen nor in tumors between the dietary groups. It should be noted that we evaluated mRNA expression in the tumor tissue that were collected on day 35 post tumor injection. Thus, it is likely that cytokine expression levels may have been upregulated in the early phases of tumor growth during recruitment of inflammatory cells, and that by day 35, the expressed mediators may have been used for the respective signaling processes. Unexpectedly, we observed that the mRNA expression of IL10 in tumors from ω-3 diet-fed mice was significantly higher (six fold) relative to the expression in the tumors from the ω-6 diet-fed mice. Further, the levels of IL10 mRNA were inversely correlated with the tumor size indicating a potential role of IL10 in the suppression of tumor growth. However, further mechanistic studies are required to confirm the role of IL10 in LC-ω-3FA mediated tumor suppression.

It is estimated that metastasis is responsible for about 90% of deaths due to cancer and represents the central clinical challenge of oncology of all types of cancers including BC [502, 503]. Our studies shows lower incidence and frequencies of metastatic tumor growths in multiple organs in mice fed a diet high in LC-ω-3FAs, which are in correspondence with a significant longer survival of mice in the group compared to the mice fed ω-6 diet. The death due to metastasis (typically in BC) is not due arresting of few tumor cells from blood stream into a distant organ, rather it is due to the consequences related to the uncontrolled proliferation of metastatic tumor cells in the organ, affecting its physiological functions needed for life. Metastasis is a sequential process and for a successful metastatic growth, roles of both tumor microenvironments and pre-metastatic tissue microenvironments are crucial [504-506]. Most of metastasis and survival studies

focus on tumor microenvironments and less emphasis is given on the role of pre-metastatic niche. As per seed and soil hypothesis, all organs are not hospitable for all tumor types so specific tumor types have organ preferences for metastasis. However, as showed by our studies, dietary factors such as PUFAs can modulate organ microenvironments modulating the metastatic growth in the organ. Thus, further studies should be done to understand the role tissue microenvironments and the modifying factors that can modulate pre-metastatic niche in favoring of tumor growths.

In conclusion, from the NTB studies, we showed that a dietary ω-3 and ω-6 PUFAs differentially modulated the microenvironments of the primary tumor site and one of the metastatic sites (liver), which can regulate 4T1 mammary tumor growth and metastasis. Specifically, dietary LC-ω-3FAs lowers MG ductal density, epithelial cell proliferation and adipose tissue inflammation in MGs and lowers hepatic steatosis, hepatocyte apoptosis and EMM in livers of NTB mice. In 4T1 mammary tumors, dietary LC-ω-3FAs delayed tumor initiation, growth and enhanced survival of the mice by lowering the incidence and frequencies of metastases to common and uncommon sites. The potential mechanism includes modulation of inflammatory microenvironments in tumors, specifically increased infiltration of T-cells and IL10 mediated anti-inflammatory activities.

6.2. Future directions

The present study is the first study analyzing the effects of PUFAs administered as isocaloric, isolipidic diets using a pair-fed model. From our NTB and TB studies, we reported many novel observations of tissue microenvironment modulations by dietary PUFA composition regulating mammary tumor progression and answered critical questions regarding the importance of PUFA composition in diets. However, our studies

have raised many important questions that can be addressed in future studies, some of which are discussed below.

1. We observed the differences in MG ductal branching and sprouting between mice fed ω-6 and ω-3 diets. Progesterone and prolactin are the major hormones regulating branching during normal MG developments. We used adult, nulliparous mice and did not see differences in those hormones. So, it is likely that an alternative mechanism could play role in the regulation of branching morphogenesis by dietary PUFAs.
2. There were significantly smaller adipocytes in MG and abdominal fats in a ω-3 diet-fed mice compared to the ω-6 group. The observation raises the question that dietary PUFA composition potentially regulates FA storage versus metabolism, which can be addressed in future metabolic studies.
3. There was significantly more hepatic steatosis but lower glycogen deposits in the hepatocytes of mice fed an ω-6 diet relative to the ω-3 group. It is unclear if increases in fat droplets in hepatocytes are limiting glycogen storage, or vice versa. It is possible a different mechanism related to the choice of fat versus glycogen pathways, is regulated by PUFA composition.
4. In metastasis studies, we evaluated multiple organs (lungs, liver, heart, kidneys, ovaries, and bone) and found differences in the incidence and frequency of metastasis in those organs. However, in our NTB studies, we analyzed hepatic microenvironments only as one of the representative metastatic sites. It is likely that dietary PUFA composition might have modulated microenvironments of the other organs to regulate metastatic growth to these sites. Further studies analyzing each of these organs are needed to address these questions.

5. Bone metastasis in breast cancer is regulated by cross talk between osteoclasts and tumor cells. The understanding of how dietary PUFA composition modulates osteoclastic activities in the presence and absence of tumor will help to understand if PUFAs aid in the formation of pre-metastatic niches in bone.
6. We analyzed inflammatory microenvironments of tumors on day 35 post tumor injection for the evaluation of inflammatory cells and cytokines/growth factors. Since tumor immunology depends on the stage of tumor growth and progression, time dependent studies will help in understanding PUFA regulation of tumor immunology during tumor development and metastasis.
7. Examine the therapeutic potential of ω-3 PUFA interventions.
8. Determine the longitudinal response to ω-3 “change over” in tumor bearing mice
9. Determine a dietary PUFA regulation of mammary tumor on brain metastasis.
10. Analyses of metastatic burden between the mice from the dietary groups that are having similar tumor size.

References

1. Center for disease control and prevention, *U.S. Cancer Statistics Working Group. U.S. Cancer Statistics Data Visualizations Tool, based on November 2017 submission data (1999-2015)*. June 2018 [cited 2018 August 2018]; Available from: https://gis.cdc.gov/Cancer/USCS/DataViz.html.
2. National cancer institute, *Cancer Stat Facts: Female Breast Cancer*. 2018 [cited 2018 August 16]; Available from: https://seer.cancer.gov/statfacts/html/breast.html.
3. GLOBOCAN, W.H.O. *Breast Cancer: Estimated Incidence, Mortality and Prevalence Worldwide in 2012*. 2015 [cited 2018 August, 2018]; Available from: http://globocan.iarc.fr/old/FactSheets/cancers/breast-new.asp.
4. Center for disease control and prevntion, *What Are the Risk Factors for Breast Cancer?* 2018; Available from: https://www.cdc.gov/cancer/breast/basic_info/risk_factors.htm.
5. Dieterich, M., et al., *Influence of Lifestyle Factors on Breast Cancer Risk.* Breast Care, 2014. **9**(6): p. 407-414.
6. Thiebaut, A.C., et al., *Dietary fat and postmenopausal invasive breast cancer in the National Institutes of Health-AARP Diet and Health Study cohort.* J Natl Cancer Inst, 2007. **99**(6): p. 451-62.
7. Kim, E.J., et al., *Dietary fat increases solid tumor growth and metastasis of 4T1 murine mammary carcinoma cells and mortality in obesity-resistant BALB/c mice.* Breast Cancer Research : BCR, 2011. **13**(4): p. R78-R78.
8. Xia, H., et al., *Meta-Analysis of Saturated Fatty Acid Intake and Breast Cancer Risk.* Medicine (Baltimore), 2015. **94**(52): p. e2391.
9. Devkumar, M., et al., *MRI reveals increased tumorigenesis following high fat feeding in a mouse model of triple-negative breast cancer.* NMR in Biomedicine, 2017. **30**(10): p. e3758.
10. Yang, B., et al., *Ratio of n-3/n-6 PUFAs and risk of breast cancer: a meta-analysis of 274135 adult females from 11 independent prospective studies.* BMC Cancer, 2014. **14**: p. 105.
11. Thiebaut, A.C., et al., *Dietary intakes of omega-6 and omega-3 polyunsaturated fatty acids and the risk of breast cancer.* Int J Cancer, 2009. **124**(4): p. 924-31.
12. Gomes, M.A., et al., *The role of background diet on the effects of eicosapentaenoic acid and docosahexaenoic acid supplementation in healthy pre-menopausal women: a randomized, cross-over, controlled study.* Lipids Health Dis, 2016. **15**(1): p. 168.
13. Fay, M.P., et al., *Effect of different types and amounts of fat on the development of mammary tumors in rodents: a review.* Cancer Res, 1997. **57**(18): p. 3979-88.
14. Zheng, J.S., et al., *Intake of fish and marine n-3 polyunsaturated fatty acids and risk of breast cancer: meta-analysis of data from 21 independent prospective cohort studies.* Bmj, 2013. **346**: p. f3706.
15. Murff, H.J., et al., *Dietary polyunsaturated fatty acids and breast cancer risk in Chinese women: a prospective cohort study.* Int J Cancer, 2011. **128**(6): p. 1434-41.
16. Kiyabu, G.Y., et al., *Fish, n - 3 polyunsaturated fatty acids and n - 6 polyunsaturated fatty acids intake and breast cancer risk: The Japan Public Health Center-based prospective study.* Int J Cancer, 2015. **137**(12): p. 2915-26.
17. Astorg, P., *Dietary N-6 and N-3 polyunsaturated fatty acids and prostate cancer risk: a review of epidemiological and experimental evidence.* Cancer Causes Control, 2004. **15**(4): p. 367-86.

18. Patterson, E., et al., *Health Implications of High Dietary Omega-6 Polyunsaturated Fatty Acids.* Journal of Nutrition and Metabolism, 2012. **2012**: p. 539426.
19. Calder, P.C. and R.F. Grimble, *Polyunsaturated fatty acids, inflammation and immunity.* Eur J Clin Nutr, 2002. **56 Suppl 3**: p. S14-9.
20. Simopoulos, A.P., *An Increase in the Omega-6/Omega-3 Fatty Acid Ratio Increases the Risk for Obesity.* Nutrients, 2016. **8**(3): p. 128.
21. Weylandt, K.H., et al., *Omega-3 Polyunsaturated Fatty Acids: The Way Forward in Times of Mixed Evidence.* BioMed Research International, 2015. **2015**: p. 143109.
22. Russo, G.L., *Dietary n-6 and n-3 polyunsaturated fatty acids: from biochemistry to clinical implications in cardiovascular prevention.* Biochem Pharmacol, 2009. **77**(6): p. 937-46.
23. Brenna, J.T., et al., *alpha-Linolenic acid supplementation and conversion to n-3 long-chain polyunsaturated fatty acids in humans.* Prostaglandins Leukot Essent Fatty Acids, 2009. **80**(2-3): p. 85-91.
24. Fabian, C.J., B.F. Kimler, and S.D. Hursting, *Omega-3 fatty acids for breast cancer prevention and survivorship.* Breast Cancer Research, 2015. **17**(1): p. 62.
25. Simopoulos, A.P., *Evolutionary aspects of diet, the omega-6/omega-3 ratio and genetic variation: nutritional implications for chronic diseases.* Biomed Pharmacother, 2006. **60**(9): p. 502-7.
26. Burdge, G.C. and P.C. Calder, *Dietary alpha-linolenic acid and health-related outcomes: a metabolic perspective.* Nutr Res Rev, 2006. **19**(1): p. 26-52.
27. Arterburn, L.M., E.B. Hall, and H. Oken, *Distribution, interconversion, and dose response of n-3 fatty acids in humans.* Am J Clin Nutr, 2006. **83**(6 Suppl): p. 1467s-1476s.
28. Saini, R.K. and Y.-S. Keum, *Omega-3 and omega-6 polyunsaturated fatty acids: Dietary sources, metabolism, and significance — A review.* Life Sciences, 2018. **203**: p. 255-267.
29. Stremmel, W., *Uptake of fatty acids by jejunal mucosal cells is mediated by a fatty acid binding membrane protein.* J Clin Invest, 1988. **82**(6): p. 2001-10.
30. Abumrad, N.A., et al., *Cloning of a rat adipocyte membrane protein implicated in binding or transport of long-chain fatty acids that is induced during preadipocyte differentiation. Homology with human CD36.* J Biol Chem, 1993. **268**(24): p. 17665-8.
31. Jia, Z., et al., *The fatty acid transport protein (FATP) family: very long chain acyl-CoA synthetases or solute carriers?* J Mol Neurosci, 2007. **33**(1): p. 25-31.
32. Masson, C.J., et al., *Fatty acid- and cholesterol transporter protein expression along the human intestinal tract.* PLoS One, 2010. **5**(4): p. e10380.
33. Burdge, G.C., *Metabolism of α-linolenic acid in humans.* Prostaglandins, Leukotrienes and Essential Fatty Acids, 2006. **75**(3): p. 161-168.
34. Sprecher, H., *The roles of anabolic and catabolic reactions in the synthesis and recycling of polyunsaturated fatty acids.* Prostaglandins, Leukotrienes and Essential Fatty Acids, 2002. **67**(2): p. 79-83.
35. Russo, G.L., *Dietary n−6 and n−3 polyunsaturated fatty acids: From biochemistry to clinical implications in cardiovascular prevention.* Biochemical Pharmacology, 2009. **77**(6): p. 937-946.
36. Calder, P.C., *Omega-3 polyunsaturated fatty acids and inflammatory processes: nutrition or pharmacology?* Br J Clin Pharmacol, 2013. **75**(3): p. 645-62.
37. Stulnig, T.M., et al., *Polyunsaturated Eicosapentaenoic Acid Displaces Proteins from Membrane Rafts by Altering Raft Lipid Composition.* Journal of Biological Chemistry, 2001. **276**(40): p. 37335-37340.

38. Tilley, S.L., T.M. Coffman, and B.H. Koller, *Mixed messages: modulation of inflammation and immune responses by prostaglandins and thromboxanes.* The Journal of Clinical Investigation, 2001. **108**(1): p. 15-23.
39. Lewis, R.A., K.F. Austen, and R.J. Soberman, *Leukotrienes and other products of the 5-lipoxygenase pathway. Biochemistry and relation to pathobiology in human diseases.* N Engl J Med, 1990. **323**(10): p. 645-55.
40. Calder, P.C., *Polyunsaturated fatty acids and inflammatory processes: New twists in an old tale.* Biochimie, 2009. **91**(6): p. 791-795.
41. Davies, P., et al., *The Role of Arachidonic Acid Oxygenation Products in Pain and Inflammation.* Annual Review of Immunology, 1984. **2**(1): p. 335-357.
42. Omori, K., et al., *Multiple roles of the PGE2 -EP receptor signal in vascular permeability.* Br J Pharmacol, 2014. **171**(21): p. 4879-89.
43. Phipps, R.P., S.H. Stein, and R.L. Roper, *A new view of prostaglandin E regulation of the immune response.* Immunol Today, 1991. **12**(10): p. 349-52.
44. Nakayama, T., et al., *Prostaglandin E2 promotes degranulation-independent release of MCP-1 from mast cells.* J Leukoc Biol, 2006. **79**(1): p. 95-104.
45. Lemos, H.P., et al., *Prostaglandin mediates IL-23/IL-17-induced neutrophil migration in inflammation by inhibiting IL-12 and IFNγ production.* Proceedings of the National Academy of Sciences, 2009. **106**(14): p. 5954-5959.
46. Williams, J.A. and E. Shacter, *Regulation of Macrophage Cytokine Production by Prostaglandin E2 : DISTINCT ROLES OF CYCLOOXYGENASE-1 AND -2.* Journal of Biological Chemistry, 1997. **272**(41): p. 25693-25699.
47. Vane, J.R. and R.M. Botting, *The mechanism of action of aspirin.* Thrombosis Research, 2003. **110**(5): p. 255-258.
48. Goto, T., et al., *Cyclic AMP as a mediator of prostaglandin E-induced suppression of human natural killer cell activity.* J Immunol, 1983. **130**(3): p. 1350-5.
49. Aronoff, D.M., C. Canetti, and M. Peters-Golden, *Prostaglandin E2 inhibits alveolar macrophage phagocytosis through an E-prostanoid 2 receptor-mediated increase in intracellular cyclic AMP.* J Immunol, 2004. **173**(1): p. 559-65.
50. Rincon, M., et al., *Prostaglandin E2 and the increase of intracellular cAMP inhibit the expression of interleukin 2 receptors in human T cells.* Eur J Immunol, 1988. **18**(11): p. 1791-6.
51. Kunkel, S.L., et al., *Prostaglandin E2 regulates macrophage-derived tumor necrosis factor gene expression.* Journal of Biological Chemistry, 1988. **263**(11): p. 5380-5384.
52. Byron, K.A., et al., *Interferon-gamma production in atopic dermatitis: a role for prostaglandins?* Int Arch Allergy Immunol, 1992. **99**(1): p. 50-5.
53. Wang, M.T., K.V. Honn, and D. Nie, *Cyclooxygenases, prostanoids, and tumor progression.* Cancer Metastasis Rev, 2007. **26**(3-4): p. 525-34.
54. Snijdewint, F.G., et al., *Prostaglandin E2 differentially modulates cytokine secretion profiles of human T helper lymphocytes.* J Immunol, 1993. **150**(12): p. 5321-9.
55. Sheibanie, A.F., et al., *The proinflammatory effect of prostaglandin E2 in experimental inflammatory bowel disease is mediated through the IL-23-->IL-17 axis.* J Immunol, 2007. **178**(12): p. 8138-47.
56. Huang, M., et al., *Non-small cell lung cancer cyclooxygenase-2-dependent regulation of cytokine balance in lymphocytes and macrophages: up-regulation of interleukin 10 and down-regulation of interleukin 12 production.* Cancer Res, 1998. **58**(6): p. 1208-16.

57. Obermajer, N., et al., *Positive feedback between PGE2 and COX2 redirects the differentiation of human dendritic cells toward stable myeloid-derived suppressor cells.* Blood, 2011. **118**(20): p. 5498-505.
58. Walker, C.G., et al., *The Pattern of Fatty Acids Displaced by EPA and DHA Following 12 Months Supplementation Varies between Blood Cell and Plasma Fractions.* Nutrients, 2015. **7**(8): p. 6281-93.
59. Drobnic, F., et al., *Erythrocyte Omega-3 Fatty Acid Content in Elite Athletes in Response to Omega-3 Supplementation: A Dose-Response Pilot Study.* Journal of Lipids, 2017. **2017**: p. 1472719.
60. Kang, J.X., et al., *Fat-1 mice convert n-6 to n-3 fatty acids.* Nature, 2004. **427**: p. 504.
61. Januszewicz, P., *[Role of prostaglandins in immunological reactions].* Pol Tyg Lek, 1981. **36**(12): p. 457-8.
62. Chapkin, R.S., C.C. Akoh, and C.C. Miller, *Influence of dietary n-3 fatty acids on macrophage glycerophospholipid molecular species and peptidoleukotriene synthesis.* J Lipid Res, 1991. **32**(7): p. 1205-13.
63. Lee, T.H., et al., *Effect of dietary enrichment with eicosapentaenoic and docosahexaenoic acids on in vitro neutrophil and monocyte leukotriene generation and neutrophil function.* N Engl J Med, 1985. **312**(19): p. 1217-24.
64. Schmidt, E.B., et al., *Cod liver oil inhibits neutrophil and monocyte chemotaxis in healthy males.* Atherosclerosis, 1989. **77**(1): p. 53-7.
65. Yamada, H., et al., *In vivo and in vitro inhibition of monocyte adhesion to endothelial cells and endothelial adhesion molecules by eicosapentaenoic acid.* Arterioscler Thromb Vasc Biol, 2008. **28**(12): p. 2173-9.
66. Miles, E.A., F.A. Wallace, and P.C. Calder, *Dietary fish oil reduces intercellular adhesion molecule 1 and scavenger receptor expression on murine macrophages.* Atherosclerosis, 2000. **152**(1): p. 43-50.
67. Goua, M., et al., *Regulation of adhesion molecule expression in human endothelial and smooth muscle cells by omega-3 fatty acids and conjugated linoleic acids: involvement of the transcription factor NF-kappaB?* Prostaglandins Leukot Essent Fatty Acids, 2008. **78**(1): p. 33-43.
68. Honda, K.L., et al., *EPA and DHA exposure alters the inflammatory response but not the surface expression of toll-like receptor 4 in macrophages.* Lipids, 2015. **50**(2): p. 121-129.
69. Zhao, Y., et al., *Eicosapentaenoic acid prevents LPS-induced TNF-alpha expression by preventing NF-kappaB activation.* J Am Coll Nutr, 2004. **23**(1): p. 71-8.
70. Khalfoun, B., et al., *Docosahexaenoic and eicosapentaenoic acids inhibit in vitro human endothelial cell production of interleukin-6.* Adv Exp Med Biol, 1997. **400b**: p. 589-97.
71. Allam-Ndoul, B., et al., *Effect of n-3 fatty acids on the expression of inflammatory genes in THP-1 macrophages.* Lipids in Health and Disease, 2016. **15**: p. 69.
72. Serhan, C.N., et al., *Novel functional sets of lipid-derived mediators with antiinflammatory actions generated from omega-3 fatty acids via cyclooxygenase 2-nonsteroidal antiinflammatory drugs and transcellular processing.* J Exp Med, 2000. **192**(8): p. 1197-204.
73. Oh, S.F., et al., *Pro-resolving actions and stereoselective biosynthesis of 18S E-series resolvins in human leukocytes and murine inflammation.* J Clin Invest, 2011. **121**(2): p. 569-81.
74. Arita, M., C.B. Clish, and C.N. Serhan, *The contributions of aspirin and microbial oxygenase to the biosynthesis of anti-inflammatory resolvins: novel oxygenase products*

from omega-3 polyunsaturated fatty acids. Biochem Biophys Res Commun, 2005. **338**(1): p. 149-57.
75. Lannan, K.L., et al., *Maresin 1 induces a novel pro-resolving phenotype in human platelets.* J Thromb Haemost, 2017. **15**(4): p. 802-813.
76. Serhan, C.N., et al., *Anti-inflammatory actions of neuroprotectin D1/protectin D1 and its natural stereoisomers: assignments of dihydroxy-containing docosatrienes.* J Immunol, 2006. **176**(3): p. 1848-59.
77. Serhan, C.N., et al., *Maresins: novel macrophage mediators with potent antiinflammatory and proresolving actions.* J Exp Med, 2009. **206**(1): p. 15-23.
78. Hong, S., et al., *Novel docosatrienes and 17S-resolvins generated from docosahexaenoic acid in murine brain, human blood, and glial cells. Autacoids in anti-inflammation.* J Biol Chem, 2003. **278**(17): p. 14677-87.
79. Arita, M., et al., *Stereochemical assignment, antiinflammatory properties, and receptor for the omega-3 lipid mediator resolvin E1.* J Exp Med, 2005. **201**(5): p. 713-22.
80. Arita, M., et al., *Resolvin E1 selectively interacts with leukotriene B4 receptor BLT1 and ChemR23 to regulate inflammation.* J Immunol, 2007. **178**(6): p. 3912-7.
81. Levy, B.D., et al., *Protectin D1 is generated in asthma and dampens airway inflammation and hyperresponsiveness.* J Immunol, 2007. **178**(1): p. 496-502.
82. Duffield, J.S., et al., *Resolvin D series and protectin D1 mitigate acute kidney injury.* J Immunol, 2006. **177**(9): p. 5902-11.
83. Hudert, C.A., et al., *Transgenic mice rich in endogenous omega-3 fatty acids are protected from colitis.* Proc Natl Acad Sci U S A, 2006. **103**(30): p. 11276-81.
84. Hellmann, J., et al., *Resolvin D1 decreases adipose tissue macrophage accumulation and improves insulin sensitivity in obese-diabetic mice.* Faseb j, 2011. **25**(7): p. 2399-407.
85. Sulciner, M.L., et al., *Resolvins suppress tumor growth and enhance cancer therapy.* The Journal of Experimental Medicine, 2017.
86. Duvall, M.G. and B.D. Levy, *DHA- and EPA-derived resolvins, protectins, and maresins in airway inflammation.* European journal of pharmacology, 2016. **785**: p. 144-155.
87. Dalli, J., et al., *The novel 13S,14S-epoxy-maresin is converted by human macrophages to maresin 1 (MaR1), inhibits leukotriene A4 hydrolase (LTA4H), and shifts macrophage phenotype.* Faseb j, 2013. **27**(7): p. 2573-83.
88. Vatnick, D.R., et al., *Control of Breast Cancer through the Resolution of Inflammation.* The FASEB Journal, 2016. **30**(1_supplement): p. 698.3-698.3.
89. Calder, P.C., *Omega-3 Fatty Acids and Inflammatory Processes.* Nutrients, 2010. **2**(3): p. 355-374.
90. Cardiff, R.D. and S.R. Wellings, *The Comparative Pathology of Human and Mouse Mammary Glands.* Journal of Mammary Gland Biology and Neoplasia, 1999. **4**(1): p. 105-122.
91. Russo, J., et al., *Comparative study of human and rat mammary tumorigenesis.* Lab Invest, 1990. **62**(3): p. 244-78.
92. Wärri, A.M., N.M. Saarinen, and S.I. Mäkelä, *Can Modulation of Mammary Gland Development by Dietary Factors Support Breast Cancer Prevention?* Hormone Research in Paediatrics, 2007. **68**(5): p. 248-260.
93. Carroll, J.S., et al., *Deciphering the divergent roles of progestogens in breast cancer.* Nature Reviews Cancer, 2016. **17**: p. 54.
94. Byng, J.W., et al., *The quantitative analysis of mammographic densities.* Phys Med Biol, 1994. **39**(10): p. 1629-38.

95. Boyd, N.F., et al., *Mammographic density and the risk and detection of breast cancer.* N Engl J Med, 2007. **356**(3): p. 227-36.
96. Mandelson, M.T., et al., *Breast density as a predictor of mammographic detection: comparison of interval- and screen-detected cancers.* J Natl Cancer Inst, 2000. **92**(13): p. 1081-7.
97. Boyd, N.F., et al., *Quantitative classification of mammographic densities and breast cancer risk: results from the Canadian National Breast Screening Study.* J Natl Cancer Inst, 1995. **87**(9): p. 670-5.
98. Huo, C.W., et al., *High mammographic density is associated with an increase in stromal collagen and immune cells within the mammary epithelium.* Breast Cancer Research : BCR, 2015. **17**(1): p. 79.
99. McGinley, J.N. and H.J. Thompson, *Quantitative Assessment of Mammary Gland Density in Rodents Using Digital Image Analysis.* Biological Procedures Online, 2011. **13**: p. 4-4.
100. Blacher, S., et al., *Quantitative Assessment of Mouse Mammary Gland Morphology Using Automated Digital Image Processing and TEB Detection.* Endocrinology, 2016. **157**(4): p. 1709-16.
101. Russo, I.H. and J. Russo, *Developmental stage of the rat mammary gland as determinant of its susceptibility to 7,12-dimethylbenz[a]anthracene.* J Natl Cancer Inst, 1978. **61**(6): p. 1439-49.
102. Nielsen, T.S., et al., *Prepubertal exposure to cow's milk reduces susceptibility to carcinogen-induced mammary tumorigenesis in rats.* Int J Cancer, 2011. **128**(1): p. 12-20.
103. Sharma, D., et al., *Quantification of epithelial cell differentiation in mammary glands and carcinomas from DMBA- and MNU-exposed rats.* PLoS One, 2011. **6**(10): p. e26145.
104. Russo, J., et al., *Molecular and cellular basis of the mammary gland susceptibility to carcinogenesis.* Environ Health Perspect, 1983. **49**: p. 185-99.
105. Hawes, D., et al., *Dense breast stromal tissue shows greatly increased concentration of breast epithelium but no increase in its proliferative activity.* Breast Cancer Research, 2006. **8**(2): p. R24-R24.
106. Stomper, P.C., et al., *Cellular proliferative activity of mammographic normal dense and fatty tissue determined by DNA S phase percentage.* Breast Cancer Res Treat, 1996. **37**(3): p. 229-36.
107. Huh, S.J., et al., *The Proliferative Activity of Mammary Epithelial Cells in Normal Tissue Predicts Breast Cancer Risk in Premenopausal Women.* Cancer Research, 2016. **76**(7): p. 1926-1934.
108. Alowami, S., et al., *Mammographic density is related to stroma and stromal proteoglycan expression.* Breast Cancer Res, 2003. **5**(5): p. R129-35.
109. Abrahamsson, A., et al., *Dense breast tissue in postmenopausal women is associated with a pro-inflammatory microenvironment in vivo.* Oncoimmunology, 2016. **5**(10): p. e1229723.
110. Khadge, S., et al., *Long-Chain Omega-3 Polyunsaturated Fatty Acids Modulate Mammary Gland Composition and Inflammation.* Journal of Mammary Gland Biology and Neoplasia, 2018. **23**(1): p. 43-58.
111. Parmar, H. and G.R. Cunha, *Epithelial-stromal interactions in the mouse and human mammary gland in vivo.* Endocr Relat Cancer, 2004. **11**(3): p. 437-58.
112. Alfonso, J.C., et al., *In-silico insights on the prognostic potential of immune cell infiltration patterns in the breast lobular epithelium.* Sci Rep, 2016. **6**: p. 33322.
113. Nazari, S.S. and P. Mukherjee, *An overview of mammographic density and its association with breast cancer.* Breast Cancer (Tokyo, Japan), 2018. **25**(3): p. 259-267.

114. Hilakivi-Clarke, L., et al., *A maternal diet high in n - 6 polyunsaturated fats alters mammary gland development, puberty onset, and breast cancer risk among female rat offspring.* Proc Natl Acad Sci U S A, 1997. **94**(17): p. 9372-7.
115. Hilakivi-Clarke, L., R. Clarke, and M. Lippman, *The influence of maternal diet on breast cancer risk among female offspring.* Nutrition, 1999. **15**(5): p. 392-401.
116. Ion, G., J.A. Akinsete, and W.E. Hardman, *Maternal consumption of canola oil suppressed mammary gland tumorigenesis in C3(1) TAg mice offspring.* BMC Cancer, 2010. **10**: p. 81.
117. Su, H.M., P.H. Hsieh, and H.F. Chen, *A maternal high n-6 fat diet with fish oil supplementation during pregnancy and lactation in rats decreases breast cancer risk in the female offspring.* J Nutr Biochem, 2010. **21**(11): p. 1033-7.
118. Olivo, S.E. and L. Hilakivi-Clarke, *Opposing effects of prepubertal low- and high-fat n-3 polyunsaturated fatty acid diets on rat mammary tumorigenesis.* Carcinogenesis, 2005. **26**(9): p. 1563-72.
119. Manna, S., et al., *Protective role of fish oil (Maxepa) on early events of rat mammary carcinogenesis by modulation of DNA-protein crosslinks, cell proliferation and p53 expression.* Cancer Cell International, 2007. **7**(1): p. 6.
120. Hardman, W.E., et al., *Dietary walnut suppressed mammary gland tumorigenesis in the C(3)1 TAg mouse.* Nutr Cancer, 2011. **63**(6): p. 960-70.
121. Hardman, W.E., *Dietary canola oil suppressed growth of implanted MDA-MB 231 human breast tumors in nude mice.* Nutr Cancer, 2007. **57**(2): p. 177-83.
122. Innis, S.M., *Metabolic programming of long-term outcomes due to fatty acid nutrition in early life.* Matern Child Nutr, 2011. **7 Suppl 2**: p. 112-23.
123. Mennitti, L.V., et al., *Type of fatty acids in maternal diets during pregnancy and/or lactation and metabolic consequences of the offspring.* J Nutr Biochem, 2015. **26**(2): p. 99-111.
124. Anderson, B.M., et al., *Lifelong exposure to n-3 PUFA affects pubertal mammary gland development.* Appl Physiol Nutr Metab, 2014. **39**(6): p. 699-706.
125. MacLennan, M.B., et al., *Mammary tumor development is directly inhibited by lifelong n-3 polyunsaturated fatty acids.* The Journal of Nutritional Biochemistry, 2013. **24**(1): p. 388-395.
126. Kang, J.X., *Fat-1 transgenic mice: a new model for omega-3 research.* Prostaglandins Leukot Essent Fatty Acids, 2007. **77**(5-6): p. 263-7.
127. Wei, N., et al., *Effects of different dietary fatty acids on the fatty acid compositions and the expression of lipid metabolic-related genes in mammary tumor tissues of rats.* Nutr Cancer, 2008. **60**(6): p. 810-25.
128. Ghosh-Choudhury, T., et al., *Fish oil targets PTEN to regulate NFkappaB for downregulation of anti-apoptotic genes in breast tumor growth.* Breast Cancer Res Treat, 2009. **118**(1): p. 213-28.
129. Corsetto, P.A., et al., *Effects of n-3 PUFAs on breast cancer cells through their incorporation in plasma membrane.* Lipids Health Dis, 2011. **10**: p. 73.
130. Liang, P., et al., *Effect of dietary omega-3 fatty acids on tumor-associated macrophages and prostate cancer progression.* The Prostate, 2016. **76**(14): p. 1293-1302.
131. Kuno, T., et al., *Promoting effects of high-fat corn oil and high-fat mixed lipid diets on 7,12-dimethylbenz[a]anthracene-induced mammary tumorigenesis in F344 rats.* Oncol Rep, 2003. **10**(3): p. 699-703.
132. Malarkey, D.E., et al., *New Insights into Functional Aspects of Liver Morphology.* Toxicologic Pathology, 2005. **33**(1): p. 27-34.

133. R.M.N., M., et al., *Pathology of the liver, 4th edition.* Diagnostic Cytopathology, 2003. **29**(1): p. 43-43.
134. Kimitaka, K., et al., *A comparative study of the anatomy of rat and human livers.* Journal of Hepato-Biliary-Pancreatic Surgery, 1999. **6**(2): p. 171-175.
135. Boorman, G., et al., *Pathology ofthe Fischer Rat*. 1990, Academic Press.
136. Harada, T., et al., *Pathology of the mouse*. 1999, Cache River Press.
137. Matsumoto, T. and M. Kawakami, *The unit-concept of hepatic parenchyma--a re-examination based on angioarchitectural studies.* Acta Pathol Jpn, 1982. **32 Suppl 2**: p. 285-314.
138. Ramaiah, S.K. and A. Banerjee, *CHAPTER 37 - Liver Toxicity of Chemical Warfare Agents A2 - Gupta, Ramesh C*, in *Handbook of Toxicology of Chemical Warfare Agents*. 2009, Academic Press: San Diego. p. 549-560.
139. Braet, F. and E. Wisse, *Structural and functional aspects of liver sinusoidal endothelial cell fenestrae: a review.* Comparative hepatology, 2002. **1**(1): p. 1.
140. Bykov, I., et al. *Functional differences between periportal and perivenous Kupffer cells isolated by digitonin-collagenase perfusion*. in *Comparative hepatology*. 2004. BioMed Central.
141. Kawada, N. *Molecular mechanism of stellate cell activation and therapeutic strategy for liver fibrosis*. in *Comparative hepatology*. 2004. BioMed Central.
142. Geerts, A., *History, Heterogeneity, Developmental Biology, and Functions of Quiescent Hepatic Stellate Cells.* Semin Liver Dis, 2001. **21**(03): p. 311-336.
143. King, D.G. *Lobule of pig liver*. 2002 January, 2002 [cited 2018; Available from: http://www.siumed.edu/~dking2/erg/GI152b.htm.
144. Kim, C.H., *Homeostatic and pathogenic extramedullary hematopoiesis.* Journal of blood medicine, 2010. **1**: p. 13-19.
145. Craig, C.E., A. Quaglia, and A.P. Dhillon, *Extramedullary haematopoiesis in massive hepatic necrosis.* Histopathology, 2004. **45**(5): p. 518-25.
146. Toro, K., M. Hubay, and E. Keller, *Extramedullary haematopoiesis in liver of sudden infant death cases.* Forensic Sci Int, 2007. **170**(1): p. 15-9.
147. Tsamandas, A.C., et al., *Extramedullary hematopoiesis in the allograft liver.* Mod Pathol, 1995. **8**(6): p. 671-4.
148. Wong, Y., et al., *Imaging features of focal intrahepatic extramedullary haematopoiesis.* Br J Radiol, 1999. **72**(861): p. 906-10.
149. Yamamoto, K., et al., *Extramedullary hematopoiesis: Elucidating the function of the hematopoietic stem cell niche (Review).* Mol Med Rep, 2016. **13**(1): p. 587-91.
150. O'Malley, D.P., *Benign extramedullary myeloid proliferations.* Mod Pathol, 2007. **20**(4): p. 405-15.
151. Eliasson, P. and J.I. Jonsson, *The hematopoietic stem cell niche: low in oxygen but a nice place to be.* J Cell Physiol, 2010. **222**(1): p. 17-22.
152. E, C.J. and B.G. E, *Extramedullary hematopoiesis in the adult mouse liver is associated with specific hepatic sinusoidal endothelial cells.* Hepatology, 1997. **26**(1): p. 165-175.
153. Dusad, A., et al., *High fat and alcoholic diets increase hepatic EMH, osteolysis and spontaneous metastases by orthotopic mammary tumors.* Journal for Immunotherapy of Cancer, 2013. **1**(Suppl 1): p. P258-P258.
154. Wang, H.J., et al., *Inflammation in Alcoholic Liver Disease.* Annual review of nutrition, 2012. **32**: p. 343-368.
155. Toita, R., et al., *Increased hepatic inflammation in a normal-weight mouse after long-term high-fat diet feeding.* Journal of Toxicologic Pathology, 2018. **31**(1): p. 43-47.

156. Agius, L., *Glucokinase and molecular aspects of liver glycogen metabolism.* Biochem J, 2008. **414**(1): p. 1-18.
157. Rui, L., *Energy Metabolism in the Liver.* Comprehensive Physiology, 2014. **4**(1): p. 177-197.
158. Adeva-Andany, M.M., et al., *Glycogen metabolism in humans.* BBA Clinical, 2016. **5**: p. 85-100.
159. Zhang, T., et al., *Acetylation negatively regulates glycogen phosphorylase by recruiting protein phosphatase 1.* Cell Metab, 2012. **15**(1): p. 75-87.
160. Karpe, F., J.R. Dickmann, and K.N. Frayn, *Fatty Acids, Obesity, and Insulin Resistance: Time for a Reevaluation.* Diabetes, 2011. **60**(10): p. 2441-2449.
161. Dole, V.P., *A relation between non-esterified fatty acids in plasma and the metabolism of glucose.* J Clin Invest, 1956. **35**(2): p. 150-4.
162. Alves-Bezerra, M. and D.E. Cohen, *Triglyceride Metabolism in the Liver.* Compr Physiol, 2017. **8**(1): p. 1-8.
163. Kersten, S., et al., *Peroxisome proliferator-activated receptor alpha mediates the adaptive response to fasting.* J Clin Invest, 1999. **103**(11): p. 1489-98.
164. Le, M.H., et al., *Prevalence of non-alcoholic fatty liver disease and risk factors for advanced fibrosis and mortality in the United States.* PLoS ONE, 2017. **12**(3): p. e0173499.
165. Williams, C.D., et al., *Prevalence of nonalcoholic fatty liver disease and nonalcoholic steatohepatitis among a largely middle-aged population utilizing ultrasound and liver biopsy: a prospective study.* Gastroenterology, 2011. **140**(1): p. 124-31.
166. Choi, S.S. and A.M. Diehl, *Hepatic triglyceride synthesis and nonalcoholic fatty liver disease.* Curr Opin Lipidol, 2008. **19**(3): p. 295-300.
167. Kawano, Y. and D.E. Cohen, *Mechanisms of hepatic triglyceride accumulation in non-alcoholic fatty liver disease.* Journal of Gastroenterology, 2013. **48**(4): p. 434-441.
168. Tiniakos, D.G., M.B. Vos, and E.M. Brunt, *Nonalcoholic fatty liver disease: pathology and pathogenesis.* Annu Rev Pathol, 2010. **5**: p. 145-71.
169. Warensjo, E., et al., *Associations between estimated fatty acid desaturase activities in serum lipids and adipose tissue in humans: links to obesity and insulin resistance.* Lipids Health Dis, 2009. **8**: p. 37.
170. Hall, D., et al., *Peroxisomal and microsomal lipid pathways associated with resistance to hepatic steatosis and reduced pro-inflammatory state.* J Biol Chem, 2010. **285**(40): p. 31011-23.
171. Tripathy, S., M. Torres-Gonzalez, and D.B. Jump, *Elevated hepatic fatty acid elongase-5 activity corrects dietary fat-induced hyperglycemia in obese C57BL/6J mice.* J Lipid Res, 2010. **51**(9): p. 2642-54.
172. Jump, D.B., *Fatty acid regulation of hepatic lipid metabolism.* Current Opinion in Clinical Nutrition and Metabolic Care, 2011. **14**(2): p. 115-120.
173. Jump, D.B., *N-3 polyunsaturated fatty acid regulation of hepatic gene transcription.* Curr Opin Lipidol, 2008. **19**(3): p. 242-7.
174. Clamp, A.G., et al., *The influence of dietary lipids on the composition and membrane fluidity of rat hepatocyte plasma membrane.* Lipids, 1997. **32**(2): p. 179-184.
175. Ma, D.W.L., et al., *Plasma phospholipids and fatty acid composition differ between liver biopsy-proven nonalcoholic fatty liver disease and healthy subjects.* Nutrition &Amp; Diabetes, 2016. **6**: p. e220.

176. Kusunoki, M., et al., *Correlation between lipid and glycogen contents in liver and insulin resistance in high-fat-fed rats treated with the lipoprotein lipase activator NO-1886.* Metabolism, 2002. **51**(6): p. 792-5.
177. López-Soldado, I., et al., *Liver Glycogen Reduces Food Intake and Attenuates Obesity in a High-Fat Diet–Fed Mouse Model.* Diabetes, 2015. **64**(3): p. 796-807.
178. Ocak Duran, A., et al., *Hepatic steatosis is associated with higher incidence of liver metastasis in patients with metastatic breast cancer; an observational clinical study.* J buon, 2015. **20**(4): p. 963-9.
179. Wu, W., et al., *Fatty liver decreases the risk of liver metastasis in patients with breast cancer: a two-center cohort study.* Breast Cancer Res Treat, 2017. **166**(1): p. 289-297.
180. Balkwill, F. and A. Mantovani, *Inflammation and cancer: back to Virchow?* The Lancet, 2001. **357**(9255): p. 539-545.
181. Renehan, A.G., et al., *Body-mass index and incidence of cancer: a systematic review and meta-analysis of prospective observational studies.* Lancet, 2008. **371**(9612): p. 569-78.
182. Gilbert, C.A. and J.M. Slingerland, *Cytokines, obesity, and cancer: new insights on mechanisms linking obesity to cancer risk and progression.* Annu Rev Med, 2013. **64**: p. 45-57.
183. Hosogai, N., et al., *Adipose tissue hypoxia in obesity and its impact on adipocytokine dysregulation.* Diabetes, 2007. **56**(4): p. 901-11.
184. Lawler, H.M., et al., *Adipose Tissue Hypoxia, Inflammation, and Fibrosis in Obese Insulin-Sensitive and Obese Insulin-Resistant Subjects.* J Clin Endocrinol Metab, 2016. **101**(4): p. 1422-8.
185. Tornatore, L., et al., *The nuclear factor kappa B signaling pathway: integrating metabolism with inflammation.* Trends Cell Biol, 2012. **22**(11): p. 557-66.
186. Murano, I., et al., *Dead adipocytes, detected as crown-like structures, are prevalent in visceral fat depots of genetically obese mice.* J Lipid Res, 2008. **49**(7): p. 1562-8.
187. Cinti, S., et al., *Adipocyte death defines macrophage localization and function in adipose tissue of obese mice and humans.* J Lipid Res, 2005. **46**(11): p. 2347-55.
188. Cha, Y.J., E.-S. Kim, and J.S. Koo, *Tumor-associated macrophages and crown-like structures in adipose tissue in breast cancer.* Breast Cancer Research and Treatment, 2018. **170**(1): p. 15-25.
189. Berger, N.A., *Crown-like Structures in Breast Adipose Tissue from Normal Weight Women: Important Impact.* Cancer Prevention Research, 2017. **10**(4): p. 223-225.
190. Wang, B., I.S. Wood, and P. Trayhurn, *Hypoxia induces leptin gene expression and secretion in human preadipocytes: differential effects of hypoxia on adipokine expression by preadipocytes.* J Endocrinol, 2008. **198**(1): p. 127-34.
191. Ollberding, N.J., et al., *Prediagnostic leptin, adiponectin, C-reactive protein, and the risk of postmenopausal breast cancer.* Cancer Prev Res (Phila), 2013. **6**(3): p. 188-95.
192. Ishikawa, M., J. Kitayama, and H. Nagawa, *Enhanced expression of leptin and leptin receptor (OB-R) in human breast cancer.* Clin Cancer Res, 2004. **10**(13): p. 4325-31.
193. Hu, X., et al., *Leptin—A Growth Factor in Normal and Malignant Breast Cells and for Normal Mammary Gland Development.* JNCI: Journal of the National Cancer Institute, 2002. **94**(22): p. 1704-1711.
194. Strong, A.L., et al., *Leptin produced by obese adipose stromal/stem cells enhances proliferation and metastasis of estrogen receptor positive breast cancers.* Breast Cancer Res, 2015. **17**: p. 112.
195. Fouad, Y.A. and C. Aanei, *Revisiting the hallmarks of cancer.* American Journal of Cancer Research, 2017. **7**(5): p. 1016-1036.

196. Zhao, X., et al., *Prognostic significance of tumor-associated macrophages in breast cancer: a meta-analysis of the literature.* Oncotarget, 2017. **8**(18): p. 30576-30586.
197. Gwak, J.M., et al., *Prognostic value of tumor-associated macrophages according to histologic locations and hormone receptor status in breast cancer.* PLoS One, 2015. **10**(4): p. e0125728.
198. Nielsen, S.R. and M.C. Schmid, *Macrophages as Key Drivers of Cancer Progression and Metastasis.* Mediators of Inflammation, 2017. **2017**: p. 9624760.
199. Hagerling, C., A.-J. Casbon, and Z. Werb, *Balancing the innate immune system in tumor development.* Trends in cell biology, 2015. **25**(4): p. 214-220.
200. Italiani, P. and D. Boraschi, *From Monocytes to M1/M2 Macrophages: Phenotypical vs. Functional Differentiation.* Frontiers in Immunology, 2014. **5**(514).
201. Wei, B., et al., *The neutrophil lymphocyte ratio is associated with breast cancer prognosis: an updated systematic review and meta-analysis.* OncoTargets and therapy, 2016. **9**: p. 5567-5575.
202. Gregory, A.D. and A.M. Houghton, *Tumor-associated neutrophils: new targets for cancer therapy.* Cancer Res, 2011. **71**(7): p. 2411-6.
203. De Larco, J.E., et al., *Atypical methylation of the interleukin-8 gene correlates strongly with the metastatic potential of breast carcinoma cells.* Proceedings of the National Academy of Sciences, 2003. **100**(24): p. 13988-13993.
204. Fridlender, Z.G., et al., *Polarization of tumor-associated neutrophil phenotype by TGF-beta: "N1" versus "N2" TAN.* Cancer Cell, 2009. **16**(3): p. 183-94.
205. Queen, M.M., et al., *Breast cancer cells stimulate neutrophils to produce oncostatin M: potential implications for tumor progression.* Cancer Res, 2005. **65**(19): p. 8896-904.
206. Talmadge, J.E. and D.I. Gabrilovich, *History of myeloid derived suppressor cells (MDSCs) in the macro- and micro-environment of tumour-bearing hosts.* Nature reviews. Cancer, 2013. **13**(10): p. 739-752.
207. Ost, M., et al., *Myeloid-Derived Suppressor Cells in Bacterial Infections.* Front Cell Infect Microbiol, 2016. **6**: p. 37.
208. Guo, C., et al., *Myeloid-derived suppressor cells have a proinflammatory role in the pathogenesis of autoimmune arthritis.* Ann Rheum Dis, 2016. **75**(1): p. 278-85.
209. Chen, S., et al., *Diminished immune response to vaccinations in obesity: role of myeloid-derived suppressor and other myeloid cells.* Obes Res Clin Pract, 2015. **9**(1): p. 35-44.
210. Bronte, V., et al., *Recommendations for myeloid-derived suppressor cell nomenclature and characterization standards.* Nature Communications, 2016. **7**: p. 12150.
211. Veglia, F., M. Perego, and D. Gabrilovich, *Myeloid-derived suppressor cells coming of age.* Nature Immunology, 2018. **19**(2): p. 108-119.
212. Umansky, V., et al., *The Role of Myeloid-Derived Suppressor Cells (MDSC) in Cancer Progression.* Vaccines, 2016. **4**(4): p. 36.
213. Condamine, T., et al., *Regulation of Tumor Metastasis by Myeloid-derived Suppressor Cells.* Annual review of medicine, 2015. **66**: p. 97-110.
214. Gabrilovich, D.I. and S. Nagaraj, *Myeloid-derived-suppressor cells as regulators of the immune system.* Nature reviews. Immunology, 2009. **9**(3): p. 162-174.
215. Ezernitchi, A.V., et al., *TCR ζ Down-Regulation under Chronic Inflammation Is Mediated by Myeloid Suppressor Cells Differentially Distributed between Various Lymphatic Organs.* The Journal of Immunology, 2006. **177**(7): p. 4763-4772.
216. Hanson, E.M., et al., *Myeloid-derived suppressor cells down-regulate L-selectin expression on CD4+ and CD8+ T cells.* J Immunol, 2009. **183**(2): p. 937-44.

217. Srivastava, M.K., et al., *Myeloid-derived suppressor cells inhibit T-cell activation by depleting cystine and cysteine.* Cancer Res, 2010. **70**(1): p. 68-77.
218. Ravelli, A., et al., *Tumor-infiltrating lymphocytes and breast cancer: Beyond the prognostic and predictive utility.* Tumour Biol, 2017. **39**(4): p. 1010428317695023.
219. Mao, Y., et al., *The value of tumor infiltrating lymphocytes (TILs) for predicting response to neoadjuvant chemotherapy in breast cancer: a systematic review and meta-analysis.* PLoS One, 2014. **9**(12): p. e115103.
220. Mahmoud, S.M., et al., *Tumor-infiltrating CD8+ lymphocytes predict clinical outcome in breast cancer.* Journal of clinical oncology, 2011. **29**(15): p. 1949-1955.
221. Gu-Trantien, C., et al., *CD4+ follicular helper T cell infiltration predicts breast cancer survival.* The Journal of clinical investigation, 2013. **123**(7): p. 2873-2892.
222. Shou, J., et al., *Worse outcome in breast cancer with higher tumor-infiltrating FOXP3+ Tregs : a systematic review and meta-analysis.* BMC Cancer, 2016. **16**: p. 687.
223. Shang, B., et al., *Prognostic value of tumor-infiltrating FoxP3+ regulatory T cells in cancers: a systematic review and meta-analysis.* Sci Rep, 2015. **5**: p. 15179.
224. Chen, W., et al., *Conversion of peripheral CD4+CD25- naive T cells to CD4+CD25+ regulatory T cells by TGF-beta induction of transcription factor Foxp3.* J Exp Med, 2003. **198**(12): p. 1875-86.
225. Oderup, C., et al., *Cytotoxic T lymphocyte antigen-4-dependent down-modulation of costimulatory molecules on dendritic cells in CD4+ CD25+ regulatory T-cell-mediated suppression.* Immunology, 2006. **118**(2): p. 240-9.
226. Simpson, T.R., et al., *Fc-dependent depletion of tumor-infiltrating regulatory T cells co-defines the efficacy of anti-CTLA-4 therapy against melanoma.* J Exp Med, 2013. **210**(9): p. 1695-710.
227. Paget, S., *The distribution of secondary growths in cancer of the breast. 1889.* Cancer Metastasis Rev, 1989. **8**(2): p. 98-101.
228. Aslakson, C.J. and F.R. Miller, *Selective events in the metastatic process defined by analysis of the sequential dissemination of subpopulations of a mouse mammary tumor.* Cancer Res, 1992. **52**(6): p. 1399-405.
229. Hart, I.R. and I.J. Fidler, *Role of organ selectivity in the determination of metastatic patterns of B16 melanoma.* Cancer Res, 1980. **40**(7): p. 2281-7.
230. Langley, R.R. and I.J. Fidler, *The seed and soil hypothesis revisited - the role of tumor-stroma interactions in metastasis to different organs.* International journal of cancer. Journal international du cancer, 2011. **128**(11): p. 2527-2535.
231. Fidler, I.J. and M.L. Kripke, *Metastasis results from preexisting variant cells within a malignant tumor.* Science, 1977. **197**(4306): p. 893-5.
232. Fidler, I.J. and J.E. Talmadge, *Evidence that intravenously derived murine pulmonary melanoma metastases can originate from the expansion of a single tumor cell.* Cancer Res, 1986. **46**(10): p. 5167-71.
233. Talmadge, J.E. and I.J. Fidler, *Enhanced metastatic potential of tumor cells harvested from spontaneous metastases of heterogeneous murine tumors.* J Natl Cancer Inst, 1982. **69**(4): p. 975-80.
234. Talmadge, J.E. and I.J. Fidler, *AACR Centennial Series: The Biology of Cancer Metastasis: Historical Perspective.* Cancer research, 2010. **70**(14): p. 5649-5669.
235. Liu, Y. and X. Cao, *Characteristics and Significance of the Pre-metastatic Niche.* Cancer Cell, 2016. **30**(5): p. 668-681.
236. Liu, S., et al., *Vascular endothelial growth factor plays a critical role in the formation of the pre-metastatic niche via prostaglandin E2.* Oncol Rep, 2014. **32**(6): p. 2477-84.

237. Hiratsuka, S., et al., *Tumour-mediated upregulation of chemoattractants and recruitment of myeloid cells predetermines lung metastasis.* Nat Cell Biol, 2006. **8**(12): p. 1369-75.
238. Weilbaecher, K.N., T.A. Guise, and L.K. McCauley, *Cancer to bone: a fatal attraction.* Nat Rev Cancer, 2011. **11**(6): p. 411-25.
239. Coleman, R.E., *Clinical features of metastatic bone disease and risk of skeletal morbidity.* Clin Cancer Res, 2006. **12**(20 Pt 2): p. 6243s-6249s.
240. Roodman, G.D., *Mechanisms of bone metastasis.* N Engl J Med, 2004. **350**(16): p. 1655-64.
241. Suva, L.J., R.J. Griffin, and I. Makhoul, *MECHANISMS OF BONE METASTASES OF BREAST CANCER.* Endocrine-related cancer, 2009. **16**(3): p. 703-713.
242. Yin, J.J., et al., *TGF-β signaling blockade inhibits PTHrP secretion by breast cancer cells and bone metastases development.* The Journal of Clinical Investigation, 1999. **103**(2): p. 197-206.
243. Buchs, N., et al., *Calcium stimulates parathyroid hormone-related protein production in Leydig tumor cells through a putative cation-sensing mechanism.* European Journal of Endocrinology, 2000. **142**(5): p. 500-505.
244. Kobayashi, Y., et al., *Prostaglandin E2 enhances osteoclastic differentiation of precursor cells through protein kinase A-dependent phosphorylation of TAK1.* J Biol Chem, 2005. **280**(12): p. 11395-403.
245. Tian, L., et al., *Prevalence of osteoporosis and related lifestyle and metabolic factors of postmenopausal women and elderly men: A cross-sectional study in Gansu province, Northwestern of China.* Medicine, 2017. **96**(43): p. e8294.
246. Alvisa-Negrín, J., et al., *Osteopenia in Alcoholics: Effect of Alcohol Abstinence.* Alcohol and Alcoholism, 2009. **44**(5): p. 468-475.
247. Styner, M., et al., *Bone marrow fat accumulation accelerated by high fat diet is suppressed by exercise.* Bone, 2014. **64**: p. 39-46.
248. Sealls, W., et al., *Dietary polyunsaturated fatty acids (C18:2 omega6 and C18:3 omega3) do not suppress hepatic lipogenesis.* Biochim Biophys Acta, 2008. **1781**(8): p. 406-14.
249. Gonzalez, M., et al., *Defining a relationship between dietary fatty acids and the cytochrome P450 system in a mouse model of fatty liver disease.* Physiol Genomics, 2011. **43**(3): p. 121-35.
250. Livak, K.J. and T.D. Schmittgen, *Analysis of relative gene expression data using real-time quantitative PCR and the 2(-Delta Delta C(T)) Method.* Methods, 2001. **25**(4): p. 402-408.
251. Olson, L.K., et al., *Pubertal exposure to high fat diet causes mouse strain-dependent alterations in mammary gland development and estrogen responsiveness.* Int J Obes (Lond), 2010. **34**(9): p. 1415-26.
252. Fasano, E., et al., *Long-Chain n-3 PUFA against breast and prostate cancer: which are the appropriate doses for intervention studies in animals and humans?* Crit Rev Food Sci Nutr, 2015: p. 0.
253. Hilakivi-Clarke, L., et al., *Mechanisms mediating the effects of prepubertal (n-3) polyunsaturated fatty acid diet on breast cancer risk in rats.* J Nutr, 2005. **135**(12 Suppl): p. 2946S-2952S.
254. MacLennan, M.B., B.M. Anderson, and D.W. Ma, *Differential mammary gland development in FVB and C57Bl/6 mice: implications for breast cancer research.* Nutrients, 2011. **3**(11): p. 929-36.
255. Zhu, Z., et al., *Mammary gland density predicts the cancer inhibitory activity of the N-3 to N-6 ratio of dietary fat.* Cancer Prev Res (Phila), 2011. **4**(10): p. 1675-85.

256. Hilakivi-Clarke, L., et al., *A maternal diet high in n − 6 polyunsaturated fats alters mammary gland development, puberty onset, and breast cancer risk among female rat offspring.* Proceedings of the National Academy of Sciences of the United States of America, 1997. **94**(17): p. 9372-9377.
257. Hilakivi-Clarke, L., *Nutritional modulation of terminal end buds: its relevance to breast cancer prevention.* Curr Cancer Drug Targets, 2007. **7**(5): p. 465-74.
258. Davis, C.D. and E.O. Uthus, *DNA methylation, cancer susceptibility, and nutrient interactions.* Exp Biol Med (Maywood), 2004. **229**(10): p. 988-95.
259. Maller, O., H. Martinson, and P. Schedin, *Extracellular Matrix Composition Reveals Complex and Dynamic Stromal-Epithelial Interactions in the Mammary Gland.* Journal of Mammary Gland Biology and Neoplasia, 2010. **15**(3): p. 301-318.
260. Iyengar, N.M., C.A. Hudis, and A.J. Dannenberg, *Obesity and inflammation: new insights into breast cancer development and progression.* Am Soc Clin Oncol Educ Book, 2013: p. 46-51.
261. Hovey, R.C. and L. Aimo, *Diverse and Active Roles for Adipocytes During Mammary Gland Growth and Function.* Journal of Mammary Gland Biology and Neoplasia, 2010. **15**(3): p. 279-290.
262. Couldrey, C., et al., *Adipose tissue: a vital in vivo role in mammary gland development but not differentiation.* Dev Dyn, 2002. **223**(4): p. 459-68.
263. MacLennan, M. and D.W. Ma, *Role of dietary fatty acids in mammary gland development and breast cancer.* Breast Cancer Res, 2010. **12**(5): p. 211.
264. Olson, L.K., et al., *Pubertal exposure to high fat diet causes mouse strain-dependent alterations in mammary gland development and estrogen responsiveness.* Int J Obes, 2010. **34**(9): p. 1415-1426.
265. Anderson, B.M., et al., *Lifelong exposure to n-3 PUFA affects pubertal mammary gland development.* Applied Physiology, Nutrition, and Metabolism, 2014. **39**(6): p. 699-706.
266. Khadge, S., et al., *Dietary omega-3 and omega-6 polyunsaturated fatty acids modulate hepatic pathology.* J Nutr Biochem, 2018. **52**: p. 92-102.
267. Belzung, F., T. Raclot, and R. Groscolas, *Fish oil n-3 fatty acids selectively limit the hypertrophy of abdominal fat depots in growing rats fed high-fat diets.* Am J Physiol, 1993. **264**(6 Pt 2): p. R1111-8.
268. Peyron-Caso, E., et al., *Dietary fish oil increases lipid mobilization but does not decrease lipid storage-related enzyme activities in adipose tissue of insulin-resistant, sucrose-fed rats.* J Nutr, 2003. **133**(7): p. 2239-43.
269. Casado-Diaz, A., et al., *The omega-6 arachidonic fatty acid, but not the omega-3 fatty acids, inhibits osteoblastogenesis and induces adipogenesis of human mesenchymal stem cells: potential implication in osteoporosis.* Osteoporos Int, 2013. **24**(5): p. 1647-61.
270. Massaro, M., et al., *The omega-3 fatty acid docosahexaenoate attenuates endothelial cyclooxygenase-2 induction through both NADP(H) oxidase and PKC epsilon inhibition.* Proc Natl Acad Sci U S A, 2006. **103**(41): p. 15184-9.
271. Ukropec, J., et al., *The hypotriglyceridemic effect of dietary n-3 FA is associated with increased beta-oxidation and reduced leptin expression.* Lipids, 2003. **38**(10): p. 1023-9.
272. Wójcik, C., et al., *Modulation of adipocyte differentiation by omega-3 polyunsaturated fatty acids involves the ubiquitin-proteasome system.* Journal of Cellular and Molecular Medicine, 2014. **18**(4): p. 590-599.
273. Brenna, J.T., *Efficiency of conversion of alpha-linolenic acid to long chain n-3 fatty acids in man.* Curr Opin Clin Nutr Metab Care, 2002. **5**(2): p. 127-32.

274. Zhu, Z.R., et al., *Fatty acid composition of breast adipose tissue in breast cancer patients and in patients with benign breast disease.* Nutr Cancer, 1995. **24**(2): p. 151-60.
275. Bagga, D., et al., *Long-chain n-3-to-n-6 polyunsaturated fatty acid ratios in breast adipose tissue from women with and without breast cancer.* Nutr Cancer, 2002. **42**(2): p. 180-5.
276. Palomer, X., et al., *Palmitic and Oleic Acid: The Yin and Yang of Fatty Acids in Type 2 Diabetes Mellitus.* Trends in Endocrinology & Metabolism. **29**(3): p. 178-190.
277. Hilakivi-Clarke, L., et al., *Consumption of a high-fat diet alters estrogen receptor content, protein kinase C activity, and mammary gland morphology in virgin and pregnant mice and female offspring.* Cancer Res, 1998. **58**(4): p. 654-60.
278. Hilakivi-Clarke, L., et al., *Dietary modulation of pregnancy estrogen levels and breast cancer risk among female rat offspring.* Clin Cancer Res, 2002. **8**(11): p. 3601-10.
279. McGinley, J.N. and H.J. Thompson, *Quantitative assessment of mammary gland density in rodents using digital image analysis.* Biol Proced Online, 2011. **13**(1): p. 4.
280. Zhu, Z., et al., *Mammary Gland Density Predicts the Cancer Inhibitory Activity of the N-3 to N-6 Ratio of Dietary Fat.* Cancer Prevention Research, 2011. **4**(10): p. 1675-1685.
281. McCormack, V.A. and I. dos Santos Silva, *Breast Density and Parenchymal Patterns as Markers of Breast Cancer Risk: A Meta-analysis.* Cancer Epidemiology Biomarkers & Prevention, 2006. **15**(6): p. 1159-1169.
282. Sandhu, N., et al., *Influence of obesity on breast density reduction by omega-3 fatty acids: Evidence from a randomized clinical trial.* Cancer Prevention Research, 2015.
283. Wolfson, B., et al., *A High-Fat Diet Promotes Mammary Gland Myofibroblast Differentiation through MicroRNA 140 Downregulation.* Mol Cell Biol, 2017. **37**(4).
284. Xue, L., et al., *Model of mouse mammary gland hyperproliferation and Hyperplasia Induced by a western-style diet.* Nutrition and Cancer, 1996. **26**(3): p. 281-287.
285. Hidaka, B.H., et al., *Omega-3 and Omega-6 Fatty Acids in Blood and Breast Tissue of High-Risk Women and Association with Atypical Cytomorphology.* Cancer Prevention Research, 2015. **8**(5): p. 359-364.
286. Fabian, C.J., et al., *Modulation of Breast Cancer Risk Biomarkers by High Dose Omega-3 Fatty Acids: Phase II Pilot Study in Pre-menopausal Women.* Cancer prevention research (Philadelphia, Pa.), 2015. **8**(10): p. 922-931.
287. Yee, L.D., et al., *The inhibition of early stages of HER-2/neu-mediated mammary carcinogenesis by dietary n-3 polyunsaturated fatty acids.* Molecular nutrition & food research, 2013. **57**(2): p. 10.1002/mnfr.201200445.
288. Manni, A., et al., *Influence of omega-3 fatty acids on Tamoxifen-induced suppression of rat mammary carcinogenesis.* Int J Cancer, 2014. **134**(7): p. 1549-57.
289. Cunha, G.R., et al., *Elucidation of a role for stromal steroid hormone receptors in mammary gland growth and development using tissue recombinants.* J Mammary Gland Biol Neoplasia, 1997. **2**(4): p. 393-402.
290. Mueller, S.O., et al., *Mammary gland development in adult mice requires epithelial and stromal estrogen receptor alpha.* Endocrinology, 2002. **143**(6): p. 2357-65.
291. Ciarloni, L., S. Mallepell, and C. Brisken, *Amphiregulin is an essential mediator of estrogen receptor α function in mammary gland development.* Proceedings of the National Academy of Sciences, 2007. **104**(13): p. 5455-5460.
292. Kenney, N.J., et al., *Induction of ductal morphogenesis and lobular hyperplasia by amphiregulin in the mouse mammary gland.* Cell Growth Differ, 1996. **7**(12): p. 1769-81.

293. Ruan, W., M.E. Monaco, and D.L. Kleinberg, *Progesterone Stimulates Mammary Gland Ductal Morphogenesis by Synergizing with and Enhancing Insulin-Like Growth Factor-I Action.* Endocrinology, 2005. **146**(3): p. 1170-1178.
294. Hadsell, D.L. and S.G. Bonnette, *IGF and insulin action in the mammary gland: lessons from transgenic and knockout models.* J Mammary Gland Biol Neoplasia, 2000. **5**(1): p. 19-30.
295. Drolet, R., et al., *Hypertrophy and hyperplasia of abdominal adipose tissues in women.* Int J Obes (Lond), 2008. **32**(2): p. 283-91.
296. LeMieux, M.J., et al., *Eicosapentaenoic acid reduces adipocyte hypertrophy and inflammation in diet-induced obese mice in an adiposity-independent manner.* J Nutr, 2015. **145**(3): p. 411-7.
297. Obst, B.E., et al., *Adipocyte size and number in dietary obesity resistant and susceptible rats.* American Journal of Physiology - Endocrinology And Metabolism, 1981. **240**(1): p. E47-E53.
298. Haramizu, S., et al., *Different contribution of muscle and liver lipid metabolism to endurance capacity and obesity susceptibility of mice.* J Appl Physiol (1985), 2009. **106**(3): p. 871-9.
299. Buckley, J.D. and P.R.C. Howe, *Long-Chain Omega-3 Polyunsaturated Fatty Acids May Be Beneficial for Reducing Obesity—A Review.* Nutrients, 2010. **2**(12): p. 1212-1230.
300. Mori, T., et al., *Dietary fish oil upregulates intestinal lipid metabolism and reduces body weight gain in C57BL/6J mice.* J Nutr, 2007. **137**(12): p. 2629-34.
301. Flachs, P., et al., *Polyunsaturated fatty acids of marine origin upregulate mitochondrial biogenesis and induce beta-oxidation in white fat.* Diabetologia, 2005. **48**(11): p. 2365-75.
302. Ailhaud, G., et al., *Temporal changes in dietary fats: role of n-6 polyunsaturated fatty acids in excessive adipose tissue development and relationship to obesity.* Prog Lipid Res, 2006. **45**(3): p. 203-36.
303. Massiera, F., et al., *A Western-like fat diet is sufficient to induce a gradual enhancement in fat mass over generations.* Journal of Lipid Research, 2010. **51**(8): p. 2352-2361.
304. Gaillard, D., et al., *Requirement and role of arachidonic acid in the differentiation of pre-adipose cells.* Biochem J, 1989. **257**(2): p. 389-97.
305. Kim, H.K., et al., *Docosahexaenoic acid inhibits adipocyte differentiation and induces apoptosis in 3T3-L1 preadipocytes.* J Nutr, 2006. **136**(12): p. 2965-9.
306. Kalupahana, N.S., et al., *Eicosapentaenoic acid prevents and reverses insulin resistance in high-fat diet-induced obese mice via modulation of adipose tissue inflammation.* J Nutr, 2010. **140**(11): p. 1915-22.
307. Skurk, T., et al., *Relationship between adipocyte size and adipokine expression and secretion.* J Clin Endocrinol Metab, 2007. **92**(3): p. 1023-33.
308. Frederich, R.C., et al., *Leptin levels reflect body lipid content in mice: evidence for diet-induced resistance to leptin action.* Nat Med, 1995. **1**(12): p. 1311-4.
309. Meilleur, K.G., et al., *Circulating Adiponectin Is Associated with Obesity and Serum Lipids in West Africans.* The Journal of Clinical Endocrinology & Metabolism, 2010. **95**(7): p. 3517-3521.
310. Meyer, L.K., et al., *Adipose tissue depot and cell size dependency of adiponectin synthesis and secretion in human obesity.* Adipocyte, 2013. **2**(4): p. 217-226.
311. Friedman, J.M. and J.L. Halaas, *Leptin and the regulation of body weight in mammals.* Nature, 1998. **395**(6704): p. 763-70.

312. Kim, E.J., et al., *Dietary fat increases solid tumor growth and metastasis of 4T1 murine mammary carcinoma cells and mortality in obesity-resistant BALB/c mice.* Breast Cancer Res, 2011. **13**(4): p. R78.
313. Pérez-Matute, P., et al., *Eicosapentaenoic acid actions on adiposity and insulin resistance in control and high-fat-fed rats: role of apoptosis, adiponectin and tumour necrosis factor-α.* British Journal of Nutrition, 2007. **97**(2): p. 389-398.
314. Neschen, S., et al., *Fish oil regulates adiponectin secretion by a peroxisome proliferator-activated receptor-gamma-dependent mechanism in mice.* Diabetes, 2006. **55**(4): p. 924-8.
315. Loffreda, S., et al., *Leptin regulates proinflammatory immune responses.* Faseb j, 1998. **12**(1): p. 57-65.
316. Hu, X., et al., *Leptin--a growth factor in normal and malignant breast cells and for normal mammary gland development.* J Natl Cancer Inst, 2002. **94**(22): p. 1704-11.
317. Sjögren, K., et al., *Liver-derived insulin-like growth factor I (IGF-I) is the principal source of IGF-I in blood but is not required for postnatal body growth in mice.* Proceedings of the National Academy of Sciences of the United States of America, 1999. **96**(12): p. 7088-7092.
318. Chang, H.R., et al., *Macrophage and adipocyte IGF1 maintain adipose tissue homeostasis during metabolic stresses.* Obesity (Silver Spring), 2016. **24**(1): p. 172-83.
319. Spadaro, O., et al., *IGF1 Shapes Macrophage Activation in Response to Immunometabolic Challenge.* Cell Reports. **19**(2): p. 225-234.
320. Richert, M.M. and T.L. Wood, *The insulin-like growth factors (IGF) and IGF type I receptor during postnatal growth of the murine mammary gland: sites of messenger ribonucleic acid expression and potential functions.* Endocrinology, 1999. **140**(1): p. 454-61.
321. Jones, R.A., et al., *Transgenic overexpression of IGF-IR disrupts mammary ductal morphogenesis and induces tumor formation.* Oncogene, 2007. **26**(11): p. 1636-44.
322. Tamimi, R.M., et al., *EXPRESSION OF IGF1R IN NORMAL BREAST TISSUE AND SUBSEQUENT RISK OF BREAST CANCER.* Breast cancer research and treatment, 2011. **128**(1): p. 243-250.
323. Gouon-Evans, V., M.E. Rothenberg, and J.W. Pollard, *Postnatal mammary gland development requires macrophages and eosinophils.* Development, 2000. **127**(11): p. 2269-82.
324. Iyengar, N.M., et al., *Metabolic Obesity, Adipose Inflammation and Elevated Breast Aromatase in Women with Normal Body Mass Index.* Cancer Prevention Research, 2017. **10**(4): p. 235-243.
325. Iyengar, N.M., et al., *Menopause Is a Determinant of Breast Adipose Inflammation.* Cancer Prevention Research, 2015. **8**(5): p. 349-358.
326. Monk, J.M., et al., *Fish-Oil–Derived n–3 PUFAs Reduce Inflammatory and Chemotactic Adipokine-Mediated Cross-talk between Co-cultured Murine Splenic CD8+ T Cells and Adipocytes.* The Journal of Nutrition, 2015. **145**(4): p. 829-838.
327. Sun, X., et al., *CCL2-driven inflammation increases mammary gland stromal density and cancer susceptibility in a transgenic mouse model.* Breast Cancer Research : BCR, 2017. **19**: p. 4.
328. Spychalla, J.P., A.J. Kinney, and J. Browse, *Identification of an animal omega-3 fatty acid desaturase by heterologous expression in Arabidopsis.* Proc Natl Acad Sci U S A, 1997. **94**(4): p. 1142-7.

329. Simopoulos, A.P., *The importance of the omega-6/omega-3 fatty acid ratio in cardiovascular disease and other chronic diseases.* Exp Biol Med (Maywood), 2008. **233**(6): p. 674-88.
330. Calder, P.C., *Fatty acids and inflammation: the cutting edge between food and pharma.* Eur J Pharmacol, 2011. **668 Suppl 1**: p. S50-8.
331. Kuehl, F. and R. Egan, *Prostaglandins, arachidonic acid, and inflammation.* Science, 1980. **210**(4473): p. 978-984.
332. Serhan, C.N., et al., *Resolvins.* A Family of Bioactive Products of Omega-3 Fatty Acid Transformation Circuits Initiated by Aspirin Treatment that Counter Proinflammation Signals, 2002. **196**(8): p. 1025-1037.
333. Poulsen, R.C., et al., *Identification of inflammatory and proresolving lipid mediators in bone marrow and their lipidomic profiles with ovariectomy and omega-3 intake.* Am J Hematol, 2008. **83**(6): p. 437-45.
334. Blasbalg, T.L., et al., *Changes in consumption of omega-3 and omega-6 fatty acids in the United States during the 20th century.* Am J Clin Nutr, 2011. **93**(5): p. 950-62.
335. Aziz, A.A., et al., *Increasing Dietary alpha-linolenic acid enhances tissue levels of long-chain n-3 PUFA when linoleic acid intake is low in hamsters.* Ann Nutr Metab, 2010. **57**(1): p. 50-8.
336. Harris, W.S., W.C. Poston, and C.K. Haddock, *Tissue n − 3 and n − 6 fatty acids and risk for coronary heart disease events.* Atherosclerosis, 2007. **193**(1): p. 1-10.
337. Song, J., et al., *Association of serum phospholipid PUFAs with cardiometabolic risk: beneficial effect of DHA on the suppression of vascular proliferation/inflammation.* Clin Biochem, 2014. **47**(6): p. 361-8.
338. Abeywardena, M.Y. and G.S. Patten, *Role of ω3 long-chain polyunsaturated fatty acids in reducing cardio-metabolic risk factors.* Endocr Metab Immune Disord Drug Targets, 2011. **11**(3): p. 232-46.
339. Kimura, Y., et al., *Meat, fish and fat intake in relation to subsite-specific risk of colorectal cancer: The Fukuoka Colorectal Cancer Study.* Cancer Sci, 2007. **98**(4): p. 590-7.
340. Berquin, I.M., I.J. Edwards, and Y.Q. Chen, *Multi-targeted therapy of cancer by omega-3 fatty acids.* Cancer Lett, 2008. **269**(2): p. 363-77.
341. Luzio, G.A., V.K. Parnaik, and R.M. Mayer, *A D-glucosylated form of dextransucrase: demonstration of partial reactions.* Carbohydrate research, 1983. **121**: p. 269-78.
342. Mejia-Barradas, C.M., et al., *The consumption of n-3 polyunsaturated fatty acids differentially modulates gene expression of peroxisome proliferator-activated receptor alpha and gamma and hypoxia-inducible factor 1 alpha in subcutaneous adipose tissue of obese adolescents.* Endocrine, 2014. **45**(1): p. 98-105.
343. Capanni, M., et al., *Prolonged n-3 polyunsaturated fatty acid supplementation ameliorates hepatic steatosis in patients with non-alcoholic fatty liver disease: a pilot study.* Aliment Pharmacol Ther, 2006. **23**(8): p. 1143-51.
344. Tanaka, N., et al., *Highly purified eicosapentaenoic acid treatment improves nonalcoholic steatohepatitis.* J Clin Gastroenterol, 2008. **42**(4): p. 413-8.
345. Szczepaniak, L.S., et al., *Magnetic resonance spectroscopy to measure hepatic triglyceride content: prevalence of hepatic steatosis in the general population.* Am J Physiol Endocrinol Metab, 2005. **288**(2): p. E462-8.
346. Bellentani, S., et al., *Prevalence of and risk factors for hepatic steatosis in Northern Italy.* Ann Intern Med, 2000. **132**(2): p. 112-7.

347. van der Meer, R.W., et al., *Effects of short-term high-fat, high-energy diet on hepatic and myocardial triglyceride content in healthy men.* J Clin Endocrinol Metab, 2008. **93**(7): p. 2702-8.
348. Shah, K., et al., *Diet and exercise interventions reduce intrahepatic fat content and improve insulin sensitivity in obese older adults.* Obesity (Silver Spring), 2009. **17**(12): p. 2162-8.
349. Vitola, B.E., et al., *Weight loss reduces liver fat and improves hepatic and skeletal muscle insulin sensitivity in obese adolescents.* Obesity (Silver Spring), 2009. **17**(9): p. 1744-8.
350. Charlton, M., et al., *Fast food diet mouse: novel small animal model of NASH with ballooning, progressive fibrosis, and high physiological fidelity to the human condition.* Am J Physiol Gastrointest Liver Physiol, 2011. **301**(5): p. G825-34.
351. Depner, C.M., K.A. Philbrick, and D.B. Jump, *Docosahexaenoic acid attenuates hepatic inflammation, oxidative stress, and fibrosis without decreasing hepatosteatosis in a Ldlr(-/-) mouse model of western diet-induced nonalcoholic steatohepatitis.* J Nutr, 2013. **143**(3): p. 315-23.
352. Srivastava, M.K., et al., *Myeloid-derived suppressor cells inhibit T-cell activation by depleting cystine and cysteine.* Cancer research, 2010. **70**(1): p. 68-77.
353. Feldstein, A.E., et al., *Hepatocyte apoptosis and fas expression are prominent features of human nonalcoholic steatohepatitis.* Gastroenterology, 2003. **125**(2): p. 437-43.
354. Abdelhalim, M.A. and S.A. Moussa, *Biochemical changes of hemoglobin and osmotic fragility of red blood cells in high fat diet rabbits.* Pak J Biol Sci, 2010. **13**(2): p. 73-7.
355. Vazquez, S.E., M.A. Inlay, and T. Serwold, *CD201 and CD27 identify hematopoietic stem and progenitor cells across multiple murine strains independently of Kit and Sca-1.* Exp Hematol, 2015. **43**(7): p. 578-85.
356. Li, X., et al., *Isocaloric Pair-Fed High-Carbohydrate Diet Induced More Hepatic Steatosis and Inflammation than High-Fat Diet Mediated by miR-34a/SIRT1 Axis in Mice.* Sci Rep, 2015. **5**: p. 16774.
357. Bertola, A., et al., *Mouse model of chronic and binge ethanol feeding (the NIAAA model).* Nat Protoc, 2013. **8**(3): p. 627-37.
358. Bonnet, N., E. Somm, and C.J. Rosen, *Diet and gene interactions influence the skeletal response to polyunsaturated fatty acids.* Bone, 2014. **68**: p. 100-7.
359. Rosqvist, F., et al., *Overfeeding polyunsaturated and saturated fat causes distinct effects on liver and visceral fat accumulation in humans.* Diabetes, 2014. **63**(7): p. 2356-68.
360. Boozer, C.N., G. Schoenbach, and R.L. Atkinson, *Dietary fat and adiposity: a dose-response relationship in adult male rats fed isocalorically.* Am J Physiol, 1995. **268**(4 Pt 1): p. E546-50.
361. Buckley, J.D. and P.R. Howe, *Anti-obesity effects of long-chain omega-3 polyunsaturated fatty acids.* Obes Rev, 2009. **10**(6): p. 648-59.
362. Baillie, R.A., et al., *Coordinate induction of peroxisomal acyl-CoA oxidase and UCP-3 by dietary fish oil: a mechanism for decreased body fat deposition.* Prostaglandins Leukot Essent Fatty Acids, 1999. **60**(5-6): p. 351-6.
363. Perez-Matute, P., et al., *Eicosapentaenoic acid actions on adiposity and insulin resistance in control and high-fat-fed rats: role of apoptosis, adiponectin and tumour necrosis factor-alpha.* Br J Nutr, 2007. **97**(2): p. 389-98.
364. Hassanali, Z., et al., *Dietary supplementation of n-3 PUFA reduces weight gain and improves postprandial lipaemia and the associated inflammatory response in the obese JCR:LA-cp rat.* Diabetes Obes Metab, 2010. **12**(2): p. 139-47.

365. Amri, E.Z., G. Ailhaud, and P.A. Grimaldi, *Fatty acids as signal transducing molecules: involvement in the differentiation of preadipose to adipose cells.* J Lipid Res, 1994. **35**(5): p. 930-7.
366. Clarke, S.D. and D. Jump, *Polyunsaturated fatty acids regulate lipogenic and peroxisomal gene expression by independent mechanisms.* Prostaglandins Leukot Essent Fatty Acids, 1997. **57**(1): p. 65-9.
367. Schwinkendorf, D.R., et al., *Effects of central administration of distinct fatty acids on hypothalamic neuropeptide expression and energy metabolism.* Int J Obes (Lond), 2011. **35**(3): p. 336-44.
368. James, M.J., R.A. Gibson, and L.G. Cleland, *Dietary polyunsaturated fatty acids and inflammatory mediator production.* Am J Clin Nutr, 2000. **71**(1 Suppl): p. 343S-8S.
369. Hodson, L., et al., *Docosahexaenoic acid enrichment in NAFLD is associated with improvements in hepatic metabolism and hepatic insulin sensitivity: a pilot study.* Eur J Clin Nutr, 2017.
370. Mohamed, A.I., et al., *The effect of dietary menhaden, olive, and coconut oil fed with three levels of vitamin E on plasma and liver lipids and plasma fatty acid composition in rats.* J Nutr Biochem, 2002. **13**(7): p. 435-441.
371. Kassem, A.A., et al., *Dietary (n-6 : n-3) fatty acids alter plasma and tissue fatty acid composition in pregnant Sprague Dawley rats.* ScientificWorldJournal, 2012. **2012**: p. 851437.
372. Ruxton, C.H., et al., *The impact of long-chain n-3 polyunsaturated fatty acids on human health.* Nutr Res Rev, 2005. **18**(1): p. 113-29.
373. Astorg, P., et al., *Plasma n-6 and n-3 polyunsaturated fatty acids as biomarkers of their dietary intakes: a cross-sectional study within a cohort of middle-aged French men and women.* Eur J Clin Nutr, 2008. **62**(10): p. 1155-61.
374. Abayasekara, D.R. and D.C. Wathes, *Effects of altering dietary fatty acid composition on prostaglandin synthesis and fertility.* Prostaglandins Leukot Essent Fatty Acids, 1999. **61**(5): p. 275-87.
375. Zivkovic, A.M., et al., *Dietary omega-3 fatty acids aid in the modulation of inflammation and metabolic health.* Calif Agric (Berkeley), 2011. **65**(3): p. 106-111.
376. Thies, F., et al., *Association of n-3 polyunsaturated fatty acids with stability of atherosclerotic plaques: a randomised controlled trial.* Lancet, 2003. **361**(9356): p. 477-85.
377. Bozzetto, L., et al., *Liver fat is reduced by an isoenergetic MUFA diet in a controlled randomized study in type 2 diabetic patients.* Diabetes Care, 2012. **35**(7): p. 1429-35.
378. Bessesen, D.H., S.H. Vensor, and M.R. Jackman, *Trafficking of dietary oleic, linolenic, and stearic acids in fasted or fed lean rats.* Am J Physiol Endocrinol Metab, 2000. **278**(6): p. E1124-32.
379. Liehr, M., et al., *Olive oil bioactives protect pigs against experimentally-induced chronic inflammation independently of alterations in gut microbiota.* PLoS One, 2017. **12**(3): p. e0174239.
380. Wang, X., et al., *Liver fatty acid composition in mice with or without nonalcoholic fatty liver disease.* Lipids Health Dis, 2011. **10**: p. 234.
381. Deng, Q.G., et al., *Steatohepatitis induced by intragastric overfeeding in mice.* Hepatology, 2005. **42**(4): p. 905-14.
382. Jump, D.B., et al., *Impact of dietary fat on the development of non-alcoholic fatty liver disease in Ldlr(−/−) mice.* The Proceedings of the Nutrition Society, 2016. **75**(1): p. 1-9.

383. Lieber, C.S., et al., *Model of nonalcoholic steatohepatitis.* Am J Clin Nutr, 2004. **79**(3): p. 502-9.
384. Nobili, V., et al., *Docosahexaenoic acid supplementation decreases liver fat content in children with non-alcoholic fatty liver disease: double-blind randomised controlled clinical trial.* Arch Dis Child, 2011. **96**(4): p. 350-3.
385. Bialostosky, K., et al., *Dietary intake of macronutrients, micronutrients, and other dietary constituents: United States 1988-94.* Vital Health Stat 11, 2002(245): p. 1-158.
386. Porras, D., et al., *Protective effect of quercetin on high-fat diet-induced non-alcoholic fatty liver disease in mice is mediated by modulating intestinal microbiota imbalance and related gut-liver axis activation.* Free Radic Biol Med, 2017. **102**: p. 188-202.
387. Tetri, L.H., et al., *Severe NAFLD with hepatic necroinflammatory changes in mice fed trans fats and a high-fructose corn syrup equivalent.* Am J Physiol Gastrointest Liver Physiol, 2008. **295**(5): p. G987-95.
388. Jovicic, N., et al., *Differential Immunometabolic Phenotype in Th1 and Th2 Dominant Mouse Strains in Response to High-Fat Feeding.* PLoS One, 2015. **10**(7): p. e0134089.
389. Alwayn, I.P., et al., *Omega-3 fatty acid supplementation prevents hepatic steatosis in a murine model of nonalcoholic fatty liver disease.* Pediatr Res, 2005. **57**(3): p. 445-52.
390. Ahmed, A.A., et al., *Novel regulatory roles of omega-3 fatty acids in metabolic pathways: a proteomics approach.* Nutr Metab (Lond), 2014. **11**(1): p. 6.
391. Brenner, C., et al., *Decoding cell death signals in liver inflammation.* J Hepatol, 2013. **59**(3): p. 583-94.
392. Vansaun, M.N., A.M. Mendonsa, and D. Lee Gorden, *Hepatocellular proliferation correlates with inflammatory cell and cytokine changes in a murine model of nonalchoholic fatty liver disease.* PLoS One, 2013. **8**(9): p. e73054.
393. DeSantis, C.E., et al., *Breast cancer statistics, 2017, racial disparity in mortality by state.* CA Cancer J Clin, 2017. **67**(6): p. 439-448.
394. McCracken, M., et al., *Cancer incidence, mortality, and associated risk factors among Asian Americans of Chinese, Filipino, Vietnamese, Korean, and Japanese ethnicities.* CA Cancer J Clin, 2007. **57**(4): p. 190-205.
395. Ziegler, R.G., et al., *Migration patterns and breast cancer risk in Asian-American women.* J Natl Cancer Inst, 1993. **85**(22): p. 1819-27.
396. Evans, D.G., et al., *Breast cancer risk in a screening cohort of Asian and white British/Irish women from Manchester UK.* BMC Public Health, 2018. **18**(1): p. 178.
397. Zheng, J.-S., et al., *Intake of fish and marine n-3 polyunsaturated fatty acids and risk of breast cancer: meta-analysis of data from 21 independent prospective cohort studies.* BMJ : British Medical Journal, 2013. **346**.
398. Weylandt, K.H., et al., *Omega-3 fatty acids and their lipid mediators: towards an understanding of resolvin and protectin formation.* Prostaglandins Other Lipid Mediat, 2012. **97**(3-4): p. 73-82.
399. Khadge, S., et al., *Lipid Inflammatory Mediators in Cancer Progression and Therapy.* Adv Exp Med Biol, 2017. **1036**: p. 145-156.
400. D'Eliseo, D. and F. Velotti, *Omega-3 Fatty Acids and Cancer Cell Cytotoxicity: Implications for Multi-Targeted Cancer Therapy.* J Clin Med, 2016. **5**(2).
401. MacLennan, M.B., et al., *Mammary tumor development is directly inhibited by lifelong n-3 polyunsaturated fatty acids.* J Nutr Biochem, 2013. **24**(1): p. 388-95.
402. McCormack, V.A. and I. dos Santos Silva, *Breast density and parenchymal patterns as markers of breast cancer risk: a meta-analysis.* Cancer Epidemiol Biomarkers Prev, 2006. **15**(6): p. 1159-69.

403. Vaysse, C., et al., *Inflammation of mammary adipose tissue occurs in overweight and obese patients exhibiting early-stage breast cancer.* npj Breast Cancer, 2017. **3**(1): p. 19.
404. Fidler, I.J., *Metastasis: quantitative analysis of distribution and fate of tumor emboli labeled with 125 I-5-iodo-2'-deoxyuridine.* J Natl Cancer Inst, 1970. **45**(4): p. 773-82.
405. Peters, I.T.A., et al., *Prevalence and Risk Factors of Ovarian Metastases in Breast Cancer Patients < 41 Years of Age in the Netherlands: A Nationwide Retrospective Cohort Study.* PLoS ONE, 2017. **12**(1): p. e0168277.
406. Bussani, R., et al., *Cardiac metastases.* Journal of Clinical Pathology, 2007. **60**(1): p. 27-34.
407. Nasu, H., et al., *Breast cancer metastatic to the kidney with renal vein involvement.* Jpn J Radiol, 2015. **33**(2): p. 107-11.
408. Tao, K., et al., *Imagable 4T1 model for the study of late stage breast cancer.* BMC Cancer, 2008. **8**: p. 228.
409. Hiraga, T., et al., *Zoledronic acid inhibits visceral metastases in the 4T1/luc mouse breast cancer model.* Clin Cancer Res, 2004. **10**(13): p. 4559-67.
410. Zhang, Y., et al., *Surgically-Induced Multi-organ Metastasis in an Orthotopic Syngeneic Imageable Model of 4T1 Murine Breast Cancer.* Anticancer Res, 2015. **35**(9): p. 4641-6.
411. Yoneda, T., et al., *Actions of bisphosphonate on bone metastasis in animal models of breast carcinoma.* Cancer, 2000. **88**(12 Suppl): p. 2979-88.
412. Watkins, B.A., et al., *Dietary ratio of (n-6)/(n-3) polyunsaturated fatty acids alters the fatty acid composition of bone compartments and biomarkers of bone formation in rats.* J Nutr, 2000. **130**(9): p. 2274-84.
413. Yuan, J., et al., *The effects of polyunsaturated fatty acids and their metabolites on osteoclastogenesis in vitro.* Prostaglandins Other Lipid Mediat, 2010. **92**(1-4): p. 85-90.
414. Wonnacott, K.E., et al., *Dietary omega-3 and -6 polyunsaturated fatty acids affect the composition and development of sheep granulosa cells, oocytes and embryos.* Reproduction, 2010. **139**(1): p. 57-69.
415. Khan, R.S., et al., *Fish oil selectively improves heart function in a mouse model of lipid-induced cardiomyopathy.* Journal of cardiovascular pharmacology, 2013. **61**(4): p. 345-354.
416. Zeng, Z., et al., *Omega-3 Polyunsaturated Fatty Acids Attenuate Fibroblast Activation and Kidney Fibrosis Involving MTORC2 Signaling Suppression.* Scientific Reports, 2017. **7**: p. 46146.
417. Talmadge, J.E., *Models of metastasis in drug discovery.* Methods Mol Biol, 2010. **602**: p. 215-33.
418. Younos, I.H., et al., *Tumor regulation of myeloid-derived suppressor cell proliferation and trafficking.* Int Immunopharmacol, 2012. **13**(3): p. 245-56.
419. Lelekakis, M., et al., *A novel orthotopic model of breast cancer metastasis to bone.* Clin Exp Metastasis, 1999. **17**(2): p. 163-70.
420. H Heppner, G., F. R Miller, and P.V. Malathy Shekhar, *Nontransgenic models of breast cancer.* Breast Cancer Research : BCR, 2000. **2**(5): p. 331-334.
421. Morecki, S., et al., *Allogeneic cell therapy for a murine mammary carcinoma.* Cancer Res, 1998. **58**(17): p. 3891-5.
422. Faria, S.S., et al., *The neutrophil-to-lymphocyte ratio: a narrative review.* ecancermedicalscience, 2016. **10**: p. 702.
423. Bing, C., et al., *Adipose atrophy in cancer cachexia: morphologic and molecular analysis of adipose tissue in tumour-bearing mice.* Br J Cancer, 2006. **95**(8): p. 1028-37.

424. Porporato, P.E., *Understanding cachexia as a cancer metabolism syndrome.* Oncogenesis, 2016. **5**: p. e200.
425. Ebadi, M. and V.C. Mazurak, *Evidence and Mechanisms of Fat Depletion in Cancer.* Nutrients, 2014. **6**(11): p. 5280-5297.
426. Yee, L.D., et al., *Dietary (n-3) polyunsaturated fatty acids inhibit HER-2/neu-induced breast cancer in mice independently of the PPARgamma ligand rosiglitazone.* J Nutr, 2005. **135**(5): p. 983-8.
427. Yee, L.D., et al., *The inhibition of early stages of HER-2/neu-mediated mammary carcinogenesis by dietary n-3 PUFAs.* Mol Nutr Food Res, 2013. **57**(2): p. 320-7.
428. Olivo-Marston, S.E., et al., *Gene signaling pathways mediating the opposite effects of prepubertal low-fat and high-fat n-3 polyunsaturated fatty acid diets on mammary cancer risk.* Cancer Prev Res (Phila), 2008. **1**(7): p. 532-45.
429. Paschall, A.V. and K. Liu, *An Orthotopic Mouse Model of Spontaneous Breast Cancer Metastasis.* Journal of visualized experiments : JoVE, 2016(114): p. 10.3791/54040.
430. Ghochikyan, A., et al., *Primary 4T1 tumor resection provides critical "window of opportunity" for immunotherapy.* Clinical & experimental metastasis, 2014. **31**(2): p. 185-198.
431. Chung, H., et al., *Omega-3 fatty acids reduce obesity-induced tumor progression independent of GPR120 in a mouse model of postmenopausal breast cancer.* Oncogene, 2014. **34**: p. 3504.
432. Xue, M., et al., *Docosahexaenoic acid inhibited the Wnt/beta-catenin pathway and suppressed breast cancer cells in vitro and in vivo.* J Nutr Biochem, 2014. **25**(2): p. 104-10.
433. Pulaski, B.A. and S. Ostrand-Rosenberg, *Reduction of Established Spontaneous Mammary Carcinoma Metastases following Immunotherapy with Major Histocompatibility Complex Class II and B7.1 Cell-based Tumor Vaccines.* Cancer Research, 1998. **58**(7): p. 1486-1493.
434. Saxena, M. and G. Christofori, *Rebuilding cancer metastasis in the mouse.* Molecular Oncology, 2013. **7**(2): p. 283-296.
435. Wright, L.E., et al., *Murine models of breast cancer bone metastasis.* BoneKEy Reports, 2016. **5**: p. 804.
436. Bolin, C., et al., *Novel mouse mammary cell lines for in vivo bioluminescence imaging (BLI) of bone metastasis.* Biological Procedures Online, 2012. **14**: p. 6-6.
437. Mandal, C.C., et al., *Fish oil prevents breast cancer cell metastasis to bone.* Biochem Biophys Res Commun, 2010. **402**(4): p. 602-7.
438. Rahman, M., et al., *DHA is a more potent inhibitor of breast cancer metastasis to bone and related osteolysis than EPA.* Breast cancer research and treatment, 2013. **141**(3): p. 10.1007/s10549-013-2703-y.
439. Kruger, M.C. and L.M. Schollum, *Is docosahexaenoic acid more effective than eicosapentaenoic acid for increasing calcium bioavailability?* Prostaglandins Leukot Essent Fatty Acids, 2005. **73**(5): p. 327-34.
440. Watkins, B.A., Y. Li, and M.F. Seifert, *Dietary ratio of n-6/n-3 PUFAs and docosahexaenoic acid: actions on bone mineral and serum biomarkers in ovariectomized rats.* J Nutr Biochem, 2006. **17**(4): p. 282-9.
441. Huo, Z., et al., *Metastasis of breast cancer to renal cancer: report of a rare case.* International Journal of Clinical and Experimental Pathology, 2015. **8**(11): p. 15417-15421.

442. K., K.I., *Cardiac lymphatic involvement by metastatic tumor.* Cancer, 1972. **29**(3): p. 799-808.
443. B., L.W. and B.W. L., *The changing prevalence of secondary cardiac neoplasms as related to cancer therapy.* Cancer, 1980. **45**(10): p. 2659-2662.
444. Reynen, K., U. Köckeritz, and R.H. Strasser, *Metastases to the heart.* Annals of Oncology, 2004. **15**(3): p. 375-381.
445. PIMENTEL, C., et al., *Ovarian Metastases from Breast Cancer: A Series of 28 Cases.* Anticancer Research, 2016. **36**(8): p. 4195-4200.
446. Lee, S.-J., et al., *Clinical Characteristics of Metastatic Tumors to the Ovaries.* Journal of Korean Medical Science, 2009. **24**(1): p. 114-119.
447. Eilati, E., et al., *Flaxseed enriched diet-mediated reduction in ovarian cancer severity is correlated to the reduction of prostaglandin E2 in laying hen ovaries.* Prostaglandins, Leukotrienes and Essential Fatty Acids (PLEFA), 2013. **89**(4): p. 179-187.
448. Wan, X.H., X. Fu, and G. Ababaikeli, *Docosahexaenoic Acid Induces Growth Suppression on Epithelial Ovarian Cancer Cells More Effectively than Eicosapentaenoic Acid.* Nutr Cancer, 2016. **68**(2): p. 320-7.
449. Wang, Y.-C., et al., *Docosahexaenoic Acid Modulates Invasion and Metastasis of Human Ovarian Cancer via Multiple Molecular Pathways.* International Journal of Gynecological Cancer, 2016. **26**(6): p. 994-1003.
450. Chen, Y., et al., *Epidemiology of Contralateral Breast Cancer.* Cancer Epidemiology Biomarkers & Prevention, 1999. **8**(10): p. 855-861.
451. Alkner, S., et al., *Contralateral breast cancer can represent a metastatic spread of the first primary tumor: determination of clonal relationship between contralateral breast cancers using next-generation whole genome sequencing.* Breast Cancer Research, 2015. **17**(1): p. 102.
452. Raghavendra, A., et al., *Mammographic breast density is associated with the development of contralateral breast cancer.* Cancer, 2017. **123**(11): p. 1935-1940.
453. Khadge, S., et al., *Long-Chain Omega-3 Polyunsaturated Fatty Acids Modulate Mammary Gland Composition and Inflammation.* J Mammary Gland Biol Neoplasia, 2018.
454. Schley, P.D., et al., *Mechanisms of omega-3 fatty acid-induced growth inhibition in MDA-MB-231 human breast cancer cells.* Breast Cancer Research and Treatment, 2005. **92**(2): p. 187-195.
455. Jiang, W., et al., *Identification of a Molecular Signature Underlying Inhibition of Mammary Carcinoma Growth by Dietary N-3 Fatty Acids.* Cancer Research, 2012. **72**(15): p. 3795-3806.
456. El Fadli, M., et al., *Breast cancer metastasis to the spleen: a case report and literature review.* Oxford Medical Case Reports, 2017. **2017**(12): p. omx069.
457. Roomi, M.W., et al., *In vitro and in vivo effects of a nutrient mixture on breast cancer progression.* Int J Oncol, 2014. **44**(6): p. 1933-44.
458. DuPre, S.A. and K.W. Hunter, Jr., *Murine mammary carcinoma 4T1 induces a leukemoid reaction with splenomegaly: association with tumor-derived growth factors.* Exp Mol Pathol, 2007. **82**(1): p. 12-24.
459. Younos, I., et al., *Tumor- and organ-dependent infiltration by myeloid-derived suppressor cells.* Int Immunopharmacol, 2011. **11**(7): p. 816-26.
460. Gonzalez, M.J., et al., *Dietary fish oil inhibits human breast carcinoma growth: a function of increased lipid peroxidation.* Lipids, 1993. **28**(9): p. 827-32.
461. Hammamieh, R., et al., *Control of the growth of human breast cancer cells in culture by manipulation of arachidonate metabolism.* BMC Cancer, 2007. **7**(1): p. 138.

462. Albino, A.P., et al., *Cell Cycle Arrest and Apoptosis of Melanoma Cells by Docosahexaenoic Acid: Association with Decreased pRb Phosphorylation.* Cancer Research, 2000. **60**(15): p. 4139-4145.
463. Istfan, N.W., J. Wan, and Z.Y. Chen, *Fish oil and cell proliferation kinetics in a mammary carcinoma tumor model.* Adv Exp Med Biol, 1995. **375**: p. 149-56.
464. Murray, M., et al., *Anti-tumor activities of lipids and lipid analogues and their development as potential anticancer drugs.* Pharmacol Ther, 2015. **150**: p. 109-28.
465. Merendino, N., et al., *Dietary ω-3 Polyunsaturated Fatty Acid DHA: A Potential Adjuvant in the Treatment of Cancer.* BioMed Research International, 2013. **2013**: p. 11.
466. Hardman, W.E., et al., *Three percent dietary fish oil concentrate increased efficacy of doxorubicin against MDA-MB 231 breast cancer xenografts.* Clin Cancer Res, 2001. **7**(7): p. 2041-9.
467. Reddy, S., M. Raffin, and V. Kaklamani, *Targeting Angiogenesis in Metastatic Breast Cancer.* The Oncologist, 2012. **17**(8): p. 1014-1026.
468. Fidler, I.J. and L.M. Ellis, *The implications of angiogenesis for the biology and therapy of cancer metastasis.* Cell, 1994. **79**(2): p. 185-8.
469. Zhang, G., et al., *Epoxy metabolites of docosahexaenoic acid (DHA) inhibit angiogenesis, tumor growth, and metastasis.* Proc Natl Acad Sci U S A, 2013. **110**(16): p. 6530-5.
470. Albini, A., et al., *Tumor inflammatory angiogenesis and its chemoprevention.* Cancer Res, 2005. **65**(23): p. 10637-41.
471. Lewis, C.E., et al., *Cytokine regulation of angiogenesis in breast cancer: the role of tumor-associated macrophages.* J Leukoc Biol, 1995. **57**(5): p. 747-51.
472. Nozawa, H., C. Chiu, and D. Hanahan, *Infiltrating neutrophils mediate the initial angiogenic switch in a mouse model of multistage carcinogenesis.* Proceedings of the National Academy of Sciences, 2006. **103**(33): p. 12493-12498.
473. Wroblewski, M., et al., *Mast cells decrease efficacy of anti-angiogenic therapy by secreting matrix-degrading granzyme B.* Nature Communications, 2017. **8**(1): p. 269.
474. Kzhyshkowska, J., et al., *Role of tumor associated macrophages in tumor angiogenesis and lymphangiogenesis.* Frontiers in Physiology, 2014. **5**(75).
475. Mantovani, A. and M. Locati, *Macrophage Metabolism Shapes Angiogenesis in Tumors.* Cell Metabolism, 2016. **24**(5): p. 653-654.
476. Bingle, L., et al., *Macrophages promote angiogenesis in human breast tumour spheroids in vivo.* British Journal Of Cancer, 2005. **94**: p. 101.
477. Denkert, C., et al., *Tumor-associated lymphocytes as an independent predictor of response to neoadjuvant chemotherapy in breast cancer.* J Clin Oncol, 2010. **28**(1): p. 105-13.
478. Zhang, X. and W. Xu, *Neutrophils diminish T-cell immunity to foster gastric cancer progression: the role of GM-CSF/PD-L1/PD-1 signalling pathway.* Gut, 2017.
479. Jiao, Y., et al., *Docosahexaenoic acid and disulfiram act in concert to kill cancer cells: a mutual enhancement of their anticancer actions.* Oncotarget, 2017. **8**(11): p. 17908-17920.
480. Hajjaji, N. and P. Bougnoux, *Selective sensitization of tumors to chemotherapy by marine-derived lipids: a review.* Cancer Treat Rev, 2013. **39**(5): p. 473-88.
481. Slagsvold, J.E., et al., *DHA alters expression of target proteins of cancer therapy in chemotherapy resistant SW620 colon cancer cells.* Nutr Cancer, 2010. **62**(5): p. 611-21.
482. Hamidullah, B. Changkija, and R. Konwar, *Role of interleukin-10 in breast cancer.* Breast Cancer Res Treat, 2012. **133**(1): p. 11-21.

483. Bhattacharjee, H.K., et al., *Is Interleukin 10 (IL10) Expression in Breast Cancer a Marker of Poor Prognosis?* Indian Journal of Surgical Oncology, 2016. **7**(3): p. 320-325.
484. Ahmad, N., et al., *IL-6 and IL-10 are associated with good prognosis in early stage invasive breast cancer patients.* Cancer Immunol Immunother, 2018. **67**(4): p. 537-549.
485. Fujii, S., et al., *Interleukin-10 promotes the maintenance of antitumor CD8(+) T-cell effector function in situ.* Blood, 2001. **98**(7): p. 2143-51.
486. Mumm, J.B., et al., *IL-10 elicits IFNgamma-dependent tumor immune surveillance.* Cancer Cell, 2011. **20**(6): p. 781-96.
487. Sun, Z., et al., *IL10 and PD-1 Cooperate to Limit the Activity of Tumor-Specific CD8+ T Cells.* Cancer Res, 2015. **75**(8): p. 1635-44.
488. L., B.R., F.F. M., and M.F. Eleftheria, *Dietary Fatty Acids Differentially Regulate Production of TNF-α and IL-10 by Murine 3T3-L1 Adipocytes.* Obesity, 2008. **16**(5): p. 938-944.
489. Foitzik, T., et al., *Omega-3 fatty acid supplementation increases anti-inflammatory cytokines and attenuates systemic disease sequelae in experimental pancreatitis.* JPEN J Parenter Enteral Nutr, 2002. **26**(6): p. 351-6.
490. Donkor, M.K., et al., *Mammary tumor heterogeneity in the expansion of myeloid-derived suppressor cells.* Int Immunopharmacol, 2009. **9**(7-8): p. 937-48.
491. Kowanetz, M., et al., *Granulocyte-colony stimulating factor promotes lung metastasis through mobilization of Ly6G+Ly6C+ granulocytes.* Proceedings of the National Academy of Sciences, 2010. **107**(50): p. 21248-21255.
492. Roche-Nagle, G., et al., *Antimetastatic activity of a cyclooxygenase-2 inhibitor.* British Journal Of Cancer, 2004. **91**: p. 359.
493. Brault, M.S. and R.A. Kurt, *Impact of Tumor-Derived CCL2 on Macrophage Effector Function.* Journal of Biomedicine and Biotechnology, 2005. **2005**(1): p. 37-43.
494. Waight, J.D., et al., *Tumor-Derived G-CSF Facilitates Neoplastic Growth through a Granulocytic Myeloid-Derived Suppressor Cell-Dependent Mechanism.* PLoS ONE, 2011. **6**(11): p. e27690.
495. Koopman, K.E., et al., *Hypercaloric diets with increased meal frequency, but not meal size, increase intrahepatic triglycerides: A randomized controlled trial.* Hepatology (Baltimore, Md.), 2014. **60**(2): p. 545-553.
496. Akiyama, T., et al., *High-fat hypercaloric diet induces obesity, glucose intolerance and hyperlipidemia in normal adult male Wistar rat.* Diabetes Res Clin Pract, 1996. **31**(1-3): p. 27-35.
497. Elkum, N., et al., *Obesity is a significant risk factor for breast cancer in Arab women.* BMC Cancer, 2014. **14**: p. 788.
498. Golay, A. and E. Bobbioni, *The role of dietary fat in obesity.* Int J Obes Relat Metab Disord, 1997. **21 Suppl 3**: p. S2-11.
499. Macias, H. and L. Hinck, *Mammary Gland Development.* Wiley interdisciplinary reviews. Developmental biology, 2012. **1**(4): p. 533-557.
500. Hoy, A.J., S. Balaban, and D.N. Saunders, *Adipocyte-Tumor Cell Metabolic Crosstalk in Breast Cancer.* Trends Mol Med, 2017. **23**(5): p. 381-392.
501. Brook, C., J.K. Lloyd, and O. Wolf, *Relation between age of onset of obesity and size and number of adipose cells.* Br med J, 1972. **2**(5804): p. 25-27.
502. Chaffer, C.L. and R.A. Weinberg, *A perspective on cancer cell metastasis.* Science, 2011. **331**(6024): p. 1559-64.
503. Redig, A.J. and S.S. McAllister, *Breast cancer as a systemic disease: a view of metastasis.* Journal of internal medicine, 2013. **274**(2): p. 113-126.

504. Psaila, B. and D. Lyden, *The Metastatic Niche: Adapting the Foreign Soil.* Nature reviews. Cancer, 2009. **9**(4): p. 285-293.
505. Murgai, M., A. Giles, and R. Kaplan, *Physiological, Tumor, and Metastatic Niches: Opportunities and Challenges for Targeting the Tumor Microenvironment.* Critical reviews in oncogenesis, 2015. **20**(3-4): p. 301-314.
506. Brodt, P., *Role of the Microenvironment in Liver Metastasis: From Pre- to Prometastatic Niches.* Clinical Cancer Research, 2016. **22**(24): p. 5971-5982.